Phenomenology of glueballs and scalar-isoscalar quarkonia within an effective hadronic model of QCD

Stanislaus Janowski

Dissertation zur Erlangung des
Doktorgrades der Naturwissenschaften

vorgelegt beim Fachbereich Physik
der Johann Wolfgang Goethe-Universität
in Frankfurt am Main

Frankfurt am Main (September 2015)
(D 30)

vom Fachbereich Physik der

Johann Wolfgang Goethe-Universität als Dissertation angenommen.

Dekan: Prof. Dr. Rene Reifarth

1. Gutachter: PD. Dr. Francesco Giacosa

2. Gutachter: Prof. Dr. Dirk-Hermann Rischke

Datum der Disputation: voraussichtlich 06.11.2015

Eidesstattliche Versicherung

Ich erkläre hiermit an Eides Statt, dass ich die vorliegende Dissertation selbständig angefertigt und mich anderer Hilfsmittel als der in ihr angegebenen nicht bedient habe, insbesondere, dass alle Entlehnungen aus anderen Schriften mit Angabe der betreffenden Schrift gekennzeichnet sind. Auf Textpassagen, Abbildungen und Tabellen, die aus eigenen Publikationen [1, 2, 3, 4, 5, 6, 7, 8, 9] entnommen sind, wird lediglich zu Beginn des jeweiligen Kapitels entsprechend hingewiesen.
Ich versichere, die Grundsätze der guten wissenschaftlichen Praxis beachtet, und nicht die Hilfe einer kommerziellen Promotionsvermittlung in Anspruch genommen zu haben.

Frankfurt am Main, den 21.08.2015

How many bodies are required before we have a problem? G.E. Brown points out that this can be answered by a look at history. In eighteenth-century Newtonian mechanics, the three-body problem was insoluble. With the birth of relativity around 1910 and quantum electrodynamics in 1930, the two- and one-body problems became insoluble. And within modern quantum field theory, the problem of zero bodies (vacuum) is insoluble. So, if we are out after exact solutions, no bodies at all is already too many!

R.D. Mattuck

Abstract

A natural consequence of the pure Yang-Mills sector of quantum chromodynamics (QCD) is the existence of gauge-invariant states composed of gluons, so-called glueballs. Since the early 1970s their properties have been investigated in a variety of approaches but a conclusive picture of glueballs is still missing. Lattice QCD confirmed their existence and determined the full spectrum of glueballs where the ground state is a scalar glueball ($J^{PC} = 0^{++}$) with a mass of about 1.7 GeV.

A further fundamental issue of QCD is the understanding of the scalar-isoscalar sector, $I^G(J^{PC}) = 0^+(0^{++})$, in the low-energy region below 2 GeV. In the last four decades many states with these quantum numbers were discovered and discussed. At the present time five scalar-isoscalar resonances are well-established and listed by the *Particle Data Group* (PDG). There are the two resonances $f_0(500)$ and $f_0(980)$ whose masses lie below 1 GeV. Many studies suggest that these resonances are neither quarkonia nor glueballs. Together with $a_0(980)$ and $K_0^*(800)$ they rather form a nonet of tetraquark states or they can be interpreted as mesonic molecular states. The remaining three resonances are $f_0(1370)$, $f_0(1500)$, and $f_0(1710)$ and lie in the energy region between 1 and 2 GeV. Thus, it is natural to expect that one of them is the scalar glueball.

This thesis is addressed to study the vacuum phenomenology of the scalar-isoscalar sector in the energy region between 1 and 2 GeV in the framework of the extended linear sigma model (eLSM). This effective field-theoretical model is based on symmetries and anomalies of QCD such as the global chiral symmetry and the trace anomaly. The degrees of freedom of the eLSM are from the very beginning hadrons: there are quark-antiquark mesons as well as one scalar glueball, which is described by excitations of a scalar dilaton field. The $\bar{q}q$ fields include not only scalar ($S, 0^{++}$) and pseudoscalar (P, 0^{-+}) mesons, but also vector (V_μ, 1^{--}) and axial-vector (A_μ, 1^{++}) mesons. The eLSM in the case $N_f = 2$, where N_f is the number of flavors, yields a two-body mixing scenario in the scalar-isoscalar sector where the bare non-strange quark-antiquark meson $\sigma_N \cong \left(\bar{u}u + \bar{d}d\right)/\sqrt{2}$ and the bare scalar glueball G are involved. In the eLSM with $N_f = 3$ an additional scalar-isoscalar $\bar{q}q$ state, the strange one $\sigma_S \cong \bar{s}s$, arises. Hence, two bare quarkonia and a bare glueball mix and generate the physical resonances $f_0(1370)$, $f_0(1500)$, and $f_0(1710)$. Finally, the fields σ_N, σ_S, and G possess the quantum numbers of the vacuum, hence three types of condensates arise in our model: the non-strange and the strange quark condensate $\left\langle \bar{u}u + \bar{d}d \right\rangle/\sqrt{2} \neq 0$ and $\langle \bar{s}s \rangle \neq 0$ as well as the gluon condensate $\left\langle \frac{\alpha_s}{\pi} G^a_{\mu\nu} G^{a,\mu\nu} \right\rangle \neq 0$. Thus, it is interesting to learn how large are the respective contributions to the generation of hadron masses.

We found two solutions of the eLSM in the case of $N_f = 2$. In both solutions the resonance $f_0(1370)$ was predominantly the non-strange $\bar{q}q$ state while the glueball was in one solution predominantly $f_0(1500)$ and in the other one predominantly $f_0(1710)$. Calculations of the three-flavored eLSM yield an unambiguous result where $f_0(1370)$ was, as previously, predominantly the non-strange, while $f_0(1500)$ is predominantly the strange quark-antiquark meson, and finally the resonance $f_0(1710)$ turns out to be predominantly a scalar glueball. Our calculations are based on the assumption that the decay width of the scalar glueball is narrow ($\Gamma_G \lesssim 100$ GeV) which is in accordance with large-N_c arguments. As a consequence, we obtained for the energy scale parameter Λ_{dil}, which arises from the trace anomaly, a large value, which implies a large gluon condensate. Furthermore, we found that the mass of the ρ meson is mostly generated by the gluon condensate. Consequently, we expect that its mass in medium scales as the gluon condensate rather than the quark condensate.

We emphasize that the inclusion of the (axial-)vector degrees of freedom was crucial for the results of our approach. These fields affect the phenomenology in the (pseudo)scalar sector, e.g. our model suggests that $f_0(1370)$ is the chiral partner of the pion. In addition, it is, to our knowledge, the first time where a full mixing, $N_f = 3$, above 1 GeV of two scalar-isoscalar quarkonia and a scalar glueball, described by a dilaton field, in a chiral hadronic model with (axial-)vector fields, was studied.

Moreover, we studied the vacuum properties of a pseudoscalar glueball $\tilde{G}$. To this end, we constructed in conformity with the eLSM the effective Lagrangian which couples this glueball to the quark-antiquark mesons. The corresponding mass $m_{\tilde{G}} = 2.6$ GeV is predicted by lattice QCD in the quenched approximation and lies in the energy region which can be investigated by the upcoming *AntiProton ANnihilations at DArmstadt* ($\bar{\text{P}}$ANDA) experiment at the *Facility for Antiproton and Ion Research* (FAIR) as well as the *GLUonic EXcitations* (GlueX) experiment of the *Jefferson national LABoratory* (JLAB). In case of the pseudoscalar glueball we present our results as branching ratios in order to make parameter-free predictions which can be used as a guideline for the search of glueballs. We found that $\tilde{G} \to KK\pi$ is the dominant decay channel ($\sim 47\%$) of the pseudoscalar glueball followed by $\tilde{G} \to \eta\pi\pi$ ($\sim 16\%$) and $\tilde{G} \to \eta'\pi\pi$ ($\sim 10\%$), while $\tilde{G} \to \pi\pi\pi$ is predicted to vanish. We repeat the calculations for a glueball mass of 2.37 GeV which corresponds to the mass of the pseudoscalar resonance $X(2370)$ observed in the *BEijing Spectrometer* (BES) III experiment. In the future, the very same procedure can be applied to other glueballs. A very interesting case is that of the vector glueball $\mathcal{O}_\mu$ with a mass of $m_{\mathcal{O}_\mu} = 3.8$ GeV obtained by lattice QCD, whose decay into quark-antiquark mesons will be studied. In this work we present the Lagrangian and the main features.

Contents

Chapter 1

Introduction

In this chapter we briefly recapitulate the theoretical background which is relevant in order to construct our effective model, by using the following references [10, 11, 12, 13, 14, 15, 16, 17, 18, 19]. In addition, by following the references [1, 2, 3, 4, 5, 6, 7, 8, 9, 20], we give an overview of the subjects and the associated *physical* issues which this thesis addresses.

1.1 Units and conventions

We use *natural units* [10]

$$\hbar = c = \varepsilon_0 = k_B = 1 \,, \tag{1.1}$$

which implies

$$[\text{energy}] = [\text{mass}] = [\text{temperature}] = [\text{length}]^{-1} = [\text{time}]^{-1} \,, \tag{1.2}$$

as well the *Minkowski space* where

$$g_{\mu\nu} = g^{\mu\nu} = diag(1, -1, -1, -1) \tag{1.3}$$

is the *metric tensor* and

$$x \equiv x^{\mu} = (t, \vec{x})^T \,, \quad x_{\mu} = g_{\mu\nu} x^{\nu} = (t, -\vec{x}) \tag{1.4}$$

are the *co-* and *contravariant vectors* of the *space-time* with Greek indices running over 0,1,2,3.

1.2 Aspects of Quantum Chromodynamics (QCD)

At the present time four fundamental forces are known. The *Strong interaction* together with the *weak* and the *electromagnetic interaction* represent the interactions of the *Standard Model of Particle Physics* (SM)[1]. The latter is formulated as a *local quantum field theory* (QFT) with the symmetry group

$$SU(3) \times SU(2) \times U(1) \,, \tag{1.5}$$

[1]The fourth fundamental force is gravity, which is described by the theory of general relativity, see e.g. Ref. [21]. Unfortunately, this theory could be not yet satisfactorily implemented into the SM due to conceptional problems such as non-renormalisability and the tensor nature of gravitons.

where $U(N)$ and $SU(N)$ are the *unitary* and *special unitary groups*, respectively, in N dimensions, see e.g. Refs. [10, 11, 12, 13, 22, 23] and later on in this thesis. The theory of the strong interaction is *quantum chromodynamics*, on which this work is based on. Therefore, its relevant aspects will be discussed in the following.

1.2.1 From hadrons and quarks to QCD

In the last century a huge amount of strongly interacting particles, so-called *hadrons*, were discovered e.g.,

$$proton, neutron, \pi, K, \Lambda, \omega, \rho, \eta, \phi, J/\psi ... \ .$$

Already before the underlying theory of the strong interaction, QCD, was developed and well-established, a classification of hadrons was undertaken. To this end one assumed that hadrons are composed of elementary pieces of matter, which are called *quarks* according to a suggestion of Murray Gell-Mann, and used for their classification the $SU_f(N_f)$ *flavor symmetry*, where $N_f = 3$ is the number of flavors [24, 25, 26, 27]. This was the birth of the *quark model*, which is today in a more sophisticated form embedded in QCD [28].

Later on, the development of the *parton model*[2] by Richard P. Feynman and James D. Bjorken was of primary importance in order to describe and interpret *deep inelastic lepton-nucleon scattering*.[3] Such high-energy experiments indicate that quarks with spin $\frac{1}{2}$ exist. At the present time six quark flavors are known ($N_f = 6$) which we summarize in Table 1.1.

Quark Flavor	**Notation**	**Current Mass [MeV]**
up	u	$2.3^{+0.7}_{-0.5}$
down	d	$4.8^{+0.5}_{-0.3}$
strange	s	95 ± 5
charm	c	$(1.275 \pm 0.025) \cdot 10^3$
bottom	b	$(4.18 \pm 0.03) \cdot 10^3$
top	t	$(173.21 \pm 0.51 \pm 0.71) \cdot 10^3$

Table 1.1: Quark flavors and their *current masses* [11]. According to these masses they are compartmentalized into the *light* (u, d, s) and *heavy* quarks (c, b, t).

All experiments exhibit that very soon after a collision quarks form hadrons. The time-scale of this procedure, called *hadronization*, is Λ_{QCD}^{-1}, where $\Lambda_{QCD} \simeq 200$ MeV is the typical hadronic energy scale. This implies also that the size of a hadron is about 1 fm. Quarks are then confined

[2] It turned out that inter alia partons can be interpreted as quarks. Hence, the parton model is a dynamical quark model, while the quark model of Murray Gell-Mann and George Zweig is only a static one.

[3] Leptons are, just as quarks, elementary building blocks of matter of the SM. They include the *electron* (e^-) with its two heavier counterparts, *muon* (μ^-) and *tau* (τ^-), as well as the corresponding *neutrinos* ν_e, ν_μ, and ν_τ. Protons and neutrons are called nucleons.

inside hadrons and it is not possible to isolate them. This so-called *confinement* is a feature of the strong interaction which is experimentally verified but theoretically still not completely understood.

In addition, quarks carry fractions of the *electric charge* $e_q = ze$, where $z = \frac{2}{3}$ for u, c, t and $z = -\frac{1}{3}$ for d, s, b. Nevertheless, due to the confinement, conservation of electric charge is fulfilled, since the observable hadrons only exhibit multiples of e. Moreover, quarks as particles of spin $S = \frac{1}{2}$ are *fermions* according to the *spin-statistic theorem* of Wolfgang Pauli [29].

Using quarks and *antiquarks*[4] as building blocks of matter, two types of hadrons with respect to their spin can be formed, the so-called *baryons* and *mesons*.

Baryons

Baryons possess half-integer spin, $S = n + \frac{1}{2}$ with $n \in \mathbb{N}_0$, and are therefore fermions. Furthermore, they are defined through the baryon number $B = 1$ which is a conserved quantity. *Ordinary* baryons[5] are composed of three quarks (qqq). By using the reduction formula for irreducible representation of $SU(3)$ one obtains

$$3 \otimes 3 \otimes 3 = 10 \oplus 8 \oplus 8 \oplus 1 \,, \tag{1.6}$$

i.e., a *decuplet*, two *octets*, and a *singlet*, which contain 27 baryons. For instance, in the case of $S = \frac{1}{2}$ the *proton* is placed in one of the two octets and its *valence quarks*[6] are (u, u, d).

Mesons

Mesons are particles with an integer spin, $S = n$ with $n \in \mathbb{N}_0$, which are according to the spin-statistic theorem *bosons*. The ordinary mesons are made of a quark and an antiquark $(q\bar{q})$ where according to the reduction formula for irreducible representation of $SU(3)$ one obtains

$$3 \otimes \bar{3} = 8 \oplus 1 \,, \tag{1.7}$$

i.e., there exist an octet and a singlet. In case of mesons, there is no corresponding conserved mesonic number, but by definition these kinds of hadrons possess always a vanishing baryon number ($B = 0$). Hence, there are other possibilities to built mesons from quarks and antiquarks, e.g. *tetraquarks*, first proposed by Robert L. Jaffe, which are composed of a diquark and an anti-diquark $(qq\bar{q}\bar{q})$. Beyond that, from the theoretical point of view there is a further group of mesons, so-called *glueballs*, which are not composed of valence quarks. These states will face us many times because they play a crucial role in this work.

[4] To every quark flavor there is a corresponding antiquark. They possess exactly the same mass as the respective quark but all their additive *quantum numbers*, such as the electric charge, are opposite.

[5] There are also other possibilities to combine baryons which are in agreement with all required conservation laws or symmetries, e.g. the pentaquarks $(qqqq\bar{q})$. Their existence is controversial, but see, however, the very recent results of Ref. [30]. Moreover, the definition of the baryon number B implies that $B_q = \frac{1}{3}$ and $B_{\bar{q}} = -\frac{1}{3}$.

[6] The so-called valence quarks define the quantum numbers, such as spin, of a hadron.

Color charge

The flavor symmetry as a fundamental symmetry of the strong interaction proved to be problematic. Due to the non-vanishing intrinsic mass of quarks, the so-called current mass reported in Table 1.1, this symmetry is not an exact symmetry of the strong interaction. In particular, the breaking of the flavor symmetry between the light and heavy quarks is sizeable. However, a substantial problem of the quark model described by $SU_f(3)$ flavor symmetry was that the *wave function* of the *delta resonance*[7] Δ^{++}, currently denoted as $\Delta(1232)$ [11], should be totally symmetric,

$$\Psi^{totsym}_{\Delta^{++}} = \Psi^{sym}_{space}(L=0)\Psi^{sym}_{spin}(S=3/2)\Psi^{sym}_{flavor}(uuu)\,, \tag{1.8}$$

but this would violate the Pauli principle. In order to preserve it, since it is considered to be physically fundamental, an additional intrinsic degree of freedom was proposed in 1964, so-called *color* [31]. The simplest possibility to antisymmetrize the wave function of Δ^{++} (1.21) was to assume that every quark flavor occurs in three different colors *red*, *green*, and *blue*. This is the usual convention and the corresponding antisymmetric color wave function reads

$$\Psi^{antisym}_{color} = (rgb + gbr + brg - rbg - grb - bgr)/\sqrt{6}\,. \tag{1.9}$$

At that time the concept of color was controversial due to missing experimental evidence. But in course of time, as the development of QCD proceeded and experimental evidence increased, one recognized the deep physical meaning of color as the *'charge'* of the strong interaction [14].

Evidence for color charge

In the following we show two experimental arguments that verify the existence of color charge [11, 12].

- The *amplitude* of a decaying neutral *pion* into two *photons* is proportional to the number of colors,

  $$\mathcal{A}_{\pi^0\to\gamma\gamma} \propto N_c \tag{1.10}$$

  see the corresponding *Feynman diagram*[8] in Figure 1.1,

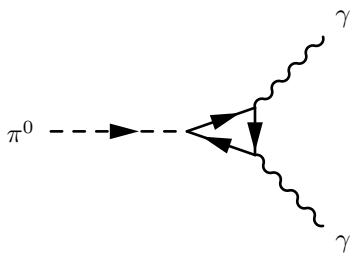

Figure 1.1: Feynman diagram of the decay process $\pi^0 \to \gamma\gamma$.

[7] Resonances are particles or physical excitations with a typical lifetime of $t \approx 10^{-23}s$. They are defined as the poles of a *propagator*, where the real part corresponds to the *Breit-Wigner mass* and the imaginary part to half of the *Breit-Wigner full width*.

[8] These diagrams are named after its inventor and illustrate processes of QFT, which can be transformed into corresponding analytical expressions.

and the theoretical *decay width* is given by

$$\Gamma^{th}_{\pi^0\to\gamma\gamma} = 7.87 \cdot \left(\frac{N_c}{3}\right)^2 \text{eV} \,. \tag{1.11}$$

The corresponding decay process observed experimentally yields a decay width of

$$\Gamma^{ex}_{\pi^0\to\gamma\gamma} = (7.95 \pm 0.05)\,\text{eV} \,. \tag{1.12}$$

Hence these results are only compatible if the number of colors is $N_c = 3$.

- The *ratio* of the *cross sections* for hadronic and leptonic *electron-positron annihilation* reads

$$R = \frac{\sigma(e^+e^- \to hadrons)}{\sigma(e^+e^- \to \mu^+\mu^-)} = N_c \sum_f e_{q,f}^2 = N_c \begin{cases} 5/9 \text{ for } N_f = 2 \\ 2/3 \text{ for } N_f = 3 \\ 10/9 \text{ for } N_f = 4 \\ 11/9 \text{ for } N_f = 5 \\ 5/3 \text{ for } N_f = 6 \end{cases} . \tag{1.13}$$

It is clear that the production of particles depends on the *centre-of-mass energy* (cme) $\sqrt{s}$ of the annihilating leptons. The cme for creating particles which include strange quarks must be large enough in order to produce them. This energy is clearly larger than the one required to produce hadrons only composed of up and down quarks, see Figure 1.2. Similar to the case of the decaying π^0, the theoretical results of Eq. (1.13) are only in agreement with experimental data if the number of colors is $N_c = 3$.

The experimental verification of the color charge which occurs in three different types, as was proposed by the antisymmetrization of the wave function of $\Delta(1232)$, was essential for the progress of QCD. In analogy to *quantum electrodynamics* (QED) one introduces a quantum field theory with a *local* $SU_c(N_c)$ *color symmetry*, where $N_c = 3$, to describe the strong interaction. Similarly, the *gauge theory of the weak interaction*,[9] is based on the same idea.

According to the color wave function (1.9), each three qqq baryon has such a *'white'* color configuration, that is to say that they are *color singlets* under the transformations of the local $SU_c(N_c = 3)$ color symmetry. Analogously, each $\bar{q}q$ meson has a *'white'* color wave function given by

$$\Psi^{white}_{\bar{q}q} = (\bar{r}r + \bar{g}g + \bar{b}b)/\sqrt{3} \,. \tag{1.14}$$

Gluons and their evidence

A local QFT requires *gauge fields* (boson fields with spin 1) which are the mediators of the corresponding interaction. The gauge fields of QCD are the so-called *gluons* which, due to the *non-abelian* structure of the color symmetry, are themselves colored objects. Their existence was verified by the experiment *Positron Elektron Tandem Ring Anlage* (PETRA) at the *Deutsches*

[9] Sheldon Glashow, Steven Weinberg, and Abdus Salam successfully unified the electromagnetic and the weak interaction to the *electroweak interaction*, see e.g. Refs. [10, 22] and references therein. A further unification to the grand unified theory (GUT), where also QCD is included, is still not satisfactorily completed, because such theories predict a decay of the proton, but up to now this could not be experimentally verified.

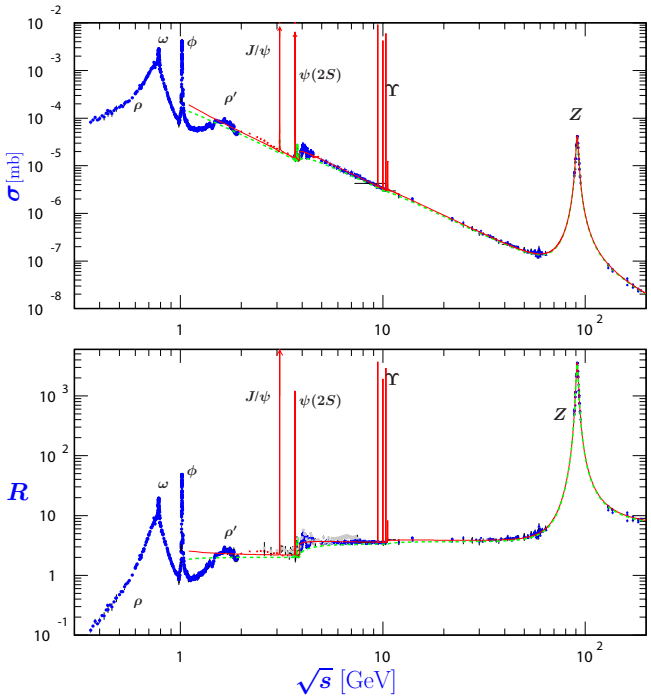

Figure 1.2: World data on the total cross section of $e^+e^- \rightarrow hadrons$ and the ratio $R(\sqrt{s})$= $\sigma(e^+e^- \rightarrow hadrons)/(\sigma(e^+e^- \rightarrow \mu^+\mu^-)$. This figure is taken from Ref. [11].

Elektronen SYnchrotron (DESY) facility in Hamburg in 1979, where in e^-e^+ annihilation processes *three jet events* were observed, as shown in Figure 1.3 and 1.4 [32, 33, 34, 35]. The interpretation of these hadronic jets is based on the QCD prediction that the production of quark-antiquark pairs are accompanied by hard non-collinear gluons [32]. In addition, the analysis of the *Ellis-Karliner angle* distribution of such three jet events shows that gluons are particles of spin 1 as QCD requires. The discovery of the gluons was a further important experimental milestone of QCD.

Moreover, at the *DEtector with Lepton, Photon and Hadron Identification* (DELPHI) at the *Large Electron Positron Collider* (LEP) at the *European Organization for Nuclear Research* (CERN) a clear proof of the *gluon selfcoupling* was given by studying *four-jet events* in 1991 [36]. Such four-jet events can be observed by hadronic decays of the weak gauge boson Z^0, where the angle between the planes which are made of the two low- and high-energetic jets, respectively, corresponds to the *Bengtsson-Zerwas angle*. From this angle the amount of *three-gluon vertices*[10], shown in Figure 1.5, can be extracted which differ from those of theories without *gauge selfcoupling* [14, 36, 37, 38].

[10] A vertex is the interaction point of a Feynman diagram, which is proportional to the *coupling constant* of the corresponding interaction.

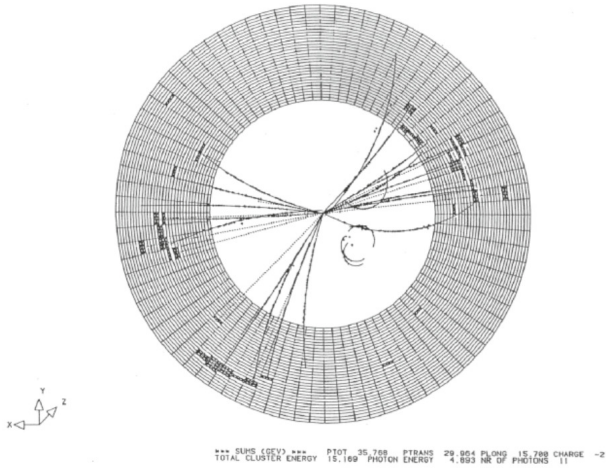

Figure 1.3: A three jet event registered in the *JApan, Deutschland and England* detector (JADE) at PETRA at a total energy of $\sqrt{s} = 31$ GeV. This figure is taken from Ref. [33].

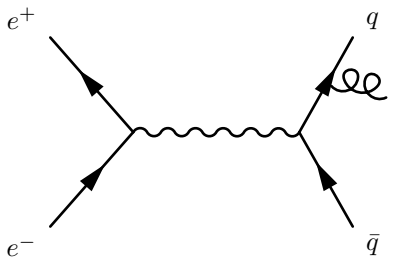

Figure 1.4: Feynman diagram of a three jet process.

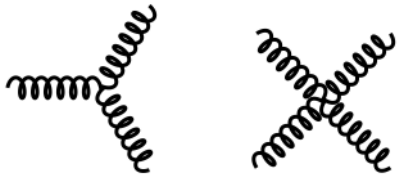

Figure 1.5: Feynman diagrams of a three- and four-gluon selfcoupling. This figure is taken from Ref. [39]

An interesting experimental fact is that until now a *'white'* gluon, where

$$\Psi_g^{singlet} = \left(\bar{r}r + \bar{g}g + \bar{b}b\right)/\sqrt{3} \tag{1.15}$$

is the corresponding wave function, is not observed. In turn, this means that the special unitary gauge group describes the color symmetry correctly, since in that case the condition

$$\det(U) = 1 \tag{1.16}$$

requires eight traceless matrices as the *generators*, T^a with $a = 1, ..., N_c^2 - 1$, of the group which correspond to the eight colored gluons. If a unitary gauge group would be taken in order to describe the color symmetry then the condition (1.16) is not compulsive. Thus the generators, T^a with $a = 1, ..., N_c^2$, are not constrained by

$$\mathrm{Tr}(T^a) \stackrel{!}{=} 0\,. \tag{1.17}$$

In that case one could take, together with the eight traceless matrices, an additional matrix, e.g. the *identity matrix* which corresponds to the ninth gluon, the singlet one of Eq. (1.15). As a consequence, such gluons would couple to *'white'* objects but the properties of such a theory would be completely different from what we observe in nature.

Theoretical mainstays and some open questions of QCD

From the theoretical point of view the analytical proof of *renormalisability of gauge theories* [40] and that of *asymptotic freedom*[11] [41, 42] in the beginning of the 1970s was crucial for establishing of QCD as the theory of the strong interaction. In the following we briefly discuss these features.

Calculations of internal *loops* of Feynman diagrams yield divergent results. In order to obtain a useful theory one first has to eliminate these divergences by the method of *renormalization*, according to which infinite *'bare'* quantities such as masses and coupling constants lead to *'finite'* and physical masses and coupling constants. If this procedure is realizable then the corresponding theory, like QCD, is renormalizable. This requirement is essential for a fundamental theory of nature.

The coupling *'constant'* of QCD, which is defined analogously to the *fine-structure constant* of QED,

$$\alpha_s = \frac{g_s^2}{4\pi}\,, \tag{1.18}$$

is actually *not* a constant but a function of an *energy scale*[12] Q as proven in a variety of measurements [11], see Figure 1.6. According to that the coupling (1.18) decreases with increasing energy where finally in the limit

$$Q \to \infty \Rightarrow \alpha_s(Q) \to 0 \tag{1.19}$$

asymptotic freedom emerges. This means that very energetic quarks interact softly with each other. Hence, the application of *perturbative methods* in order to study the *high-energy region* is a useful approach.

[11] This is a feature only of non-abelian theories.

[12] This corresponds to the squared four-momentum transfer Q^2, see e.g. Refs. [14, 16].

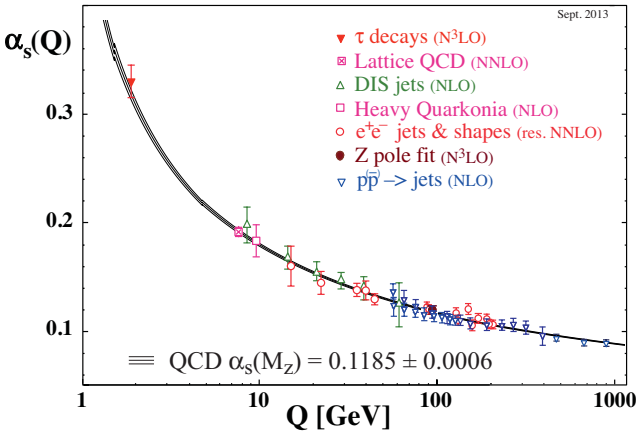

Figure 1.6: Summary of measurements of α_s as a function of the energy scale Q. This figure is taken from Ref. [11].

When the momentum transfer or the energy scale decreases, the strength of the coupling $\alpha_s(Q)$ increases, where its *new world average value* is given in Figure 1.6 which implies

$$g_s(M_Z) \approx 1.49\,, \tag{1.20}$$

where $M_Z = (91.1876 \pm 0.002)$ GeV is the mass of the Z^0 gauge boson of the weak interaction [11]. Thus, using *perturbation theory* in that energy region fails and the phenomenon of confinement emerges, whose analytical proof within the QCD does not yet exist. Due to the confinement and the fact that gluons interact strongly with each other the existence of colorless states composed of gluons, the glueballs, is expected. Unfortunately, their unambiguous experimental verification, just as full understanding of their nature, is up to now not completed. Namely, the exact determination of these glueballs would require an exact solution in $(3+1)$ dimensions of the *pure Yang-Mills* part of the *QCD Lagrangian*

$$\mathcal{L}_{QCD} = \sum_{f=1}^{N_f} \bar{q}_f (i\gamma^\mu D_\mu - m_f) q_f - \frac{1}{4} G^a_{\mu\nu} G^{\mu\nu}_a \tag{1.21}$$

which is still not available. The key problem is the non-linearity of the Yang-Mills equations. Still, *effective models* and *lattice QCD* are a way out, see the discussion later on.

Approaches of low-energy QCD

In order to study glueballs and the confined region of QCD, respectively, a variety of *effective quantum field theories* were developed. They are based on the QCD Lagrangian, where the realization of its symmetries is central, see e.g. Refs. [43, 44, 45, 46, 47, 48, 49] and references therein. In this work we follow such an approach, therefore we will introduce and discuss in detail our effective model in chapter 2. Now we present two applications of non-perturbative QCD which will be relevant and useful for our future construction of an effective model. These non-perturbative methods are the so-called *large-N_c expansion* and lattice QCD.

Large-N_c limit In connection to effective models, a further useful tool is the large-N_c expansion of QCD, where the limit of an infinite number of colors, $N_c \to \infty$, is used [50, 51]. Indeed, it is neither possible to solve QCD nor to fully understand confinement by using the large-N_c expansion, but still many calculations within effective models simplify. Therefore we outline the scaling properties of some quantities in the large-N_c limit, which are essential for our research and considerations with respect to our model [18].

An important feature in the limit $N_c \to \infty$ is that the masses of $\bar{q}q$ mesons as well as of glueballs are constant and hence they scale as

$$m_{\bar{q}q} \propto N_c^0 \,, \;\; m_G \propto N_c^0 \,. \tag{1.22}$$

When $n \geq 2$ ordinary mesons interact with each other, then the corresponding amplitude behaves as follows

$$\mathcal{A}_{\bar{q}q} \propto N_c^{-\frac{n-2}{2}} \,. \tag{1.23}$$

Thus, this amplitude decreases when the number of colors N_c increases. An important example for Eq. (1.23) is for $n = 3$, which corresponds to a two-body decay process $\bar{q}q \to 2\bar{q}q$, where

$$\mathcal{A}_{\bar{q}q \to 2\bar{q}q} \propto N_c^{-\frac{1}{2}} \,. \tag{1.24}$$

This implies that the corresponding decay width scales as

$$\Gamma_{\bar{q}q \to 2\bar{q}q} \propto \left|\mathcal{A}_{\bar{q}q \to 2\bar{q}q}\right|^2 \propto N_c^{-1} \,. \tag{1.25}$$

In case of $n \geq 2$ interacting glueballs the scaling of the amplitude reads

$$\mathcal{A}_G \propto N_c^{-(n-2)} \,. \tag{1.26}$$

An amplitude for n ordinary mesons, which interact with m glueballs, scales for $n \geq 1$ and $m \geq 1$ as

$$\mathcal{A}_{\bar{q}qG} \propto N_c^{-\left(\frac{n}{2}+m-1\right)} \,. \tag{1.27}$$

An important example in this case is when $m = 1$ and $n = 2$. This corresponds to the decay of a glueball into two ordinary mesons

$$\mathcal{A}_{G \to 2\bar{q}q} \propto N_c^{-1} \Rightarrow \Gamma_{G \to 2\bar{q}q} \propto \left|\mathcal{A}_{G \to 2\bar{q}q}\right|^2 \propto N_c^{-2} \,. \tag{1.28}$$

In comparison with Eq. (1.25) one sees that the decays of glueballs are stronger suppressed than decays of ordinary mesons. A further interesting case is when $n = m = 1$, which yields

$$\mathcal{A}_{\bar{q}qG} \propto N_c^{-\frac{1}{2}} \tag{1.29}$$

and corresponds to a mixing between an ordinary meson and a glueball which is large-N_c suppressed.

Lattice QCD Another very important method is lattice QCD where enormous efforts have been made in order to solve QCD numerically[13]. One uses a discretized lattice of points in *Euclidean space-time* with a spacing a in a four-dimensional space-time volume L_3T. The fermions are located on the sites of the lattice whereas the gauge fields correspond to the links between these sites. This idea which exactly preserves gauge invariance goes back to Kenneth G. Wilson in 1974 [62]. In order to calculate masses of hadrons one uses the *two-point correlation function*

$$C(t) = \langle\Omega|\hat{\phi}^\dagger(t)\hat{\phi}(0)|\Omega\rangle \propto \int dU \int d\psi \int d\bar{\psi} \sum_{\vec{x}} \hat{\phi}^\dagger(t,\vec{x})\hat{\phi}(0,0)e^{-S_F(\beta)-S_G(\beta)} \,, \tag{1.30}$$

where $|\Omega\rangle$ is the *ground state* of QCD, the so-called *vacuum*, and $\hat{\phi}^\dagger$ as well as $\hat{\phi}$ are the *creation* and *annihilation operators*, respectively. U, ψ, and $\bar{\psi}$ are the gauge and fermion fields of the *path integral* whereas a statistical probability for their particular configuration is given by the *Boltzmann weight* $e^{-S_F(\beta)-S_G(\beta)}$, where $S_F(\beta)$ and $S_G(\beta)$ are the fermion and gauge *action*, respectively. The parameter β ist the *lattice coupling* which controls the *continuum limit*, $a \to 0$, and hence influences the spacing a.

Using this first-principles approach of QCD a full glueball spectrum on lattice was computed, originally in the *quenched* approximation, which means that the *sea quarks*[14] and the valence quarks become static. Nevertheless, *unquenched* simulations where quark-loop corrections are considered are also done, but the computational effort is obviously larger [57, 58]. In the end the glueball mass is extracted from the decay of the function (1.30)

$$C(t) \propto e^{-m_G t} \,, \tag{1.31}$$

where the corresponding operator creates or annihilates a glueball of mass m_G at time t. In the limit $t \to \infty$ this correlator falls exponentially where the rate of the fall-off corresponds to glueball mass [54].

1.2.2 Symmetries of the QCD Lagrangian

The QCD Lagrangian (1.21) possesses a variety of symmetries, some of which are broken in several ways. An effective model of QCD should reflect as many of its symmetries as possible which will be presented next by following Refs. [10, 12, 13, 15, 17, 18, 19].

Local $SU_c(3)$ color symmetry

As previously discussed the fundamental symmetry of QCD is the local $SU_c(3)$ color symmetry. Under this *continuous* symmetry the *quark spinor fields*[15] of the Lagrangian (1.21), here denoted

[13] In this work we use, and are guided by, the values of glueball masses obtained by lattice QCD [52, 53, 54, 55, 56, 57, 58]. Therefore we recapitulate its basic ideas by following Refs. [20, 53, 54, 59, 60]. We also refer to Ref. [61] and references therein.

[14] Sea quarks are virtual quark-antiquark pairs which arise from *vacuum fluctuations*.

[15] Due to the spin and the existence of antiquarks the components of Eq. (1.32) correspond to *complex four-spinors* in *Dirac-spinor space*.

as three-vectors in color space,

$$q_f = \begin{pmatrix} q_{f,r} \\ q_{f,g} \\ q_{f,b} \end{pmatrix} , \tag{1.32}$$

transform as follows

$$q_f \to q'_f = U(x) q_f = \exp\left[-i \sum_{a=1}^{N_c^2-1} \theta^a(x) T^a \right] q_f \ , \tag{1.33}$$

$$\bar{q}_f \to \bar{q}'_f = \bar{q}_f U^\dagger(x) = \bar{q}_f \exp\left[i \sum_{a=1}^{N_c^2-1} \theta^a(x) T^a \right] , \tag{1.34}$$

where $\bar{q}_f = q_f^\dagger \gamma^0$. The matrices $T^a = \frac{\lambda^a}{2}$ are the eight generators of the $SU(3)$ group, with $a = 1, \ldots, N_c^2 - 1 = 8$, where λ^a are the Gell-Mann matrices and $\theta^a(x)$ the corresponding local parameters. The *covariant derivative* of the QCD Lagrangian (1.21)

$$D_\mu = \partial_\mu - i g_s A_\mu \tag{1.35}$$

ensures the conservation of the local color symmetry, where g_s is the *'running'* coupling constant. The four-potential A_μ represents the eight gauge fields, the gluons, and reads

$$A_\mu(x) = \sum_{a=1}^{N_c^2-1} A_\mu^a(x) T^a \ . \tag{1.36}$$

It transforms under the local $SU_c(3)$ color symmetry as

$$A_\mu(x) \to A'_\mu(x) = U(x) \left[A_\mu(x) - \frac{i}{g_s} \partial_\mu \right] U^\dagger(x) \ . \tag{1.37}$$

The Lagrangian, which we call the Dirac part of the QCD Lagrangian (1.21),

$$\mathcal{L}_D = \sum_{f=1}^{N_f} \bar{q}_f (i \gamma^\mu D_\mu - m_f) q_f \ , \tag{1.38}$$

where m_f is a *diagonal* $N_f \times N_f$ *mass matrix* of the current quarks and γ^μ are the *gamma matrices*, describes the interaction of quarks via gluons. Since color symmetry is an exact symmetry of QCD, the gluons couple to every quark flavor with the same strength. This is the so-called *flavor blindness*.

The pure Yang-Mills part of the QCD Lagrangian (1.21) describes the selfcoupling of the gauge fields and reads explicitly

$$\begin{aligned} \mathcal{L}_{YM} &= -\frac{1}{4} G^a_{\mu\nu} G_a^{\mu\nu} \\ &= -\frac{1}{2} \partial_\mu A^a_\nu (\partial^\mu A_a^\nu - \partial^\nu A_a^\mu) - g_s f^{abc} \partial_\mu A^a_\nu A_b^\mu A_c^\nu \\ &\quad -\frac{g_s^2}{4} f^{abc} f^{ade} A^a_\mu A^b_\nu A^\mu_d A^\nu_e \ , \end{aligned} \tag{1.39}$$

where we see that only three- and four-gluon selfcoupling vertices emerge. Here we use the definition of the *gluon field strength tensor*

$$G^a_{\mu\nu} \equiv \partial_\mu A^a_\nu - \partial_\nu A^a_\mu + g_s f^{abc} A^b_\mu A^c_\nu \ , \tag{1.40}$$

where f^{abc} are the antisymmetric structure constants of the $SU(3)$ group. Hence, the last term of Eq. (1.40) is the difference to an *abelian* theory like QED with the relevant consequences of gauge-field selfcoupling. The gluon field strength tensor transforms under the local color symmetry as follows

$$G^a_{\mu\nu}T^a \to \left(G^a_{\mu\nu}T^a\right)' = U(x)G^a_{\mu\nu}T^aU^\dagger(x) \ . \tag{1.41}$$

The sum of the Lagrangians (1.38) and (1.39) yields the QCD Lagrangian

$$\mathcal{L}_{QCD} = \mathcal{L}_D + \mathcal{L}_{YM} \ . \tag{1.42}$$

Centre symmetry

The *discrete centre symmetry* Z_n belongs to a special unitary group and is therefore a part of the $SU_c(N_c)$ color symmetry

$$U = \exp\left(-i\sum_{a=1}^{N_c^2-1}\theta^aT^a\right) \ , \tag{1.43}$$

where θ^a are such that

$$Z_n = \exp\left(-\frac{2\pi n}{N_c}\mathbb{1}\right) \ , \ n = 0,1,2,...,N_c-1 \ . \tag{1.44}$$

The gauge fields and the quark spinor fields transform under the transformations of the centre symmetry as follows

$$A_\mu \to A'_\mu = Z_nA^\dagger_\mu Z_n = A_\mu \ , \tag{1.45}$$

$$q_f \to q'_f = Z_nq_f \ . \tag{1.46}$$

The Lagrangian of QCD is clearly invariant under this symmetry[16]. But if one considers phenomena at non-vanishing temperature then the Z_n symmetry is spontaneously broken above a critical temperature in the pure Yang-Mills sector of QCD. In that case the *deconfinement* takes place where the *Polyakov loop* is the corresponding order parameter, see e.g. Refs. [63, 64, 65, 66] for details.

Discrete symmetries C, P, and T

The QCD Lagrangian is separately invariant under the following discrete symmetries: *parity* P (inversion of the spatial coordinates), *charge conjugation* C (inversion of particle into antiparticle), and *time reversal* T. Clearly, QCD, as every QFT [67], is invariant under CPT transformations.

The quark spinor fields transform under parity as

$$q(t,\vec{x}) \to q'(t,\vec{x}) = \gamma^0q(t,-\vec{x}) \ , \tag{1.47}$$

$$\bar{q}(t,\vec{x}) \to \bar{q}'(t,\vec{x}) = \bar{q}(t,-\vec{x})\gamma^0 \tag{1.48}$$

[16] At non-vanishing temperature, due the presence of quarks, the centre symmetry is not exactly realized because the fermionic fields not fulfill antisymmetric boundary conditions.

and under charge conjugation as

$$q(x) \to q'(x) = \hat{C}\bar{q}(x)^T \,, \tag{1.49}$$

$$\bar{q}(x) \to \bar{q}'(x) = q(x)^T\hat{C} \,, \tag{1.50}$$

where the operator $\hat{C}$ reads

$$\hat{C} = -i\gamma^0\gamma^2 \,. \tag{1.51}$$

Note, the gamma matrices in Eq. (1.51) have to be in the Dirac representation.

Moreover, these symmetries are related to quantum numbers which characterize hadrons. Namely, the parity of a quark-antiquark meson can be obtained via

$$P = (-1)^{L+1} \tag{1.52}$$

and its charge conjugation quantum number through

$$C = (-1)^{L+S} \,, \tag{1.53}$$

where L is the *angular momentum* and S the spin of the $\bar{q}q$ system. Due to the fact that charge conjugation is only an exact symmetry for neutral states but not for charged ones, the so-called G *parity*, which combines parity with *isospin symmetry* (I) [11, 68], was introduced as:

$$G = (-1)^{L+S+I} \,. \tag{1.54}$$

Global chiral symmetry

The *global chiral symmetry* is a further continuous symmetry of QCD described by the unitary group

$$U_R(N_f) \times U_L(N_f) \,, \tag{1.55}$$

which is isomorphic to the group

$$U_V(N_f) \times U_A(N_f) \equiv SU_V(N_f) \times U_V(1) \times SU_A(N_f) \times U_A(1) \,. \tag{1.56}$$

This symmetry undergoes several breaking mechanisms which are of *explicit* as well as *spontaneous* type. In order to investigate the Dirac part of the QCD Lagrangian (1.21) with respect to this symmetry, we first use the *chiral projection operators* which are defined as follows

$$\hat{\mathcal{P}}_{R,L} = \frac{1}{2}\left(\mathbb{1} \pm \gamma^5\right) \,, \tag{1.57}$$

where

$$\gamma^5 = i\gamma^0\gamma^1\gamma^2\gamma^3 = \gamma_5 \,. \tag{1.58}$$

Thus, the quark spinor fields can be decomposed into right- and left-handed Dirac spinors

$$q_f = \left(\hat{\mathcal{P}}_R + \hat{\mathcal{P}}_L\right) q_f \equiv q_{f,R} + q_{f,L} \,, \tag{1.59}$$

$$\bar{q}_f = \bar{q}_f \left(\hat{\mathcal{P}}_L + \hat{\mathcal{P}}_R\right) \equiv \bar{q}_{f,R} + \bar{q}_{f,L} \,. \tag{1.60}$$

Using the *anticommutation relation* of the gamma matrices

$$\left\{\gamma^5, \gamma^\mu\right\} = 0 \tag{1.61}$$

and

$$\hat{\mathcal{P}}_{R,L}\gamma^\mu = \gamma^\mu \hat{\mathcal{P}}_{L,R} \tag{1.62}$$

we obtain for the Dirac part of the QCD-Lagrangian

$$\mathcal{L}_D = \sum_{f=1}^{N_f} \left(i\bar{q}_{f,R}\gamma^\mu D_\mu q_{f,R} + i\bar{q}_{f,L}\gamma^\mu D_\mu q_{f,L} - i\bar{q}_{f,R} m_f q_{f,L} - i\bar{q}_{f,L} m_f q_{f,R}\right) . \tag{1.63}$$

The global chiral transformations of the quark spinor fields in flavor space read

$$q_{f,R,L} \to q'_{f,R,L} = U_{R,L} q_{f,R,L} = \exp\left(-i \sum_{i=0}^{N_f^2-1} \theta^i_{R,L} T^i\right) q_{f,R,L} \ , \tag{1.64}$$

$$\bar{q}_{f,R,L} \to \bar{q}'_{f,R,L} = \bar{q}_{f,R,L} U^\dagger_{R,L} = \bar{q}_{f,R,L} \exp\left(i \sum_{i=0}^{N_f^2-1} \theta^i_{R,L} T^i\right) , \tag{1.65}$$

where $\theta^i_{R,L}$ are the parameters and T^i with

$$T^0 = \sqrt{\frac{1}{2N_f}} \mathbb{1}_{N_f} \tag{1.66}$$

the generators of the $U(N_f)$ group.

According to the *Noether theorem* [69], there are in the chiral limit and neglecting anomalies $2N_f^2$ conserved *currents*. These are the right-handed

$$R^\mu = V^\mu - A^\mu \ , \tag{1.67}$$

and the left-handed

$$L^\mu = V^\mu + A^\mu \ , \tag{1.68}$$

currents, respectively, which can be expressed as vector

$$V^\mu = \frac{R^\mu + L^\mu}{2} \tag{1.69}$$

and axial-vector currents

$$A^\mu = \frac{L^\mu - R^\mu}{2} \ . \tag{1.70}$$

The advantage of the latter representation is that V^μ and A^μ have a definite parity, 1 and −1, respectively. A direct calculation from the QCD Lagrangian yields [43]

$$V^\mu_0 = \bar{q}\gamma^\mu q \ , \tag{1.71}$$

$$V^\mu_i = \bar{q}\gamma^\mu T^i q \ , \tag{1.72}$$

$$A^\mu_0 = \bar{q}\gamma^\mu\gamma_5 q \ , \tag{1.73}$$

$$A_i^\mu = \bar{q}\gamma^\mu\gamma_5 T^i q \,, \tag{1.74}$$

with

$$\partial_\mu V_0^\mu = 0 \,, \tag{1.75}$$

$$\partial_\mu V_i^\mu = i\bar{q}\left[m_f, T^i\right] q \,, \tag{1.76}$$

$$\partial_\mu A_0^\mu = 2i\bar{q} m_f \gamma_5 q \,, \tag{1.77}$$

$$\partial_\mu A_i^\mu = i\bar{q}\left\{m_f, T^i\right\}\gamma_5 q \,. \tag{1.78}$$

Applying the parity transformations (1.47) and (1.48) to the vector and axial-vector currents (1.71)-(1.74) yields

$$V_0(t,\vec{x}) \to V_0'(t,\vec{x}) = V_0(t,-\vec{x}) \,, \tag{1.79}$$

$$V_i(t,\vec{x}) \to V_i'(t,\vec{x}) = -V_i(t,-\vec{x}) \tag{1.80}$$

and

$$A_0(t,\vec{x}) \to A_0'(t,\vec{x}) = -A_0(t,-\vec{x}) \,, \tag{1.81}$$

$$A_i(t,\vec{x}) \to A_i'(t,\vec{x}) = A_i(t,-\vec{x}) \,. \tag{1.82}$$

Explicit breaking of the global chiral symmetry The chiral symmetry is explicitly broken classically due to the non-vanishing quark masses as well as at the quantum level due to loop corrections. In the *chiral limit*, $m_f = 0$, the chiral symmetry is classically conserved. Thus, the Dirac part of the QCD Lagrangian (1.63) is invariant under the transformations (1.64) and (1.65), but if $m_f \neq 0$ then non-vanishing mass terms occur in the Lagrangian (1.63), which mix the right- and the left-handed quark spinor fields and explicitly break the chiral symmetry. In the case of degenerate quark masses, the so-called *flavor limit*,

$$m_u = m_d = ... = m_{N_f} \,, \tag{1.83}$$

the N_f^2 currents of the $U_A(N_f)$ symmetry are explicitly broken

$$U_R(N_f) \times U_L(N_f) \to U_V(N_f) \,, \tag{1.84}$$

see Eqs. (1.77) and (1.78). In the case when quark masses are not degenerate,

$$m_u \neq m_d \neq ... \neq m_{N_f} \,, \tag{1.85}$$

then also the $N_f^2 - 1$ currents of the $SU_V(N_f)$ symmetry are broken

$$U_R(N_f) \times U_L(N_f) \to U_V(1) \,, \tag{1.86}$$

where $U_V(1)$ corresponds to conservation of the baryon number, see Eqs. (1.75) and (1.76).

At the quantum level even in the chiral limit the chiral symmetry is explicitly broken to

$$U_R(N_f) \times U_L(N_f) \to U_V(N_f) \times SU_A(N_f) \,. \tag{1.87}$$

The reason is that after quantization the singlet of the axial current does not vanish

$$\partial_\mu A_0^\mu = 2i\bar{q} m_f \gamma_5 q - \frac{g_s^2 N_f}{32\pi^2} G_{\mu\nu}^a \tilde{G}_a^{\mu\nu} \neq 0 \,, \tag{1.88}$$

where

$$\tilde{G}_a^{\mu\nu} = \frac{1}{2}\epsilon^{\mu\nu\rho\sigma} G^a_{\rho\sigma} \tag{1.89}$$

is the *dual gluon field strength tensor*. This phenomenon, which is known as the *chiral* or $U_A(1)$ *anomaly*, was first seen in QED and is analogously realized in QCD [70]. In QFT anomalies play an important role. In general anomalies are symmetries of a classical Lagrangian that are broken at the quantum level [15].

The non-zero quark masses, see Table 1.1, originate from the so-called *Higgs mechanism*, which is named after Peter W. Higgs and describes a *spontaneous breaking of a gauge symmetry*[17] [71, 72, 73]. The corresponding part of the *Higgs Lagrangian* is given by

$$\mathcal{L}^{int}_{Higgs} = \lambda_f H \bar{\Psi}_f \Psi_f \ , \tag{1.90}$$

where H is the *scalar Higgs field* ($J^{PC} = 0^{++}$), Ψ_f a field of a quark flavor $f \in \{u, d, s, ..., N_f\}$ and λ_f the corresponding coupling constant. Since the Higgs field has the quantum numbers of vacuum it may condense. Hence, one *shifts* this field

$$H \to v + H \ , \tag{1.91}$$

where $v \equiv \langle H \rangle$ is the *vacuum expectation value* (vev) of the Higgs field H. Inserting the shift (1.91) into the Lagrangian (1.90) one obtains

$$\mathcal{L}^{int}_{Higgs} \to \lambda_f v \bar{\Psi}_f \Psi_f + \lambda_f H \bar{\Psi}_f \Psi_f \ , \tag{1.92}$$

where

$$m_f = \lambda_f v \tag{1.93}$$

is the current mass of the corresponding quark flavor.

The Higgs boson was discovered in 2012 at the *A Toroidal LHC ApparatuS* (ATLAS) and the *Compact Muon Solenoid* (CMS) experiment at the *Large Hadron Collider* (LHC) [74, 75]. It was the last missing particle of the SM[18] with a mass [11]

$$m_H = (125.7 \pm 0.4)\ \text{GeV} \ . \tag{1.94}$$

It should be stressed that the generation of the baryonic mass through the Higgs mechanism is only about $\lesssim 5\%$ and therefore negligible. The main contribution originates from the spontaneous breaking of the global chiral symmetry.

Spontaneous breaking of the global chiral symmetry Apart from the explicit breaking of the chiral symmetry in the vacuum of QCD, $|\Omega\rangle$, there is also the spontaneous breaking of chiral symmetry:

$$U_V(N_f) \times SU_A(N_f) \to U_V(N_f) \ , \tag{1.95}$$

[17] The Higgs mechanism also explains why the gauge bosons of the weak interaction, Z^0 and $W^\pm$, have a mass.

[18] It is interesting that the Higgs particle is the only scalar among the elementary particles of the SM. The search for the Higgs particle was the main reason for building the LHC.

see e.g. Refs. [76, 77, 78]. In this case the vacuum is only invariant under the transformations of the vector symmetry but is not left invariant by the axial-vector symmetry

$$\tilde{T}^a|\Omega\rangle \neq |\Omega\rangle \,, \tag{1.96}$$

where $\tilde{T}^a = \gamma_5 \frac{\tau^a}{2}$ is a generator of the axial-vector transformations which act on the QCD vacuum. This leads to a non-vanishing *quark* or *chiral condensate*

$$\langle \bar{q}q \rangle = \langle \bar{q}_R q_L + \bar{q}_L q_R \rangle \neq 0 \tag{1.97}$$

and according to the *Goldstone theorem* there arise $N_f^2 - 1$ massless states, the *Nambu-Goldstone bosons* [44, 45, 79]. Hence, the spontaneous breaking of the chiral symmetry explains some important features of the hadronic mass spectrum. For instance, the *pion*, which is a *pseudoscalar-isotriplet*

$$I^G(J^{PC}) = 1^-(0^{-+}) \tag{1.98}$$

corresponds to the Nambu-Goldstone bosons for $N_f = 2$. Indeed, the pion is not a massless state but possesses a mass of about 140 MeV [11]. However, this mass originates not from the Goldstone but from the Higgs sector. The pion field,

$$\vec{\pi} \equiv i\bar{q}\gamma_5 \vec{\tau} q \,, \tag{1.99}$$

transforms under the vector as well as axial-vector symmetry as follows

$$\vec{\pi} \to \vec{\pi}' = \vec{\pi} + \vec{\theta} \times \vec{\pi} \,, \tag{1.100}$$

$$\vec{\pi} \to \vec{\pi}' = \vec{\pi} + \vec{\theta}\sigma \,, \tag{1.101}$$

where

$$\sigma \equiv \bar{q}q \tag{1.102}$$

is a *scalar-isoscalar* field

$$I^G(J^{PC}) = 0^+(0^{++}) \,. \tag{1.103}$$

Hence, the pion field is invariant under the vector transformations, see Eq. (1.100), but not under the axial-vector transformations, because it transforms into the so-called *chiral partner* which is the sigma field, see Eq. (1.101). Thus, one would expect that both the pion and the sigma field have the same mass. Formerly, the chiral partner of the pion was identified with the resonance $f_0(500)$ [11] but at the present time many works show that the resonance $f_0(1370)$ [11] with a mass of

$$m_{f_0(1370)} = (1200 - 1500)\ \text{MeV} \tag{1.104}$$

is the chiral partner of the pion, see e.g. Refs. [1, 3, 19, 80, 81] and later on in this work. This large mass splitting between the pion and its chiral partner can only be explained by spontaneous but not by explicit breaking of the chiral symmetry. At a sufficiently large non-zero temperature restoration of the chiral symmetry takes place and the masses of the chiral partners become degenerate, see e.g. Refs. [82, 83].

Since the realization of the spontaneous breaking of the chiral symmetry is crucial in our hadronic model, we demonstrate this idea by using the simple classical ϕ^4-*theory* which can be found in many standard text books on QFT, e.g. [10].

The corresponding Lagrangian with a scalar field ϕ reads

$$\mathcal{L}_{\phi^4} = \frac{1}{2}\partial_\mu\phi\partial^\mu\phi + \mathcal{V}_{\phi^4}(\phi) \,, \tag{1.105}$$

where

$$\mathcal{V}_{\phi^4}(\phi) = \frac{1}{2}m^2\phi^2 + \frac{\lambda}{4!}\phi^4 \,. \tag{1.106}$$

This Lagrangian possesses a discrete Z_2 symmetry,

$$\phi \to \phi' = -\phi \,. \tag{1.107}$$

If $m^2 > 0$ and $\lambda > 0$ then only one minimum of the potential (1.106) at $\phi = \phi_0 = 0$ exists. In this case the ground state fulfills the Z_2 symmetry and possesses the same symmetry as the Lagrangian (1.105). However, when one requires $m^2 \overset{!}{<} 0$, then one finds two minima of the potential (1.106),

$$\phi_{1,2} = \pm\phi_0 = \pm\sqrt{-\frac{6m^2}{\lambda}} \,, \tag{1.108}$$

see Figure 1.7, where each one of them may correspond to the ground state of the physical system described by the ϕ^4-theory.

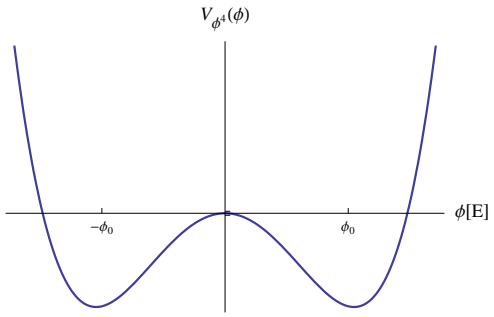

Figure 1.7: Potential of the ϕ^4-theory (1.106) for $m^2 < 0$ and $\lambda > 0$.

Now, the ground state is not any more symmetric under the Z_2 transformation (1.107) which indicates spontaneous symmetry breaking. Which of the two equivalent minima is the vev of the physical system is randomly chosen by the system itself. In order to study the physical excitations or fluctuations around the vacuum one has to shift the field

$$\phi \to \phi_0 + \phi \,. \tag{1.109}$$

Thus, the corresponding quadratic mass can be studied as well as additional three-point vertices, which originate from the spontaneous symmetry breaking.

Lorentz symmetry

An essential requirement for a fundamental theory like QCD is invariance under *Lorentz transformations*. These transformations correspond to three *rotations* as well as three *boosts* with six generators in total. The Lorentz transformations in Dirac-spinor representation read

$$S(\Lambda) = \exp\left(-\frac{i}{4}\omega_{\mu\nu}\sigma^{\mu\nu}\right) , \tag{1.110}$$

where $\omega_{\mu\nu} = -\omega_{\nu\mu}$ are the parameters of the Lorentz group and

$$\sigma^{\mu\nu} = \frac{1}{2}[\gamma^{\mu}, \gamma^{\nu}] \tag{1.111}$$

represent the corresponding generators. Accordingly, the quark spinor fields of the QCD Lagrangian (1.21) transform under Lorentz symmetry as follows:

$$q_f(x) \to q'_f(x') = S(\Lambda) q_f(\Lambda^{-1}x) , \tag{1.112}$$

$$\bar{q}_f(x) \to \bar{q}'_f(x') = \bar{q}_f(\Lambda^{-1}x) S(\Lambda)^{-1} . \tag{1.113}$$

Dilatation symmetry

We complete our considerations of the symmetries of QCD by discussing the *dilatation symmetry* which belongs to the *conformal group* under which the classical QCD Lagrangian with $m_f = 0$ is invariant [84, 85]. The conformal group has fifteen generators, where six of them are those of the Lorentz group, discussed previously. Furthermore, when translations of space-time are considered, four additional generators occur. These ten generators constitute the *Poincaré* or *inhomogeneous Lorentz group*. Finally, among the last five generators, four correspond to *special conformal* transformations and the last one to the dilatation symmetry.

The dilatation transformation reads

$$x^{\mu} \to x'^{\mu} = \lambda^{-1} x^{\mu} , \tag{1.114}$$

where λ^{-1} is a scale parameter which changes the scale of the Minkowski-space by affecting the metric, but without violating the conservation of length intervals and angles. The fields of an arbitrary Lagrangian transform as follows

$$\varphi_i(x) \to \varphi'_i(x) = \lambda^d \varphi_i(\lambda x) , \tag{1.115}$$

where d is the naive scaling dimension of the corresponding field and i indicates its components. Note that $\varphi'_i(x') = \lambda^d \varphi_i(\lambda\lambda^{-1}x) = \lambda^d \varphi_i(x)$. The quark spinor fields transform under dilation as

$$q_f \to q'_f = \lambda^{3/2} q_f \tag{1.116}$$

and the gauge fields of QCD as

$$A^a_{\mu} \to A'^a_{\mu} = \lambda A^a_{\mu} . \tag{1.117}$$

This implies that, at the classical level, where no loop corrections are taken into account, and in the chiral limit, $m_f = 0$, the QCD action is invariant under the transformations of the dilatation symmetry:

$$\begin{aligned} S'_{\mathcal{L}_{QCD}} &= \int d^4x' \mathcal{L}'_{QCD} = \int d^4x' \left(\bar{q}' i\gamma^\mu D'_\mu q' - \frac{1}{4} G'^a_{\mu\nu} G'^{\mu\nu}_a \right) \\ &= \int \lambda^{-4} d^4x \left(\lambda^{3/2} \bar{q} \lambda i\gamma^\mu D_\mu \lambda^{3/2} q - \frac{1}{4} \lambda^2 G^a_{\mu\nu} \lambda^2 G^{\mu\nu}_a \right) \\ &= \int d^4x \mathcal{L}_{QCD} = S_{\mathcal{L}_{QCD}} \ . \end{aligned} \tag{1.118}$$

This is evident because no dimensionful parameter occurs in Eq. (1.118). According to the Noether theorem a corresponding current

$$J^\mu_{YM} = x_\nu T^{\mu\nu}_{YM} \tag{1.119}$$

exists, where $T^{\mu\nu}_{YM}$ is the energy-momentum tensor of the pure Yang-Mills part of QCD Lagrangian

$$T^{\mu\nu}_{YM} = \frac{\partial \mathcal{L}_{YM}}{\partial(\partial_\mu A_\rho)} \partial^\nu A_\rho - g^{\mu\nu} \mathcal{L}_{YM} \ . \tag{1.120}$$

Provided that energy-momentum is conserved, $\partial_\mu T^{\mu\nu}_{YM} = 0$, one obtains in the case of dilatation invariance

$$\partial_\mu J^\mu_{YM} = T^\mu_{YM,\mu} = 0 \ . \tag{1.121}$$

Explicit breaking of the dilatation symmetry The dilatation symmetry is explicitly broken in two ways. Firstly, due to the non-vanishing current quark masses

$$T^\mu_\mu = \sum_{f=1}^{N_f} m_f \bar{q} q \neq 0 \ , \tag{1.122}$$

but if only the light quark flavors are considered this breaking is small because the masses of these quarks are small compared to those of hadrons.

Nevertheless, the explicit breaking of dilatation symmetry by quantum effects is more significant. This phenomenon is called *trace* or *scale anomaly* which plays a fundamental role in QCD. Namely, in QCD one obtains

$$\partial_\mu J^\mu_{YM,dil} = T^\mu_{YM,\mu} = \frac{\beta(g_s)}{4g_s} G^a_{\mu\nu} G^{\mu\nu}_a \neq 0 \ , \tag{1.123}$$

where

$$\beta(g_s) = \mu \frac{\partial g_s}{\partial \mu} \ , \tag{1.124}$$

is the *β-function of the renormalization group* of QCD. A calculation at one-loop level yields

$$\beta(g_s) = -b g_s^3 = -\frac{11 N_c}{48\pi^2} g_s^3 \ , \tag{1.125}$$

whereas in full QCD with N_f flavors the constant b reads

$$b = \frac{11 N_c - 2 N_f}{48\pi^2} \ . \tag{1.126}$$

Thus, when quantum fluctuations are included and renormalization is carried out, the coupling constant of QCD g_s becomes a *'running'* (renormalized) one

$$g_s \to g_s(\mu) \,, \tag{1.127}$$

where μ is the energy-scale parameter[19]. The solution of Eq. (1.124) is given by

$$g_s^2(\mu) = \frac{g_0^2}{1 + 2bg_0^2 \ln \frac{\mu}{\mu_0}} \,. \tag{1.128}$$

In order to obtain an asymptotically free theory, in which the *'running'* coupling constant decreases by increasing the energy and vice versa, the following constraint must hold

$$b > 0 \Leftrightarrow N_f < \frac{11N_c}{2} \,, \tag{1.129}$$

which is the case in nature, where $N_f = 6$ and $N_c = 3$. This implies that in the *low-energy region* gluons as well as quarks couple strongly and are therefore confined in hadrons, which are invariant under the transformations of $SU_c(3)$-symmetry.

The pole of the *'running'* coupling (1.128) is given by

$$1 + 2bg_0^2 \ln \frac{\mu}{\mu_0} \stackrel{!}{=} 0 \Rightarrow \mu_L \equiv \Lambda_L = \Lambda_{YM} = \mu_0 e^{-\frac{1}{2bg_0^2}} \,, \tag{1.130}$$

which is called the *Landau pole* and can be interpreted in the following way. Due to the large value of the strong coupling constant in the low-energy region perturbative calculations are impossible [11], but this does not imply that the running coupling becomes infinite at the Landau pole, $g_s(\mu_L) \to \infty$. In fact, the β-function implies that at the scale $\mu \approx \Lambda_{YM}$ QCD becomes a strongly coupled theory where perturbative methods fail and Eq. (1.128) reads

$$g_s(\mu)^2 = \frac{1}{2b \ln \frac{\mu}{\Lambda_{YM}}} \,, \tag{1.131}$$

where Λ_{YM} is the Yang-Mills scale. Thus, the β-function induces an energy scale which in turn generates a dimension in QCD which originally was, at the classical level and in the chiral limit, dimensionless. This important phenomenon is called *dimensional transmutation*. Unfortunately, the value of Λ_{YM}, or of $\Lambda_{QCD} \gtrsim \Lambda_{YM}$, when quarks are taken into account, cannot be calculated theoretically, because g_0 in Eq. (1.130) for a fixed μ_0 is unknown. However, at a typical hadronic scale which corresponds approximately to the radius of a nucleon,

$$\Lambda_{QCD}^{-1} \simeq 1 \text{ fm} \,, \tag{1.132}$$

one obtains

$$\Lambda_{QCD} \simeq 200 \text{ MeV} \,. \tag{1.133}$$

For a more precise determinations we refer e.g. to Ref. [86]. As a consequence of the trace anomaly, the vev of the $T^{\mu}_{YM,\mu}$ (1.123) does not vanish and represents the so-called gluon condensate:

$$\left\langle T^{\mu}_{YM,\mu} \right\rangle = -\frac{11N_c}{48} \left\langle \frac{\alpha_s}{\pi} G^a_{\mu\nu} G^{\mu\nu}_a \right\rangle = -\frac{11N_c}{48} C^4 \neq 0 \,, \tag{1.134}$$

[19]The energy dependence of the strong coupling g_s is the only reason why the divergence of the scale current (1.123) does not vanish.

where

$$C^4 \simeq (330 - 600 \text{ MeV})^4 \, . \tag{1.135}$$

The numerical value (1.135) has been obtained through QCD sum rules (lower bound of the interval) [87, 88, 89, 90, 91, 92, 93, 94, 95] and lattice-QCD simulations (upper bound of the interval) [96, 97, 98, 99, 100, 101, 102, 103, 104, 105].

1.3 Glueballs

As already mentioned, glueballs, the bound states of gluons, are naturally expected in QCD due to the non-abelian nature of the theory. The gluons, which possess the quantum numbers

$$I(J^P) = 0(1^-) \, , \tag{1.136}$$

interact strongly with themselves and thus they can bind and form colorless states. The bare mass of gluons is $m_g = 0$ [11], but through the interaction of a gluon with the vacuum an effective mass emerges

$$m_g = 0 \rightarrow m_g^* \simeq (400 - 900) \text{ MeV} \, . \tag{1.137}$$

It is important to stress that the generation of this effective gluonic mass takes place without breaking the local symmetry, see Refs. [106, 107, 108] for technical details.
The effective gluonic mass should be interpreted as an energy scale which emerges upon non-perturbative physics. It is then responsible for the emergence of the masses of the glueballs as well. This is in analogy to the quark sector where the masses of the *constituent quarks*, for instance of the light ones,

$$m_{q_{uds}}^* \simeq (300 - 450) \text{ MeV} \, , \tag{1.138}$$

are considerable larger than their corresponding current masses, see Table 1.1. The existence of glueballs has been studied in the framework of the effective *bag model*[20] for QCD already four decades ago [110, 111, 112, 113, 114] and it has been further investigated in a variety of approaches [60, 115, 116, 117]. Numerical calculations in lattice QCD of the Yang-Mills sector of QCD also find a glueball spectrum with different quantum numbers, in which the scalar glueball is the lightest state, see Figure 1.8 [52, 53, 54, 55, 56, 57, 58].

An important feature of glueballs is that due to the *'democratic'* coupling of the gluons to all quark flavors, the glueball should be a flavor-blind object. Moreover, glueballs can mix with other mesonic states, most importantly with quarkonia ($\bar{q}q$), with the same quantum numbers. This makes an experimental verification of glueballs more complicated, because measurable physical resonances emerge as admixtures. The search for states which are predominantly glueballs represents an active experimental and theoretical area of research, see Refs. [60, 115, 116, 117] and references therein. The reason for these efforts is that a better understanding of the glueball properties would be an important step in the comprehension of the non-perturbative behavior of QCD. However, although up to now particular glueball candidates exist, some of which will

[20] This model is often called *M.I.T. bag model*, because it was first introduced at the *Massachusetts Institute of Technology*. For a detailed introduction we refer to Ref. [109].

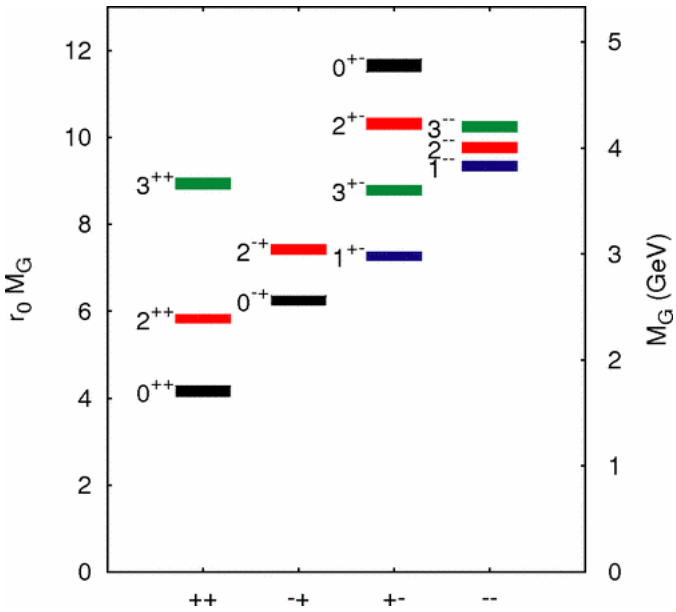

Figure 1.8: The mass spectrum of glueballs in the pure $SU_c(N_c = 3)$ gauge theory. The masses are given both in terms of the Sommer parameter r_0 (r_0^{-1} = 410 MeV) and GeV. The thickness of each colored box indicates the statistical uncertainty of the mass. This figure is taken from Ref. [55].

be discussed later on, no state which is predominantly and unambiguously a glueball has been identified.

In the following we will discuss some *gluon-rich* physical production processes, see Fig 1.9, in which the formation of glueballs as well as their detection is most probable [20, 60, 59, 118].

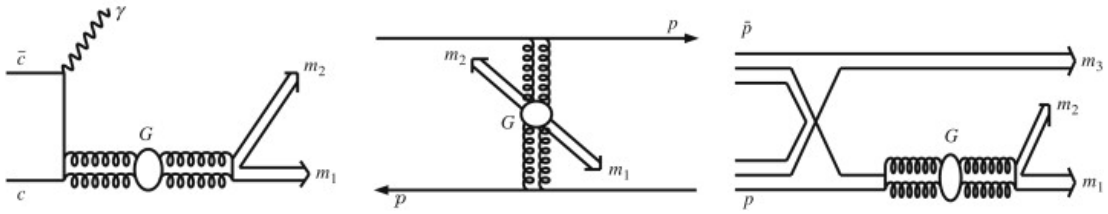

Figure 1.9: Feynman diagrams possibly leading to the formation of glueballs: (left) *radiative J/ψ decays*, (middle) *pomeron-pomeron scattering* in hadron-hadron *central collisions*, (right) $\bar{p}p$ annihilation. This figure is taken from Ref. [20].

- *Radiative decay of J/ψ*

  J/ψ, is a $\bar{c}c$ meson or a *charmonium*, which possesses the quantum numbers of the photon $J^{PC} = 1^{--}$, and is with a decay width of

$$\Gamma_{J/\psi} = 92.9 \pm 2.8 \text{ keV} \tag{1.139}$$

a very narrow resonance [11]. The reason is that the decay

$$J/\psi \to \bar{D}D \,, \tag{1.140}$$

which is actually favored, according to the *OZI rule*,[21] because D mesons contain a charm quark, is kinematically not allowed. Namely,

$$m_{J/\psi} = (3096.916 \pm 0.011) \text{ MeV} \,, \tag{1.141}$$

is below the threshold of the $\bar{D}D$ mesons [11]. In addition, the decay of J/ψ into mesons which are made of light quarks is OZI suppressed. Such decays proceed for instance via gluons which then convert into hadrons, but these kinds of decays are of high multiplicity and therefore difficult to detect. Another decay process of J/ψ is into a photon and two gluons. These gluons can form a glueball as an intermediate state, which in turn decays further into ordinary mesons. Moreover, the scalar and tensor glueballs cannot be part of three-gluon process. For this very reason the radiative decay of J/ψ is of prime importance for the search for glueballs. At the BESIII experiment huge data samples of such decays are studied [123].

- *Central collisions*

  A central collision is a scattering process of two high-energy hadrons, such as protons. In this process the hadrons lose energy via emission and exchange of gluons. Here a glueball can be formed, which then further decays into $\bar{q}q$ mesons.

- *$\bar{p}p$ annihilation*

  In experiments where protons and antiprotons annihilate, a gluon-rich environment emerges due to annihilation of quark and antiquark pairs into gluons. Hence glueballs can be directly formed or they can be produced together with other particles as intermediate states, which subsequently decay into ordinary mesons. The upcoming $\bar{\text{P}}$ANDA experiment will use an antiproton beam with energy range of 1.5 GeV to 15 GeV colliding with a proton target at rest [124, 125, 126, 127]. Thus, glueballs with masses of

  $$m_{glueball} = \sqrt{2m_p(m_p + E_{\bar{p}})} = 2.1 - 5.5 \text{ GeV} \tag{1.142}$$

  can be directly formed. Note that m_p is the mass of the proton or antiproton and $E_{\bar{p}} = \left(\sqrt{\vec{k}^2 + m_p^2}, \vec{k}\right)$ is the energy of the antiproton.

Here we discussed processes in which it is highly probable that glueballs can be produced. On the other side $\gamma\gamma$ *fusion* is a process, in which the production of glueballs should be strongly suppressed because of the fact that photons only couple to the intrinsic electric charge but not to the intrinsic color charge. Therefore it is not expected to see a substantial production of glueballs in $\gamma\gamma$ processes.

[21] The OZI rule, named after Susumu Okubo, George Zweig, and Jugoro Iizuka, means that competing processes, in which exchange of gluons is required, are suppressed, contrary to those in which the quark lines are not interrupted, see Refs. [27, 119, 120, 121, 122].

Scalar glueball

According to the *Particle Data Group* (PDG) in the scalar-isoscalar sector,

$$I^G\left(J^{PC}\right) = 0^+\left(0^{++}\right) \ ,$$

there are currently five resonances in the low-energy region (below 2 GeV) which we report in Table 1.2.

Resonance	**Mass [MeV]**	**Decay Width [MeV]**
$f_0(500)$	$400 - 550$	$400 - 700$
$f_0(980)$	990 ± 20	$40 - 100$
$f_0(1370)$	$1200 - 1500$	$200 - 500$
$f_0(1500)$	1505 ± 6	109 ± 7
$f_0(1710)$	1522^{+6}_{-5}	135 ± 7

Table 1.2: Masses and decay widths of the f_0 resonances [11].

It is natural to expect that one of these scalar-isoscalar resonances is the ground state of the glueball spectrum obtained by lattice QCD, the scalar glueball. However, there are two important and quite general aspects of the physics of the scalar glueball, which need to be discussed separately.

- *Is the scalar glueball broad or narrow?*

  This question is extremely important for the *phenomenology* and the assignment of the scalar glueball to an existing resonance. Yet, conflicting arguments exist:

  (i) In the large-N_c limit the glueball is predicted to be narrow. Namely, the decay of a bare glueball into two $\bar{q}q$ mesons, e.g., $G \to \pi\pi$, scales as N_c^{-2}. For comparison, the decay of a quark-antiquark state into two quark-antiquark states scales as N_c^{-1}. Since the large-N_c limit is phenomenologically successful, the quite narrow resonances $f_0(1500)$ and $f_0(1710)$ are candidates for being a scalar glueball.

  (ii) In Ref. [128] it is shown that the decay $G \to \pi\pi$ depends on the vev G_0 of the *dilaton field* as G_0^{-2}. The values of G_0 can be related to the gluon condensate of QCD by assuming that the trace anomaly is saturated by the dilaton field. Using the values of the gluon condensate from either *QCD sum rules* or lattice-QCD calculations, it turns out that the width of the decay $G \to \pi\pi$ is *very* large

  $$\Gamma_{G\to\pi\pi} \gtrsim 500 \text{ MeV} \ .$$

  The authors of Ref. [128] conclude that the search for the scalar glueball may be very difficult (if not impossible) if this state is too broad. Note that a wide glueball was also discussed in Refs. [60, 129, 130, 131, 132].

- *Assuming that the scalar glueball is narrow, is $f_0(1500)$ or $f_0(1710)$ mostly gluonic?*

  A consensus has grown that the light scalar mesons $f_0(500)$, $f_0(980)$, $a_0(980)$, $K_0^*(800)$ are *not* quark-antiquark states. The possible assignments are tetraquark or molecular states [133, 134, 135, 136, 137, 138, 139, 140, 141, 142, 143, 144, 145, 146, 147]. As a consequence, the scalar quark-antiquark states are located above 1 GeV: $a_0(1450)$ and $K_0^*(1430)$ represent the isovector and isodoublet $\bar{q}q$ states with $J^{PC} = 0^{++}$. This picture has been confirmed in Refs.[1, 148, 80, 81]. In particular, in Ref. [81] a fit to a variety of experimental data has shown that the scalar states lie between 1 and 2 GeV. Then, if the glueball is a narrow state, the main question is which of the two resonances $f_0(1500)$ and $f_0(1710)$ contains the largest gluonic amount.

Glueballs with other quantum numbers

The second lightest lattice-predicted glueball state has tensor quantum numbers ($J^{PC} = 2^{++}$) and a mass of about 2.2 GeV. A good candidate could be the very narrow resonance $f_J(2200)$ [149, 150], if the total spin of the latter will be experimentally confirmed to be $J = 2$.

The third least massive glueball predicted by lattice QCD has pseudoscalar quantum numbers ($J^{PC} = 0^{-+}$) and a mass of about 2.6 GeV. Quite remarkably, most theoretical works investigating the pseudoscalar glueball did not take into account this prediction of Yang-Mills lattice studies, but concentrated their search around 1.5 GeV in connection with the isoscalar-pseudoscalar resonances $\eta(1295), \eta(1405)$, and $\eta(1475)$. A candidate for a predominantly light pseudoscalar glueball is the middle-lying state $\eta(1405)$ due to the fact that it is largely produced in (gluon-rich) J/ψ radiative decays and is missing in $\gamma\gamma$ reactions [151, 152, 153, 154, 155, 156]. In this framework the resonances $\eta(1295)$ and $\eta(1475)$ represent radial excitations of the resonances η and η'. Indeed, in relation to η and η', a lot of work has been done in determining the gluonic amount of their wave functions. The KLOE Collaboration found that the pseudoscalar glueball fraction in the mixing of the pseudoscalar-isoscalar states η and η' can be large ($\sim 14\%$) [157], but the theoretical work of Ref. [158] found that the glueball amount in η and η' is compatible with zero, see however, also Ref. [159].

A further very interesting glueball state is the vector glueball ($J^{PC} = 1^{--}$) [160, 161, 162, 163, 164, 165, 166] with a mass of about 3.8 GeV, as lattice-QCD simulations suggest, see Ref. [55] and Figure 1.8. This glueball was first studied with respect to the so-called $\rho\pi, K^*\bar{K}$ *puzzle* [167, 168]. Otherwise, it is expected that the vector glueball is a *'clean'* state with a small admixture of $\bar{q}q$. The arguments therefore are on the one hand its structure and on the other hand its large mass. The 1^{--} glueball is composed of three gluons and hence a conversion into a quark-antiquark configuration should be difficult. Therefore one expects that this glueball is narrow as well as that its mixing with ordinary mesons is small. Contrary to the scalar glueball which is hidden among the f_0 resonances, see Table 1.2, the identification of the pseudoscalar as well as the vector glueball should be less complicated, for instance by the upcoming $\bar{\text{P}}$ANDA experiment [124, 125, 126] or *GLUonic EXcitations* (GlueX) experiment of the *Jefferson national LABoratory* (JLAB) [169].

1.4 Motivation

As previously discussed, in recent decades substantial progress in the field of strong interaction has been achieved. Nevertheless, there are still open questions, some of which we address in this work. Therefore, we repeat the relevant ones in order to outline our objectives and beyond that we give a brief idea of our approach.

1.4.1 Objectives

- The understanding of the scalar sector in the low-energy region is one of the challenges of hadronic physics. The assignment of the states of the 0^{++} nonet to the physical resonances is still not finalized. Due to the overpopulation in the scalar-isoscalar sector, see Table 1.2, a natural question is whether if one of them is predominantly the glueball. The resonances $f_0(1500)$ and $f_0(1710)$ seem to be good candidates. In order to figure out which of them has the largest gluonic content, one has to determine the *mixing matrix*.

- The search for the scalar glueball has been, and still is, in the center of vivid activity of low-energy QCD because of its importance regarding a basic phenomenon of QCD: the anomalous breaking of dilatation invariance, which is associated with the generation of the gluon condensate. Insights into the latter one can be useful to answer the question how large is the contribution of the gluon condensate in generating the meson masses.

- The existence of glueballs is a clear prediction of QCD. Due to the strong mixing in the scalar-isoscalar sector the identification of the ground-state glueball is still more complicated. Therefore, a study of glueballs with other quantum numbers, as predicted by lattice QCD, is very promising because one expects a smaller mixing with quark-antiquark mesons.

1.4.2 Approach

In the following we clarify which methods our approach is based on and what kind of input we use. We treat the addressed physical issues phenomenologically by computing physical quantities, in particular masses and decay widths, which we then compare with experimental data or we make predictions for upcoming experiments, in order to test our effective hadronic model. A general feature of such models is that one has to determine a set of free *unknown* parameters. A usual method is the χ^2 *analysis* [11] which we made use of. In addition, we present some of our results as branching ratios. This is a common procedure, because some parameters cancel when taking the ratio of two quantities.

The χ^2 function

The function of the χ^2 method reads

$$\chi^2 \equiv \chi^2(x_i) = \sum_{j=1}^{n} \left(\frac{Q_j^{th}(x_i) - Q_j^{ex}}{\Delta Q_j^{ex}} \right)^2 , \tag{1.143}$$

where Q_j^{ex} are experimental quantities, such as masses and decay widths, which have the experimental errors ΔQ_j^{ex} and $Q_j^{th}(x_i)$ are the corresponding theoretical expressions which depend on

the parameters, x_i with $i = 1...n$, of the model. After minimizing the function (1.143) we obtain a set of parameters of the model which validity is given to the value of χ^2. As an additional indicator for the reasonability of the results we make use of large-N_c arguments, according to which some parameters must be smaller than others. As an input for the χ^2 procedure we use experimental masses and decay widths of resonances listed in the PDG [11].

Branching ratios

For calculations of branching ratios where χ^2 analysis was not necessary we use as input results from the glueball mass spectrum obtained by lattice-QCD simulations in quenched approximation (e.g. neglecting quarks) [52, 53, 54, 55] and PDG data as well.

We perform our phenomenological study in vacuum, i.e., at vanishing *temperature* ($T = 0$) and *chemical potential* ($\mu = 0$), as well as at *tree level*, i.e., our calculations are done without loop corrections. The computations are performed with *Mathematica*. In the following we show the formulas which are used in this work for calculating both two- and three-body decay processes.

Formula for two-body decays

For the computation of *two-body decays*, $P \to P_1 P_2$, we use the well-known formula

$$\Gamma_{P\to P_1P_2} = s_f \mathcal{I} \frac{k_f}{8\pi M^2} \left| -i\mathcal{A}_{P\to P_1P_2} \right|^2 \ , \tag{1.144}$$

where

$$k_f = \frac{1}{2M} \sqrt{M^4 + (m_1^2 - m_2^2)^2 - 2M^2(m_1^2 + m_2^2)}\, \theta(M - m_1 - m_2) \tag{1.145}$$

is the modulus of the three-momentum of one of the outgoing particles (the moduli of the momenta are equal in the rest frame of the decaying particle). Moreover, M is the mass of the decaying particle P and m_1 and m_2 refer to the masses of the particles P_1 and P_2. $\mathcal{A}_{P\to P_1P_2}$ is the decay amplitude. The symmetrization factor s_f avoids double counting of identical Feynman diagrams and $\mathcal{I}$ is the isospin factor which considers all subchannels of a particular decay channel. The θ function encodes the decay threshold. Additionally, for decay processes which are on the energy threshold we perform an integration over a corresponding *spectral function* [170]. This function reads

$$d_P(X_M) = \mathcal{N} \frac{X_M^2 \Gamma_{P\to P_1P_2}(X_M)}{(X_M^2 - M^2)^2 + X_M^2 \Gamma^2_{P\to P_1P_2}(X_M)} \theta(X_M - m_1 - m_2) \ , \tag{1.146}$$

where X_M is the *'running'* mass of particle P and $\mathcal{N}$ is a normalization constant which ensures the conservation of probability

$$\int_0^\infty d_P(X_{m_P}) dX_{m_P} = 1 \ . \tag{1.147}$$

Formula for three-body decays

In case of *three-body decays*, $P \to P_1 P_2 P_3$, we use for our calculations the well-known formula

$$\Gamma_{P\to P_1P_2P_3} = \frac{s_f}{(2\pi)^3 32 M^3} \int_{(m_1+m_2)^2}^{(M-m_3)^2} dm_{12}^2 \int_{(m_{23})_{\min}}^{(m_{23})_{\max}} |-i\mathcal{A}_{P\to P_1P_2P_3}|^2 dm_{23}^2 \ , \tag{1.148}$$

where

$$(m_{23})_{\min} = (E_2^* + E_3^*)^2 - \left(\sqrt{E_2^{*2} - m_2^2} + \sqrt{E_3^{*2} - m_3^2}\right)^2 \ , \tag{1.149}$$

$$(m_{23})_{\max} = (E_2^* + E_3^*)^2 - \left(\sqrt{E_2^{*2} - m_2^2} - \sqrt{E_3^{*2} - m_3^2}\right)^2 \ , \tag{1.150}$$

and

$$E_2^* = \frac{m_{12}^2 - m_1^2 + m_2^2}{2m_{12}} \ , \ E_3^* = \frac{M^2 - m_{12}^2 - m_3^2}{2m_{12}} \ . \tag{1.151}$$

The quantities m_1, m_2, m_3 refer to the masses of the particles P_1, P_2, and P_3, $\mathcal{A}_{P\to P_1P_2P_3}$ is the decay amplitude, and s_f is a symmetrization factor. This factor equals 1 if P_1, P_2, and P_3 belong to different particles. In case of two identical particles in the final state the symmetrization factor equals 2 and for three identical particles in the final state we have $s_f = 6$.

More details and a derivation of these formulas can be found in many standard text books on particle physics, scientific works, as well as lectures, e.g. Refs. [11, 17, 19, 68, 171, 172].

Chapter 2

A Hadronic Model: The eLSM

This chapter aims to introduce an effective hadronic model of QCD in order to study physical issues of hadron spectroscopy in the mesonic sector, which we discussed in the previous chapter. This model is called *extended Linear Sigma Model* (eLSM) and was developed in Refs. [1, 2, 3, 4, 5, 6, 7, 8, 9, 17, 18, 19, 80, 81, 148, 166]. Following these references we will present and discuss the eLSM in detail in order to achieve a deep understanding of this model, which will then be used to study the physical properties of mesons.

2.1 Properties of the eLSM

2.1.1 General remarks

Let us start with a general question:

Why are hadronic models like the eLSM needed at all?

As mentioned in chapter 1 at present an exact analytical solution of QCD in $(3+1)$ dimensions does not exist. Furthermore, the *degrees of freedom* (d.o.f.) of the QCD Lagrangian are quarks and gluons but due to confinement we directly observe only free hadrons in experiments. Moreover, in the low-energy region of QCD the *'running'* coupling constant $g_s(\mu)$ becomes large and therefore the application of perturbative methods is not possible. For this reasons effective models with hadrons as d.o.f. are developed. In order to construct an effective hadronic model the following question arises immediately:

What kind of hadrons should be implemented into the effective Lagrangian?

Unfortunately, at the present time this question cannot be answered for sure but as discussed in Ref. [18] the large-N_c limit yields some indications. Namely, for $N_c \gg 1$, in the low-energy domain only free quark-antiquark and glueball mesons exist, whereas their interactions vanish. Baryons are not present because their mass increases with N_c,

$$m_{qqq} \propto N_c \,, \tag{2.1}$$

and tetraquarks may also disappear for $N_c \to \infty$, see however Ref. [173]. In the case $N_c = 3$ the interaction between $\bar{q}q$ mesons and glueballs takes place. Studying the low-energy region of QCD up to the energy of 2 GeV the following hadrons should be taken into account:

- (Pseudo)scalar and (axial-)vector quark-antiquark mesons, with quantum numbers

$$J^{PC} : 0^{++}, 0^{-+}, 1^{--}, 1^{++} ,$$

- and a scalar glueball (0^{++}) which is the lightest state of the glueball spectrum predicted by lattice QCD [52, 53, 54, 55, 56, 57, 58] with a mass of

$$m_G^{lat} \approx (1.5 - 1.7) \text{ GeV} .$$

Hence, we are looking for an effective hadronic Lagrangian which cannot be directly derived from the QCD Lagrangian due to the fact that the quarks and gluons are perturbative fields in contrast to hadrons which are non-perturbative objects. This implies the question:

Which properties should an effective hadronic model possess?

In general an effective model of QCD should be less complicated, in the sense of solvability, than QCD itself. This makes possible a verification of such a model by using experimental data and predictions for upcoming experiments can be done. In turn, the resulting insights can be useful for a better understanding of some aspects of QCD in the low-energy region.

The most crucial ingredients of an effective hadronic model are the symmetries of the QCD Lagrangian, thus the corresponding effective Lagrangian should reflect as many of the QCD symmetries as possible. The more symmetries we take into account the more constraints we can exploit by constructing the terms of the effective hadronic Lagrangian. In principle an infinite number of terms can be constructed, but this would make numerical calculations extremely difficult. In this respect it is very useful to consider the dilatation symmetry because it simplifies this issue yielding a finite number of terms. Every term which enters into the model is proportional to a free parameter, a so-called *effective coupling constant*. In order to obtain a particular solution of the hadronic model one has to determine these couplings, usually by fixing them to experimental data. However, this procedure turns out to be not always trivial. The emergence of the numerous effective couplings is the *'prize'* one has to pay for such phenomenological models.

The energy range of validity of QCD goes from zero up to the *Planck scale* (10^{19} GeV). Contrary to the fundamental QCD, the range of validity of the effective hadronic model is automatically given by the heaviest resonance which is incorporated into the model. In addition, QCD is a renormalizable theory. These requirement is inevitable for a fundamental quantum field theory but is not essential for an effective theory.

2.1.2 Symmetries of the eLSM

The d.o.f. of the eLSM studied in this work are mesons in the (pseudo)scalar as well as the (axial-)vector sector. We are interested in the phenomenology in vacuum ($T = \mu = 0$) and at tree level.

This effective Lagrangian is built in agreement with the symmetries of the QCD Lagrangian, which we discussed in chapter 1. In order to emphasize the significance of these symmetries for our model we summarize them again in the following:

- *Local $SU_c(3)$ color symmetry:* This is the fundamental symmetry of QCD, which is in the eLSM, as in each purely hadronic model, trivially fulfilled due to the fact that the eLSM contains only *'white'* states as d.o.f. .

- *Lorentz symmetry:* This is a fundamental symmetry of any quantum field theory and thus the Lagrangian of the eLSM is a *Lorentz scalar*.

- *Discrete symmetries C, P, and T:* The invariance under the simultaneous transformations of charge conjugation C, parity P and time reversal T (CPT) is a fundamental feature of quantum field theories and must be fulfilled in every hadronic model [67]. Furthermore, our hadronic Lagrangian is invariant under C, P, and T separately, in agreement with QCD.

- *Global chiral symmetry and its breakings:* This symmetry and its breakings dictate the dynamics at the hadronic level and are therefore crucial for the eLSM. The spontaneous breaking of the chiral symmetry leads to the non-vanishing quark condensate and is of primary importance.

- *Dilatation symmetry and trace anomaly:* This symmetry is crucial for a variety of reasons:

  (i) As mentioned previously, this symmetry ensures a finite number of terms in the Lagrangian of the eLSM.

  (ii) The trace anomaly of the pure Yang-Mills sector of QCD leads to a non-vanishing gluon condensate and generates via dimensional transmutation the low-energy scale $\Lambda_{QCD} \approx \Lambda_{YM}$. In the eLSM this scale corresponds to Λ_{dil} (see later on), which is in the chiral limit the only dimensionful parameter of the model.

  (iii) Introducing dilatation symmetry into the eLSM yields an additional scalar degree of freedom, the dilaton field G. This field can be interpreted as a scalar glueball, hence its mixing with scalar-isoscalar quarkonia can be studied.

2.2 The pure Yang-Mills sector of QCD

An effective theory which correctly mimics the pure Yang-Mills

$$\mathcal{L}_{YM} = -\frac{1}{4} G^a_{\mu\nu} G^{\mu\nu}_a \tag{2.2}$$

part of QCD at the quantum as well as at the confined level should contain at least a scalar field G. This field is namely linked to the gluonic field as

$$G^4 \propto G^a_{\mu\nu} G^{\mu\nu}_a \ . \tag{2.3}$$

The field G, which describes the collective field of gluons, should be embedded into a potential that generates the trace anomaly in order to induce a dimension into the effective hadronic model. The Lagrangian

$$\mathcal{L}_{dil} = \frac{1}{2}(\partial^\mu G)^2 - \mathcal{V}_{dil}(G) \,, \tag{2.4}$$

where

$$\mathcal{V}_{dil}(G) = \frac{1}{4}\frac{m_G^2}{\Lambda_{dil}^2} G^4 \left(\ln\left|\frac{G}{\Lambda_{dil}}\right| - \frac{1}{4} \right) \,, \tag{2.5}$$

fulfill exactly these requirements as shown in Refs. [174, 175, 176, 177, 178, 179, 180]. The logarithmic term, where Λ_{dil} is the energy scale which corresponds to Λ_{YM}, breaks the dilatation symmetry explicitly, similar to the β-function of the renormalization group (1.123). Hence the divergence of the corresponding current

$$J_{dil}^\mu = x_\nu T_{dil}^{\mu\nu} \tag{2.6}$$

does not vanish

$$\partial_\mu J_{dil}^\mu = T_{dil,\mu}^\mu \neq 0 \,. \tag{2.7}$$

Divergence of the trace current

In the following we compute a divergence of the trace current, $J^\mu = x_\nu T^{\mu\nu}$, for a general potential $\mathcal{V}(\varphi)$ of a Lagrangian

$$\begin{aligned} \mathcal{L} &= \frac{1}{2}\partial_\sigma\varphi\partial^\sigma\varphi - \mathcal{V}(\varphi) \\ &\equiv -\frac{1}{2}\varphi\partial_\sigma\partial^\sigma\varphi - \mathcal{V}(\varphi) \,. \end{aligned} \tag{2.8}$$

The energy-momentum tensor reads

$$\begin{aligned} T^{\mu\nu} &= \frac{\partial\mathcal{L}}{\partial(\partial_\mu\varphi)}\partial^\nu\varphi - g^{\mu\nu}\mathcal{L} \\ &= \partial^\mu\varphi\partial^\nu\varphi - g^{\mu\nu}\mathcal{L} \\ &\equiv -\varphi\partial^\mu\partial^\nu\varphi - g^{\mu\nu}\mathcal{L} \,. \end{aligned} \tag{2.9}$$

Ergo, by using

$$\partial_\mu T^{\mu\nu} = 0 \,, \tag{2.10}$$

we obtain

$$\partial_\mu J^\mu = (\partial_\mu x_\nu)\, T^{\mu\nu} = T^{00} - T^{11} - T^{22} - T^{33} \,, \tag{2.11}$$

where

$$T^{00} = \left(\partial^0\varphi\right)^2 - \left[\frac{1}{2}\left(\partial_\mu\varphi\right)^2 - \mathcal{V}(\varphi)\right] \,, \tag{2.12}$$

$$T^{11} = \left(\partial^1\varphi\right)^2 + \left[\frac{1}{2}\left(\partial_\mu\varphi\right)^2 - \mathcal{V}(\varphi)\right] \,, \tag{2.13}$$

$$T^{22} = \left(\partial^2\varphi\right)^2 + \left[\frac{1}{2}\left(\partial_\mu\varphi\right)^2 - \mathcal{V}(\varphi)\right] \,, \tag{2.14}$$

$$T^{33} = \left(\partial^3\varphi\right)^2 + \left[\frac{1}{2}\left(\partial_\mu\varphi\right)^2 - \mathcal{V}(\varphi)\right] \,. \tag{2.15}$$

Then, we obtain

$$\begin{aligned}\partial_\mu J^\mu &= \left(\partial^0\varphi\right)^2 - \left(\partial^1\varphi\right)^2 - \left(\partial^2\varphi\right)^2 - \left(\partial^3\varphi\right)^2 - 2(\partial_\mu\varphi)^2 + 4\mathcal{V}(\varphi) \\ &= -(\partial_\mu\varphi)^2 + 4\mathcal{V}(\varphi) \end{aligned} \tag{2.16}$$

and finally

$$(\partial_\mu\varphi)^2 = \partial_\mu\left(\varphi\partial^\mu\varphi\right) - \varphi\,\Box\,\varphi\,. \tag{2.17}$$

By using the *equation of motion*

$$\frac{\partial\mathcal{L}}{\partial\varphi} = \partial_\mu\frac{\partial\mathcal{L}}{\partial(\partial_\mu\varphi)} \tag{2.18}$$

we obtain

$$\Box\,\varphi = -\frac{\partial\mathcal{V}(\varphi)}{\partial\varphi}\,. \tag{2.19}$$

Therefore, by putting the elements together we obtain

$$\partial_\mu J^\mu = -\partial_\mu\left(\varphi\partial^\mu\varphi\right) - \varphi\frac{\partial\mathcal{V}(\varphi)}{\partial\varphi} + 4\mathcal{V}\left(\varphi\right)\,. \tag{2.20}$$

By neglecting the total divergence we obtain the general expression

$$\partial_\mu J^\mu = T^\mu_\mu = 4\mathcal{V}(\varphi) - \varphi\partial_\varphi\mathcal{V}(\varphi)\,. \tag{2.21}$$

Divergence of the dilaton current

Applying the dilaton potential (2.5) to Eq. (2.21) we obtain the non-vanishing divergence of the dilaton current as

$$\partial_\mu J^\mu_{dil} = T^\mu_{dil,\mu} = -\frac{1}{4}\frac{m_G^2}{\Lambda_{dil}^2}G^4 \neq 0\,. \tag{2.22}$$

The ground state of the dilaton potential reads

$$\frac{d\mathcal{V}}{dG} = \frac{m_G^2}{\Lambda_{dil}^2}G^3\ln\left|\frac{G}{\Lambda_{dil}}\right| \stackrel{!}{=} 0 \Rightarrow G_0 = \Lambda_{dil}\,. \tag{2.23}$$

Note that in Eq. (2.23) no quark-antiquark fields are present. In the general case, when $\bar{q}q$ fields are taken into account, we will obtain $G_0 \gtrsim \Lambda_{dil}$, see below. Hence, the vev of the trace of the dilaton energy-momentum tensor reads

$$\left\langle T^\mu_{dil,\mu}\right\rangle = \left\langle -\frac{1}{4}\frac{m_G^2}{\Lambda_{dil}^2}G^4\right\rangle = -\frac{1}{4}\frac{m_G^2}{\Lambda_{dil}^2}G_0^4 = -\frac{1}{4}m_G^2\Lambda_{dil}^2. \tag{2.24}$$

Requiring that the dilaton field saturates the dilaton current, we equate the vev of the dilaton current (2.24) with the vev of the trace anomaly (1.134)

$$\left\langle T^\mu_{dil,\mu}\right\rangle \equiv \left\langle T^\mu_{YM,\mu}\right\rangle\,. \tag{2.25}$$

We obtain

$$\Lambda_{dil} = \frac{\sqrt{11}}{2m_G}C^2\,. \tag{2.26}$$

2.3 The quark-gluon sector of QCD

In this section we introduce the flavor multiplets of the quark-antiquark mesons and the corresponding terms which fulfil the symmetry properties that we discussed above.

2.3.1 Mesonic fields of the eLSM

Scalar and pseudoscalar $\bar{q}q$ mesons

First, we introduce the scalar and pseudoscalar quark-antiquark mesons by defining the matrix

$$\Phi_{ij} \equiv \sqrt{2}\bar{q}_{j,R}q_{i,L} \ , \tag{2.27}$$

where $i,j \in \{u,d,s,...,N_f\}$. It is important to stress that the matrix Φ is a non-perturbative object but the quark-antiquark pair $\bar{q}_{j,R}q_{i,L}$ is indeed a perturbative quantity. Using the equivalence sign we intend to express the following:

- Both quantities transform in the same way under the global chiral symmetry. This implies that, by considering of the transformation of the quarks (1.64) and (1.65), Φ transforms under the global chiral symmetry as follows

  $$\Phi \to \Phi' = U_L \Phi U_R^\dagger \ , \quad \Phi^\dagger \to \Phi'^\dagger = U_R \Phi^\dagger U_L^\dagger \ , \tag{2.28}$$

  where $\Phi^\dagger$ is the corresponding adjoint matrix.

- The perturbative bare quarks and antiquarks can be modified dynamically through the interaction with the gluons as well as quark-antiquark pairs of the vacuum to form a non-perturbative quark-antiquark current. The non-perturbative matrix elements of Φ can now be considered approximately as composed by this current. As pointed out in Refs. [18, 19] a non-trivial connection between the objects of Eq. (2.27) can be realized by expressing of Φ_{ij} as a non-local composition of $\sqrt{2}\bar{q}_{j,R}q_{i,L}$ via

  $$\Phi_{ij} \equiv \int d^4y \sqrt{2}\bar{q}_{j,R}(x+\frac{y}{2})q_{i,L}(x-\frac{y}{2})f(y) \ , \tag{2.29}$$

  where $f(y)$ is a non-perturbative vertex function. Setting $f(y) = \delta(y)$ yields the perturbative limes of Eq. (2.27).

Using the chiral projection operators (1.57) we can rewrite the elements of the matrix Φ as follows:

$$\begin{aligned} \Phi_{ij} &\equiv \sqrt{2}\bar{q}_{j,R}q_{i,L} = \sqrt{2}\bar{q}_j\hat{\mathcal{P}}_L\hat{\mathcal{P}}_L q_i = \sqrt{2}\bar{q}_j\hat{\mathcal{P}}_L q_i \\ &= \frac{1}{\sqrt{2}}\left(\bar{q}_j q_i - \bar{q}_j\gamma^5 q_i\right) = \frac{1}{\sqrt{2}}\left(\bar{q}_j q_i + i\bar{q}_j i\gamma^5 q_i\right) \ . \end{aligned} \tag{2.30}$$

The scalar and pseudoscalar currents are defined as:

$$S_{ij} \equiv \frac{1}{\sqrt{2}}\bar{q}_j q_i \ , \quad P_{ij} \equiv \frac{1}{\sqrt{2}}\bar{q}_j i\gamma^5 q_i \ . \tag{2.31}$$

In the end we obtain the chiral field as

$$\Phi = S + iP \ , \quad \Phi^\dagger = S - iP \ , \tag{2.32}$$

where S and P are hermitian matrices and therefore they can be expressed in terms of the generators t^a of the $U(N_f)$ group, where $a = 0, 1, ..., N_f^2 - 1$, and N_f is the number of flavors:

$$S = S^a t^a \ , \quad S^a \equiv \sqrt{2}\bar{q}t^a q \ , \tag{2.33}$$

and

$$P = P^a t^a \ , \quad P^a \equiv \sqrt{2}\bar{q}i\gamma^5 t^a q \ . \tag{2.34}$$

Now, we write down a Lagrangian[1] with (pseudo)scalar $\bar{q}q$ mesons, which is invariant under the global chiral transformations (2.28)

$$\mathcal{L}_\Phi = \mathrm{Tr}\left[(\partial^\mu \Phi)^\dagger (\partial^\mu \Phi)\right] - m_0^2 \mathrm{Tr}\left(\Phi^\dagger \Phi\right) - \lambda_1 \left[\mathrm{Tr}(\Phi^\dagger \Phi)\right]^2 - \lambda_2 \mathrm{Tr}[(\Phi^\dagger \Phi)^2] \ . \tag{2.35}$$

The invariance under chiral transformation can be easily shown by using the unitarity of the operator U,

$$U^\dagger U = U U^\dagger = 1 \Leftrightarrow U^\dagger = U^{-1} \ . \tag{2.36}$$

In addition, by considering the quark transformations under parity (1.47)-(1.48) and charge conjugation (1.64)-(1.65), the chiral field Φ transforms under these transformation as follows

$$\Phi(t, \vec{x}) \overset{P}{\to} \Phi'(t, \vec{x}) = \Phi^\dagger(t, -\vec{x}) \tag{2.37}$$

and

$$\Phi(x) \overset{C}{\to} \Phi'(x) = \Phi^T(x) \ . \tag{2.38}$$

Thus, the chiral Lagrangian (2.35) is also invariant under parity and charge conjugation transformations. By applying the transformations (1.114) and (1.115) one realizes that the Lagrangian (2.35) is, due to the mass term

$$- m_0^2 \mathrm{Tr}\left(\Phi^\dagger \Phi\right) \ , \tag{2.39}$$

not invariant under dilatation symmetry. A realization of this symmetry in our model is directly connected with the implementation of a scalar glueball, which in turn is related to the trace anomaly.

Namely, dilatation invariance requires that only terms with the dimension $\left[\text{energy}^4\right]$ are allowed in the Lagrangian. Furthermore, in the chiral limit and by neglecting the $U_A(1)$ anomaly the only dimensionful parameter which enters the model should be the energy scale Λ_{dil}. This energy scale arises from the dilaton potential (2.5) and generates, such as required by the Yang-Mills sector of QCD, the trace anomaly. This implies that terms of the form

$$\alpha \left[\mathrm{Tr}(\Phi^\dagger \Phi)\right]^3 \tag{2.40}$$

[1]This Lagrangian corresponds to the one of the former versions of the LSM without (axial-)vector fields. The first LSM was introduced by Murray Gell-Mann and Maurice M. Levy in 1960 [43].

are not allowed because the coupling constant α possesses the dimension $\left[\text{energy}^{-2}\right]$. Moreover, the term

$$\frac{\beta}{G^2}[\mathrm{Tr}(\Phi^\dagger\Phi)]^3 \tag{2.41}$$

possesses a dimensionless coupling constant β, as dilatation invariance requires, but for $G = 0$ there is a singularity. In addition, at non-zero temperature when the gluon condensate which corresponds to the vev of the glueball field G_0 vanishes, the term (2.41) would also diverge. Hence, the effective hadronic Lagrangian containing a scalar glueball field (G) and (pseudo)scalar $\bar{q}q$ fields (Φ) with all symmetries discussed previously reads

$$\mathcal{L}_{G\Phi} = \mathcal{L}_{dil} + \mathrm{Tr}\left[(\partial^\mu\Phi)^\dagger(\partial^\mu\Phi)\right] - aG^2\mathrm{Tr}\left(\Phi^\dagger\Phi\right) - \lambda_1\left[\mathrm{Tr}(\Phi^\dagger\Phi)\right]^2 - \lambda_2\mathrm{Tr}\left[(\Phi^\dagger\Phi)^2\right] . \tag{2.42}$$

Due to the symmetries of the Lagrangian (2.42) the coupling of the scalar glueball to the fields of Φ is unambiguously defined. The sign of the parameter a determines whether chiral symmetry is spontaneously broken and its connection with the former mass parameter of the Lagrangian (2.35), when the scalar glueball condenses, is as follows

$$m_0^2 = aG_0^2 . \tag{2.43}$$

Hence, the coupling constant a is dimensionless as required and in order to generate the spontaneous breaking of the chiral symmetry the requirement $a \overset{!}{<} 0$ should be fulfilled.

Moreover, in the large-N_c limit the parameter a scales as

$$a \propto N_c^{-2} \tag{2.44}$$

this implies the correct scaling of the mass parameter

$$m_0^2 \propto N_c^0 . \tag{2.45}$$

The large-N_c dependence of the remaining parameters of the Lagrangian (2.42) and (2.4), respectively, is as follows. Since the glueball mass is large-N_c independent the mass parameter m_G have to scale as

$$m_G \propto N_c^0 . \tag{2.46}$$

The second parameter coming from the dilaton patential (2.5) is the energy scale Λ_{dil} which scales as

$$\Lambda_{dil} \propto N_c \tag{2.47}$$

in order to ensure that the four glueball interaction scales according to Eq. (1.26) as

$$\frac{m_G^2}{\Lambda_{dil}^2} \propto N_c^{-2} . \tag{2.48}$$

Finally, the terms which describe the four $\bar{q}q$ meson interaction scale as

$$\lambda_1 \propto N_c^{-2} , \tag{2.49}$$

$$\lambda_2 \propto N_c^{-1} . \tag{2.50}$$

The reason for the stronger suppression of the λ_1 term is due to the product of two traces which requires exchange of gluons at the quark gluon level.

Vector and axial-vector $\bar{q}q$ mesons

Analogously to the (pseudo)scalar sector (2.30), we introduce the right- and the left-handed vector and axial-vector quark-antiquark mesons by defining the matrices

$$R^{\mu}_{ij} \equiv \sqrt{2}\bar{q}_{j,R}\gamma^{\mu}q_{i,R} = \frac{1}{\sqrt{2}}\left(\bar{q}_j\gamma^{\mu}q_i - \bar{q}_j\gamma^5\gamma^{\mu}q_i\right) , \tag{2.51}$$

$$L^{\mu}_{ij} \equiv \sqrt{2}\bar{q}_{j,L}\gamma^{\mu}q_{i,L} = \frac{1}{\sqrt{2}}\left(\bar{q}_j\gamma^{\mu}q_i + \bar{q}_j\gamma^5\gamma^{\mu}q_i\right) , \tag{2.52}$$

where

$$V^{\mu}_{ij} \equiv \frac{1}{\sqrt{2}}\bar{q}_j\gamma^{\mu}q_i , \quad A^{\mu}_{ij} \equiv \frac{1}{\sqrt{2}}\bar{q}_j\gamma^5\gamma^{\mu}q_i \tag{2.53}$$

are the vector and axial-vector currents. Hence the right- and the left-handed chiral fields in the vector and axial-vector sector read

$$R^{\mu} = V^{\mu} - A^{\mu} , \quad L^{\mu} = V^{\mu} + A^{\mu} , \tag{2.54}$$

which transform under the global chiral symmetry as follows

$$R^{\mu} \to R'^{\mu} = U_R R^{\mu} U_R^{\dagger} , \tag{2.55}$$

$$L^{\mu} \to L'^{\mu} = U_L L^{\mu} U_L^{\dagger} . \tag{2.56}$$

The hermitian matrices V^{μ} and A^{μ} expressed through the generators of the $U(N_f)$ group are

$$V^{\mu} = V^{\mu}_a t_a , \quad V^{\mu}_a \equiv \sqrt{2}\bar{q}\gamma^{\mu}t_a q , \tag{2.57}$$

$$A^{\mu} = A^{\mu}_a t_a , \quad A^{\mu}_a \equiv \sqrt{2}\bar{q}\gamma^5\gamma^{\mu}t_a q . \tag{2.58}$$

In order to construct a kinetic term of (axial-)vector fields we define the right- and the left-handed field-strength tensors

$$R^{\mu\nu} = \partial^{\mu}R^{\nu} - \partial^{\nu}R^{\mu} , \tag{2.59}$$

$$L^{\mu\nu} = \partial^{\mu}L^{\nu} - \partial^{\nu}L^{\mu} , \tag{2.60}$$

which transform under chiral transformation in the following way

$$R^{\mu\nu} \to R'^{\mu\nu} = U_R R^{\mu\nu} U_R^{\dagger} , \tag{2.61}$$

$$L^{\mu\nu} \to L'^{\mu\nu} = U_L L^{\mu\nu} U_L^{\dagger} . \tag{2.62}$$

Now, a chirally and dilatation invariant Lagrangian of (axial-)vector $\bar{q}q$ fields can be constructed:

$$\begin{aligned}
\mathcal{L}_{L_\mu R_\mu} \quad = \quad & -\frac{1}{4}\mathrm{Tr}\left[(L^{\mu\nu})^2 + (R^{\mu\nu})^2\right] + \frac{m_1^2}{2}\mathrm{Tr}\left[(L^{\mu})^2 + (R^{\mu})^2\right] \\
& -i2g_2\left(\mathrm{Tr}\left\{L_{\mu\nu}\left[L^{\mu}, L^{\nu}\right]\right\} + \mathrm{Tr}\left\{R_{\mu\nu}\left[R^{\mu}, R^{\nu}\right]\right\}\right) \\
& +g_3\left[\mathrm{Tr}\left(L^{\mu}L^{\nu}L_{\mu}L_{\nu}\right) + \mathrm{Tr}\left(R^{\mu}R^{\nu}R_{\mu}R_{\nu}\right)\right] \\
& +g_4\left[\mathrm{Tr}\left(L^{\mu}L_{\mu}L^{\nu}L_{\nu}\right) + \mathrm{Tr}\left(R^{\mu}R_{\mu}R^{\nu}R_{\nu}\right)\right] \\
& +g_5\mathrm{Tr}\left(L^{\mu}L_{\mu}\right)\mathrm{Tr}\left(R^{\mu}R_{\mu}\right) \\
& +g_6\left[\mathrm{Tr}\left(L^{\mu}L_{\mu}\right)\ \mathrm{Tr}\left(L^{\mu}L_{\mu}\right) + \mathrm{Tr}\left(R^{\mu}R_{\mu}\right)\mathrm{Tr}\left(R^{\mu}R_{\mu}\right)\right] ,
\end{aligned} \tag{2.63}$$

where we consider terms up to fourth order in the fields. In the following the coupling constants g_3-g_6 are not relevant for studies in this work, since processes of four-point vertices are not considered. Although the coupling constant g_2 describes three-point vertices it is also not relevant in this work as we will see later. Furthermore, the Lagrangian (2.63) is invariant under parity and charge conjugation transformations. According to the behavior of the quarks under these discrete symmetries shown in Eqs. (1.47)-(1.48) as well as (1.64)-(1.65) the right- and the left-handed vector and axial-vector quark-antiquark fields transform under parity as

$$R^\mu(t,\vec{x}) \overset{P}{\to} R'^\mu(t,\vec{x}) = g^{\mu\nu} L_\nu(t,-\vec{x}) \,, \tag{2.64}$$

$$L^\mu(t,\vec{x}) \overset{P}{\to} L'^\mu(t,\vec{x}) = g^{\mu\nu} R_\nu(t,-\vec{x}) \tag{2.65}$$

and under charge conjugation as

$$R^\mu(x) \overset{C}{\to} R'^\mu(x) = -L^{\nu T}(x) \,, \tag{2.66}$$

$$L^\mu(x) \overset{C}{\to} L'^\mu(x) = R^{\nu T}(x) \,. \tag{2.67}$$

In analogy to the (pseudo)scalar sector we have to modify the mass term of the (axial-)vector fields in the Lagrangian (2.63) in order to realize dilatation invariance. The corresponding Lagrangian reads

$$\mathcal{L}_{GL_\mu R_\mu} = -\frac{1}{4}\mathrm{Tr}\left[(L^{\mu\nu})^2 + (R^{\mu\nu})^2\right] + \frac{b}{2}G^2\mathrm{Tr}\left[(L^\mu)^2 + (R^\mu)^2\right] \,, \tag{2.68}$$

where

$$m_1^2 = bG_0^2 > 0 \tag{2.69}$$

is the connection between the mass parameter of the Lagrangian (2.63) and the dimensionless coupling constant of the mass term of the Lagrangian (2.68).

The large-N_c dependence of the parameters of the Lagrangian (2.63) and (2.68), respectively, is as follows. Similarly, to the (pseudo)scalar sector one obtain

$$b \propto N_c^{-2} \Rightarrow m_1^2 \propto N_c^0 \,. \tag{2.70}$$

The coupling constants of the Lagrangian (2.63) scale as

$$g_2 \propto N_c^{-\frac{1}{2}} \,, \tag{2.71}$$

$$g_3, g_4 \propto N_c^{-1} \,, \tag{2.72}$$

$$g_5, g_6 \propto N_c^{-2} \,. \tag{2.73}$$

Coupling of the (pseudo)scalar and (axial-)vector $\bar{q}q$ mesons

In nature the (pseudo)scalar and (axial-)vector mesons interact with each other, therefore terms which couple these states are necessary. Firstly, we introduce a corresponding covariant derivative

$$D_\mu\Phi = \partial_\mu\Phi + ig_1(\Phi R_\mu - L_\mu\Phi) \tag{2.74}$$

and

$$(D^\mu\Phi)^\dagger = \partial^\mu\Phi^\dagger - ig_1(R^\mu\Phi^\dagger - \Phi^\dagger L^\mu)\,, \tag{2.75}$$

which behave under the chiral transformations (2.28), (2.55), and (2.56) as follows

$$\begin{aligned}(D_\mu\Phi)' &= \partial_\mu(U_L\Phi U_R^\dagger) + ig_1(U_L\Phi U_R^\dagger U_R R_\mu U_R^\dagger - U_L L_\mu U_L^\dagger U_L\Phi U_R^\dagger)\\ &= U_L(\partial_\mu\Phi)U_R^\dagger + ig_1(U_L\Phi R_\mu U_R^\dagger - U_L L_\mu\Phi U_R^\dagger)\\ &= U_L D_\mu\Phi U_R^\dagger\,.\end{aligned} \tag{2.76}$$

Similarly, we obtain

$$(D^\mu\Phi)'^\dagger = U_R\,(D^\mu\Phi)^\dagger\,U_L^\dagger\,, \tag{2.77}$$

from which the globally and locally chirally invariant kinetic term can be built

$$\mathrm{Tr}\left[(D^\mu\Phi)^\dagger(D_\mu\Phi)\right]\,. \tag{2.78}$$

However, local symmetry is not favored by phenomenology [181]. In addition, the following interaction terms of the (pseudo)scalar and (axial-)vector $\bar{q}q$ fields can be constructed

$$\frac{h_1}{2}\mathrm{Tr}[\Phi^\dagger\Phi]\mathrm{Tr}[L_\mu L^\mu + R_\mu R^\mu], \tag{2.79}$$

$$h_2\mathrm{Tr}[\Phi^\dagger L_\mu L^\mu\Phi + \Phi R_\mu R^\mu\Phi^\dagger], \tag{2.80}$$

$$2h_3\mathrm{Tr}[\Phi R_\mu\Phi^\dagger L^\mu]\,. \tag{2.81}$$

In the large-N_c limit the coupling constant g_1 scales as

$$g_1 \propto N_c^{-\frac{1}{2}} \tag{2.82}$$

and the parameters of the interaction terms (2.79), (2.80), and (2.81) as

$$h_1 \propto N_c^{-2}\,, \tag{2.83}$$

$$h_2, h_3 \propto N_c^{-1}\,. \tag{2.84}$$

Note that for the same reason as λ_1 the parameter h_1 is stronger suppressed than h_2 and h_3. Both parameters h_1 and λ_1, which are relevant for this study, vanish in the limit $N_c \to \infty$.

Explicit breaking of the chiral symmetry in eLSM

In the following we will introduce terms which describe the explicit breaking of the chiral symmetry in the eLSM.

$U_A(1)$ **anomaly** Due to the $U_A(1)$ anomaly the global chiral symmetry is even broken when quark masses vanish. There exist different ways to describe this phenomenon of the gauge sector of QCD, which arises from instantons[2], for instance by the term of Ref. [183]

$$c(\det\Phi + \det\Phi^\dagger) \tag{2.85}$$

[2]For a general introduction to instantons we refer e.g. Ref. [182] and references therein.

or via the term

$$c_1(\det\Phi - \det\Phi^\dagger)^2 \tag{2.86}$$

first discussed in Refs. [184, 185].

One can easily see that these terms generate the $U_A(1)$ anomaly by performing the axial transformations $U_A(N_f)$ on the determinant of Φ, which yields:

$$\begin{aligned}
\det\Phi &\rightarrow \det\Phi' = \det\left(U_A\Phi U_A\right) \\
&= \det\left(e^{-i\theta_A^a t^a}\Phi e^{-i\theta_A^a t^a}\right) \\
&= \det\left(e^{-i2\theta_A^a t^a}\Phi\right) \\
&= \det(e^{-i2\sum_{a=1}^{N_f^2-1}\theta_A^a t^a})\det(e^{-i2\theta_A^0 t^0})\det\Phi \\
&= \det(e^{-i2\theta_A^0 t^0})\det\Phi \\
&= e^{-i\theta_A^0\sqrt{2N_f}}\det\Phi \neq \det\Phi\,.
\end{aligned} \tag{2.87}$$

A difference between the terms (2.85) and (2.86) is that in the case of $N_f = 3$ the first one is of order $\mathcal{O}(3)$ whereas the second one of order $\mathcal{O}(6)$. This means that both terms violate the dilatation symmetry but it is not essential that terms which describe the $U_A(1)$ anomaly satisfy the dilatation symmetry. Namely, the axial anomaly is also generated by the gluonic sector of QCD, where the trace anomaly originates. Another difference between these terms is the influence on the mesonic phenomenology. The term (2.85) influences masses of scalar as well as pseudoscalar mesons while the term (2.86) only affects those of pseudoscalar-isoscalar mesons [19, 186]. Furthermore, these terms are responsible for the large mass splitting of η and $\eta'(958)$. Note, that the large-N_c scaling of the parameters c and c_1 depends on the number of quark flavors

$$c \propto N_c^{-\frac{N_f}{2}}\,, \tag{2.88}$$

$$c_1 \propto N_c^{-N_f}\,. \tag{2.89}$$

For the realization of the chiral anomaly in the implementation of the eLSM with two quark flavors we use the term (2.85) and in that of three quark flavors the term (2.86). Moreover, the term (2.86) is well suited to study the coupling of the pseudoscalar glueball $\tilde{G}$ to the ordinary scalar and pseudoscalar mesons which will be performed in chapter 6 [6, 7, 8, 9, 19, 174, 176, 187, 188].

Non-vanishing quark masses The fact that pions, as Goldstone-Bosons, are not exactly massless is a manifestation of the explicit breaking of the

$$SU_V(N_f)\times SU_A(N_f) \tag{2.90}$$

symmetry which originates from the Higgs sector [71, 72, 73]. This explicit symmetry breaking is parametrized in the eLSM in the (pseudo)scalar sector by

$$\mathrm{Tr}\left[H\left(\Phi^\dagger + \Phi\right)\right]\,, \tag{2.91}$$

where

$$H = \mathrm{diag}(h_{0u}, h_{0d}, ..., h_{0N_f}) \tag{2.92}$$

and the parameters

$$h_{0i} = const \propto m_{q_i} \tag{2.93}$$

with $i \in \{u, d, ..., N_f\}$. For the relevant cases $N_f = 2$ and $N_f = 3$ the matrix H explicitly reads

$$H = H_0 t_0 + H_3 t_3 = \begin{pmatrix} \frac{h_{0N}}{2} & 0 \\ 0 & \frac{h_{0N}}{2} \end{pmatrix} \equiv \begin{pmatrix} h_N & 0 \\ 0 & h_N \end{pmatrix} , \tag{2.94}$$

and

$$H = H_0 T_0 + H_8 T_8 = \begin{pmatrix} \frac{h_{0N}}{2} & 0 & 0 \\ 0 & \frac{h_{0N}}{2} & 0 \\ 0 & 0 & \frac{h_{0S}}{\sqrt{2}} \end{pmatrix} \equiv \begin{pmatrix} h_N & 0 & 0 \\ 0 & h_N & 0 \\ 0 & 0 & h_S \end{pmatrix} , \tag{2.95}$$

Note that the breaking of the isospin symmetry $m_{q_u} \neq m_{q_d}$ is not considered in this model hence we use $u, d \equiv N$ as well as $s \equiv S$. Analogously, in the (axial-)vector sector the corresponding term reads

$$\mathrm{Tr}\left[\Delta \left(L_\mu^2 + R_\mu^2\right)\right] , \tag{2.96}$$

where

$$\Delta = \mathrm{diag}(\delta_u, \delta_d, ..., \delta_{N_f}) , \quad \delta_i = const \propto m_{q_i} . \tag{2.97}$$

The matrix Δ explicitly reads

$$\Delta = \Delta_0 T_0 + \Delta_8 T_8 = \begin{pmatrix} \frac{\tilde{\delta}_N}{2} & 0 & 0 \\ 0 & \frac{\tilde{\delta}_N}{2} & 0 \\ 0 & 0 & \frac{\tilde{\delta}_S}{\sqrt{2}} \end{pmatrix} \equiv \begin{pmatrix} \delta_N & 0 & 0 \\ 0 & \delta_N & 0 \\ 0 & 0 & \delta_S \end{pmatrix} . \tag{2.98}$$

A crucial modification of the eLSM of Refs. [19, 81] is the introducing of a next-to-leading term in the (pseudo)scalar sector. This is necessary in order to correctly describe the phenomenology in the scalar-isoscalar sector as we will see in chapter four. The corresponding term read

$$-\mathrm{Tr}\left[E(\Phi^\dagger \Phi)\right] , \tag{2.99}$$

where

$$E = \mathrm{diag}(\epsilon_u, \epsilon_d, ..., \epsilon_{N_f}) , \quad \epsilon_i = const \propto m_{q_i} . \tag{2.100}$$

The matrix E explicitly reads

$$E = E_0 T_0 + E_8 T_8 = \begin{pmatrix} \frac{\tilde{\epsilon}_N}{2} & 0 & 0 \\ 0 & \frac{\tilde{\epsilon}_N}{2} & 0 \\ 0 & 0 & \frac{\tilde{\epsilon}_S}{\sqrt{2}} \end{pmatrix} \equiv \begin{pmatrix} \epsilon_N & 0 & 0 \\ 0 & \epsilon_N & 0 \\ 0 & 0 & \epsilon_S \end{pmatrix} . \tag{2.101}$$

The large-N_c scaling of the constants h_{0i}, δ_i, and ϵ_i reads

$$h_{0i} \propto N_c^{-\frac{1}{2}} , \tag{2.102}$$

$$\delta_i, \epsilon_i \propto N_c^0 . \tag{2.103}$$

2.3.2 Mesonic Lagrangian of the eLSM

Finally, the mesonic Lagrangian of our eLSM which is studied in the present work with respect to the three-body mixing in the scalar-isoscalar sector below 2 GeV reads

$$\begin{aligned}\mathcal{L} &= \mathcal{L}_{dil} + \mathrm{Tr}[(D^\mu\Phi)^\dagger(D_\mu\Phi)] - \mathrm{Tr}\left\{\left[m_0^2\left(\frac{G}{G_0}\right)^2 + E\right]\Phi^\dagger\Phi\right\} - \lambda_1\left[\mathrm{Tr}(\Phi^\dagger\Phi)\right]^2 - \lambda_2\ \mathrm{Tr}[(\Phi^\dagger\Phi)^2] \\ &+ c_1(\det\Phi - \det\Phi^\dagger)^2 + \mathrm{Tr}[H(\Phi^\dagger + \Phi)] + \mathrm{Tr}\left\{\left[\frac{m_1^2}{2}\left(\frac{G}{G_0}\right)^2 + \Delta\right]\left(L_\mu^2 + R_\mu^2\right)\right\} \\ &- \frac{1}{4}\mathrm{Tr}\left(L_{\mu\nu}^2 + R_{\mu\nu}^2\right) + \frac{h_1}{2}\mathrm{Tr}(\Phi^\dagger\Phi)\ \mathrm{Tr}(L_\mu L^\mu + R_\mu R^\mu) + h_2\mathrm{Tr}(\Phi^\dagger L_\mu L^\mu\Phi + \Phi R_\mu R^\mu\Phi^\dagger) \\ &+ 2h_3\mathrm{Tr}(\Phi R_\mu\Phi^\dagger L^\mu) + \ldots\,, \end{aligned} \tag{2.104}$$

where

$$\mathcal{L}_{dil} = \frac{1}{2}(\partial^\mu G)^2 - \frac{1}{4}\frac{m_G^2}{\Lambda_{dil}^2}G^4\left(\ln\left|\frac{G}{\Lambda_{dil}}\right| - \frac{1}{4}\right)\,. \tag{2.105}$$

This mesonic Lagrangian is valid for N_f quark flavors and in the large-N_c expansion. In addition, the dots in the Lagrangian (2.104) indicate further terms, e.g. those of the Lagrangian (2.63) or additional d.o.f. as for instance further glueballs.

2.4 Assignment of the fields of the eLSM

In this section we discuss the assignment of the bare quark-antiquark fields of the eLSM to the physical resonances of the PDG [11]. Therefore we explicitly show the corresponding multiplets for $N_f = 3$ as 3×3 matrices [19, 81]. In the limiting case of two quark flavors ($N_f = 2$) which will be discussed in the next chapter, the multiplets reduce to 2×2 matrices. In simplified terms this means that the third columns and rows of the original $N_f = 3$ multiplets are omitted. Hence we are only left with mesons which are composed of the two light quark flavors up and down.

2.4.1 Assignment of the fields in the scalar and pseudoscalar sector

A mesonic quark-antiquark state with spin $S = 1$ and angular momentum $L = 1$ can couple to a total angular momentum $J = 0$. In that case S and L are antiparallel to each other. Using the formulas (1.52) and (1.53) one obtains a particle with $J^{PC} = 0^{++}$ which are the quantum numbers of a scalar state. Analogously, in the case of $S = L = 0$ one obtains a particle with the quantum numbers $J^{PC} = 0^{-+}$ which corresponds to a pseudoscalar state. A further relevant quantum number is the isospin I. These quantum numbers are of great importance in order to classify physical properties or resonances according to their quantum numbers. The fields of the nonets of our hadronic model are assigned to the physical resonances of Ref. [11].

We start with the multiplets of the scalar mesons

$$S = \sum_{i=0}^{8} S^i T^i = \frac{1}{\sqrt{2}}\begin{pmatrix} \frac{\sigma_N + a_0^0}{\sqrt{2}} & a_0^+ & K_0^{\star+} \\ a_0^- & \frac{\sigma_N - a_0^0}{\sqrt{2}} & K_0^{\star0} \\ K_0^{\star-} & \bar{K}_0^{\star0} & \sigma_S \end{pmatrix} \tag{2.106}$$

and pseudoscalar mesons,

$$P = \sum_{i=0}^{8} iP^i T^i = \frac{i}{\sqrt{2}} \begin{pmatrix} \frac{(\eta_N + \pi^0)}{\sqrt{2}} & \pi^+ & K^+ \\ \pi^- & \frac{(\eta_N - \pi^0)}{\sqrt{2}} & K^0 \\ K^- & \bar{K}^0 & \eta_S \end{pmatrix} . \tag{2.107}$$

This yields the chiral field of the scalar and pseudoscalar mesons, which is a linear combination of the scalar and pseudoscalar multiplets S and P

$$\Phi = \sum_{i=0}^{8} (S^i + iP^i) T^i = \frac{1}{\sqrt{2}} \begin{pmatrix} \frac{\sigma_N + a_0^0 + i(\eta_N + \pi^0)}{\sqrt{2}} & a_0^+ + i\pi^+ & K_0^{\star +} + iK^+ \\ a_0^- + i\pi^- & \frac{\sigma_N - a_0^0 + i(\eta_N - \pi^0)}{\sqrt{2}} & K_0^{\star 0} + iK^0 \\ K_0^{\star -} + iK^- & \bar{K}_0^{\star 0} + i\bar{K}^0 & \sigma_S + i\eta_S \end{pmatrix} . \tag{2.108}$$

The corresponding adjoint chiral field is given by $\Phi^\dagger = \sum_{i=0}^{8} (S^i - iP^i) T^i$ [19, 81]. In the pseudoscalar sector we assign the fields $\vec{\pi}$ and K to the physical pion isotriplet, $I = 1$, and the two kaon isodoublets, $I = \frac{1}{2}$, [11]. The fields

$$\eta_N \cong i(\bar{u}\gamma_5 u + \bar{d}\gamma_5 d)/\sqrt{2} , \quad \eta_S \cong i\bar{s}\gamma_5 s , \tag{2.109}$$

are the non-strange and strange contributions to the physical isoscalar, $I = 0$, states η and $\eta'(958)$ [11]

$$\eta = \eta_N \cos\varphi_\eta + \eta_S \sin\varphi_\eta , \quad \eta' = -\eta_N \sin\varphi_\eta + \eta_S \cos\varphi_\eta , \tag{2.110}$$

where $\varphi_\eta = -44.6^\circ$ is the pseudoscalar mixing angle as determined as a consequence of the global fit of Ref. [81, 186]. As shown in the comprehensive study of Ref. [81], the scalar $\bar{q}q$ states lie above 1 GeV. In turn, the scalar states below 1 GeV should not be interpreted as $\bar{q}q$ states but as tetraquarks and/or mesonic molecular states, see Refs. [133, 134, 135, 136, 137, 138, 139, 140, 141, 142, 143, 144, 145, 146, 147]. Hence, in the scalar sector we assign the field $\vec{a}_0$ to the physical isotriplet resonance $a_0(1450)$ and the scalar kaon isodoublet fields $K_0^\star$ to the resonance $K_0^*(1430)$ [11]. The least clear assignment occurs in the scalar-isoscalar channel because in the region from 1 to 2 GeV there are three resonances which are listed in Ref. [11]: $f_0(1370)$, $f_0(1500)$, and $f_0(1710)$. Only two of them can be interpreted as predominantly $\bar{q}q$ states, namely the non-strange and the strange

$$\sigma_N \cong (\bar{u}u + \bar{d}d)/\sqrt{2} , \quad \sigma_S \cong \bar{s}s , \tag{2.111}$$

while the third one is probably predominantly a glueball state G. The determination of the corresponding three-body mixing matrix, as discussed in the section 1.4 and indicated in the beginning of this chapter, is one of the aims of this work and is carried out below [3, 4, 5]. Note that there are other interpretations in which $f_0(1370)$ and $f_0(1710)$ are described as resonances dynamically generated from vector-vector interactions [189, 190, 191].

2.4.2 Assignment of the fields in the vector and axial-vector sector

Particles with spin $S = 1$ and angular momentum $L = 0$ yield $J^{PC} = 1^{--}$ which are the quantum numbers of vector states. Particles with spin and angular momentum $S = L = 1$, as in the scalar case but now with a proper combination of parallel alignment, yield axial-vector states,

$J^{PC} = 1^{++}$.

The multiplets of the (axial-)vector mesons [19, 81] read

$$V^\mu = \sum_{i=0}^{8} V_i^\mu T^i = \frac{1}{\sqrt{2}} \begin{pmatrix} \frac{\omega_N^\mu + \rho^{\mu 0}}{\sqrt{2}} & \rho^{\mu +} & K^{\star \mu +} \\ \rho^{\mu -} & \frac{\omega_N^\mu - \rho^{\mu 0}}{\sqrt{2}} & K^{\star \mu 0} \\ K^{\star \mu -} & \bar{K}^{\star \mu 0} & \omega_S^\mu \end{pmatrix}, \tag{2.112}$$

$$A^\mu = \sum_{i=0}^{8} A_i^\mu T^i = \frac{1}{\sqrt{2}} \begin{pmatrix} \frac{f_{1N}^\mu + a_1^{\mu 0}}{\sqrt{2}} & a_1^{\mu +} & K_1^{\mu +} \\ a_1^{\mu -} & \frac{f_{1N}^\mu - a_1^{\mu 0}}{\sqrt{2}} & K_1^{\mu 0} \\ K_1^{\mu -} & \bar{K}_1^{\mu 0} & f_{1S}^\mu \end{pmatrix}. \tag{2.113}$$

The chiral fields of the left-handed and right-handed (axial)-vector mesons, which are linear combinations of the vector and axial-vector multiplets V^μ and A^μ, are given by

$$L^\mu = \sum_{i=0}^{8} (V_i^\mu + A_i^\mu) T^i = \frac{1}{\sqrt{2}} \begin{pmatrix} \frac{\omega_N^\mu + \rho^{\mu 0}}{\sqrt{2}} + \frac{f_{1N}^\mu + a_1^{\mu 0}}{\sqrt{2}} & \rho^{\mu +} + a_1^{\mu +} & K^{\star \mu +} + K_1^{\mu +} \\ \rho^{\mu -} + a_1^{\mu -} & \frac{\omega_N^\mu - \rho^{\mu 0}}{\sqrt{2}} + \frac{f_{1N}^\mu - a_1^{\mu 0}}{\sqrt{2}} & K^{\star \mu 0} + K_1^{\mu 0} \\ K^{\star \mu -} + K_1^{\mu -} & \bar{K}^{\star \mu 0} + \bar{K}_1^{\mu 0} & \omega_S^\mu + f_{1S}^\mu \end{pmatrix} \tag{2.114}$$

and

$$R^\mu = \sum_{i=0}^{8} (V_i^\mu - A_i^\mu) T^i = \frac{1}{\sqrt{2}} \begin{pmatrix} \frac{\omega_N^\mu + \rho^{\mu 0}}{\sqrt{2}} - \frac{f_{1N}^\mu + a_1^{\mu 0}}{\sqrt{2}} & \rho^{\mu +} - a_1^{\mu +} & K^{\star \mu +} - K_{1,A}^{\mu +} \\ \rho^{\mu -} - a_1^{\mu -} & \frac{\omega_N^\mu - \rho^{\mu 0}}{\sqrt{2}} - \frac{f_{1N}^\mu - a_1^{\mu 0}}{\sqrt{2}} & K^{\star \mu 0} - K_{1,A}^{\mu 0} \\ K^{\star \mu -} - K_{1,A}^{\mu -} & \bar{K}^{\star \mu 0} - \bar{K}_{1,A}^{\mu 0} & \omega_S^\mu - f_{1S}^\mu \end{pmatrix}. \tag{2.115}$$

The assignment of the fields of the multiplets (2.114) and (2.115) to the physical resonances is as follows. In the $J^{PC} = 1^{--}$ sector the non-strange ω_N^μ and the strange ω_S^μ isoscalar field represent the resonance $\omega(782)$ and $\phi(1020)$, respectively. The isotriplet field $\vec{\rho}^\mu$ and the isodoublet fields $K^{\star \mu}$ correspond to the resonance $\rho(770)$ and $K^*(1410)$, respectively. In the $J^{PC} = 1^{++}$ sector the non-strange f_{1N}^μ and the strange f_{1S}^μ isoscalar field are assigned to the resonance $f_1(1285)$ and $f_1(1420)$, respectively. The isotriplet field $\vec{a}_1^\mu$ is identified with the resonance $a_1(1260)$. Finally, the isodoublet fields $K_{1,A}^\mu$ correspond to a mixture of $K_1(1270)$ and $K_1(1400)$. The corresponding mixing matrix reads

$$\begin{pmatrix} K_1(1270) \\ K_1(1400) \end{pmatrix} = \begin{pmatrix} \cos\varphi_K & -i\sin\varphi_K \\ -i\sin\varphi_K & \cos\varphi_K \end{pmatrix} \begin{pmatrix} K_{1,A}^\mu \\ K_{1,B}^\mu \end{pmatrix} \tag{2.116}$$

where $\varphi_K = (33.6 \pm 4.3)^\circ$ is the mixing angle [192]. Note that the physical $I = 0$ resonances in the sector 1^{--} as well as 1^{++}, similar to other nonets like in the (pseudo)scalar sector, are admixtures of the corresponding pure isoscalar fields ω_N^μ and ω_S^μ on the one hand, and f_{1N}^μ and f_{1S}^μ on the other hand. However, the mixing angles are small and therefore the mixing of these states can be neglected.

2.5 Vacuum expectation values

In this section we introduce the vev of the eLSM (2.104) and discuss the consequences of the spontaneous breaking of the global chiral symmetry in our model by following the Refs. [1, 3, 17, 18, 19, 81].

2.5.1 Spontaneous breaking of the global chiral symmetry in the eLSM

The spontaneous breaking of chiral symmetry in the eLSM (2.104) requires that the mass parameter

$$m_0^2 \overset{!}{<} 0 \,. \tag{2.117}$$

The conservation of parity and of $SU_V(N_f)$ symmetry requires that only fields with the quantum numbers

$$I^G\left(J^{PC}\right) = 0^+\,(0^{++}) \tag{2.118}$$

can condense in vacuum. The eLSM (2.104) with $N_f = 3$ has three fields with quantum numbers of the vacuum: the two scalar-isoscalar quark-antiquark fields σ_N and σ_S as well as a scalar glueball G. Thus, the following condensates appear:

$$\langle\sigma_N\rangle \equiv \phi_N = const \neq 0 \,, \tag{2.119}$$

$$\langle\sigma_S\rangle \equiv \phi_S = const \neq 0 \,, \tag{2.120}$$

$$\langle G\rangle \equiv G_0 = const \neq 0 \,. \tag{2.121}$$

In order to study the fluctuations, i.e., the physical excitations, we shift the scalar-isoscalar fields by their vev's

$$\sigma_N \to \sigma_N + \phi_N \,, \quad \sigma_S \to \sigma_S + \phi_S \,, \quad G \to G + G_0 \,. \tag{2.122}$$

In chapter three and four we will study in detail the scalar-isoscalar Lagrangian for the case $N_f = 2$ and $N_f = 3$, respectively. Note that Eq. (2.117) corresponds to the requirement $a \overset{!}{<} 0$ in the Lagrangian (2.42) where the connection between these parameters is

$$m_0^2 = aG_0^2 \,. \tag{2.123}$$

Hence, the spontaneous breaking of the chiral symmetry originates from the explicit breaking of the dilatation symmetry, which is realized in our model by the logarithmic term of the dilaton potential (2.5).

2.5.2 Bilinear terms of the eLSM

Spontaneous breaking of chiral symmetry induces bilinear terms

$$-g_1\phi_N(f_{1N}^\mu\partial_\mu\eta_N + a_1^{\mu\pm,0}\cdot\partial_\mu\pi^{\pm,0}) - \sqrt{2}g_1\phi_S f_{1S}^\mu\partial_\mu\eta_S \,, \tag{2.124}$$

$$-\left(\frac{g_1}{\sqrt{2}}\phi_S + \frac{g_1}{2}\phi_N\right)\left(K_1^{\mu 0}\partial_\mu\bar{K}^0 + K_1^{\mu+}\partial_\mu K^- + h.c.\right) \,, \tag{2.125}$$

$$\left(i\frac{g_1}{\sqrt{2}}\phi_S - i\frac{g_1}{2}\phi_N\right)\left(\bar{K}^{\star\mu 0}\partial_\mu K_0^{\star 0} + K^{\star\mu-}\partial_\mu K_0^{\star+}\right) \,, \tag{2.126}$$

$$\left(i\frac{g_1}{2}\phi_N - i\frac{g_1}{\sqrt{2}}\phi_S\right)\left(K^{\star\mu 0}\partial_\mu\bar{K}_0^{\star 0} + K^{\star\mu+}\partial_\mu K_0^{\star-}\right) \,, \tag{2.127}$$

in the Lagrangian of the eLSM. These terms mix fields of different nonets, axial-vector with pseudoscalar and vector with scalar fields, hence they should be eliminated. This can be achieved by shifting the (axial-)vector fields as follows [19, 81, 193],

$$f_{1N/S}^\mu \to f_{1N/S}^\mu + Z_{\eta_{N/S}} w_{f_{1N/S}}\partial^\mu\eta_{N/S} \,, \quad a_1^{\mu\pm,0} \to a_1^{\mu\pm,0} + Z_\pi w_{a_1}\partial^\mu\pi^{\pm,0} \,, \tag{2.128}$$

$$K_1^{\mu\pm,0,\bar{0}} \to K_1^{\mu\pm,0,\bar{0}} + Z_K w_{K_1} \partial^\mu K^{\pm,0,\bar{0}} \,, \quad K^{\star\mu\pm,0,\bar{0}} \to K^{\star\mu\pm,0,\bar{0}} + Z_{K^\star} w_{K^\star} \partial^\mu K_0^{\star\pm,0,\bar{0}} \,. \tag{2.129}$$

After performing this procedure additional kinetic terms occur. In order to remove the latter a redefinition of the (pseudo)scalar fields is required,

$$\pi^{\pm,0} \to Z_\pi \pi^{\pm,0} \,, \quad \eta_{N/S} \to Z_{\eta_{N/S}} \eta_{N/S} \,, \tag{2.130}$$

$$K^{\pm,0,\bar{0}} \to Z_K K^{\pm,0,\bar{0}} \,, \quad K_0^{\star\pm,0,\bar{0}} \to Z_{K^\star} K_0^{\star\pm,0,\bar{0}} \,, \tag{2.131}$$

where

$$Z_\pi = Z_{\eta_N} = \frac{m_{a_1}}{\sqrt{m_{a_1}^2 - g_1^2 \phi_N^2}} \,, \quad Z_K = \frac{2 m_{K_1}}{\sqrt{4 m_{K_1}^2 - g_1^2 (\phi_N + \sqrt{2}\phi_S)^2}} \,, \tag{2.132}$$

$$Z_{K^\star} = \frac{2 m_{K^\star}}{\sqrt{4 m_{K^\star}^2 - g_1^2 (\phi_N - \sqrt{2}\phi_S)^2}} \,, \quad Z_{\eta_S} = \frac{m_{f_{1S}}}{\sqrt{m_{f_{1S}}^2 - 2 g_1^2 \phi_S^2}} \tag{2.133}$$

are the wave-function renormalization constants and

$$w_{f_{1N}} = w_{a_1} = \frac{g_1 \phi_N}{m_{a_1}^2} \,, \quad w_{f_{1S}} = \frac{\sqrt{2} g_1 \phi_S}{m_{f_{1S}}^2} \,, \tag{2.134}$$

$$w_{K^\star} = \frac{i g_1 (\phi_N - \sqrt{2}\phi_S)}{2 m_{K^\star}^2} \,, \quad w_{K_1} = \frac{g_1 (\phi_N + \sqrt{2}\phi_S)}{2 m_{K_1}^2} \,. \tag{2.135}$$

2.6 Embedding of further gluballs into the eLSM

In the following we embed further glueballs, the pseudoscalar and the vector one, into the eLSM.

2.6.1 Lagrangian of the pseudoscalar glueball

This subsection follows Refs. [6, 7, 8, 9]. In order to study the coupling of a pseudoscalar glueball $\tilde{G}$, with the corresponding quantum numbers $J^{PC} = 0^{-+}$, to quark-antiquark scalar and pseudoscalar mesons, following the Refs. [174, 176, 187, 188], we construct an effective chiral Lagrangian

$$\mathcal{L}_{\tilde{G}} = \frac{1}{2} (\partial^\mu \tilde{G})^2 - \frac{1}{2} m_{\tilde{G}}^2 \tilde{G}^2 + i c_{\tilde{G}\Phi} \tilde{G} \left(\det\Phi - \det\Phi^\dagger \right) \,, \tag{2.136}$$

where $c_{\tilde{G}\Phi}$ is an unknown coupling constant and Φ the multiplet of ordinary scalar and pseudoscalar mesons introduced in the beginning of this chapter. The pseudoscalar glueball $\tilde{G}$ is a bosonic field made of gluons and is therefore chirally invariant. Moreover, it transforms under dilatations as

$$\tilde{G}(x) \to \tilde{G}'(x) = \lambda \tilde{G}(\lambda x) \tag{2.137}$$

and under the discrete symmetries parity P and charge conjugation C as

$$\tilde{G}(t, \vec{x}) \overset{P}{\to} \tilde{G}'(t, \vec{x}) = -\tilde{G}(t, -\vec{x}) \,, \tag{2.138}$$

$$\tilde{G}(x) \overset{C}{\to} \tilde{G}'(x) = \tilde{G}(x) \,. \tag{2.139}$$

As shown in in Eq. (2.87) performing of the axial transformations of the chiral symmetry on the determinant of Φ yields

$$\begin{aligned} \det\Phi &\rightarrow \det\Phi' = \det\left(U_A \Phi U_A\right) \\ &= e^{-i\theta_A^0\sqrt{2N_f}}\det\Phi \neq \det\Phi \,. \end{aligned} \tag{2.140}$$

Similarly one can show that under vector transformations of the chiral symmetry the determinant of Φ is invariant

$$\det\Phi \rightarrow \det\Phi' = \det(U_V \Phi U_V^\dagger) = \det\Phi \,. \tag{2.141}$$

This implies that the effective Lagrangian (2.136) is invariant under $SU_R(N_f) \times SU_L(N_f)$, but not under the axial $U_A(1)$ transformation. This is in agreement with the chiral anomaly in the pseudoscalar-isoscalar sector. Applying the discrete transformations of the multiplet Φ, Eqs. (2.37) and (2.38) as well as (2.138) and (2.139), leaves the effective Lagrangian (2.136) unchanged. Additionally, in the $N_f = 3$ realization of Φ the coupling constant $c_{\tilde{G}\Phi}$ is dimensionless and the Lagrangian (2.136) is invariant under dilatations. In conclusion, one can say that the effective Lagrangian (2.136) reflect exactly the symmetries of the QCD Lagrangian.

2.6.2 Excited vector and pseudovector quark-antiquark mesons

Analogously to the (pseudo)scalar, Eq. (2.30), and (axial-)vector sector, Eqs. (2.51)-(2.52), we introduce the excited vector and pseudovector quark-antiquark fields by defining the matrices [166]

$$\tilde{\Phi}^\mu_{ij} \equiv \sqrt{2}\bar{q}_{j,R}\partial^\mu q_{i,L} = \frac{1}{\sqrt{2}}\left(\bar{q}_{j,R}\partial^\mu q_{i,L} + i\bar{q}_{j,R}\gamma^5\partial^\mu q_{i,L}\right) \,, \tag{2.142}$$

$$\tilde{\Phi}^{\mu\dagger}_{ij} \equiv \sqrt{2}\bar{q}_{j,L}\partial^\mu q_{i,R} = \frac{1}{\sqrt{2}}\left(\bar{q}_{j,L}\partial^\mu q_{i,R} - i\bar{q}_{j,L}\gamma^5\partial^\mu q_{i,R}\right) \,. \tag{2.143}$$

The excited vector and pseudovector currents are defined as:

$$E^\mu_{ij} \equiv \frac{1}{\sqrt{2}}\bar{q}_j\partial^\mu q_i \,, \tag{2.144}$$

$$B^\mu_{ij} \equiv \frac{1}{\sqrt{2}}\bar{q}_j\gamma^5\partial^\mu q_i \,. \tag{2.145}$$

Finally, the chiral fields in the excited vector and pseudovector sector read

$$\tilde{\Phi}^\mu = E^\mu + iB^\mu \,, \quad \tilde{\Phi}^\dagger = E^\mu - iB^\mu \,. \tag{2.146}$$

Since E^μ and B^μ are hermitian matrices they can be expressed through the generators of the $U(N_f)$ group

$$E^\mu = E^\mu_a t_a \,, \quad E^\mu_a \equiv \sqrt{2}\bar{q}\partial^\mu t_a q \,, \tag{2.147}$$

$$B^\mu = B^\mu_a t_a \,, \quad B^\mu_a \equiv \sqrt{2}\bar{q}\gamma^5\partial^\mu t_a q \,. \tag{2.148}$$

The fields (2.146) transform under the global chiral symmetry in the following way

$$\tilde{\Phi}^\mu \rightarrow \tilde{\Phi}'^\mu = U_L\tilde{\Phi}^\mu U_R^\dagger \,, \tag{2.149}$$

$$\tilde{\Phi}^{\mu\dagger} \to \tilde{\Phi}'^{\mu\dagger} = U_R \tilde{\Phi}^{\mu\dagger} U_L^\dagger \,. \tag{2.150}$$

Furthermore, by considering the quark transformations under parity, Eqs. (1.47)-(1.48), and charge conjugation, Eqs. (1.64)-(1.65), the chiral field $\tilde{\Phi}^\mu$ transforms under these transformation as follows

$$\tilde{\Phi}^\mu \overset{P}{\to} \tilde{\Phi}'^\mu = \tilde{\Phi}^\dagger_\mu \tag{2.151}$$

and

$$\tilde{\Phi}^\mu \overset{C}{\to} \tilde{\Phi}'^\mu = \tilde{\Phi}^{\mu T} \,. \tag{2.152}$$

2.6.3 Assignment of the fields in the excited vector and pseudovector sector

According to Eqs. (1.52) and (1.53) the quantum numbers $S = 1$ and $L = 2$ yield a vector meson $J^{PC} = 1^{--}$ but due to a higher angular momentum it is an excited one (E^μ). In case of $S = 0$ and $L = 1$ one obtains a particle with the quantum numbers $J^{PC} = 1^{+-}$ which describes a pseudovector meson (B^μ). The $N_f = 3$ multiplets of these mesons read

$$E^\mu = \sum_{i=0}^{8} E_i^\mu T^i = \frac{1}{\sqrt{2}} \begin{pmatrix} \frac{\omega^\mu_{N,E} + \rho_E^{\mu 0}}{\sqrt{2}} & \rho_E^{\mu +} & K_E^{\star \mu +} \\ \rho_E^{\mu -} & \frac{\omega^\mu_{N,E} - \rho_E^{\mu 0}}{\sqrt{2}} & K_E^{\star \mu 0} \\ K_E^{\star \mu -} & \bar{K}_E^{\star \mu 0} & \omega^\mu_{S,E} \end{pmatrix}, \tag{2.153}$$

$$B^\mu = \sum_{i=0}^{8} i B_i^\mu T^i = \frac{i}{\sqrt{2}} \begin{pmatrix} \frac{h^\mu_{1N} + b_1^{\mu 0}}{\sqrt{2}} & b_1^{\mu +} & K^{\mu +}_{1,B} \\ b_1^{\mu -} & \frac{h^\mu_{1N} - b_1^{\mu 0}}{\sqrt{2}} & K^{\mu 0}_{1,B} \\ K^{\mu -}_{1,B} & \bar{K}^{\mu 0}_{1,B} & h^\mu_{1S} \end{pmatrix}, \tag{2.154}$$

which yield the chiral field in the excited vector and pseudovector sector

$$\tilde{\Phi} = \sum_{i=0}^{8} (E_i^\mu + i B_i^\mu) T^i = \frac{1}{\sqrt{2}} \begin{pmatrix} \frac{\omega^\mu_{N,E} + \rho_E^{\mu 0} + i(h^\mu_{1N} + b_1^{\mu 0})}{\sqrt{2}} & \rho_E^{\mu +} + i b_1^{\mu +} & K_E^{\star \mu +} + i K^{\mu +}_{1,B} \\ \rho_E^{\mu -} + i b_1^{\mu -} & \frac{\omega^\mu_{N,E} - \rho_E^{\mu 0} + i(h^\mu_{1N} - b_1^{\mu 0})}{\sqrt{2}} & K_E^{\star \mu 0} + i K^{\mu 0}_{1,B} \\ K_E^{\star \mu -} + i K^{\mu -}_{1,B} & \bar{K}_E^{\star \mu 0} + i \bar{K}^{\mu 0}_{1,B} & \omega^\mu_{S,E} + i h^\mu_{1S} \end{pmatrix}, \tag{2.155}$$

where the corresponding adjoint chiral field is given by $\tilde{\Phi}^\dagger = \sum_{i=0}^{8} (E_i^\mu - i B_i^\mu) T^i$. The assignment of the fields of the multiplets (2.153) and (2.154) to the physical resonances is as follows. In the excited vector sector where $J^{PC} = 1^{--}$ and $L = 2$ the non-strange $\omega^\mu_{N,E}$ and the strange $\omega^\mu_{S,E}$ field represent the resonance $\omega(1650)$ and $\phi(1680)$, respectively. The isotriplet field $\vec{\rho}^\mu_E$ and the isodoublet fields $K_E^{\star \mu}$ correspond to the resonance $\rho(1700)$ and $K^*(1680)$, respectively. In the $J^{PC} = 1^{+-}$ sector the non-strange h^μ_{1N} and the strange h^μ_{1S} field are assigned to the resonance $h_1(1170)$ and $h_1(1380)$. The isotriplet field $\vec{b}_1^\mu$ is identified with the resonance $b_1(1230)$. Finally, the isodoublet fields $K^\mu_{1,B}$ corresponds to a mixture of $K_1(1270)$ and $K_1(1400)$ [192] where the corresponding mixing matrix reads

$$\{b_1(1230),\ K_{1,B},\ h_1(1170),\ h_1(1380)\}.$$

In both nonets the strange-non-strange isoscalar mixing is neglected, thus $f_1(1285)$ and $h_1(1170)$ are purely non-strange states, while $f_1(1420)$ and $h_1(1380)$ are purely strange states.

2.6.4 Lagrangian of the vector glueball

In the following we construct a chiral Lagrangian of the vector glueball, which decays via two- and three-body processes into (pseudo)scalar, (axial-)vector, as well as excited vector and pseudovector quark-antiquark mesons [166]. This Lagrangian reads

$$\mathcal{L}_{\mathcal{O}_\mu} = -\frac{1}{4}\mathcal{O}_{\mu\nu}\mathcal{O}^{\mu\nu} - \frac{1}{2}m^2_{\mathcal{O}_\mu}\mathcal{O}_\mu\mathcal{O}^\mu + \mathcal{L}^{int}_{\mathcal{O}_\mu,1} + \mathcal{L}^{int}_{\mathcal{O}_\mu,2} + \mathcal{L}^{int}_{\mathcal{O}_\mu,3} \ , \tag{2.156}$$

where $\mathcal{O}_\mu$ is the vector glueball and

$$\mathcal{O}_{\mu\nu} = \partial_\mu\mathcal{O}_\nu - \partial_\nu\mathcal{O}_\mu \tag{2.157}$$

the corresponding field-strength tensor. The vector glueball is clearly invariant under chiral symmetry and transforms under dilatation symmetry, see Eq. (1.115), as

$$\mathcal{O}^\mu(x) \to \mathcal{O}'^\mu(x) = \lambda\mathcal{O}^\mu(\lambda x) \ . \tag{2.158}$$

In addition, it transforms under parity as

$$\mathcal{O}_\mu \to \mathcal{O}'_\mu = \mathcal{O}^\mu \tag{2.159}$$

and under charge conjugation as

$$\mathcal{O}_\mu \to \mathcal{O}'_\mu = -\mathcal{O}_\mu \ . \tag{2.160}$$

The interaction Lagrangian $\mathcal{L}^{int}_{\mathcal{O}_\mu,1}$ describes the coupling of the vector glueball to the (pseudo)scalar and (axial-)vector $\bar{q}q$ mesons and reads

$$\mathcal{L}^{int}_{\mathcal{O}_\mu,1} = \kappa_1\mathcal{O}_\mu\mathrm{Tr}\left(L^\mu\Phi\Phi^\dagger + R^\mu\Phi^\dagger\Phi\right) \ , \tag{2.161}$$

where κ_1 is a dimensionless coupling constant. One can easily see that this Lagrangian fulfills the symmetries of the QCD Lagrangian. It is invariant under the chiral transformations (2.28), (2.55), and (2.56),

$$\mathcal{L}'^{int}_{\mathcal{O}_{\mu,1}} = \kappa_1\mathcal{O}_\mu\mathrm{Tr}\left(U_L L^\mu U_L^\dagger U_L\Phi U_R^\dagger U_R\Phi^\dagger U_L^\dagger + U_R R^\mu U_R^\dagger U_R\Phi^\dagger U_L^\dagger U_L\Phi U_R^\dagger\right) = \mathcal{L}^{int}_{\mathcal{O}_{\mu,1}} \tag{2.162}$$

as well as dilatation-symmetric, Eq. (1.115),

$$S'_{\mathcal{L}_{\mathcal{O}_{\mu,1}}} = \int \lambda^{-4}d^4x'\kappa_1\lambda\mathcal{O}_\mu\mathrm{Tr}\left(\lambda L^\mu\lambda\Phi\lambda\Phi^\dagger + \lambda R^\mu\lambda\Phi^\dagger\lambda\Phi\right) = S_{\mathcal{L}_{\mathcal{O}_{\mu,1}}} \ . \tag{2.163}$$

Finally, using the parity transformations (2.37), (2.64) and (2.65) one obtains

$$\mathcal{L}'^{int}_{\mathcal{O}_{\mu,1}} = \kappa_1\mathcal{O}^\mu\mathrm{Tr}\left(R_\mu\Phi^\dagger\Phi + L_\mu\Phi\Phi^\dagger\right) = \mathcal{L}^{int}_{\mathcal{O}_{\mu,1}} \ , \tag{2.164}$$

and analogously we obtain using the charge conjugation transformations (2.38), (2.66), and (2.67)

$$\begin{aligned}\mathcal{L}'^{int}_{\mathcal{O}_{\mu,1}} &= \kappa_1(-\mathcal{O}_\mu)\mathrm{Tr}\left(-R^{\mu T}\Phi^T\Phi^{\dagger T} - L^{\mu T}\Phi^{\dagger T}\Phi^T\right)\\ &= -\kappa_1\mathcal{O}_\mu\mathrm{Tr}\left(-\Phi^\dagger\Phi R^\mu - \Phi\Phi^\dagger L^\mu\right)\\ &= \kappa_1\mathcal{O}_\mu\mathrm{Tr}\left(R^\mu\Phi^\dagger\Phi - L^\mu\Phi\Phi^\dagger\right) = \mathcal{L}^{int}_{\mathcal{O}_{\mu,1}} \ .\end{aligned} \tag{2.165}$$

The Lagrangian $\mathcal{L}_{\mathcal{O}_\mu,2}$, which couples to the (pseudo)scalar, excited vector, and pseudovector quark-antiquark mesons as well as to the scalar glueball, reads

$$\mathcal{L}_{\mathcal{O}_\mu,2} = \kappa_2 G \mathcal{O}_\mu \mathrm{Tr}\left(\Phi^\dagger \tilde{\Phi}^\mu + \tilde{\Phi}^{\mu\dagger}\Phi\right) , \tag{2.166}$$

where κ_2 is a dimensionless coupling constant. Exactly as in the previous case, also this Lagrangian (2.166) fulfils the symmetries of the QCD Lagrangian. Finally, the Lagrangian $\mathcal{L}_{\mathcal{O}_\mu,3}$ reads

$$\mathcal{L}^{int}_{\mathcal{O}_\mu,3} = \alpha \mathcal{O}_{\mu\nu} \mathrm{Tr}\left(R^\mu \Phi^\dagger L^\nu \Phi - L^\mu \Phi R^\nu \Phi^\dagger\right) . \tag{2.167}$$

As the Lagrangian (2.161) this Lagrangian couples to the ordinary mesons in the (pseudo)scalar and (axial-)vector sector. But in this case we obtain interaction terms of the type

$$\partial_\mu \mathcal{O}_\nu V^\mu A^\nu \tag{2.168}$$

which are proportional to the condensates ϕ_N and ϕ_S as well as the *Clebsch-Gordan coefficients*. Note that the Lagrangian breaks the dilatation symmetry hence the coupling constant α is not dimensionless but carries the dimension [energy^{-2}].

The calculation of the corresponding decay widths and branching ratios, respectively, are in progress and will be presented in Ref. [166].

Chapter 3

Mixing in the Scalar-Isoscalar Sector of the $N_f = 2$ eLSM

In this chapter we discuss the two-body mixing of the scalar-isoscalar states within the eLSM in the case of two quark flavors, following Refs. [1, 2, 17]. In this approximation the model contains only two

$$I^G\left(J^{PC}\right) = 0^+\,(0^{++})$$

fields. Several mixing scenarios are possible, which should be taken into account. Considering the results of Ref. [80], we start our study with the natural assignment [1, 17]

$$\sigma_N \cong f_0(1370)\,, \quad G \cong f_0(1500) \tag{3.1}$$

and then we test the alternative scenario [1]

$$\sigma_N \cong f_0(1370)\,, \quad G \cong f_0(1710)\,. \tag{3.2}$$

Additionally, we also tested assignments with the resonance $f_0(500)$ (or σ) as predominantly non-strange $\bar{q}q$ meson [1, 2]. Up to 2012 $f_0(500)$ was actually named $f_0(600)$ [194] with the following Breit-Wigner mass and width:

$$m_{f_0(600)} = (400 - 1200)\ \text{MeV}\,, \tag{3.3}$$

$$\Gamma_{f_0(600)} = (600 - 1000)\ \text{MeV}\,. \tag{3.4}$$

In Ref. [195], see also Refs. [196, 197, 198, 199], the estimate of the mass and width of this resonance was more precise

$$m_{f_0(500)} = (400 - 550)\ \text{MeV}\,, \tag{3.5}$$

$$\Gamma_{f_0(500)} = (400 - 700)\ \text{MeV}\,, \tag{3.6}$$

for that reason we repeat the calculations of this scenario [2] in order to confirm or disprove the results of Ref. [1].

The numerical results presented in this chapter are obtained from the *Mathematica* algorithm developed in Ref. [17].

3.1 eLSM in the case of $N_f = 2$

The Lagrangian of the eLSM used for calculations in the case of two quark flavors [1, 2, 17] reads

$$\begin{aligned}\mathcal{L} &= \mathcal{L}_{dil} + \mathrm{Tr}[(D^\mu\Phi)^\dagger(D_\mu\Phi)] - \mathrm{Tr}\left[m_0^2\left(\frac{G}{G_0}\right)^2\Phi^\dagger\Phi\right] - \lambda_1\left[\mathrm{Tr}(\Phi^\dagger\Phi)\right]^2 - \lambda_2\ \mathrm{Tr}[(\Phi^\dagger\Phi)^2] \\ &+ c(\det\Phi + \det\Phi^\dagger) + \mathrm{Tr}[H(\Phi^\dagger + \Phi)] + \mathrm{Tr}\left[\frac{m_1^2}{2}\left(\frac{G}{G_0}\right)^2\left(L_\mu^2 + R_\mu^2\right)\right] \\ &- \frac{1}{4}\mathrm{Tr}\left(L_{\mu\nu}^2 + R_{\mu\nu}^2\right) + \frac{h_1}{2}\mathrm{Tr}(\Phi^\dagger\Phi)\ \mathrm{Tr}(L_\mu L^\mu + R_\mu R^\mu) + h_2\mathrm{Tr}(\Phi^\dagger L_\mu L^\mu\Phi + \Phi R_\mu R^\mu\Phi^\dagger) \\ &+ 2h_3\mathrm{Tr}(\Phi R_\mu\Phi^\dagger L^\mu) + \dots\,, \end{aligned} \tag{3.7}$$

where

$$\mathcal{L}_{dil} = \frac{1}{2}(\partial^\mu G)^2 - \frac{1}{4}\frac{m_G^2}{\Lambda_{dil}^2}G^4\left(\ln\left|\frac{G}{\Lambda_{dil}}\right| - \frac{1}{4}\right)\,. \tag{3.8}$$

This Lagrangian follows from the Lagrangian (2.104) by setting

$$h_{0S} = \Delta = E = 0\,, \tag{3.9}$$

see Eqs. (2.95), (2.98), and (2.101).

3.1.1 Assignment of the fields in the $N_f = 2$ eLSM

The multiplets in the (pseudo)scalar and (axial-)vector sector of the eLSM in the case of $N_f = 2$ read explicitly:

$$\Phi = (\sigma_N + i\eta_N)\,t^0 + (\vec{a}_0 + i\vec{\pi})\cdot\vec{t}\,, \tag{3.10}$$

$$\Phi^\dagger = (\sigma_N - i\eta_N)\,t^0 + (\vec{a}_0 - i\vec{\pi})\cdot\vec{t}\,, \tag{3.11}$$

$$L^\mu = (\omega_N^\mu + f_{1N}^\mu)\,t^0 + (\vec{\rho}^\mu + \vec{a}_1^\mu)\cdot\vec{t}\,, \tag{3.12}$$

$$R^\mu = (\omega_N^\mu - f_{1N}^\mu)\,t^0 + (\vec{\rho}^\mu - \vec{a}_1^\mu)\cdot\vec{t}\,, \tag{3.13}$$

where t^0, $\vec{t}$ are the generators of the group $U(2)$. The assignment of the fields to the physical resonances listed in Ref. [11] corresponds to those discussed in section 2.4. The main difference to the eLSM with $N_f = 3$ is that only fields composed of *up* and *down* quarks are present. This implies that e.g. in the pseudoscalar-isoscalar sector only the pure field η_N occurs, which corresponds to the $SU(2)$ counterpart of the η meson. The mass of η_N, which is about 700 MeV [200, 157], can be obtained by *'unmixing'* the physical η and $\eta'(958)$ mesons which both contain $\bar{s}s$ contributions, see Eq. (2.110). As shown in Ref.[80], the σ_N field should be interpreted as a predominantly $\bar{q}q$ state because its decay width decreases as N_c^{-1} in the limit of a large number of colors. In the scalar-isoscalar sector only two fields, σ_N and G, are present, thus a mixing of two $0^+(0^{++})$ states takes place. The physical fields σ' and G' are obtained through an $SO(2)$ rotation, as we will show in the following. Then the assignments

$$\{\sigma', G'\} \equiv \{f_0(1370), f_0(1500)\}\,, \quad \{\sigma', G'\} \equiv \{f_0(1370), f_0(1710)\} \tag{3.14}$$

as well as

$$\{\sigma', G'\} \equiv \{f_0(500), f_0(1500)\} \ , \quad \{\sigma', G'\} \equiv \{f_0(500), f_0(1710)\} \tag{3.15}$$

will be discussed.

3.1.2 Explicit symmetry breaking terms

In the case of $N_f = 2$ the leading-order term which describes the explicit breaking of the chiral symmetry in the (pseudo)scalar sector reads

$$\mathrm{Tr}[H(\Phi + \Phi^\dagger)] \equiv h_N \sigma_N \ , \tag{3.16}$$

where

$$H = \mathrm{diag}(h_N, h_N) \tag{3.17}$$

and

$$h_N = const. \propto m_{q_N} \ , \tag{3.18}$$

which allows us to take into account the non-vanishing value m_q of the current quark mass. This term contains the dimensionful parameter h_N with $[h_N] = [\mathrm{energy}^3]$ and also explicitly breaks dilatation invariance, just as the quark masses do in the underlying QCD Lagrangian. Finally, the chiral anomaly is described by the term [183]:

$$c\,(\det\Phi + \det\Phi^\dagger) \ . \tag{3.19}$$

For $N_f = 2$ the parameter c carries the dimension $[\mathrm{energy}^2]$ and represents a further breaking of dilatation invariance. This term arises from instantons, which are also a property of the Yang-Mills sector of QCD.

3.1.3 Lagrangian, masses, and mixing matrix of the scalar-isoscalar fields in the case $N_f = 2$

In order to study the non-vanishing vev's of the two 0^{++} isoscalar fields, σ_N and G, of the $N_f = 2$ model we set all the other fields of the Lagrangian (3.7) to zero and obtain

$$\begin{aligned}\mathcal{L}_{\sigma_N G} &= \frac{1}{2}(\partial^\mu G)^2 - \frac{1}{4}\frac{m_G^2}{\Lambda_{dil}^2} G^4 \left(\ln\left|\frac{G}{\Lambda_{dil}}\right| - \frac{1}{4}\right) \\ &\quad + \frac{1}{2}(\partial^\mu \sigma_N)^2 - \frac{1}{2}\left[m_0^2\left(\frac{G}{G_0}\right)^2 - c\right]\sigma_N^2 - \frac{1}{4}\left(\lambda_1 + \frac{\lambda_2}{2}\right)\sigma_N^4 + h_N \sigma_N \ .\end{aligned} \tag{3.20}$$

Upon shifting the fields by their vev's, $\sigma_N \to \sigma_N + \phi_N$ and $G \to G + G_0$, and expanding the potential of $\mathcal{L}_{\sigma_N G}$ (3.20) up to second order, we obtain the bare masses of the states [1, 80],

$$m_{\sigma_N}^2 = m_0^2 - c + 3\left(\lambda_1 + \frac{\lambda_2}{2}\right)\phi_N^2 \ , \tag{3.21}$$

$$M_G^2 = m_0^2 \frac{\phi_N^2}{G_0^2} + m_G^2 \frac{G_0^2}{\Lambda_{dil}^2}\left(1 + 3\ln\left|\frac{G_0}{\Lambda_{dil}}\right|\right) \ . \tag{3.22}$$

The pure glueball mass M_G depends also on the quark condensate ϕ_N, but correctly reduces to m_G in the limit $m_0^2 = 0$, i.e., when quarkonium and glueball decouple. In the presence of quarkonia, $m_0^2 \neq 0$, the vev G_0 is given by the equation

$$-\frac{m_0^2 \phi_N^2 \Lambda_{dil}^2}{m_G^2} = G_0^4 \ln\left|\frac{G_0}{\Lambda_{dil}}\right| , \tag{3.23}$$

which implies that $G_0 \gtrsim \Lambda_{dil}$. For large values of Λ_{dil} one has $G_0 \simeq \Lambda_{dil}$, while for small values G_0 can be somewhat larger than Λ_{dil}. The shift of the fields by their vev's introduces a bilinear mixing term $\propto \sigma_N G$ in the Lagrangian (3.7), such that mass term of the tree-level potential reads

$$V^{(2)}_{\sigma_N G} = \frac{1}{2}\Sigma^T M \Sigma , \tag{3.24}$$

with

$$M \equiv \begin{pmatrix} m^2_{\sigma_N} & 2m_0^2\phi_N G_0^{-1} \\ 2m_0^2\phi_N G_0^{-1} & M_G^2 \end{pmatrix} , \quad \Sigma \equiv \begin{pmatrix} \sigma_N \\ G \end{pmatrix} . \tag{3.25}$$

Performing a diagonalization, which corresponds to an $SO(2)$ rotation, yields the diagonal matrix

$$M' = BMB^T \tag{3.26}$$

with the masses of the physical fields σ'_N and G'

$$m^2_{\sigma'_N} = m^2_{\sigma_N}\cos^2\theta + M_G^2 \sin^2\theta + 2\, m_0^2 \frac{\phi_N}{G_0}\sin(2\theta) , \tag{3.27}$$

$$M^2_{G'} = M_G^2 \cos^2\theta + m^2_{\sigma_N}\sin^2\theta - 2\, m_0^2 \frac{\phi_N}{G_0}\sin(2\theta) . \tag{3.28}$$

The orthogonal transformation matrix

$$B = \begin{pmatrix} \cos\theta & \sin\theta \\ -\sin\theta & \cos\theta \end{pmatrix} \tag{3.29}$$

links the pure scalar-isoscalar fields to the physical resonances as follows

$$\Sigma' = \begin{pmatrix} \sigma'_N \\ G' \end{pmatrix} = B\,\Sigma = B \begin{pmatrix} \sigma_N \\ G \end{pmatrix} . \tag{3.30}$$

The corresponding mixing angle θ reads

$$\theta = \frac{1}{2}\arctan\left(-4\,\frac{\phi_N}{G_0}\,\frac{m_0^2}{M_G^2 - m^2_{\sigma_N}}\right) . \tag{3.31}$$

The quantity m_0^2 can be calculated from the masses of the pion, η_N, and the bare σ_N mass [80]

$$m_0^2 = \left(\frac{m_\pi}{Z}\right)^2 + \frac{1}{2}\left[\left(\frac{m_{\eta_N}}{Z}\right)^2 - m^2_{\sigma_N}\right] . \tag{3.32}$$

If $m_0^2 - c < 0$, spontaneous breaking of chiral symmetry is realized.

3.1.4 Parameters of the $N_f = 2$ eLSM

The Lagrangian of the eLSM in the case of two flavors (3.7) contains the following twelve free parameters [1, 2, 17]:

$$m_0, \lambda_1, \lambda_2, m_1, g_1, c, h_N, h_1, h_2, h_3, m_G, \Lambda_{dil} = \sqrt{11}\, C^2/(2m_G) \,. \tag{3.33}$$

The processes that we shall consider depend only on the combination $h_1 + h_2 + h_3$, thus reducing the number of parameters to ten. We replace the set of ten parameters by the following equivalent set

$$m_\pi \,,\, m_{\eta_N} \,,\, m_\rho \,,\, m_{a_1} \,,\, \phi_N \,,\, Z_\pi \,,\, m_{\sigma_N} \,,\, m_G \,,\, m_1 \,,\, C \,. \tag{3.34}$$

The masses $m_\pi = 139.57$ MeV and $m_\rho = 775.49$ MeV are fixed to their PDG values [11]. As outlined in Refs. [80, 201], the mass of the η_N meson can be calculated by using the mixing of strange and non-strange contributions in the physical fields η and $\eta'(958)$, of Eq. (2.110). Here we use $\varphi_\eta \simeq -36^\circ$ [200], which corresponds to the value $m_{\eta_N} = 716$ MeV. Given the well-known uncertainty of the value of the angle φ_η, one could also consider other values, e.g., $\varphi_\eta = -41.4^\circ$, as published by the KLOE Collaboration [157], which corresponds to $m_{\eta_N} = 755$ MeV. Variations of the pseudoscalar mixing angle affect the results presented in this chapter only slightly. The value of m_{a_1} is fixed to 1050 MeV according to the study of Ref. [202]. We stress that taking the present PDG estimate of 1230 MeV does not change the quality of our results. The chiral condensate is fixed as

$$\phi_N = Z_\pi f_\pi \tag{3.35}$$

and the renormalization constant Z_π is determined by the study of the process $a_1 \to \pi\gamma$ where $Z_\pi = 1.67 \pm 0.2$ [80].

Then, we are left with the following four free parameters

$$C \,,\, m_{\sigma_N} \,,\, m_G \,,\, m_1 \,, \tag{3.36}$$

where C parametrizes the gluon condensate (1.134), m_{σ_N} and m_G are the bare masses of the 0^{++} isoscalar fields (3.21) and (3.22), and m_1 is the mass parameter of the (axial-)vector fields. For these parameters a fit was performed which depends on the chosen assignment in the detailed discussion later on.

3.2 Results and Discussion

3.2.1 Assigning σ'_N and G' to $f_0(1370)$ and $f_0(1500)$

The σ'_N field denotes an isoscalar $J^{PC} = 0^{++}$ state and its assignment to a physical state is a long-debated problem of low-energy QCD [52, 53, 54, 55, 56, 57, 58, 60, 115, 116, 117, 133, 134, 138, 145, 146, 147, 203, 204, 205, 206]. The two major candidates are the resonances $f_0(500)$ and the $f_0(1370)$ [11]. The study of Ref. [80] has shown that $f_0(1370)$ is favoured to be a state which is predominantly $\bar{q}q$. As stated above, the resonance $f_0(1500)$ is a convincing glueball candidate [80]. For these reasons we first test the scenario

$$\{\sigma', G'\} \equiv \{f_0(1370), f_0(1500)\} \,, \tag{3.37}$$

which turns out to be phenomenologically feasible in the eLSM in the case $N_f = 2$ [1, 17].

The χ^2 analysis for the scenario $\{\sigma', G'\} \equiv \{f_0(1370), f_0(1500)\}$

In order to determine the free parameters we use the χ^2 analysis and perform a fit. In this case we fit the four free parameters listed in Eq. (3.36) to five experimental quantities. As experimental input we utilize the masses of the two scalar-isoscalar resonances [11], where we use for the mass of $f_0(1370)$ the mean value

$$m^{ex}_{\sigma'_N} = (1350 \pm 150)\ \text{MeV} \tag{3.38}$$

and

$$m_{G'} \equiv m_{f_0(1500)} = (1505 \pm 6)\ \text{MeV}\ . \tag{3.39}$$

Furthermore, we use the three well-known decay widths of the well-measured resonance $f_0(1500)$: $f_0(1500) \to \pi\pi$, $f_0(1500) \to \eta\eta$, and $f_0(1500) \to KK$.

Note that, although our framework is based on $N_f = 2$, we can calculate the amplitudes for the decays into mesons containing strange quarks by making use of the flavor symmetry $SU_f(3)$ [207, 208, 209]. It is then possible to calculate the following $f_0(1500)$ decay widths into pseudoscalar mesons containing s-quarks: $f_0(1500) \to KK$, $f_0(1500) \to \eta\eta$, and $f_0(1500) \to \eta\eta'$. The χ^2 method yields

$$\chi^2/d.o.f. = 0.29\ . \tag{3.40}$$

The values of the parameters and the masses as well as the decay widths of the scalar-isoscalar resonances are given in Tables 3.1 and 3.2, which correspond to the solution in which $\sigma'_N \equiv f_0(1370) \cong (\bar{u}u+\bar{d}d)/\sqrt{2}$ is predominantly a non-strange $\bar{q}q$ state and $G' \equiv f_0(1500)$ predominantly a glueball state.

Parameter	**Value [MeV]**
C	699 ± 40
m_{σ_N}	1275 ± 30
m_G	1369 ± 26
m_1	809 ± 18

Table 3.1: Parameters obtained from the fit with the solution: $\{\sigma'_N, G'\} \equiv \{f_0(1370), f_0(1500)\}$.

We have also examined the uniqueness of our fit for this assignment [1]. To this end, we have considered χ^2 by fixing three of the four parameters entering the fit at their best values and varying the remaining fourth parameter. In each of the four cases we observe only one minimum of the χ^2 function, see Figures 3.1-3.4. Each minimum leads exactly to the parameter values stated in Table 3.1. We also observe no changes of the results for the errors of the parameters. These findings give us confidence that the obtained minimum corresponds to the absolute minimum of the χ^2 function.

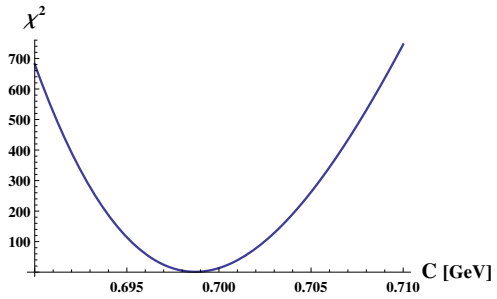

Figure 3.1: χ^2 as a function of the parameter C.

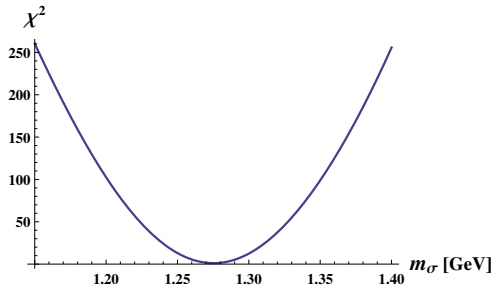

Figure 3.2: χ^2 as a function of the parameter m_σ.

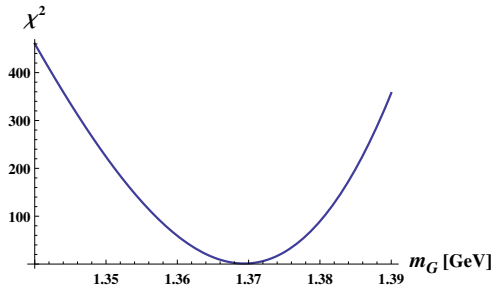

Figure 3.3: χ^2 as a function of the bare glueball mass m_G.

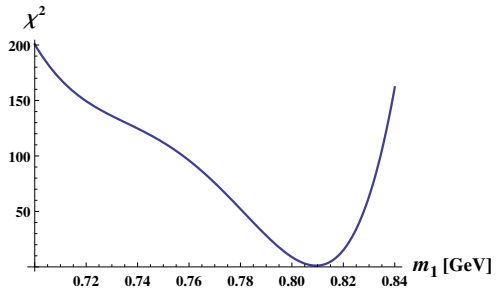

Figure 3.4: χ^2 as a function of the parameter m_1.

Quantity	Fit [MeV]	Experiment [MeV]
$m_{\sigma'_N}$	1191 ± 26	1200-1500
$m_{G'}$	1505 ± 6	1505 ± 6
$G' \to \pi\pi$	38 ± 5	38.04 ± 4.95
$G' \to \eta\eta$	5.3 ± 1.3	5.56 ± 1.34
$G' \to KK$	9.3 ± 1.7	9.37 ± 1.69

Table 3.2: Fit in the scenario $\{\sigma',\, G'\} = \{f_0(1370),\, f_0(1500)\}$. Note that, the $f_0(1370)$ mass ranges between 1200 MeV and 1500 MeV [11] and therefore, as an estimate, we are using the value $m_{\sigma'} = (1350 \pm 150)$ MeV in the fit.

Consequences of the χ^2 analysis for the solution $\{\sigma'_N, G'\} \equiv \{f_0(1370), f_0(1500)\}$

- The quarkonium-glueball mixing angle reads

$$\theta = (29.7 \pm 3.6)^\circ \,. \tag{3.41}$$

  This, in turn, implies that the resonance $f_0(1500)$ consists to 76% of a glueball and to the remaining 24% of a quark-antiquark state. The inverse is true for $f_0(1370)$.

- Our fit allows us to determine the gluon condensate:

$$C = (699 \pm 40) \text{ MeV} \,. \tag{3.42}$$

  This result implies that the upper value in Eq. (1.135) is favored by our analysis. It is interesting that insights into this basic quantity of QCD can be obtained from the PDG data on mesons.

- Further results for the $f_0(1500)$ meson are reported in the first two entries of Table 3.3. The decay into 4π is calculated as a product of an intermediate $\rho\rho$ decay. To this end the usual integration over the ρ spectral function is performed [80]. Our result yields 30 MeV in the 4π decay channel and is about half of the experimental value

$$\Gamma_{f_0(1500)\to 4\pi} = (54.0 \pm 7.1) \text{ MeV} \,. \tag{3.43}$$

  However, it should be noted that an intermediate state consisting of two $f_0(500)$ mesons, which is also expected to contribute in this decay channel, is not included in the present model. The decay into the $\eta\eta'$ channel is also evaluated, see Table 3.3. This channel is subtle because it is exactly on the threshold of the $f_0(1500)$ mass, namely [11]

$$m_\eta + m_{\eta'} = 1505.642 \text{ MeV} \,. \tag{3.44}$$

  Therefore, an integration over the spectral function of the decaying meson $f_0(1500)$ is necessary. The result is in a qualitative agreement with the experiment, see Table 3.3.

- The results for the $f_0(1370)$ meson are reported in the last four rows of Table 3.3. They are in agreement with the experimental data regarding the full width [11]:

$$\Gamma_{f_0(1370)} = (200 - 500) \text{ MeV} \,. \tag{3.45}$$

Unfortunately, the experimental results in the different channels are not yet conclusive. Our theoretical results point towards a dominant direct $\pi\pi$ and a non-negligible $\eta\eta$ contribution. These results correspond well to the experimental analysis of Ref. [210] where

$$\Gamma_{f_0(1370)\to\pi\pi} = 325 \text{ MeV} \tag{3.46}$$

and

$$\frac{\Gamma_{f_0(1370)\to\eta\eta}}{\Gamma_{f_0(1370)\to\pi\pi}} = 0.19 \pm 0.07 \tag{3.47}$$

are obtained. We find that the four-pion decay of

$$f_0(1370) \to \rho\rho \to 4\pi \tag{3.48}$$

is strongly suppressed, as was also found in Ref. [80]. This is unlike Ref. [210], where a small but non-negligible value of about 50 MeV is found. However, it should be noted that due to interference effects our result for this decay channel varies strongly when the parameters are even slightly modified.

- The mass of the ρ meson can be expressed as

$$m_\rho^2 = m_1^2 + \phi^2 \left(h_1 + h_2 + h_3\right)/2 \,. \tag{3.49}$$

In order that the contribution of the chiral condensate is not negative, the condition $m_1 \leq m_\rho$ should hold. In the framework of our fit this condition is fulfilled at the two-sigma level. This result points towards a dominant m_1 contribution to the ρ mass. This property, in turn, means that the ρ mass is predominantly generated from the gluon condensate and not from the chiral condensate. It is therefore expected that the ρ mass in the medium scales as the gluon condensate rather than as the chiral condensate [211]. In view of the fact that m_1 is slightly larger than m_ρ we have also repeated the fit by fixing $m_1 = m_\rho$. The minimum has a $\chi^2/$ d.o.f. $\simeq 1$ and the results are very similar to the previous case. The corresponding discussion about the phenomenology is unchanged. As we shall see, this result is confirmed in the full $N_f = 3$ case [3], see chapter four.

- As already stressed in Refs. [80, 212], the inclusion of (axial-)vector mesons plays a central role to obtain the present results. The artificial decoupling of (axial-)vector states would generate a by far too wide $f_0(1370)$ state. For this reason the glueball-quarkonium mixing scenario above 1 GeV has been previously studied only in phenomenological models with flavor symmetry [60, 115, 116, 117, 207, 208, 209] but not in the context of chirally invariant models.

Further tests of the stability of the fit

Given that the resonance $f_0(1370)$ has a large mass uncertainty, we have also examined the behaviour of the fit at different points of the PDG mass interval [1]. Considering the minimal value $m^{\min}_{f_0(1370)} = (1220 \pm 20)$ MeV we obtain $\chi^2 = 0.2/d.o.f.$ The resulting value of the mixing

Decay Channel	Our Value [MeV]	Experiment [MeV]
$G' \to \rho\rho \to 4\pi$	30	54.0 ± 7.1
$G' \to \eta\eta'$	0.6	2.1 ± 1.0
$\sigma'_N \to \pi\pi$	284 ± 43	-
$\sigma'_N \to \eta\eta$	72 ± 6	-
$\sigma'_N \to KK$	4.6 ± 2.1	-
$\sigma'_N \to \rho\rho \to 4\pi$	0.09	-

Table 3.3: Further results regarding the $\sigma'_N \equiv f_0(1370)$ and $G' \equiv f_0(1500)$ decays.

angle $\theta = (30.3 \pm 3.4)^\circ$ is practically the same as the value $\theta = (29.7 \pm 3.6)^\circ$ obtained in the case where $m_{f_0(1370)} = (1350 \pm 150)$ MeV was considered. Other results are also qualitatively similar to the case of $m_{f_0(1370)} = (1350 \pm 150)$ MeV. For the upper boundary of the $f_0(1370)$ mass, the error interval of ± 20 MeV turns out to be too restrictive as it leads to unacceptably large χ^2 values. Consequently, increasing the error interval decreases the χ^2 values – we observe that $m^{\max}_{f_0(1370)} = (1480 \pm 120)$ MeV leads to an acceptable χ^2 value of 1.14 . Consequently, we obtain $\theta = (30.0 \pm 3.5)^\circ$, practically unchanged in comparison with the value $\theta = (29.7 \pm 3.6)^\circ$ in the case where $m_{f_0(1370)} = (1350 \pm 150)$ MeV. Also other quantities remain basically the same as in the case of $m_{f_0(1370)} = (1350 \pm 150)$ MeV.

We have also considered the fit at several points between the lower and upper boundaries of the $m_{f_0(1370)}$ mass range. We have chosen points of 50 MeV difference starting at $m_{f_0(1370)} = 1250$ MeV (i.e., we have considered $m_{f_0(1370)} \in \{1250, 1300, 1350, 1400, 1450\}$ MeV) with errors chosen such that the $\chi^2/d.o.f.$ becomes minimal (error values are between ± 30 MeV for $m_{f_0(1370)} = 1250$ MeV and ± 100 MeV for $m_{f_0(1370)} = 1450$ MeV). We observe that the previous results presented in this section do not change significantly. Most notably, the mixing angle θ attains values between 30.2° and 30.7°, with an average error value of $\pm 3.4^\circ$.

We therefore conclude that considering different values of $m_{f_0(1370)}$ within the (1200-1500) MeV interval does not change the results significantly. In particular, the quarkonium-glueball mixing angle θ changes only slightly, by approximately 1°, and thus we confirm our conclusion that in the present scenario $f_0(1370)$ is predominantly a quarkonium and $f_0(1500)$ is predominantly a glueball.

3.2.2 Assigning σ'_N and G' to $f_0(1370)$ and $f_0(1710)$

A further glueball candidate is the resonance $f_0(1710)$ which was studied in a variety of works [207, 213, 214, 215, 216, 217]. This resonance is narrow and has a mass of $m_{f_0(1710)} = (1720 \pm 6)$ MeV which corresponds well to the scalar glueball mass predicted by lattice QCD in quenched approximation [55].

The χ^2 analysis for the scenario $\{\sigma', G'\} \equiv \{f_0(1370), f_0(1710)\}$

The resonance $f_0(1710)$ is experimentally well known. Decays into $\pi\pi$, KK, and $\eta\eta$ have been seen, while no decays into $\eta\eta'$ and into 4π have been detected. Using the total decay width $\Gamma_{f_0(1710)} = (135 \pm 8)$ MeV and the branching ratios reported in Ref. [11] it is possible to deduce the decay widths into $\pi\pi$, KK, and $\eta\eta$ presented in Table 3.5.

A fit analogous to the one in Table 3.2 yields too large errors for the decay width $\sigma'_N \equiv f_0(1370) \to \pi\pi$. For this reason we repeat our fit by adding the following constraint

$$\Gamma_{\sigma'_N \to \pi\pi} = (250 \pm 150) \text{ MeV} . \tag{3.50}$$

The large error assures that this value is in agreement with experimental data on this decay width. The χ^2 fit yields

$$\chi^2/d.o.f. = 1.72 . \tag{3.51}$$

The corresponding parameters and the fitted experimental quantities are reported in Table 3.4 and 3.5, respectively. The mixing angle between the pure quarkonium σ_N and the pure glueball G calculated from Eq. (3.31) is

$$\theta = (37.2 \pm 21.4)^\circ . \tag{3.52}$$

The χ^2 is worse than in the previous case, but the overall agreement is acceptable. The mixing angle is large and could also overshoot the value of 45°, which would imply a somewhat unexpected and unnatural reversed ordering, in which $f_0(1370)$ is predominantly glueball and $f_0(1710)$ predominantly quarkonium.

Parameter	**Value [MeV]**
C	764 ± 256
m_{σ_N}	1516 ± 80
m_G	1531 ± 233
m_1	827 ± 36

Table 3.4: Parameters obtained from the fit with the solution: $\{\sigma'_N, G'\} \equiv \{f_0(1370), f_0(1710)\}$.

Quantity	**Fit [MeV]**	**Experiment [MeV]**
$m_{\sigma'_N}$	1386 ± 134	1350 ± 150
$m_{G'}$	1720 ± 6	1720 ± 6
$G' \to \pi\pi$	29.7 ± 6.5	29.3 ± 6.5
$G' \to \eta\eta$	6.9 ± 5.8	34.3 ± 17.6
$G' \to KK$	16 ± 14	71.4 ± 29.1
$\sigma'_N \to \pi\pi$	379 ± 147	250 ± 150

Table 3.5: Fit in the scenario $\{\sigma', G'\} \equiv \{f_0(1370), f_0(1710)\}$.

Consequences of the χ^2 analysis for the solution $\{\sigma'_N, G'\} \equiv \{f_0(1370), f_0(1710)\}$

In Table 3.6 we report the decay widths $\Gamma_{G'\to\rho\rho\to 4\pi}$, $\Gamma_{G'\to\eta\eta'}$, $\Gamma_{\sigma'_N\to\eta\eta}$, and $\Gamma_{\sigma'_N\to KK}$, which can be calculated as a consequence of the fit of Table 3.5. A clear problem of this scenario is that the decay width

$$G' \equiv f_0(1710) \to \rho\rho \to 4\pi \tag{3.53}$$

is large, while experimentally it has not been seen. Therefore, we conclude that this scenario is slightly less favored than the previous one. Still, no final statement can be done. Indeed, as we will see in the next chapter, in a full $N_f = 3$ treatment, $f_0(1710)$ will be predominantly gluonic.

Decay Channel	**Our Value [MeV]**	**Experiment [MeV]**
$G' \to \rho\rho \to 4\pi$	115	-
$G' \to \eta\eta'$	16	-
$\sigma'_N \to \eta\eta$	153 ± 79	-
$\sigma'_N \to KK$	$2.1^{+13.6}_{-2.1}$	-

Table 3.6: Further results from the fit with $\{\sigma'$, $G'\} \equiv \{f_0(1370)$, $f_0(1710)\}$.

3.2.3 Assignments with $f_0(500)$ as σ'_N

Scenarios with $\sigma'_N \equiv f_0(600)$

The scenarios with the old data of Ref. [194] for $f_0(600)$

$$\{\sigma'_N, G'\} \equiv \{f_0(600), f_0(1500)\} \tag{3.54}$$

and

$$\{\sigma'_N, G'\} \equiv \{f_0(600), f_0(1710)\} \tag{3.55}$$

have also been tested. In both cases the mixing angle turns out to be smaller, $\theta \lesssim 15^\circ$, thus the state $f_0(600)$ is predominantly quarkonium. Then, in these cases the analysis of Ref. [80] applies: a simultaneous description of the $\pi\pi$ scattering lengths and the $\sigma_N \to \pi\pi$ decay width cannot be achieved. For these reasons the mixing scenarios with the resonance $f_0(600)$ as a quarkonium state are not favored.

Scenarios with $\sigma'_N \equiv f_0(500)$

We have also tested the assignments

$$\{\sigma'_N, G'\} \equiv \{f_0(500), f_0(1500)\} \tag{3.56}$$

and

$$\{\sigma'_N, G'\} \equiv \{f_0(500), f_0(1710)\} \tag{3.57}$$

using the new available experimental data of the $f_0(500)$ resonance [11]. We used for the calculation the mean value of its mass,

$$m^{ex}_{\sigma'_N} = (475 \pm 75)\ \text{MeV} . \tag{3.58}$$

In both assignments the mixing angle turns out to be small, $\theta \lesssim 13°$, and this implies that the state $f_0(500)$ is almost a pure quarkonium. The problem of these scenarios is that the decay into two pions is too narrow,

$$\Gamma_{\sigma'_N \to \pi\pi} \lesssim 180\ \text{MeV} , \tag{3.59}$$

as already found in Ref. [1], in comparison to the experimental one,

$$\Gamma_{f_0(500)\to\pi\pi} = (400 - 700)\ \text{MeV} . \tag{3.60}$$

We thus confirm our result in Ref. [1] that the scenarios with the resonance $f_0(500)$ as a quarkonium state are not favored. Note that we do not test any scenarios with the resonance $f_0(980)$ because as shown in Refs. [19, 80, 81] its interpretation as a quarkonium state is as well not favored. The resonances $f_0(500)$ and $f_0(980)$, which form a low lying scalar nonet, together with the isotriplet $a_0(980)$ and the isodoublet states $K_0^*(800)$, can be interpreted as tetraquark states and/or mesonic molecular states, see Refs. [133, 134, 135, 136, 137, 138, 139, 140, 141, 142, 143, 144, 145, 146, 147].

3.3 Final remarks

By the study of the mixing scenario within the eLSM in the case of two quark flavors we found two solutions. One solution exhibits the resonance $f_0(1500)$ being predominantly a glueball, in the other one $f_0(1710)$ was found to be predominantly gluonic. It should be stressed that the $N_f = 2$ treatment is not complete. The absence of the third bare field σ_S together with possible interference effects of the amplitudes are jointly responsible for inconclusive results. In order to obtain an unambiguous result a full study of the mixing scenario is required. This means that a study within a chiral approach with (axial-)vector quark-antiquark d.o.f. where the bare scalar-isoscalar fields σ_N and G as well as σ_S which generate $f_0(1370)$, $f_0(1500)$, and $f_0(1710)$ are present, must be performed. However, the resonance $f_0(1710)$ is actually even more favorable than $f_0(1500)$.

- Now, if the resonance $f_0(1500)$ is interpreted as predominantly a glueball then the following issues occur. Flavor blindness requires of a pure glueball state

$$\frac{\Gamma_{G\to\pi\pi}}{\Gamma_{G\to KK}} = \frac{3}{4} . \tag{3.61}$$

  This branching ratio reads for the two putative scalar glueball candidates

$$\frac{\Gamma_{f_0(1500)\to\pi\pi}}{\Gamma_{f_0(1500)\to KK}} = 4.06 \tag{3.62}$$

  and

$$\frac{\Gamma_{f_0(1710)\to\pi\pi}}{\Gamma_{f_0(1710)\to KK}} = 0.41 . \tag{3.63}$$

This shows that the requirement of flavor blindness is rather fulfilled by the resonance $f_0(1710)$ than $f_0(1500)$. Moreover, the errors of the decay widths of $f_0(1710)$ are sufficiently large to find a match between theoretical expectation and the experiment, see Table 3.5. This is not possible for the resonance $f_0(1500)$, see Table 3.2.

- Furthermore, lattice-QCD calculations predict on the one hand a scalar glueball mass of $m_G^{lat} \approx 1.7$ GeV which corresponds to the mass of $f_0(1710)$ [55, 216, 217]. On the other hand, the production rate in radiative J/ψ decay is higher for $f_0(1710)$ than $f_0(1500)$ [215]. This arguments support the scenario in which $G' \equiv f_0(1710)$. Indeed, a full $N_f = 3$ study confirms that $f_0(1710)$ is the glueball state to a good level of accuracy, see the next chapter.

Chapter 4

Mixing in the Scalar-Isoscalar Sector of the $N_f = 3$ eLSM

In this chapter we study the three-body mixing problem in the scalar-isoscalar sector of the eLSM with a scalar glueball in the case $N_f = 3$. The intention is to improve on the case $N_f = 2$ studied in the previous chapter, which could not clarify which resonance $f_0(1500$ or $f_0(1710)$ is predominantly gluonic. For that purpose we use the $N_f = 3$ version of the eLSM developed in Refs. [3, 19, 81] and follow Refs. [3, 4, 5].

The numerical results of the eLSM presented in this chapter are obtained from a *Mathematica* algorithm which was developed in Refs. [3, 4, 5] and this work.

4.1 Lagrangian, masses, and mixing matrix of the scalar-isoscalar fields

The essential difference with respect to the $N_f = 2$ case is that here we do not neglect the strange d.o.f., thus an additional condensate occurs which has a high impact on the phenomenology, as we will see in the following.

The three scalar-isoscalar fields σ_N, σ_S, and G are the only fields of the model with quantum numbers of the vacuum, $I^G(J^{PC}) = 0^+(0^{++})$. In order to study the vacuum expectation values (vev's) and the mixing behavior of these fields we set all other fields of the chiral Lagrangian (2.104) to zero and obtain the scalar-isoscalar Lagrangian

$$\begin{aligned}\mathcal{L}_{\sigma_N\sigma_S G} = \mathcal{L}_{dil} &+ \frac{1}{2}(\partial_\mu\sigma_N)^2 + \frac{1}{2}(\partial_\mu\sigma_S)^2 - \frac{m_0^2}{2}\left(\frac{G}{G_0}\right)^2\left(\sigma_N^2+\sigma_S^2\right)\\ &- \lambda_1\left(\frac{\sigma_N^2}{2}+\frac{\sigma_S^2}{2}\right)^2 - \frac{\lambda_2}{4}\left(\frac{\sigma_N^4}{2}+\sigma_S^4\right) + h_{\sigma_N}\sigma_N + h_{\sigma_S}\sigma_S - \frac{1}{2}\epsilon_S\sigma_S^2\,, \end{aligned} \tag{4.1}$$

where

$$\mathcal{L}_{dil} = \frac{1}{2}(\partial^\mu G)^2 - \frac{1}{4}\frac{m_G^2}{\Lambda_{dil}^2}G^4\left(\ln\left|\frac{G}{\Lambda_{dil}}\right| - \frac{1}{4}\right) . \tag{4.2}$$

Now we perform the shifts of the scalar-isoscalar fields by their vev's, $\sigma_N \to \sigma_N + \phi_N$, $\sigma_S \to \sigma_S + \phi_S$, and $G \to G + G_0$, in order to obtain the bare masses and the bilinear mixing terms $\propto \sigma_N\sigma_S$, $\propto \sigma_N G$, and $\propto \sigma_S G$. The bare masses of the non-strange and strange $\bar{q}q$ fields read

$$m_{\sigma_N}^2 = C_1 + 2\lambda_1\phi_N^2 + \frac{3}{2}\lambda_2\phi_N^2 , \quad m_{\sigma_S}^2 = C_1 + 2\lambda_1\phi_S^2 + 3\lambda_2\phi_S^2 + \epsilon_S , \tag{4.3}$$

where

$$C_1 = m_0^2 + \lambda_1\left(\phi_N^2 + \phi_S^2\right) \tag{4.4}$$

is a constant [81] (see Table 4.1),

$$\phi_N = Z_\pi f_\pi , \quad \phi_S = \frac{2Z_K f_K - \phi_N}{\sqrt{2}} , \tag{4.5}$$

are the condensates of the non-strange and strange quark-antiquark states, where $Z_{\pi/K}$ are the wave-function renormalization constants given in Eq. (2.132) and $f_{\pi/K}$ are the vacuum decay constants. The bare mass of the scalar glueball reads

$$M_G^2 = \frac{m_0^2}{G_0^2}\left(\phi_N^2 + \phi_S^2\right) + \frac{m_G^2 G_0^2}{\Lambda_{dil}^2}\left(1 + 3\ln\left|\frac{G_0}{\Lambda_{dil}}\right|\right) . \tag{4.6}$$

Note that the bare glueball mass also depends on the quark condensates ϕ_N and ϕ_S, but correctly reduces to m_G in the limit $m_0^2 = 0$, when quarkonia and the glueball decouple. When quarkonia couple to the glueball, $m_0^2 \neq 0$, the vev G_0 is given by the equation

$$-\frac{m_0^2\Lambda_{dil}^2}{m_G^2}\left(\phi_N^2 + \phi_S^2\right) = G_0^4 \ln\left|\frac{G_0}{\Lambda_{dil}}\right| . \tag{4.7}$$

This equation shows that $G_0 \gtrsim \Lambda_{dil}$. For large values of Λ_{dil} one has $G_0 \simeq \Lambda_{dil}$, while for small values G_0 can be somewhat larger than Λ_{dil}, see the analogous $N_f = 2$ equation. Note that here ϕ_S appears, but the coupling constant c is no longer present.

The contribution to the tree-level potential which is of second order in the fields reads

$$V^{(2)}_{\sigma_N\sigma_S G} = \frac{1}{2}\Sigma^T M \Sigma , \tag{4.8}$$

where

$$M \equiv \begin{pmatrix} m_{\sigma_N}^2 & 2\lambda_1\phi_N\phi_S & 2m_0^2\phi_N G_0^{-1} \\ 2\lambda_1\phi_N\phi_S & m_{\sigma_S}^2 & 2m_0^2\phi_S G_0^{-1} \\ 2m_0^2\phi_N G_0^{-1} & 2m_0^2\phi_S G_0^{-1} & M_G^2 \end{pmatrix} , \quad \Sigma \equiv \begin{pmatrix} \sigma_N \\ \sigma_S \\ G \end{pmatrix} . \tag{4.9}$$

Following the usual diagonalization procedure, an orthogonal matrix B is introduced such that the matrix $M' = BMB^T$ is diagonal. As a consequence, B links the bare scalar-isoscalar fields to the physical resonances

$$\begin{pmatrix} f_0(1370) \\ f_0(1500) \\ f_0(1710) \end{pmatrix} \equiv \Sigma' = \begin{pmatrix} \sigma'_N \\ \sigma'_S \\ G' \end{pmatrix} = B\,\Sigma = B\begin{pmatrix} \sigma_N \\ \sigma_S \\ G \end{pmatrix} . \tag{4.10}$$

4.2 Determination of the mixing matrix B: Preliminary studies

In the following section we present the determination of the scalar-isoscalar mixing matrix B.

4.2.1 Parameters of the model

In Ref. [81] a global fit was performed, in which 21 experimental quantities were fitted to eleven parameters of the eLSM. Due to their peculiar status, scalar-isoscalar mesons were not part of the fit. This allowed to exclude the coupling constants λ_1 and h_1 from the fit, which are large-N_c suppressed and therefore expected to be small. Since we are now explicitly interested in the scalar-isoscalar resonances, these two coupling constants must be considered, which brings the number of parameters to 13. Furthermore, in the fit of Ref. [81], the glueball was considered to be frozen. This approximation is justifiable in the large-N_c limit because the coupling of one scalar glueball to m ordinary mesons scales as $\propto N_c^{-m/2}$. In the present study the scalar glueball decay is non-zero, which introduces two additional parameters Λ_{dil} and m_G, so that we have 15 parameters. Moreover, there is an additional mass term $\propto \epsilon_S$, see Eq. (2.99), not present in the study of Ref. [81], and thus our chiral Lagrangian (2.104) contains 16 parameters. However, the parameter g_2, which is contained in the dots in Eq. (2.104), does not play any role in the present study. The reason is that only one two-body decay process which depends on g_2 is of interest: the intermediate decay $\rho \to \pi\pi$ of the full decay $f_0 \to \rho\rho \to 4\pi$, where an integration over the ρ spectral function is required and for the numerical calculations we use the corresponding experimental value $\Gamma_{\rho\to\pi\pi} \simeq 149$ MeV [11]. Hence, we can omit g_2 in the following, bringing the total number of relevant parameters to be fitted to 15

$$\Lambda_{dil}\ ,\ m_G\ ,\ m_0\ ,\ m_1\ ,\ \lambda_1\ ,\ \lambda_2\ ,\ h_1\ ,\ h_2\ ,\ h_3\ ,\ g_1\ ,\ c_1\ ,\ h_{0N}\ ,\ h_{0S}\ ,\ \delta_S\ ,\ \epsilon_S\ . \tag{4.11}$$

For the calculations in this work we use the values of the parameters entering the Lagrangian (2.104) , i.e., λ_2, h_2, h_3, g_1, c_1, h_{0N}, h_{0S}, δ_S, as well as the two combinations C_1, Eq. (4.4), and

$$C_2 = m_1^2 + \frac{h_1}{2}\left(\phi_N^2 + \phi_S^2\right) \tag{4.12}$$

determined in Ref. [81] and shown in Table 4.1.

Parameter	**Value**	**Parameter**	**Value**
C_1	-0.918×10^6 MeV^2	C_2	0.413×10^6 MeV^2
c_1	$450 \cdot 10^{-6}$ MeV^{-2}	δ_S	0.151×10^6MeV^2
g_1	5.84	λ_2	68.3
h_2	9.88	h_3	3.87
ϕ_N	164.6 MeV	ϕ_S	126.2 MeV

Table 4.1: Values of the parameters from Ref. [81].

Hence there are five free parameters remaining which enter into the Lagrangian (2.104) of Ref. [3]

$$\Lambda_{dil}\ ,\ m_G\ ,\ \lambda_1\ ,\ h_1\ ,\ \epsilon_S\ . \tag{4.13}$$

Moreover, in order to be consistent in this work we also use the values of the quantities given in Table 4.2 which results from the global fit of Ref. [81].

Quantity	**Fit [MeV]**	**Experiment [MeV]**
f_π	96.3 ± 0.7	92.2 ± 4.6
f_K	106.9 ± 0.6	110.4 ± 5.5
m_π	141 ± 5.8	137.3 ± 6.9
m_K	485.6 ± 3	495.6 ± 24.8
m_η	509.4 ± 3	547.9 ± 27.4
m_ρ	783.1 ± 7	775.5 ± 38.8
m_{a_1}	1186 ± 6	1230 ± 62
$m_{f_1(1420)}$	1372.5 ± 5.3	1426.4 ± 71.3

Table 4.2: Values of vacuum constants and masses from the global fit of Ref. [81].

4.2.2 Simplified procedure

In view of the fact that we started our study from the Lagrangian of the eLSM of Ref. [81] in which the mass parameter ϵ_S was not present, we first studied the simplified case with four parameters Λ_{dil}, m_G, λ_1, h_1. Equations (4.3) show that the masses of the pure fields σ_N and σ_S depend on λ_1 but not on h_1. The parameter h_1 occurs in the amplitudes of the scalar-isoscalar fields and is therefore only relevant when calculating the corresponding decay widths, see Appendix A. Moreover, the coupling constants λ_1 and h_1 occur in the model (2.104) in terms which contain a product of traces and are therefore large-N_c suppressed. Hence the couplings scale as N_c^{-2} and not as N_c^{-1}, and they are expected to be small.

We first focus on the determination of the mixing matrix by using the mass eigenvalues of the scalar-isoscalar fields, where the parameters Λ_{dil}, m_G, and λ_1 can be calculated by diagonalization of the mass matrix M of the tree-level potential (4.8). Where we consider both relevant assignments of the pure scalar-isoscalar fields to the resonances $f_0(1370)$, $f_0(1500)$, and $f_0(1710)$ [11], namely

$$\sigma_N \cong f_0(1370)\ ,\ \sigma_S \cong f_0(1500) \text{ and } G \cong f_0(1710) \tag{4.14}$$

and

$$\sigma_N \cong f_0(1370)\ ,\ \sigma_S \cong f_0(1710) \text{ and } G \cong f_0(1500)\ . \tag{4.15}$$

This should provide a first step as well as show the direction to determinate the final mixing matrix, because in this procedure an exact solution is expected. Afterwards, using the obtained parameters, the values of which are given in Table 4.3, as well as the mixing matrix (4.16) we can

try to describe the decays of the 0^{++} isoscalar fields for a small numerical range of the large-N_c suppressed coupling h_1.

If this simple approach will turn out unsatisfactory then a fit of the parameters Λ, m_G, λ_1, and h_1 should be performed.

Solution at the mass level

The numerical values of the free parameters presented in Table 4.3 have been obtained by requiring that the three following masses of the scalar-isoscalar fields [11] hold. For the mass of $f_0(1370)$ we use the mean value of the mass given in Ref. [11] $m_{f_0(1370)} = (1350 \pm 150)$ MeV, while for the two other masses we use the well-known values of $m_{f_0(1500)} = (1505 \pm 6)$ MeV and $m_{f_0(1710)} = (1720 \pm 6)$ MeV. It turns out that the resonances $f_0(1370)$ and $f_0(1500)$ are predominantly non-strange and strange $\bar{q}q$ states, and that the resonance $f_0(1710)$ is predominantly a scalar glueball. No other solution [e.g. for the other scenario (4.15)] was found.

Parameter	**Value**
Λ_{dil}	930 MeV
m_G	1580 MeV
λ_1	2.03

Table 4.3: Parameters obtained from calculating the mass eigenvalues of the scalar-isoscalar fields with the assignment: $\{\sigma_N', \sigma_S', G'\} \equiv \{f_0(1370), f_0(1500), f_0(1710)\}$ [4].

The mixing matrix corresponding to the parameters of Table 4.3 reads [4]

$$B = \begin{pmatrix} 0.92 & -0.05 & 0.39 \\ -0.22 & -0.89 & -0.40 \\ -0.33 & -0.45 & 0.83 \end{pmatrix}. \tag{4.16}$$

Testing the solution at the mass level by considering decays

We now test the mixing matrix (4.16) by evaluating the decay widths, where we use the parameters of Table 4.3. It turns out that using this solution it is not possible to describe the decay processes of the f_0 resonances into $\pi\pi$ and KK, as shown in Figures 4.1 - 4.6. These results are clearly *too large* and cannot be cured by varying the only remaining free parameter h_1, which should anyhow be small. Corresponding results in the large-N_c limit, for which $h_1 = 0$, are summarized in Table 4.4. Thus, the decay widths do not support this scenario as being physical. Note that such a large decay width of the predominantly glueball state is in agreement with the study of Ref. [128].

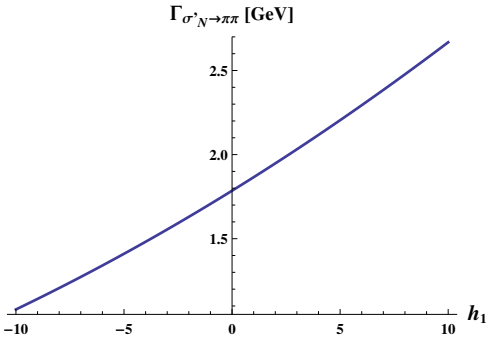

Figure 4.1: Decay of $\sigma'_N \to \pi\pi$ using the mixing matrix B of Ref. [4].

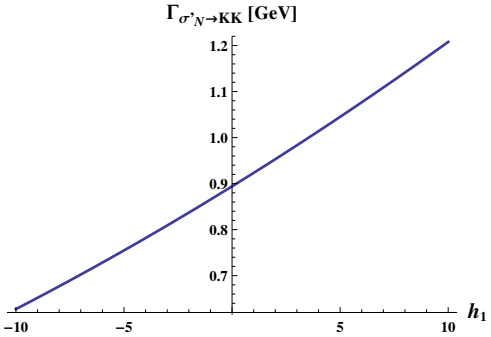

Figure 4.2: Decay of $\sigma'_N \to KK$ using the mixing matrix B of Ref. [4].

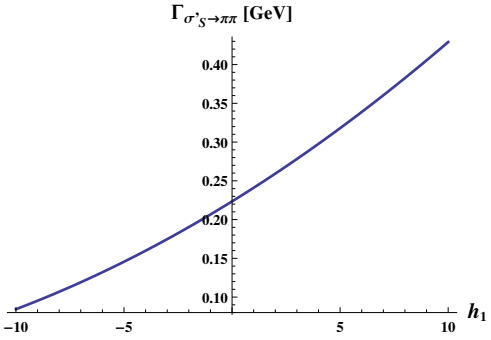

Figure 4.3: Decay of $\sigma'_S \to \pi\pi$ using the mixing matrix B of Ref. [4].

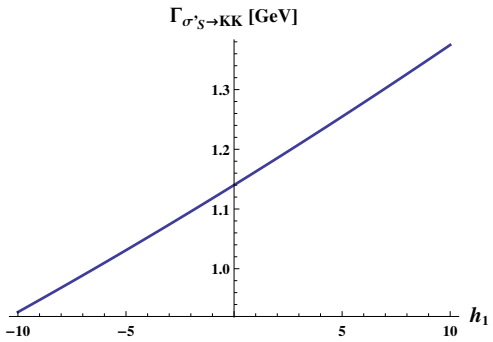

Figure 4.4: Decay of $\sigma'_S \to KK$ using the mixing matrix B of Ref. [4].

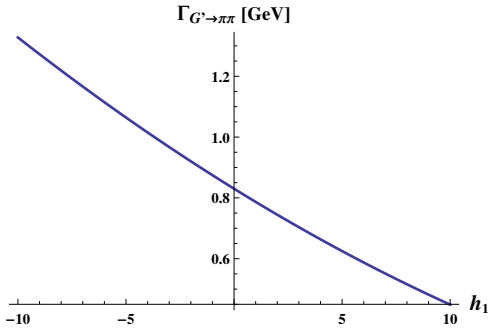

Figure 4.5: Decay of $G' \to \pi\pi$ using the mixing matrix B of Ref. [4].

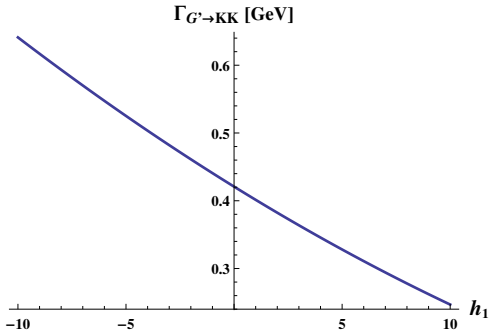

Figure 4.6: Decay of $G' \to KK$ using the mixing matrix B of Ref. [4].

Decay Channel	Our Value [MeV]	Experiment [MeV]
$f_0(1370) \to \pi\pi$	1785	-
$f_0(1370) \to KK$	894	-
$f_0(1500) \to \pi\pi$	830	38.04 ± 4.95
$f_0(1500) \to KK$	421	9.37 ± 1.69
$f_0(1710) \to \pi\pi$	223	29.3 ± 6.5
$f_0(1710) \to KK$	1140	71.4 ± 29.1

Table 4.4: Consequences of the solution at the mass level in the large-N_c limit, $h_1 = 0$, using Eq. (4.16) in which $\{\sigma'_N, \sigma'_S, G'\} \equiv \{f_0(1370), f_0(1500), f_0(1710)\}$ [4, 5].

Further discussion

The search for an acceptable solution is extremely difficult due to interference effects in the decay amplitudes. As an alternative approach, we use as an input the bare glueball mass $m_G = 1.7$ GeV in agreement with lattice QCD [52]. Then, due to the fact that $f_0(1710)$ was too broad in the previous solution, we increase the value of the dimensionful parameter Λ_{dil}. For the choice $\Lambda_{dil} \simeq 2$ GeV the resonance $f_0(1710)$ is sufficiently narrow. By further tuning $\lambda_1 \simeq -10$ and $h_1 \simeq -5$, we obtain the mixing matrix [5]

$$B = \begin{pmatrix} 0.90 & 0.41 & -0.05 \\ -0.42 & 0.90 & -0.03 \\ -0.04 & -0.05 & -0.99 \end{pmatrix}. \tag{4.17}$$

The resonance $f_0(1710)$ is (almost) a pure glueball. The masses and decay widths that are determined by these parameters are are still too large, see Table 4.5.

Quantity	Our Value [MeV]	Experiment [MeV]
$m_{f_0(1370)}$	1060	1200-1500
$m_{f_0(1500)}$	1480	1505 ± 6
$m_{f_0(1710)}$	1700	1720 ± 6
$f_0(1370) \to \pi\pi$	120	-
$f_0(1370) \to KK$	70	-
$f_0(1500) \to \pi\pi$	140	38.04 ± 4.95
$f_0(1500) \to KK$	130	9.37 ± 1.69
$f_0(1710) \to \pi\pi$	82	29.3 ± 6.5
$f_0(1710) \to KK$	64	71.4 ± 29.1

Table 4.5: Consequences of the solution (4.17), in which $\{\sigma'_N, \sigma'_S, G'\} \equiv \{f_0(1370), f_0(1500), f_0(1710)\}$ [5].

While the decays of $f_0(1370)$ and $f_0(1710)$ are at least in qualitative agreement with the experiment, this is not the case for $f_0(1500)$ for which the decays are still too large. Note

also that the quite large value of Λ_{dil} implies a large gluon condensate. Lattice-QCD results [96, 97, 98, 99, 100, 101, 102, 103, 104, 105] suggest that $\Lambda_{dil} \lesssim 0.6$ GeV, see the discussion in Ref. [1]. Thus, at this level this solution can point to an interesting direction where to look for it: a large bare glueball mass in agreement with lattice (1.7 GeV) and a large value of the gluon condensate. Another possibility is to improve the underlying effective model of Ref. [81], by studying the influence of a quadratic mass term in the (pseudo)scalar sector. This is a minimal change of Ref. [81], which however can have interesting phenomenological implications due to the fact that the strange current quark mass is not negligible. For a value of the gluon condensate in agreement with lattice QCD, a not too broad glueball can only be found if destructive interferences between the different amplitudes occur. This is why an improved numerical analysis, which allows to study in detail the whole parameter space, would also be helpful.

4.2.3 Decay of the pure glueball and the gluon condensate

In Figure 4.7 we anticipate our result for the decay of a pure, i.e., unmixed, scalar glueball into two pions as function of the vev G_0. For values of G_0 which belong to the range obtained by QCD sum rules and lattice QCD (the vertical band[1]), $G \to \pi\pi$ is also *very* large, in complete agreement with Ref. [128]. The two curves correspond to the cases with and without (axial-)vector states. One can see that the inclusion of (axial-)vector d.o.f. reduces the decay width, but this effect is not sufficient to make it small enough (when G_0 is inside the vertical band). When mixing is taken into account, due to interference phenomena the strong coupling of G to pions may be reduced for the physical resonances. Yet, since the quarkonium state $\bar{n}n$ is also expected to be broad, it is not possible to obtain two narrow resonances $f_0(1500)$ and $f_0(1710)$ in a three-body mixing scenario. Thus, we realize that we cannot obtain a good description of the phenomenology of the states $f_0(1370)$, $f_0(1500)$, and $f_0(1710)$ if we impose that G_0 corresponds to the range given by QCD sum rules or lattice QCD.

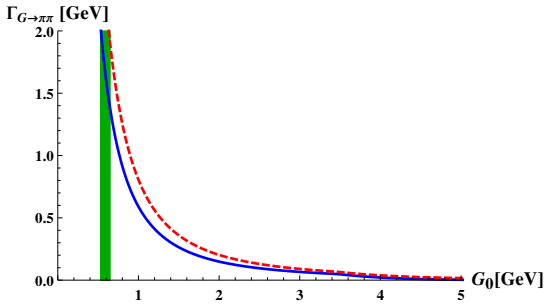

Figure 4.7: Decay of the pure glueball field into $\pi\pi$ for a bare glueball mass m_G = 1525 MeV. Dashed red line: (Axial-)vector mesons are decoupled (Z_π = 1). Solid blue line: (Axial-)vector mesons are included ($Z_\pi \neq 1$).

[1]The vertical band in Figure 1 is slightly shifted to the right when compared to the range of Λ_{dil} determined from Eqs. (1.135) and (2.26). This results from Eq. (4.7) which shows that $G_0 \gtrsim \Lambda_{dil}$. For large values of Λ_{dil} one has $G_0 \simeq \Lambda_{dil}$, while for small values G_0 can be somewhat larger than Λ_{dil}.

4.3 Determination of the mixing matrix B: The full study

In the following we present the full determination of the scalar-isoscalar mixing matrix B, where Λ_{dil} is fitted as well.

4.3.1 The χ^2 analysis

Using the χ^2 analysis,

$$\chi^2 \equiv \chi^2(x_i) = \sum_{j=1}^{8} \left(\frac{Q_j^{th}(x_i) - Q_j^{ex}}{\Delta Q_j^{ex}} \right)^2 \quad , \text{with } i = 1, \ldots, 5 \ , \tag{4.18}$$

we fit eight experimental quantities to the five parameters

$$x_i = \Lambda_{dil} \ , \ m_G \ , \ \lambda_1 \ , \ h_1 \ , \ \epsilon_S \tag{4.19}$$

of our chiral model summarized in Tables 4.6 and 4.7.

For the mass of $f_0(1370)$ we use the value $m_{f_0(1370)} = (1350 \pm 150)$ MeV and we increase the experimental errors of $m_{f_0(1500)} = (1505 \pm 6)$ MeV and $m_{f_0(1710)} = (1720 \pm 6)$ [11] to 5%. This procedure was also applied in Ref. [81], arguing that the precision of our model cannot be better than 5% since it does not account e.g. for isospin breaking effects. Moreover, in order to better constrain the fit we use the value $\Gamma_{f_0(1370)\to\pi\pi} = 325$ MeV [210] together with an estimated uncertainty of about 100 MeV, which is not given in Ref. [210]. The parameters in Table 4.6, for which

$$\chi^2/d.o.f. \approx 0.35 \tag{4.20}$$

was achieved, and the masses as well as the decay widths of the scalar-isoscalar resonances in Table 4.7 correspond to the solution in which $\sigma_N' \equiv f_0(1370) \cong (\bar{u}u + \bar{d}d)/\sqrt{2}$ is predominantly a non-strange, $\sigma_S' \equiv f_0(1500) \cong \bar{s}s$ predominantly a strange $\bar{q}q$ state, and $G' \equiv f_0(1710)$ predominantly a glueball state.

Parameter	**Value**
Λ_{dil}	3297 [MeV]
m_G	1525 [MeV]
λ_1	6.25
h_1	−3.22
ϵ_S	0.421×10^6 [MeV^2]

Table 4.6: Parameters obtained from the fit with the solution: $\{\sigma_N', \ \sigma_S', \ G'\} \equiv \{f_0(1370), \ f_0(1500), \ f_0(1710)\}$.

Quantity	Fit [MeV]	Experiment [MeV]
$m_{f_0(1370)}$	1444	1200-1500
$m_{f_0(1500)}$	1534	1505 ± 6
$m_{f_0(1710)}$	1750	1720 ± 6
$f_0(1370) \to \pi\pi$	423.6	-
$f_0(1500) \to \pi\pi$	39.2	38.04 ± 4.95
$f_0(1500) \to KK$	9.1	9.37 ± 1.69
$f_0(1710) \to \pi\pi$	28.3	29.3 ± 6.5
$f_0(1710) \to KK$	73.4	71.4 ± 29.1

Table 4.7: Fit with the solution: $\{\sigma_N', \sigma_S', G'\} \equiv \{f_0(1370), f_0(1500), f_0(1710)\}$.

The bare fields $\sigma_N \cong \left(\bar{u}u + \bar{d}d\right)/\sqrt{2}$, $\sigma_S \cong \bar{s}s$, and G generate the resonances $f_0(1370)$, $f_0(1500)$, and $f_0(1710)$, where the corresponding mixing matrix B, cf. Eq. (4.10), is given by

$$B = \begin{pmatrix} -0.91 & 0.24 & -0.33 \\ 0.30 & 0.94 & -0.17 \\ -0.27 & 0.26 & 0.93 \end{pmatrix} , \tag{4.21}$$

which implies the following admixtures of the bare fields to the resonances

$$\begin{aligned} f_0(1370): &\quad 83\%\,\sigma_N\,, \quad 6\%\,\sigma_S\,, \quad 11\%\,G\,, \\ f_0(1500): &\quad 9\%\,\sigma_N\,, \quad 88\%\,\sigma_S\,, \quad 3\%\,G\,, \\ f_0(1710): &\quad 8\%\,\sigma_N\,, \quad 6\%\,\sigma_S\,, \quad 86\%\,G\,. \end{aligned} \tag{4.22}$$

For other results of the mixing matrix B using different theoretical models, we refer to Refs. [20, 203, 204, 205, 207, 213, 214] and references therein. Moreover, our branching ratio

$$\frac{\Gamma_{f_0(1710)\to\pi\pi}}{\Gamma_{f_0(1710)\to KK}} = 0.39 \tag{4.23}$$

is very close to the experimental one

$$\frac{\Gamma_{f_0(1710)\to\pi\pi}}{\Gamma_{f_0(1710)\to KK}} = 0.41\,, \tag{4.24}$$

see Table 3.6. The branching ratio (4.23) is also in good agreement with those of Refs.[218, 219, 220]. Note that the resonance $f_0(1710)$ is not a pure glueball but contains quark-antiquark components, therefore the branching ratios (4.23) and (4.24) can differ from the expected one of a pure glueball

$$\frac{\Gamma_{G\to\pi\pi}}{\Gamma_{G\to KK}} = \frac{3}{4}\,. \tag{4.25}$$

For further approaches which favor the resonance $f_0(1710)$ as predominantly gluonic we refer to Refs. [215, 216, 217, 221, 222] and references therein.

4.3.2 Discussion of the χ^2 analysis

The parameters λ_1 and h_1 are small, in agreement with the large-N_c expectation (they scale as N_c^{-2} and not as N_c^{-1}). The numerical value $\Lambda_{dil} \approx 3.3$ GeV suppresses the quarkonium-glueball

mixing: this is why the admixtures in Eq. (4.22) are small.

In the pure Yang-Mills sector the vev of the dilaton field G is given by $G_0 = \Lambda_{dil}$. The numerical value $\Lambda_{dil} \approx 3.3$ GeV implies that the resulting gluon condensate in pure Yang-Mills theory, which is parametrized by the constant C defined in Eq. (1.134), reads $C \approx 1.8$ GeV, which is a factor 3 larger than the lattice value $C \approx 0.61$ GeV obtained in Ref. [105] in the quenched approximation. When quarks are included, the value of G_0 is such that $G_0 \approx \Lambda_{dil}$ to a very good level of precision, see Eq. (4.7). Similarly, using Eq. (4.6) the value of the bare glueball mass in the presence of quarks reads $M_G \approx m_G$. The fact that $G_0 \approx \Lambda_{dil}$ and $M_G \approx m_G$ is also a consequence of the large value of Λ_{dil}. For small $\Lambda_{dil} \lesssim 0.6$ GeV the differences are larger.

Our determination of the parameter C is based on the assumption that the glueball is narrow, see Figure 4.7 and the discussion in section 1.3. If this assumption does not hold, the glueball is very broad and would probably remain undetected. If, however, the narrow-glueball hypothesis is correct, our results imply that either (i) the value of the constant C cannot be directly compared to the corresponding one appearing in lattice QCD or QCD sum rules (which is entirely possible because there may be corrections to the tree-level Lagrangian (2.105) arising from renormalization), or (ii) that it is *not* allowed to assume that the dilaton field saturates the trace anomaly. In turn, Eqs. (2.22) and (2.24) would not hold and other contributions should appear in order to reconcile the mismatch.

The stability of the fit has been also tested by repeating the minimum search for different values of the parameters, by increasing or reducing the errors in some channels and by including and/or removing some experimental quantities. The same pattern has always been found: in all solutions the resonance $f_0(1710)$ is (by far) predominantly a glueball, while $f_0(1370)$ and $f_0(1500)$ are predominantly $(\bar{u}u + \bar{d}d)/\sqrt{2}$ and $\bar{s}s$ quark-antiquark states, respectively.

In the future, one should also go beyond the present two-step fit and perform a unique fit in which all 15 parameters (4.11) are determined at once. However, we do not expect large variations for the parameters determined in Ref. [81] and listed in Table 4.1 otherwise the agreement with mesonic masses and decays calculated in Ref. [81] would inevitably be spoiled.

4.3.3 Consequences of the χ^2 analysis

As a consequence of our fit we calculate the decay processes given in Table 4.8. We discuss our results in the following.

- At present, the different decay channels of the resonance $f_0(1370)$ are experimentally not yet well known because conflicting experimental results exist [11]. Only the full decay width is listed in Ref. [11]: $\Gamma^{exp}_{f_0(1370)} = (200 - 500)$ MeV. In our solution the dominant decay channel of $f_0(1370)$ is the one into two pions with a decay width of about 400 MeV. This corroborates that $f_0(1370)$ is predominantly a non-strange $\bar{q}q$ state as also found in Refs. [1, 80, 81]. The total decay width of $f_0(1370)$ obtained with the parameters of Table 4.6 is 598 MeV. In addition, we found non-negligible contributions from the decays

$f_0(1370) \to \eta\eta$ and $f_0(1370) \to \rho\rho \to 4\pi$, where in the latter case we have integrated over the corresponding ρ spectral function. These results are in qualitative agreement with the experimental analysis of Ref. [210], where

$$\Gamma_{f_0(1370)\to\pi\pi} = 325 \text{ MeV} , \tag{4.26}$$

$$\Gamma_{f_0(1370)\to 4\pi} \approx 50 \text{ MeV} , \tag{4.27}$$

and

$$\frac{\Gamma_{f_0(1370)\to\eta\eta}}{\Gamma_{f_0(1370)\to\pi\pi}} = 0.19 \pm 0.07 . \tag{4.28}$$

Note that the channel

$$f_0(1370) \to f_0(500) f_0(500) \to 4\pi \tag{4.29}$$

is not included in our model, so our determination of the 4π–decay mode is not complete.

- When omitting the quantity $\Gamma_{f_0(1370)\to\pi\pi}$ from the fit, a solution with a similar phenomenology is found. However, the state $f_0(1370)$ would be somewhat too wide (≈ 700 MeV.) This is why we have decided to include the value $\Gamma_{f_0(1370)\to\pi\pi} = 325$ MeV [210] in the fit.

- The decay channel $f_0(1500) \to \eta\eta$ turns out to be in good agreement with the experiment.

- Experimentally, there is also a sizeable contribution of the channel

$$f_0(1500) \to 4\pi : \Gamma^{exp}_{f_0(1500)\to 4\pi} = (54.0 \pm 7.1) \text{ MeV} . \tag{4.30}$$

  We have calculated the decay of $f_0(1500)$ into 4π only through the intermediate $\rho\rho$ state, as in the case of $f_0(1370)$ and $f_0(1710)$, respectively, including the ρ spectral function. We found that this decay channel is strongly suppressed. However, we expect a further and much larger contribution to this decay channel through the intermediate state of two $f_0(500)$ resonances, but $f_0(500)$ is not implemented in the present model.

- The decay channel $f_0(1710) \to \eta\eta$ is slightly larger than the experiment.

- In comparison with the $N_f = 2$ results of Ref. [1], we now find that the decay channel $f_0(1710) \to \rho\rho \to 4\pi$ is strongly suppressed. The reason is the scaling

$$\Gamma_{f_0(1710)\to\rho\rho\to 4\pi} \propto G_0^{-1} . \tag{4.31}$$

  This is indeed an important point: in Ref. [1] two scenarios were phenomenologically acceptable, one in which $f_0(1500)$ and one in which $f_0(1710)$ is predominantly a glueball. The latter case was, however, slightly disfavored because $\Gamma_{f_0(1710)\to\rho\rho\to 4\pi}$ was too large in virtue of the vev $G_0 \approx \Lambda_{dil}$, which was much smaller in that case. A solution of that type was possible because only one quarkonium existed and less experimental information was taken into account.

Decay Channel	**Our Value [MeV]**	**Experiment [MeV]**
$f_0(1370) \to KK$	117.5	–
$f_0(1370) \to \eta\eta$	43.3	–
$f_0(1370) \to \rho\rho \to 4\pi$	13.8	–
$f_0(1500) \to \eta\eta$	4.7	5.56 ± 1.34
$f_0(1500) \to \rho\rho \to 4\pi$	0.2	$> 54.0 \pm 7.1$
$f_0(1710) \to \eta\eta$	57.9	34.3 ± 17.6
$f_0(1710) \to \rho\rho \to 4\pi$	0.5	–

Table 4.8: Consequences of the fit with the solution: $\{\sigma'_N,\ \sigma'_S,\ G'\} \equiv \{f_0(1370),\ f_0(1500),\ f_0(1710)\}$.

Chapter 5

Pseudoscalar Glueball within the eLSM

In this chapter we present and discuss the results for the pseudoscalar glueball $\tilde{G}$, $J^{PC} = 0^{-+}$, following Refs. [6, 7, 8, 9]. The corresponding effective chiral interaction chiral Lagrangian

$$\mathcal{L}_{\tilde{G}}^{int} = ic_{\tilde{G}\Phi}\tilde{G}\left(\det\Phi - \det\Phi^{\dagger}\right) , \tag{5.1}$$

which we already introduced in chapter 2, enables us to study the decay widths for the processes $\tilde{G} \to PPP$ and $\tilde{G} \to PS$, where P and S are pseudoscalar and scalar quark-antiquark fields, respectively. Our intention is to study the properties of the pseudoscalar glueball in order to give a useful hints for an experimental search of this still undetected but theoretically expected state, e.g. the ongoing BESIII experiment [123] and the upcoming $\bar{\text{P}}$ANDA experiment at the FAIR facility near Darmstadt [124].

The numerical results of the pseudoscalar glueball within the eLSM presented in this chapter are obtained from a *Mathematica* algorithm which was developed in Refs. [6, 7, 8, 9] and this work, except for the calculations in (5.3.4) which have been done by Klaus Neuschwander in Ref. [223] and the calculations in (5.4) which have been done by Antje Peters in Ref. [224].

5.1 Implications of the chiral interaction Lagrangian $\mathcal{L}_{\tilde{G}}^{int}$

5.1.1 Assignment of the fields and the free parameter

For our calculations we fixed the mass of the pseudoscalar glueball to $m_{\tilde{G}} = 2.6$ GeV. This value is obtained by studying of the pure Yang-Mills sector in lattice QCD [52, 53, 54, 55, 56, 57]. The assignment of the (pseudo)scalar quark-antiquark fields of the multiplet Φ to the physical resonances corresponds to the discussion of section[1] 2.4. By evaluating the decays of the pseudoscalar glueball $\tilde{G}$ we have to take into account that the spontaneous breaking of chiral symmetry takes

[1]For the numerical calculations in this chapter we used for all masses the values of Ref. [11] as well as the standard values $f_\pi = 0.0922$ GeV and $f_K = 0.110$ GeV [11].

place. This implies the usual shift of the scalar-isoscalar fields as well as the procedure of eliminating the bilinear terms in the (axial-)vector sector which we already performed in chapter 2. Thus the chiral interaction Lagrangian (5.1) contains the relevant tree-level vertices for the two- and three-body decay processes of $\tilde{G}$, $\tilde{G} \to PPP$, and $\tilde{G} \to PS$, which are explicitly shown in Appendix B.1.

This chiral Lagrangian contains only one unknown coupling constant $c_{\tilde{G}\Phi}$, whose determination would require experimental data or a more microscopic model. The branching ratios can be calculated and do not depend on $c_{\tilde{G}\Phi}$: they are a clear prediction of the model and may present a useful guideline for experimental search of the pseudoscalar glueball in the energy region between 2 to 3 GeV. In this respect, the planned $\bar{\text{P}}$ANDA experiment at the FAIR facility [124] will be capable to scan the mass region above 2.5 GeV. The experiment is based on proton-antiproton scattering, thus the pseudoscalar glueball $\tilde{G}$ can be directly produced as an intermediate state. We shall therefore present our results for the branching ratios for a putative pseudoscalar glueball with a mass of 2.6 GeV.

On the other hand, it is also possible that the pseudoscalar glueball $\tilde{G}$ has a mass that is a bit lower than the lattice-QCD prediction and that it has been already observed in the BESIII experiment, where pseudoscalar resonances have been investigated in J/ψ decays [225, 226, 227]. In particular, the resonance $X(2370)$ which has been clearly observed in the $\pi^+\pi^-\eta'$ channel represents a good candidate, because it is quite narrow (~ 80 MeV) and its mass lies just below the lattice-QCD prediction. For this reason we repeat our calculation for a pseudoscalar glueball mass of 2.37 GeV, and thus make predictions for the resonance $X(2370)$, which can be tested in the near future.

5.1.2 Constraints on the coupling constant $c_{\tilde{G}\Phi}$

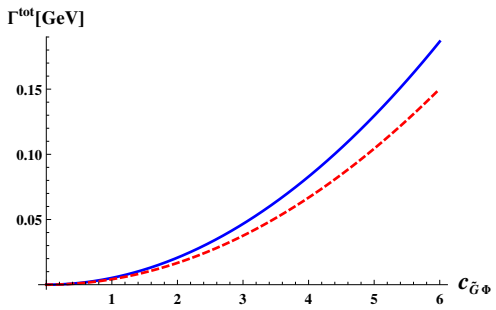

Figure 5.1: Solid (blue) line: Total decay width of the pseudoscalar glueball with the bare mass $m_{\tilde{G}}$= 2.6 GeV as function of the coupling constant $c_{\tilde{G}\Phi}$. Dashed (red) line: Same curve for $m_{\tilde{G}}$= 2.37 GeV [6].

As mentioned previously, the chiral interaction Lagrangian contains an unknown coupling constant which cannot be determined without experimental data. In Figure 5.1 we show the behavior

of the total decay width

$$\Gamma_{\tilde{G}}^{tot} = \Gamma_{\tilde{G}\to PPP} + \Gamma_{\tilde{G}\to PS} \tag{5.2}$$

as a function of the coupling constant $c_{\tilde{G}\Phi}$ for both choices of the pseudoscalar glueball mass. We assume here that other decay channels, such as decays into vector mesons or baryons are negligible. In the case of $m_{\tilde{G}} = 2.6$ GeV, one expects from large-N_c considerations that the total decay width

$$\Gamma_{\tilde{G}}^{tot} \lesssim 100 \text{ MeV} . \tag{5.3}$$

In fact, as discussed in the Introduction, the scalar glueball candidates $f_0(1500)$ and $f_0(1710)$ are roughly 100 MeV broad and the tensor candidate $f_J(2220)$ is even narrower. In the present work, the condition (5.3) implies that

$$c_{\tilde{G}\Phi} \lesssim 5 . \tag{5.4}$$

Moreover, in the case of $m_{\tilde{G}} = 2.37$ GeV in which the identification $\tilde{G} \equiv X(2370)$ has been made, we can indeed use the experimental knowledge on the full decay width

$$\Gamma_{X(2370)} = 83 \pm 17 \text{ MeV} \tag{5.5}$$

[225, 226, 227] to determine the coupling constant to be

$$c_{\tilde{G}\Phi} = 4.48 \pm 0.46 . \tag{5.6}$$

However, we also refer to the recent work of Ref. [228], where the possibility of a broad pseudoscalar glueball is discussed.

5.1.3 Mixing in the pseudoscalar-isoscalar sector

Once the shifts of the scalar-isoscalar fields by their vacuum expectation values have been performed, there are also bilinear mixing terms in the $J^{PC} = 0^{-+}$ isoscalar sector of the form $\propto \eta_N \tilde{G}$ and $\propto \eta_S \tilde{G}$ which lead to a non-diagonal mass matrix. In principle, one should take these terms into account, in addition to the already mentioned η_N-η_S mixing (2.110) [19, 81, 157, 186, 200], and solve a three-body mixing problem in order to determine the physical masses of the pseudoscalar particles. This will also affect the calculation of the decay widths. However, due to the large mass difference of the bare glueball field $\tilde{G}$ to the other quark-antiquark pseudoscalar fields, the corresponding admixtures of $\tilde{G}$ are expected be very small and can be safely neglected. In the following we will present the calculation of this three-body mixing problem in order to show that for the numerical calculations of the decay widths the field $\tilde{G}$ can be considered as a pure state.

The contribution of the pseudoscalar-isoscalar fields to the tree-level potential of the chiral interaction Lagrangian (5.1), which is of second order in the fields, reads

$$V^{(2)}_{\eta_N \eta_S \tilde{G}} = \frac{1}{2} \tilde{\Sigma}^T \tilde{M} \tilde{\Sigma} , \; \tilde{\Sigma} \equiv \begin{pmatrix} \eta_N \\ \eta_S \\ \tilde{G} \end{pmatrix} , \tag{5.7}$$

where

$$\tilde{M} \equiv \begin{pmatrix} m_{\eta_N}^2 & -c_1 Z_\pi Z_{\eta_S} \phi_N^3 \phi_S/2 & -c_{\tilde{G}\Phi} Z_\pi \phi_N \phi_S/\sqrt{2} \\ -c_1 Z_{\eta_S} Z_\pi \phi_N^3 \phi_S/2 & m_{\eta_S}^2 & -c_{\tilde{G}\Phi} Z_\pi \phi_N/2\sqrt{2} \\ -c_{\tilde{G}\Phi} Z_\pi \phi_N \phi_S/\sqrt{2} & -c_{\tilde{G}\Phi} Z_\pi \phi_N/2\sqrt{2} & m_{\tilde{G}}^2 \end{pmatrix} \tag{5.8}$$

is the non-diagonal mass matrix and

$$-c_1 Z_\pi Z_{\eta_S} \phi_N^3 \phi_S/2 \tag{5.9}$$

is the mixing parameter of the η_N-η_S mixing studied in Refs. [19, 81, 186]. Following the usual diagonalization procedure, which corresponds to an $SO(3)$ rotation, an orthogonal matrix $\tilde{B}$ is introduced such that the matrix $\tilde{M}' = \tilde{B}\tilde{M}\tilde{B}^T$ is diagonal. As a consequence, $\tilde{B}$ links the bare pseudoscalar-isoscalar fields to the physical resonances η and $\eta'(958)$ and to a *hypothetical* pseudoscalar glueball, which we denote as η_g, as follows

$$\begin{pmatrix} \eta \\ \eta'(958) \\ \eta_g \end{pmatrix} \equiv \tilde{\Sigma}' = \begin{pmatrix} \eta'_N \\ \eta'_S \\ \tilde{G}' \end{pmatrix} = \tilde{B}\,\tilde{\Sigma} = \tilde{B} \begin{pmatrix} \eta_N \\ \eta_S \\ \tilde{G} \end{pmatrix}. \tag{5.10}$$

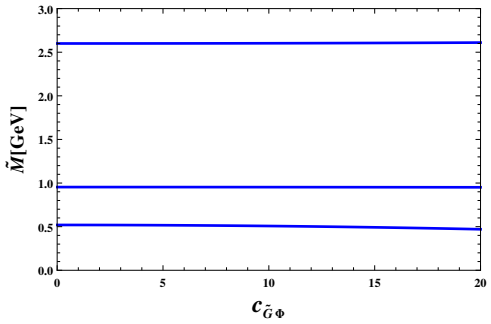

Figure 5.2: Physical masses of pseudoscalar-isoscalar fields as a function of the coupling constant $c_{\tilde{G}\Phi}$.

In Figure 5.2 we show the masses of the pseudoscalar states, after diagonalization of the bare mass matrix (5.8), as a function of the coupling constant $c_{\tilde{G}\Phi}$. It turns out that the mass of the mixed state which is predominantly a glueball increases very slowly. For the value of the coupling constant, $c_{\tilde{G}\Phi} = 4.48 \pm 0.46$, determined in the previous subsection, where we assumed that the resonance $X(2370)$ is a glueball, we obtain the physical masses of the pseudoscalar states presented in Table 5.1. For solving the three-body mixing issue we used for the masses of the bare fields $m_{\eta_N} = 766$ MeV, $m_{\eta_S} = 770$ MeV [186] and the mass $m_{\tilde{G}} = 2.6$ GeV which corresponds to a lattice-QCD calculation in the quenched approximation [52, 53, 54, 55, 56, 57].

The corresponding mixing matrix reads

$$\tilde{B} = \begin{pmatrix} 0.71 & 0.70 & 0.02 \\ -0.70 & 0.71 & -0.01 \\ -0.02 & -0.01 & 0.99 \end{pmatrix}, \tag{5.11}$$

Mass	eLSM [MeV]	Experiment [MeV]
m_η	517	(547.862 ± 0.018)
$m_{\eta'(958)}$	954	(957.78 ± 0.06)
m_{η_g}	2600.52	–

Table 5.1: Masses of the pseudoscalar-isoscalar mesons.

which implies the following admixtures of the bare fields to the two physical resonances as well as to the *hypothetical* state η_g

$$\begin{aligned} \eta: &\quad 51\%\,\eta_N\,, \quad 49\%\,\eta_S\,, \quad \approx 0\%\,\tilde{G}\,, \\ \eta'(958): &\quad 49\%\,\eta_N\,, \quad 51\%\,\eta_S\,, \quad \approx 0\%\,\tilde{G}\,, \\ \eta_g: &\quad \approx 0\%\,\eta_N\,, \quad \approx 0\%\,\eta_S\,, \quad \approx 100\%\,\tilde{G}\,. \end{aligned} \tag{5.12}$$

Equations (5.11) and (5.12) show that the mixing of the two pseudoscalar-isoscalar quark-antiquark fields is almost maximal as also determined in Ref. [19, 81, 186] and the mixing of the pseudoscalar glueball with the pseudoscalar quarkonia is almost ideal. Hence, for the numerical calculation of the decay widths we must only consider the η_N-η_S mixing and use $m_{\tilde{G}} \approx m_{\eta_g}$.

5.2 Decay of the pseudoscalar glueball $\tilde{G}$

In this section we present the analytical tree-level expressions for the decay of the pseudoscalar glueball $\tilde{G}$. The relevant vertices are extracted from the chiral interaction Lagrangian (5.1) whose explicit form is shown in Appendix B.1. These vertices are then applied to the decay formulas (1.144) and (1.148).

5.2.1 Decay widths of the type $\tilde{G} \to PPP$

We begin with listing the decay amplitudes and widths of the pseudoscalar glueball into three ordinary pseudoscalar mesons.

Decay channel $\tilde{G} \to KK\eta$:

$$-i\mathcal{A}_{\tilde{G}\to K^-K^+\eta} = -i\mathcal{A}_{\tilde{G}\to K^0\bar{K}^0\eta} = \frac{1}{2} c_{\tilde{G}\Phi} Z_K^2 Z_\pi \cos^2\varphi_\eta\,, \tag{5.13}$$

$$\Gamma_{\tilde{G}\to KK\eta} = 2\Gamma_{\tilde{G}\to K^-K^+\eta}\,. \tag{5.14}$$

Decay channel $\tilde{G} \to KK\eta'$:

$$-i\mathcal{A}_{\tilde{G}\to K^-K^+\eta'} = -i\mathcal{A}_{\tilde{G}\to K^0\bar{K}^0\eta'} = \frac{1}{2} c_{\tilde{G}\Phi} Z_K^2 Z_\pi \sin^2\varphi_\eta\,, \tag{5.15}$$

$$\Gamma_{\tilde{G}\to KK\eta'} = 2\Gamma_{\tilde{G}\to K^-K^+\eta'}\,. \tag{5.16}$$

Decay channel $\tilde{G} \to \eta\eta\eta$:

$$-i\mathcal{A}_{\tilde{G}\to\eta\eta\eta} = \frac{1}{2\sqrt{2}} c_{\tilde{G}\Phi} Z_{\eta_S} Z_\pi^2 \cos^4\varphi_\eta \sin^2\varphi_\eta \,, \tag{5.17}$$

$$\Gamma_{\tilde{G}\to\eta\eta\eta} \propto 6\left|-i\mathcal{A}_{\tilde{G}\to\eta\eta\eta}\right|^2 \,. \tag{5.18}$$

Decay channel $\tilde{G} \to \eta\eta\eta'$:

$$-i\mathcal{A}_{\tilde{G}\to\eta\eta\eta'} = \frac{1}{2\sqrt{2}} c_{\tilde{G}\Phi} Z_{\eta_S} Z_\pi^2 (\cos^3\varphi_\eta - 2\sin^2\varphi_\eta \cos\varphi_\eta) \,, \tag{5.19}$$

$$\Gamma_{\tilde{G}\to\eta\eta\eta'} \propto 2\left|-i\mathcal{A}_{\tilde{G}\to\eta\eta\eta'}\right|^2 \,. \tag{5.20}$$

Decay channel $\tilde{G} \to \eta\eta'\eta'$:

$$-i\mathcal{A}_{\tilde{G}\to\eta\eta'\eta'} = \frac{1}{2\sqrt{2}} c_{\tilde{G}\Phi} Z_{\eta_S} Z_\pi^2 (\sin^3\varphi_\eta - 2\cos^2\varphi_\eta \sin\varphi_\eta) \,, \tag{5.21}$$

$$\Gamma_{\tilde{G}\to\eta\eta'\eta'} \propto 2\left|-i\mathcal{A}_{\tilde{G}\to\eta\eta'\eta'}\right|^2 \,. \tag{5.22}$$

Decay channel $\tilde{G} \to KK\pi$:

$$-i\mathcal{A}_{\tilde{G}\to K^-K^+\pi^0} = -i\mathcal{A}_{\tilde{G}\to K^0\bar{K}^0\pi^0} = \frac{1}{2} c_{\tilde{G}\Phi} Z_K^2 Z_\pi \,, \tag{5.23}$$

$$-i\mathcal{A}_{\tilde{G}\to\bar{K}^0K^+\pi^-} = -i\mathcal{A}_{\tilde{G}\to K^0K^-\pi^+} = \frac{1}{\sqrt{2}} c_{\tilde{G}\Phi} Z_K^2 Z_\pi \,, \tag{5.24}$$

$$\Gamma_{\tilde{G}\to KK\pi} = \Gamma_{\tilde{G}\to K^-K^+\pi^0} + \Gamma_{\tilde{G}\to K^0\bar{K}^0\pi^0} + \Gamma_{\tilde{G}\to\bar{K}^0K^+\pi^-} + \Gamma_{\tilde{G}\to K^0K^-\pi^+} = 6\Gamma_{\tilde{G}\to K^-K^+\pi^0} \,. \tag{5.25}$$

Decay channel $\tilde{G} \to \eta\pi\pi$:

$$-i\mathcal{A}_{\tilde{G}\to\eta\pi^0\pi^0} = \frac{1}{2\sqrt{2}} c_{\tilde{G}\Phi} Z_{\eta_S} Z_\pi^2 \sin\varphi_\eta \,, \tag{5.26}$$

$$-i\mathcal{A}_{\tilde{G}\to\eta\pi^+\pi^-} = \frac{1}{\sqrt{2}} c_{\tilde{G}\Phi} Z_{\eta_S} Z_\pi^2 \sin\varphi_\eta \,, \tag{5.27}$$

$$\Gamma_{\tilde{G}\to\eta\pi\pi} = 2\Gamma_{\tilde{G}\to\eta\pi^0\pi^0} + \Gamma_{\tilde{G}\to\eta\pi^+\pi^-} \,. \tag{5.28}$$

Decay channel $\tilde{G} \to \eta'(958)\pi\pi$:

$$-i\mathcal{A}_{\tilde{G}\to\eta\pi^0\pi^0} = \frac{1}{2\sqrt{2}} c_{\tilde{G}\Phi} Z_{\eta_S} Z_\pi^2 \sin\varphi_\eta \,, \tag{5.29}$$

$$-i\mathcal{A}_{\tilde{G}\to\eta\pi^+\pi^-} = \frac{1}{\sqrt{2}} c_{\tilde{G}\Phi} Z_{\eta_S} Z_\pi^2 \sin\varphi_\eta \,, \tag{5.30}$$

$$\Gamma_{\tilde{G}\to\eta\pi\pi} = 2\Gamma_{\tilde{G}\to\eta\pi^0\pi^0} + \Gamma_{\tilde{G}\to\eta\pi^+\pi^-} \,. \tag{5.31}$$

5.2.2 Decay widths of the type $\tilde{G} \to PS$

Now we consider the decay channels of the pseudoscalar glueball into an ordinary pseudoscalar and a scalar meson.

Decay channel $\tilde{G} \to KK_0^\star$:

$$-i\mathcal{A}_{\tilde{G}\to K^- K_0^{\star+}} = -i\mathcal{A}_{\tilde{G}\to K^+ K_0^{\star-}} = -i\mathcal{A}_{\tilde{G}\to \bar{K}^0 K_0^{\star 0}} = -i\mathcal{A}_{\tilde{G}\to K^0 \bar{K}_0^{\star 0}} = \frac{1}{2\sqrt{2}} c_{\tilde{G}\Phi} Z_{K^\star} Z_K \phi_N \,, \tag{5.32}$$

$$\Gamma_{\tilde{G}\to K_0^\star K} = \Gamma_{\tilde{G}\to K^- K_0^{\star+}} + \Gamma_{\tilde{G}\to K^+ K_0^{\star-}} + \Gamma_{\tilde{G}\to \bar{K}^0 K_0^{\star 0}} + \Gamma_{\tilde{G}\to K^0 \bar{K}_0^{\star 0}} = 4\Gamma_{\tilde{G}\to K^- K_0^{\star+}} \,. \tag{5.33}$$

Decay channel $\tilde{G} \to \pi a_0$:

$$-i\mathcal{A}_{\tilde{G}\to \pi^0 a_0^0} = -i\mathcal{A}_{\tilde{G}\to \pi^+ a_0^-} = i\mathcal{A}_{\tilde{G}\to \pi^- a_0^+} = \frac{1}{\sqrt{2}} c_{\tilde{G}\Phi} Z_\pi \phi_S \,, \tag{5.34}$$

$$\Gamma_{\tilde{G}\to \pi a_0} = \Gamma_{\tilde{G}\to \pi^0 a_0^0} + \Gamma_{\tilde{G}\to \pi^+ a_0^-} + \Gamma_{\tilde{G}\to \pi^- a_0^+} = 3\Gamma_{\tilde{G}\to \pi^0 a_0^0} \,. \tag{5.35}$$

Decay channel $\tilde{G} \to \eta\sigma_N$:

$$-i\mathcal{A}_{\tilde{G}\to \eta\sigma_N} = -\frac{1}{\sqrt{2}} c_{\tilde{G}\Phi} (Z_{\eta_S} \phi_N \sin\varphi_\eta + Z_\pi \phi_S \cos\varphi_\eta) \,, \tag{5.36}$$

$$\Gamma_{\tilde{G}\to \eta\sigma_N} \propto \left| -i\mathcal{A}_{\tilde{G}\to \eta\sigma_N} \right|^2 \,. \tag{5.37}$$

Decay channel $\tilde{G} \to \eta\sigma_S$:

$$-i\mathcal{A}_{\tilde{G}\to \eta\sigma_S} = \frac{1}{\sqrt{2}} c_{\tilde{G}\Phi} Z_\pi \phi_N \cos\varphi_\eta \,, \tag{5.38}$$

$$\Gamma_{\tilde{G}\to \eta\sigma_S} \propto \left| -i\mathcal{A}_{\tilde{G}\to \eta\sigma_S} \right|^2 \,. \tag{5.39}$$

Decay channel $\tilde{G} \to \eta'\sigma_N$:

$$-i\mathcal{A}_{\tilde{G}\to \eta'\sigma_N} = \frac{1}{\sqrt{2}} c_{\tilde{G}\Phi} (Z_{\eta_N} \phi_S \sin\varphi_\eta - Z_{\eta_S} \phi_N \cos\varphi_\eta) \,, \tag{5.40}$$

$$\Gamma_{\tilde{G}\to \eta'\sigma_N} \propto \left| -i\mathcal{A}_{\tilde{G}\to \eta'\sigma_N} \right|^2 \,. \tag{5.41}$$

Decay channel $\tilde{G} \to \eta'\sigma_S$:

$$-i\mathcal{A}_{\tilde{G}\to \eta'\sigma_S} = \frac{1}{\sqrt{2}} c_{\tilde{G}\Phi} Z_\pi \phi_N \sin\varphi_\eta \,, \tag{5.42}$$

$$\Gamma_{\tilde{G}\to \eta'\sigma_S} \propto \left| -i\mathcal{A}_{\tilde{G}\to \eta'\sigma_S} \right|^2 \,. \tag{5.43}$$

5.2.3 Amplitudes for $\tilde{G} \to P f_0$

Concerning the decay channels of $\tilde{G}$ involving scalar-isoscalar mesons one should take into account the full mixing pattern above 1 GeV, in which the resonances $f_0(1370)$, $f_0(1500)$, and $f_0(1710)$ are mixed states of the pure quark-antiquark contributions σ_N and σ_S and a pure scalar glueball field G which is absent in this study[2]. This mixing, which is described by an orthogonal 3×3 matrix, was studied in detail in chapter 3 of this work [3, 4, 5] as well as e.g. in Refs. [1, 20, 203, 204, 205, 207, 208, 213, 214, 229]. Now we present the corresponding amplitudes for the decay of the pseudoscalar glueball into η and $\eta'(958)$ and one of the f_0 resonances.

$$-i\mathcal{A}_{\tilde{G}\to\eta f_0(1370)} = -\frac{1}{\sqrt{2}} c_{\tilde{G}\Phi} (Z_{\eta_S}\phi_N \sin\varphi_\eta b_{11} + Z_\pi \phi_S \cos\varphi_\eta b_{11} + Z_\pi \phi_N \cos\varphi_\eta b_{31}) \,, \tag{5.44}$$

$$-i\mathcal{A}_{\tilde{G}\to\eta f_0(1500)} = -\frac{1}{\sqrt{2}} c_{\tilde{G}\Phi} (Z_{\eta_S}\phi_N \sin\varphi_\eta b_{12} + Z_\pi \phi_S \cos\varphi_\eta b_{12} + Z_\pi \phi_N \cos\varphi_\eta b_{32}) \,, \tag{5.45}$$

$$-i\mathcal{A}_{\tilde{G}\to\eta f_0(1710)} = -\frac{1}{\sqrt{2}} c_{\tilde{G}\Phi} (Z_{\eta_S}\phi_N \sin\varphi_\eta b_{13} + Z_\pi \phi_S \cos\varphi_\eta b_{13} + Z_\pi \phi_N \cos\varphi_\eta b_{33}) \,, \tag{5.46}$$

$$-i\mathcal{A}_{\tilde{G}\to\eta' f_0(1370)} = \frac{1}{\sqrt{2}} c_{\tilde{G}\Phi} (Z_\pi \phi_S \sin\varphi_\eta b_{11} - Z_{\eta_S}\phi_N \cos\varphi_\eta b_{11} + Z_\pi \phi_N \sin\varphi_\eta b_{31}) \,, \tag{5.47}$$

$$-i\mathcal{A}_{\tilde{G}\to\eta' f_0(1500)} = -\frac{1}{\sqrt{2}} c_{\tilde{G}\Phi} (Z_\pi \phi_S \sin\varphi_\eta b_{12} - Z_{\eta_S}\phi_N \cos\varphi_\eta b_{12} + Z_\pi \phi_N \sin\varphi_\eta b_{32}) \,, \tag{5.48}$$

and

$$-i\mathcal{A}_{\tilde{G}\to\eta' f_0(1710)} = -\frac{1}{\sqrt{2}} c_{\tilde{G}\Phi} (Z_\pi \phi_S \sin\varphi_\eta b_{13} - Z_{\eta_S}\phi_N \cos\varphi_\eta b_{13} + Z_\pi \phi_N \sin\varphi_\eta b_{33}) \,, \tag{5.49}$$

where b_{ij} with $i, j = 1, 2, 3$ are elements of a mixing matrix B of the three f_0 resonances.

5.3 Branching ratios of the decay of $\tilde{G}$

In order to make parameter-free predictions we present our numerical results as branching ratios.

5.3.1 Branching ratios of $\tilde{G} \to PPP$

The branching ratios of $\tilde{G}$ for the decays into three pseudoscalar mesons are reported in Table 5.2 for both choices of the pseudoscalar masses, 2.6 and 2.37 GeV, which are relevant for the $\bar{\text{P}}$ANDA and BESIII experiments, respectively. The branching ratios are presented relative to the total decay width of the pseudoscalar glueball $\Gamma^{tot}_{\tilde{G}}$.

[2] As already discussed scalar-isoscalar states below 1 GeV are predominantly tetraquarks or mesonic molecular states, see Refs.[133, 134, 135, 136, 137, 138, 139, 140, 141, 142, 143, 144, 145, 146, 147] and references therein, and are not considered here.

Quantity	**Case (i):** $m_{\tilde{G}} = 2.6$ **GeV**	**Case (ii):** $m_{\tilde{G}} = 2.37$ **GeV**
$\Gamma_{\tilde{G}\to KK\eta}/\Gamma_{\tilde{G}}^{tot}$	0.049	0.043
$\Gamma_{\tilde{G}\to KK\eta'}/\Gamma_{\tilde{G}}^{tot}$	0.019	0.011
$\Gamma_{\tilde{G}\to\eta\eta\eta}/\Gamma_{\tilde{G}}^{tot}$	0.016	0.013
$\Gamma_{\tilde{G}\to\eta\eta\eta'}/\Gamma_{\tilde{G}}^{tot}$	0.0017	0.00082
$\Gamma_{\tilde{G}\to\eta\eta'\eta'}/\Gamma_{\tilde{G}}^{tot}$	0.00013	0
$\Gamma_{\tilde{G}\to KK\pi}/\Gamma_{\tilde{G}}^{tot}$	0.47	0.47
$\Gamma_{\tilde{G}\to\eta\pi\pi}/\Gamma_{\tilde{G}}^{tot}$	0.16	0.17
$\Gamma_{\tilde{G}\to\eta'\pi\pi}/\Gamma_{\tilde{G}}^{tot}$	0.095	0.090

Table 5.2: Branching ratios for the decay of the pseudoscalar glueball $\tilde{G}$ into three pseudoscalar mesons.

5.3.2 Branching ratios of $\tilde{G} \to PS$

Next we turn to the decay process $\tilde{G} \to PS$. The results, for both choices of $m_{\tilde{G}}$, are reported in Table 5.3 for the cases in which the pure resonance σ_S is assigned to $f_0(1710)$ or to $f_0(1500)$.

Ratio	**Case (i):** $m_{\tilde{G}} = 2.6$ **GeV**	**Case (ii):** $m_{\tilde{G}} = 2.37$ **GeV**
$\Gamma_{\tilde{G}\to KK_S}/\Gamma_{\tilde{G}}^{tot}$	0.060	0.070
$\Gamma_{\tilde{G}\to a_0\pi}/\Gamma_{\tilde{G}}^{tot}$	0.083	0.10
$\Gamma_{\tilde{G}\to\eta\sigma_N}/\Gamma_{\tilde{G}}^{tot}$	0.0000026	0.0000030
$\Gamma_{\tilde{G}\to\eta'\sigma_N}/\Gamma_{\tilde{G}}^{tot}$	0.039	0.026
$\Gamma_{\tilde{G}\to\eta\sigma_S}/\Gamma_{\tilde{G}}^{tot}$	0.012 (0.015)	0.0094 (0.017)
$\Gamma_{\tilde{G}\to\eta'\sigma_S}/\Gamma_{\tilde{G}}^{tot}$	0 (0.0082)	0 (0)

Table 5.3: Branching ratios for the decay of the pseudoscalar glueball $\tilde{G}$ into a scalar and a pseudoscalar meson. In the last two rows σ_S is assigned to $f_0(1710)$ or to $f_0(1500)$ (values in parentheses).

5.3.3 Branching ratios of $\tilde{G} \to Pf_0$

Due to the mixing in the scalar-isoscalar channel we evaluated explicitly the decays of the pseudoscalar glueball $\tilde{G}$ into η and $\eta'(958)$, respectively, and one of the scalar-isoscalar resonances $f_0(1370), f_0(1500)$, or $f_0(1710)$. Therefore, we use the solution of the mixing scenario of our chiral approach discussed in chapter four where the corresponding mixing matrix reads

$$B = \begin{pmatrix} -0.91 & 0.24 & -0.33 \\ 0.30 & 0.94 & -0.17 \\ -0.27 & 0.26 & 0.93 \end{pmatrix} . \tag{5.50}$$

We also use two other solutions of Ref. [207] and the solution of Ref. [213] where the corresponding results can be found in Appendix B.2. The branching ratios which correspond to our solution of the mixing of the f_0 are presented in Table 5.4.

Quantity	Sol. of eLSM. (4.21)
$\Gamma_{\tilde{G}\to\eta f_0(1370)}/\Gamma^{tot}_{\tilde{G}}$	0.0012 (0.0014)
$\Gamma_{\tilde{G}\to\eta f_0(1500)}/\Gamma^{tot}_{\tilde{G}}$	0.013 (0.015)
$\Gamma_{\tilde{G}\to\eta f_0(1710)}/\Gamma^{tot}_{\tilde{G}}$	0.00078 (0.00062)
$\Gamma_{\tilde{G}\to\eta' f_0(1370)}/\Gamma^{tot}_{\tilde{G}}$	0.043 (0.029)
$\Gamma_{\tilde{G}\to\eta' f_0(1500)}/\Gamma^{tot}_{\tilde{G}}$	0.00095 (0)
$\Gamma_{\tilde{G}\to\eta' f_0(1710)}/\Gamma^{tot}_{\tilde{G}}$	0 (0)

Table 5.4: Branching ratios for the decays of the pseudoscalar glueball $\tilde{G}$ into η and η', respectively, and one of the scalar-isoscalar resonance $f_0(1370), f_0(1500)$, and $f_0(1710)$ by using the mixing matrix B, Eq. (4.21), of scalar-isoscalar states [3]. The mass of the pseudoscalar glueball is $m_{\tilde{G}} = 2.6$ GeV and $m_{\tilde{G}} = 2.37$ GeV (values in parentheses), respectively.

5.3.4 Interference phenomena

An interesting and subtle issue is that the scalar states decay further into two pseudoscalar ones. For instance, $K_0^\star \equiv K_0^*(1430)$ decays into $K\pi$. There are two possible decay amplitudes for the process $\tilde{G} \to KK\pi$. One is the direct decay mechanism reported in Table 5.2, the other is the decay chain $\tilde{G} \to KK_0^\star \to KK\pi$. Both have the same final state. The immediate question is whether interference effects emerge which spoil the results presented in Table 5.2 and 5.3. Namely, simply performing the sum of the direct three-body decay Table 5.2 and the corresponding two-body decay Table 5.3, is not fully correct.

We now describe this point in more detail by using the neutral channel $\tilde{G} \to K^0\bar{K}^0\pi$ as an illustrative case. To this end, we describe the coupling $K_0^\star$ to $K\pi$ via the Lagrangian

$$\mathcal{L}_{K_0^\star K\pi} = gK_0^\star \bar{K}_0\pi^0 + \sqrt{2}gK_0^\star K^-\pi^+ + h.c.\,. \tag{5.51}$$

The coupling constant $|g| = 2.73$ GeV is obtained by using the experimental value for the total decay width $\Gamma_{K_0^*} = 270$ MeV [11]. The full amplitude for the process $\tilde{G} \to K^0\bar{K}^0\pi^0$ results as

$$\mathcal{A}^{full}_{\tilde{G}\to K^0\bar{K}^0\pi^0} = \mathcal{A}^{direct}_{\tilde{G}\to K^0\bar{K}^0\pi^0} + \mathcal{A}^{interact}_{\tilde{G}\to K^0K_0^\star\to K^0\bar{K}^0\pi^0}\,. \tag{5.52}$$

Thus the full decay width reads:

$$\Gamma^{full}_{\tilde{G}\to K^0\bar{K}^0\pi^0} = \Gamma^{direct}_{\tilde{G}\to K^0\bar{K}^0\pi^0} + \Gamma^{interact}_{\tilde{G}\to K^0K_0^\star\to K^0\bar{K}^0\pi^0} + \zeta^{mix}_{\tilde{G}\to K^0\bar{K}^0\pi^0}\,. \tag{5.53}$$

We can then investigate how large the mixing term $\zeta^{mix}_{\tilde{G}\to K^0\bar{K}^0\pi^0}$ is, and thus the error done in neglecting it. For instance, explicit calculation for the $K^0\bar{K}^0\pi^0$ case gives a relative error of

$$\left|\frac{\zeta^{mix}_{\tilde{G}\to K^0\bar{K}^0\pi^0}}{\Gamma^{direct}_{\tilde{G}\to K^0\bar{K}^0\pi^0} + \Gamma^{interact}_{\tilde{G}\to K^0K_0^\star\to K^0\bar{K}^0\pi^0}}\right| \approx \begin{array}{ll} 7.3\% & (g>0) \\ 2.2\% & (g<0) \end{array}\,. \tag{5.54}$$

Present results from the model in Ref. [81] show that $g < 0$: the estimates presented in Ref. [6] can be regarded as upper limits. We thus conclude that the total error for the channel $\tilde{G} \to K^0\bar{K}^0\pi^0$ is not large and can be neglected at the present stage. However, future detailed and precise theoretical predictions should implement these interference effects [6, 7, 223].

5.4 Interaction of $\tilde{G}$ with baryons

In the planned $\bar{\text{P}}$ANDA experiment at FAIR [124], antiprotons collide on a proton-rich target. It is then also interesting to study how the pseudoscalar glueball interacts with the nucleon and with its chiral partner. In the so-called mirror assignment [148, 230], one starts from two nucleon fields Ψ_1 and Ψ_2 which transform under chiral transformations as follows

$$\Psi_{1R(L)} \to \Psi'_{1R(L)} = U_{R(L)}\Psi_{1R(L)} \ , \quad \Psi_{2R(L)} \to \Psi'_{2R(L)} = U_{L(R)}\Psi_{2R(L)} \ . \tag{5.55}$$

In this way, it is possible to write down a chirally invariant mass term of the type

$$\mathcal{L}_{\mu_0} = -\mu_0 \left(\bar{\Psi}_2\gamma_5\Psi_1 - \bar{\Psi}_1\gamma_5\Psi_2\right) \ . \tag{5.56}$$

Eventually, μ_0 can be seen as a condensation of a tetraquark and/or a glueball field, see details in Ref. [148]. The nucleon fields N and its chiral partner, which is associated to the resonance $N^*(1535)$, are obtained as

$$\Psi_1 = \frac{1}{\sqrt{2\cosh\delta}}\left(Ne^{\delta/2} + \gamma_5 N^* e^{-\delta/2}\right) \tag{5.57}$$

and

$$\Psi_2 = \frac{1}{\sqrt{2\cosh\delta}}\left(\gamma_5 Ne^{-\delta/2} - N^* e^{\delta/2}\right) \ , \tag{5.58}$$

where

$$\cosh\delta = \frac{m_N + m_{N^*}}{2\mu_0} \ . \tag{5.59}$$

The value $\mu_0 = (460 \pm 136)$ MeV was obtained by a fit to vacuum properties [148].

We now write down a chirally invariant Lagrangian which describes the interaction of $\tilde{G}$ with the baryon fields Ψ_1 and Ψ_2

$$\mathcal{L}^{int}_{\tilde{G}\text{-}bar} = ic_{\tilde{G}\Psi}\tilde{G}\left(\bar{\Psi}_2\Psi_1 - \bar{\Psi}_1\Psi_2\right) \ . \tag{5.60}$$

Thus, the fusion of a proton and an antiproton is described by $\mathcal{L}^{int}_{\tilde{G}\text{-}bar}$, showing that it is not chirally suppressed. Moreover, although the coupling constant $c_{\tilde{G}\Psi}$ cannot be determined, we can easily predict the ratio of the decay processes $\Gamma_{\tilde{G}\to\bar{N}N}$ and $\Gamma_{\tilde{G}\to\bar{N}^*N+h.c.}$[7, 224]:

$$\frac{\Gamma_{\tilde{G}\to\bar{N}N}}{\Gamma_{\tilde{G}\to\bar{N}^*N+h.c.}} = 1.94 \ . \tag{5.61}$$

5.5 Discussion

- The results depend only slightly on the glueball mass, thus the two columns of Table 5.2 and 5.3 are similar. It turns out that the channel $KK\pi$ is the dominant one (almost 50%). Also the $\eta\pi\pi$ and $\eta'\pi\pi$ channels are sizeable. On the contrary, the two-body decays into a scalar and a pseudoscalar are subdominant and reach only 20% of the full mesonic decay width.

- The decay of the pseudoscalar glueball into three pions vanishes:

  $$\Gamma_{\tilde{G}\to\pi\pi\pi} = 0 \ . \tag{5.62}$$

  This result represents a further simple and testable prediction of our approach.

- The decays of the pseudoscalar glueball into a scalar-isoscalar meson amount only to 5% of the total decay width. Moreover, the mixing pattern in the scalar-isoscalar sector has a negligible influence on the total decay width of $\tilde{G}$. Nevertheless, in the future it may represent an interesting and additional test for scalar-isoscalar states.

- If a standard linear sigma model without (axial-)vector mesons is studied, the replacements

$$Z_\pi = Z_K = Z_{\eta_N} = Z_{\eta_S} = 1 \tag{5.63}$$

  need to be performed. Most of the results of the branching ratios for the three-body decay are qualitatively, but not quantitatively, similar to the values of Table 5.2 (variations of about 25-30%). However, the branching ratios for the two-body decay change sizeably with respect to the results of Table 5.3. This fact shows once more that the inclusion of (axial)vector d.o.f. has sizeable effects also concerning the decays of the pseudoscalar glueball.

- In principle, the three-body final states for the decays shown in Table 5.2 can also be obtained through a sequential decay from the two-body final states shown in Table 5.3, where the scalar particle S further decays into PP, (for instance, $K_0^*(1430) \to K\pi$). There are then two possible decay amplitudes, one from the direct three-body decay and one from the sequential decay, which have to be added coherently before taking the modulus square to obtain the total three-body decay width. The results shown in Table 5.2 and 5.3 gives a first estimate which neglects interference terms for the magnitude of the total three-body decay width. We have verified that the correction from the interference term to this total three-body decay width in a given channel is at most of the order of 10% for $m_{\tilde{G}} = 2.6$ GeV and 15% for $m_{\tilde{G}} = 2.37$ GeV. For a full understanding of the contribution of the various decay amplitudes to the final three-body state, one needs to perform a detailed study of the Dalitz plot for the three-body decay.

Jede Lösung eines Problems ist ein neues Problem.
Johann Wolfgang von Goethe

Chapter 6

Conclusions and Outlook

The existence of glueballs is a clear prediction of QCD, confirmed by numerous and accurate predictions of lattice QCD, but their existence and properties need to be further studied both experimentally and theoretically. In this thesis we have studied the scalar-isoscalar sector,

$$I^G\left(J^{PC}\right) = 0^+\,(0^{++})\ ,$$

in the low-energy region below 2 GeV, where a scalar glueball is naturally expected. In addition, we have investigated the properties of a pseudoscalar glueball and written down the Lagrangian for a vector glueball. In the following we summarize the most important insights that we have achieved in this work and give some useful suggestions for future progress.

6.1 The scalar glueball

One of the challenges of hadronic physics is the full understanding of the scalar-isoscalar sector below 2 GeV where at the present five well-established f_0 resonances exist [11]. A variety of works indicate that the 0^{++} isoscalar resonances below 1 GeV,

$$f_0(500) \text{ and } f_0(980)\ ,$$

belong to a nonet of tetraquarks or are mesonic molecular states. In the energy region between 1 and 2 GeV there are three further resonances

$$f_0(1370), f_0(1500) \text{ and, } f_0(1710)\ .$$

Out of these resonances only two can be interpreted as predominantly $\bar{q}q$ mesons. Namely, one as the non-strange,

$$\sigma_N \cong \left(\bar{u}u + \bar{d}d\right)/\sqrt{2}\ ,$$

and the other one as the strange,

$$\sigma_S \cong \bar{s}s\ ,$$

meson. Hence a natural question arises whether one of them is the scalar glueball, which is, due to the quantum numbers of vacuum, directly connected with the trace anomaly of the pure

Yang-Mills sector of QCD. If that is the case then the final question is which of the f_0 resonances possesses the largest gluonic content.

In order to answer these questions we used an effective hadronic model, the extended Linear Sigma Model, whose d.o.f. are scalar and pseudoscalar (0^{-+}) as well as vector (1^{--}) and axial-vector (1^{++}) quark-antiquark mesons. The scalar glueball is described in the eLSM as the excitation of a scalar dilaton field G. Our model is built in agreement with the symmetry properties of the QCD Lagrangian. Since the eLSM is a confined effective field theory, the dynamics is dictated by the global chiral and dilation symmetries rather than the local $SU_c(3)$ symmetry, which is trivially fulfilled. In the full implementation of the eLSM ($N_f = 3$) the bare quark-antiquark mesons σ_N and σ_S as well as the bare glueball G mix and generate the physical resonances $f_0(1370)$, $f_0(1500)$, and $f_0(1710)$.

Implementation of the eLSM with two flavors ($N_f = 2$) We started our search for the scalar glueball within the two-flavor version of the eLSM, which does not contain mesons with strange quarks. In this case a two-body mixing scenario in the scalar-isoscalar sector takes place, where the bare non-strange quark-antiquark meson σ_N and the bare scalar glueball G mix and produce two physical f_0 resonances. Thus, several assignments of the bare fields σ_N and G to the f_0 resonances are possible which we investigated by using a χ^2 analysis. As an input we used physical quantities of the scalar-isoscalar resonances such as masses and decay widths [11]. Our calculations were done in vacuum, that is at vanishing temperature ($T = 0$) and chemical potential ($\mu = 0$), and at tree level, which means that loop corrections were not considered. We found two acceptable solutions where in both cases the resonance $f_0(1370)$ was predominantly the non-strange $\bar{q}q$ state while the glueball was in one solution predominantly $f_0(1500)$ and in the other one predominantly $f_0(1710)$. The reasons for the ambiguous result are that the $N_f = 2$ approach of the eLSM is not complete, mainly because the bare strange field σ_S was neglected.

The solution of the assignment

$$\sigma_N \cong f_0(1370) \text{ and } G \cong f_0(1500)$$

is slightly favored with respect to those of the assignment

$$\sigma_N \cong f_0(1370) \text{ and } G \cong f_0(1710) \,,$$

because the latter exhibits a too large

$$G' \equiv f_0(1710) \to \rho\rho \to 4\pi$$

decay width, which however is not experimentally observed [1, 17]. On the other hand, if the resonance $f_0(1500)$ is interpreted as predominantly a glueball then the following issues occur.

- Flavor blindness of a pure glueball state requires that

$$\frac{\Gamma_{G'\to\pi\pi}}{\Gamma_{G'\to KK}} = \frac{3}{4} \,. \tag{6.1}$$

This branching ratio reads for the two putative scalar glueball candidates

$$\frac{\Gamma_{f_0(1500)\to\pi\pi}}{\Gamma_{f_0(1500)\to KK}} = 4.06\ , \tag{6.2}$$

$$\frac{\Gamma_{f_0(1710)\to\pi\pi}}{\Gamma_{f_0(1710)\to KK}} = 0.41\ . \tag{6.3}$$

This shows that the requirement of flavor blindness is rather fulfilled by the resonance $f_0(1710)$ than $f_0(1500)$. Note that the branching ratio (6.1) corresponds to a pure glueball, but the f_0 resonances contain $\bar{q}q$ components. In addition, the errors of the decay widths of $f_0(1710)$ are sufficient large, thus it is possible to find a match between the theoretical expectation of Eq. (6.1) and the experiment, see Eq. 6.3 and Table 3.5. This is not possible for the resonance $f_0(1500)$, see Eq. (6.2) and Table 3.2.

- Lattice-QCD calculations predict a scalar glueball mass of

  $$m_G^{lat} \approx 1.7\ \text{GeV}$$

  which corresponds to the mass of $f_0(1710)$ rather than to $f_0(1500)$ [55, 58].

- The production rate in radiative J/ψ decay is higher for $f_0(1710)$ than for $f_0(1500)$ [215].

These arguments support the scenario in which $G' \equiv f_0(1710)$. In order to obtain a conclusive result, a study of three-body mixing scenario is required where three bare fields σ_N, σ_S, and G are involved and generate $f_0(1370)$, $f_0(1500)$, and $f_0(1710)$.

In the end, we also tested for completeness assignments with the resonance $f_0(500)$ as a predominantly non-strange $\bar{q}q$ meson [1, 2] but it turns out that its decay width is with

$$\Gamma_{\sigma_N'\to\pi\pi} \lesssim 180\ \text{MeV}\ .$$

considerably narrower than the experimental one

$$\Gamma^{ex}_{f_0(500)\to\pi\pi} = (400 - 700)\ \text{MeV}\ .$$

Therefore, scenarios in which $f_0(500)$ is interpreted as a quark-antiquark state are strongly disfavored.

Implementation of the eLSM with three flavors ($N_f = 3$) The three-flavor eLSM requires a solution of a three-body mixing problem in order to figure out which of the f_0 resonances can be interpreted as the scalar glueball. Contrary to the calculations of the eLSM in the case $N_f = 2$ we now obtained an unique result.

Our fit with

$$\chi^2/d.o.f. \approx 0.35 \tag{6.4}$$

describes the phenomenology in the scalar-isoscalar sector very well and yields

$$\frac{\Gamma_{f_0(1710)\to\pi\pi}}{\Gamma_{f_0(1710)\to KK}} = 0.39\,. \tag{6.5}$$

Similar results were also found in Refs. [218, 219, 220]. We found that the resonance $f_0(1710)$ is predominantly the scalar glueball, while the resonances $f_0(1370)$ and $f_0(1500)$ are predominantly non-strange σ_N and strange σ_S quark-antiquark meson.

$$\begin{pmatrix} f_0(1370) \\ f_0(1500) \\ f_0(1710) \end{pmatrix} = \begin{pmatrix} -0.91 & 0.24 & -0.33 \\ 0.30 & 0.94 & -0.17 \\ -0.27 & 0.26 & 0.93 \end{pmatrix} = \begin{pmatrix} \sigma_N \cong \left(\bar{u}u + \bar{d}d\right)/\sqrt{2} \\ \sigma_S \cong \bar{s}s \\ G \cong glueball \end{pmatrix}. \tag{6.6}$$

This solution is based on the assumption that the decay width of the scalar glueball is narrow ($\Gamma_G \lesssim 100$ GeV) which is in accordance with large-N_c arguments. As an interesting consequence, we obtained for the scale parameter Λ_{dil}, which arises from the trace anomaly, a large value and this implies a large gluon condensate $\left\langle \frac{\alpha_s}{\pi} G^a_{\mu\nu} G^{\mu\nu}_a \right\rangle$.

We emphasize that the inclusion of (axial-)vector d.o.f. was crucial for the results of our approach. These fields affect the phenomenology in the (pseudo)scalar sector, e.g. our model suggests that $f_0(1370)$ is the chiral partner of the pion. In addition, it is to our knowledge the first time where a full $N_f = 3$ mixing of $f_0(1370)$, $f_0(1500)$, and $f_0(1710)$ in a chiral hadronic model with a scalar glueball, described by a dilaton field, and the presence of (axial-)vector fields was studied.

6.2 The pseudoscalar glueball

Motivated by the glueball spectrum of lattice QCD, we constructed an effective interaction Lagrangian in the framework of the eLSM in order to study vacuum properties of the pseudoscalar glueball $\tilde{G}$. Accordingly, we used for our calculations the glueball mass obtained by lattice QCD in the quenched approximation $m_{\tilde{G}} = 2.6$ GeV. The upcoming $\bar{\text{P}}$ANDA experiment at FAIR near Darmstadt will cover this energy range. Our predictions can be used as a guideline for the search of glueballs.

The results regarding the pseudoscalar glueball are given as branching ratios in order to make parameter-free prediction. We found that $\tilde{G} \to KK\pi$ is the dominant decay channel ($\sim 47\%$) followed by $\tilde{G} \to \eta\pi\pi$ ($\sim 16\%$) and $\tilde{G} \to \eta'\pi\pi$ ($\sim 10\%$), while $\tilde{G} \to \pi\pi\pi$ is predicted to vanish. In addition, we repeat the calculations for a glueball mass of 2.37 GeV which corresponds to the mass of the pseudoscalar resonance $X(2370)$ observed in the BESIII experiment.

6.3 Outlook

Finally, there are further interesting developments of this work, which will be discussed in the following.

The vector glueball In case of the vector glueball $\mathcal{O}_\mu$ with a lattice-QCD mass $m_{\mathcal{O}_\mu}$ = 3.8 GeV we presented a chiral interaction Lagrangian with which the following two- and three-body decay processes can be evaluated: $\mathcal{O}_\mu \to VA$, $\mathcal{O}_\mu \to VP$, $\mathcal{O}_\mu \to PB$, $\mathcal{O}_\mu \to VPP$, $\mathcal{O}_\mu \to VSS$, $\mathcal{O}_\mu \to APS$, and $\mathcal{O}_\mu \to eVPP$. The numerical calculations are in progress and will be presented in Ref. [166].

Inclusion of light tetraquark fields In the future, one should include the nonet of light scalar states $f_0(500)$, $f_0(980)$, $a_0(980)$, and $K_0^*(800)$, which then allow to describe all scalar states up to 1.7 GeV. Indeed, in the two-flavor case the resonance $f_0(500)$ has been already included as a tetraquark/molecular field in a simplified version of the eLSM [231], in which chiral symmetry restoration at non-zero temperature has been studied, and in the extension of the eLSM to the baryonic sector [232, 233]. The role of $f_0(500)$ is important because it induces a strong attraction between nucleons and affects the properties of nuclear matter at non-zero density.

In the three-flavor case chiral models with tetraquark fields but without (axial-)vector mesons were studied [145, 146, 147]. The isovector resonances $a_0(1450)$ and $a_0(980)$ arise as a mixing of a bare quark-antiquark and a bare tetraquark/molecular field configuration. A similar situation holds in the isodoublet sector for $K_0^*(1430)$ and $K_0^*(800)$. The mixing angle turns out to be small [138]. In the scalar-isoscalar sector one has a more complicated system with the mixing of five bare fields, which leads to the five resonances $f_0(500)$, $f_0(980)$, $f_0(1370)$, $f_0(1500)$, and $f_0(1710)$ [146].

In the framework of the eLSM, the inclusion of the light scalars should also contain their coupling to (axial-)vector d.o.f. as well as to the dilaton field. A variety of decays, such as the decays of the light scalars

$$f_0(500) \to \pi\pi \ , \ f_0(980) \to KK \ ,$$

etc. as well as decays into them

$$a_1(1230) \to f_0(500)\pi \ , \ f_0(1500) \to f_0(500) f_0(500) \ ,$$

etc. can be studied. Moreover, the mixing in the isovector, isodoublet, and *most importantly* in the isoscalar sector can be investigated in such a framework. In this general scenario, a mixing of five scalar-isoscalar states takes place, which allows to describe all relevant scalar-isoscalar resonances listed in the PDG below 1.8 GeV [11]

Inclusion of other glueball fields In analogy to the scalar, pseudoscalar, and vector glueballs, further glueballs with different quantum numbers, as predicted by lattice QCD [55], can be studied in the framework of the eLSM, e.g. a pseudovector (1^{+-}) or a tensor (2^{++}) glueball. Such studies can be based on ideas similar to those pursued in this work. This can be done by making use of the symmetries of the QCD and introducing effective couplings and constructing the corresponding Lagrangians. In this way, decay ratios can be calculated which can be used as a further guide for future experimental search for gluballs.

Appendix A

Decay Widths of the Scalar-Isoscalar fields

Using the formula (1.144) we compute two-body decays of the the scalar-isoscalar fields. All relevant expressions for these decay processes are extracted from the Lagrangian (2.104) and are presented in the following [1, 3, 17, 19, 81].

A.1 Decays of the scalar-isoscalar fields into $\pi\pi$

For the decay widths of the scalar-isoscalar resonances into $\pi\pi$ we obtain

$$\Gamma_{f_0\to\pi\pi} = 6\frac{\sqrt{\frac{m_{f_0}^2}{4}-m_\pi^2}}{8\pi m_{f_0}^2}\left|-i\mathcal{A}_{f_0\to\pi\pi}(m_{f_0})\right|^2 \ , \tag{A.1}$$

where m_{f_0} is the mass of the physical f_0 resonance. The bare amplitudes (as functions of m_{f_0}) are

$$-i\mathcal{A}_{\sigma_N\to\pi\pi}(m_{f_0}) = i\left(A_{\sigma_N\pi\pi} - B_{\sigma_N\pi\pi}\frac{m_{f_0}^2-2m_\pi^2}{2} - C_{\sigma_N\pi\pi}m_\pi^2\right) \ , \tag{A.2}$$

$$-i\mathcal{A}_{\sigma_S\to\pi\pi}(m_{f_0}) = i\left(A_{\sigma_S\pi\pi} - B_{\sigma_S\pi\pi}\frac{m_{f_0}^2-2m_\pi^2}{2}\right) \ , \tag{A.3}$$

$$-i\mathcal{A}_{G\to\pi\pi}(m_{f_0}) = i\left(A_{G\pi\pi} - B_{G\pi\pi}\frac{m_{f_0}^2-2m_\pi^2}{2}\right) \ , \tag{A.4}$$

with the corresponding constants

$$A_{\sigma_N\pi\pi} = -\left(\lambda_1+\frac{\lambda_2}{2}\right)Z_\pi^2\phi_N \ , \tag{A.5}$$

$$B_{\sigma_N\pi\pi} = -2g_1Z_\pi^2w_{a_1} + (g_1^2+\frac{h_1+h_2-h_3}{2})Z_\pi^2w_{a_1}^2\phi_N \ , \tag{A.6}$$

$$C_{\sigma_N\pi\pi} = -g_1Z_\pi^2w_{a_1} \ , \tag{A.7}$$

$$A_{\sigma_S\pi\pi} = -\lambda_1Z_\pi^2\phi_S \ , \tag{A.8}$$

$$B_{\sigma_S\pi\pi} = \frac{h_1}{2} Z_\pi^2 w_{a_1}^2 \phi_S \ , \tag{A.9}$$

$$A_{G\pi\pi} = -\frac{m_0^2}{G_0} Z_\pi^2 \ , \tag{A.10}$$

$$B_{G\pi\pi} = \frac{m_1^2}{G_0} Z_\pi^2 w_{a_1}^2 \ . \tag{A.11}$$

After performing an orthogonal transformation we obtain the amplitudes for the physical scalar-isoscalar fields $\sigma'_N \equiv f_0(1370)$, $\sigma'_S \equiv f_0(1500)$, and $G' \equiv f_0(1710)$:

$$-i\mathcal{A}_{\sigma'_N\to\pi\pi}(m_{\sigma'_N}) = i\left[\mathcal{A}_{\sigma_N\to\pi\pi}(m_{\sigma'_N})b_{11} + \mathcal{A}_{\sigma_S\to\pi\pi}(m_{\sigma'_N})b_{12} + \mathcal{A}_{G\to\pi\pi}(m_{\sigma'_N})b_{13}\right] \ , \tag{A.12}$$

$$-i\mathcal{A}_{\sigma'_S\to\pi\pi}(m_{\sigma'_S}) = i\left[\mathcal{A}_{\sigma_N\to\pi\pi}(m_{\sigma'_S})b_{21} + \mathcal{A}_{\sigma_S\to\pi\pi}(m_{\sigma'_S})b_{22} + \mathcal{A}_{G\to\pi\pi}(m_{\sigma'_S})b_{23}\right] \ , \tag{A.13}$$

$$-i\mathcal{A}_{G'\to\pi\pi}(m_{G'}) = i\left[\mathcal{A}_{\sigma_N\to\pi\pi}(m_{G'})b_{31} + \mathcal{A}_{\sigma_S\to\pi\pi}(m_{G'})b_{32} + \mathcal{A}_{G\to\pi\pi}(m_{G'})b_{33}\right] \ , \tag{A.14}$$

where b_{ij}, $i,j = 1,2,3$, are the corresponding elements of the mixing matrix B from Eq. (4.10).

A.2 Decays of the scalar-isoscalar fields into KK

For the decay widths of the scalar-isoscalar resonances into KK we obtain

$$\Gamma_{f_0\to KK} = 2\frac{\sqrt{\frac{m_{f_0}^2}{4} - m_{KK}^2}}{8\pi m_{f_0}^2} \left|-i\mathcal{A}_{f_0\to KK}(m_{f_0})\right|^2 \ , \tag{A.15}$$

where the bare amplitudes are

$$-i\mathcal{A}_{\sigma_N\to KK}(m_{f_0}) = i\left[A_{\sigma_N KK} - (B_{\sigma_N KK} - 2C_{\sigma_N KK})\frac{m_{f_0}^2 - 2m_K^2}{2} + 2C_{\sigma_N KK} m_K^2\right] \ , \tag{A.16}$$

$$-i\mathcal{A}_{\sigma_S\to KK}(m_{f_0}) = i\left[A_{\sigma_S KK} - (B_{\sigma_S KK} - 2C_{\sigma_S KK})\frac{m_{f_0}^2 - 2m_K^2}{2} + 2C_{\sigma_S KK} m_K^2\right] \ , \tag{A.17}$$

$$-i\mathcal{A}_{G\to KK}(m_{f_0}) = i\left(A_{GKK} - B_{GKK}\frac{m_{f_0}^2 - 2m_K^2}{2}\right) \ , \tag{A.18}$$

and the corresponding constants read

$$A_{\sigma_N KK} = \frac{Z_K^2}{\sqrt{2}}\left[\lambda_2\left(\phi_S - \sqrt{2}\phi_N\right) - 2\sqrt{2}\lambda_1\phi_N\right] \ , \tag{A.19}$$

$$B_{\sigma_N KK} = \frac{g_1}{2} Z_K^2 w_{K_1}\left[-2 + g_1 w_{K_1}\left(\phi_N + \sqrt{2}\phi_S\right)\right] + \frac{Z_K^2 w_{K_1}^2}{2}\left[\left(2h_1 + h_2\right)\phi_N - \sqrt{2}h_3\phi_S\right] \ , \tag{A.20}$$

$$C_{\sigma_N KK} = \frac{g_1}{2} Z_K^2 w_{K_1} \ , \tag{A.21}$$

$$A_{\sigma_S KK} = \frac{Z_K^2}{\sqrt{2}}\left[\lambda_2\left(\phi_N - 2\sqrt{2}\phi_S\right) - 2\sqrt{2}\lambda_1\phi_S\right] \ , \tag{A.22}$$

$$B_{\sigma_S KK} = \frac{\sqrt{2}g_1}{2} Z_K^2 w_{K_1}\left[-2 + g_1 w_{K_1}\left(\phi_N + \sqrt{2}\phi_S\right)\right] + \frac{Z_K^2 w_{K_1}^2}{\sqrt{2}}\left[\sqrt{2}\left(h_1 + h_2\right)\phi_S - h_3\phi_N\right] \ , \tag{A.23}$$

$$C_{\sigma_S KK} = \frac{\sqrt{2}g_1}{2} Z_K^2 w_{K_1} \ , \tag{A.24}$$

$$A_{GKK} = -\frac{2m_0^2}{G_0} Z_K^2 \ , \tag{A.25}$$

$$B_{GKK} = \frac{2m_1^2}{G_0} Z_K^2 w_{K_1}^2 \ . \tag{A.26}$$

After performing an orthogonal transformation we obtain the amplitudes for the physical scalar-isoscalar fields

$$-i\mathcal{A}_{\sigma'_N \to KK}(m_{\sigma'_N}) = i\left[\mathcal{A}_{\sigma_N \to KK}(m_{\sigma'_N}) b_{11} + \mathcal{A}_{\sigma_S \to KK}(m_{\sigma'_N}) b_{12} + \mathcal{A}_{G \to KK}(m_{\sigma'_N}) b_{13}\right] \ , \tag{A.27}$$

$$-i\mathcal{A}_{\sigma'_S \to KK}(m_{\sigma'_S}) = i\left[\mathcal{A}_{\sigma_N \to KK}(m_{\sigma'_S}) b_{21} + \mathcal{A}_{\sigma_S \to KK}(m_{\sigma'_S}) b_{22} + \mathcal{A}_{G \to KK}(m_{\sigma'_S}) b_{23}\right] \ , \tag{A.28}$$

$$-i\mathcal{A}_{G' \to KK}(m_{G'}) = i\left[\mathcal{A}_{\sigma_N \to KK}(m_{G'}) b_{31} + \mathcal{A}_{\sigma_S \to KK}(m_{G'}) b_{32} + \mathcal{A}_{G \to KK}(m_{G'}) b_{33}\right] \ , \tag{A.29}$$

which we assign to the physical resonances as follows: $\sigma'_N \equiv f_0(1370)$, $\sigma'_S \equiv f_0(1500)$, and $G \equiv f_0(1710)$.

A.3 Decays of the scalar-isoscalar fields into $\eta\eta$

For the decay widths of the scalar-isoscalar resonances into $\eta\eta$ we obtain

$$\Gamma_{f_0 \to \eta\eta} = 2 \frac{\sqrt{\frac{m_{f_0}^2}{4} - m_\eta^2}}{8\pi m_{f_0}^2} \left| -i\mathcal{A}_{f_0 \to \eta\eta}(m_{f_0}) \right|^2 \ , \tag{A.30}$$

where the bare amplitudes are

$$-i\mathcal{A}_{\sigma_N \to \eta\eta}(m_{f_0}) = i\left(A_{\sigma_N \eta\eta} - B_{\sigma_N \eta\eta} \frac{m_{f_0}^2 - 2m_\eta^2}{2} + C_{\sigma_N \eta\eta} \frac{m_{f_0}^2}{2} \right) \ , \tag{A.31}$$

$$-i\mathcal{A}_{\sigma_S \to \eta\eta}(m_{f_0}) = i\left(A_{\sigma_S \eta\eta} - B_{\sigma_S \eta\eta} \frac{m_{f_0}^2 - 2m_\eta^2}{2} + C_{\sigma_S \eta\eta} \frac{m_{f_0}^2}{2} \right) \ , \tag{A.32}$$

$$\begin{aligned} -i\mathcal{A}_{G \to \eta\eta}(m_{f_0}) \quad = \quad & -i\left(A_{G\eta_N\eta_N} - B_{G\eta_N\eta_N} \frac{m_{f_0}^2 - 2m_\eta^2}{2} \right) \cos\varphi_\eta \\ & +i\left(A_{G\eta_S\eta_S} - B_{G\eta_S\eta_S} \frac{m_{f_0}^2 - 2m_\eta^2}{2} \right) \sin\varphi_\eta \end{aligned} \tag{A.33}$$

and the corresponding constants read

$$\begin{aligned} A_{\sigma_N \eta\eta} \quad = \quad & -Z_\pi^2 \phi_N \left(\lambda_1 + \frac{\lambda_2}{2} + c_1 \phi_S^2 \right) \cos^2\varphi_\eta - Z_{\eta_S}^2 \phi_N \left(\lambda_1 + \frac{c_1}{2} \phi_N^2 \right) \sin^2\varphi_\eta \\ & -\frac{3}{4} c_1 Z_\pi Z_{\eta_S} \phi_N^2 \phi_S \sin(2\varphi_\eta) \ , \end{aligned} \tag{A.34}$$

$$B_{\sigma_N \eta\eta} = -\frac{Z_\pi^2 w_{a_1}^2}{\phi_N} (m_1^2 + \frac{h_1}{2} \phi_S^2 + 2\delta_N) \cos^2\varphi_\eta + \frac{h_1}{2} Z_{\eta_S}^2 w_{f_{1S}}^2 \phi_N \sin^2\varphi_\eta \ , \tag{A.35}$$

$$C_{\sigma_N \eta\eta} = g_1 Z_\pi^2 w_{a_1} \cos^2\varphi_\eta \ , \tag{A.36}$$

$$A_{\sigma_S\eta\eta} = -Z_{\eta_S}^2\phi_S\left(\lambda_1+\lambda_2\right)\sin^2\varphi_\eta - Z_\pi^2\phi_S\left(\lambda_1+c_1\phi_N^2\right)\cos^2\varphi_\eta - \frac{1}{4}c_1 Z_\pi Z_{\eta_S}\phi_N^3\sin(2\varphi_\eta)\ , \quad \text{(A.37)}$$

$$B_{\sigma_S\eta\eta} = -\frac{Z_{\eta_S}^2 w_{f_{1S}}^2}{\phi_S}\left(m_1^2+\frac{h_1}{2}\phi_N^2+2\delta_S\right)\sin^2\varphi_\eta + \frac{h_1}{2}Z_\pi^2 w_{a_1}^2\phi_S\cos^2\varphi_\eta\ , \quad \text{(A.38)}$$

$$C_{\sigma_S\eta\eta} = \sqrt{2}g_1 Z_{\eta_S}^2 w_{f_{1S}}\sin^2\varphi_\eta\ , \quad \text{(A.39)}$$

$$A_{G\eta_N\eta_N} = -\frac{m_0^2}{G_0}Z_\pi^2\ , \quad \text{(A.40)}$$

$$B_{G\eta_N\eta_N} = \frac{m_1^2}{2G_0}Z_\pi^2 w_{f_{1N}}^2\ , \quad \text{(A.41)}$$

$$A_{G\eta_S\eta_S} = -\frac{m_0^2}{G_0}Z_{\eta_S}^2\ , \quad \text{(A.42)}$$

$$B_{G\eta_S\eta_S} = \frac{m_1^2}{G_0}Z_{\eta_S}^2 w_{f_{1S}}^2\ . \quad \text{(A.43)}$$

After performing an orthogonal transformation we obtain the amplitudes for the physical scalar-isoscalar fields

$$-i\mathcal{A}_{\sigma'_N\to\eta\eta}(m_{\sigma'_N}) = i\left[\mathcal{A}_{\sigma_N\to\eta\eta}(m_{\sigma'_N})b_{11}+\mathcal{A}_{\sigma_S\to\eta\eta}(m_{\sigma'_N})b_{12}+\mathcal{A}_{G\to\eta\eta}(m_{\sigma'_N})b_{13}\right]\ , \quad \text{(A.44)}$$

$$-i\mathcal{A}_{\sigma'_S\to\eta\eta}(m_{\sigma'_S}) = i\left[\mathcal{A}_{\sigma_N\to\eta\eta}(m_{\sigma'_S})b_{21}+\mathcal{A}_{\sigma_S\to\eta\eta}(m_{\sigma'_S})b_{22}+\mathcal{A}_{G\to\eta\eta}(m_{\sigma'_S})b_{23}\right]\ , \quad \text{(A.45)}$$

$$-i\mathcal{A}_{G'\to\eta\eta}(m_{G'}) = i\left[\mathcal{A}_{\sigma_N\to\eta\eta}(m_{G'})b_{31}+\mathcal{A}_{\sigma_S\to\eta\eta}(m_{G'})b_{32}+\mathcal{A}_{G\to\eta\eta}(m_{G'})b_{33}\right]\ , \quad \text{(A.46)}$$

which we assign to the physical resonances as follows: $\sigma'_N \equiv f_0(1370)$, $\sigma'_S \equiv f_0(1500)$, and $G \equiv f_0(1710)$.

A.4 Decays of the scalar-isoscalar fields into $\rho\rho \to 4\pi$

The decay processes $f_0 \to \rho\rho \to 4\pi$ are on the threshold, hence we use for the calculation of the decay widths the spectral function of the ρ meson

$$d_\rho(X_{m_\rho}) = \mathcal{N}\frac{X_{m_\rho}^2\Gamma_{\rho\to\pi\pi}(X_{m_\rho})}{(X_{m_\rho}^2-m_\rho^2)^2+X_{m_\rho}^2\Gamma_{\rho\to\pi\pi}^2(X_{m_\rho})}\theta(X_{m_\rho}-2m_\pi)\ , \quad \text{(A.47)}$$

where $\mathcal{N}$ is a normalization constant, which guaranties that

$$\int_0^\infty d_\rho(X_{m_\rho})dX_{m_\rho} = 1\ . \quad \text{(A.48)}$$

Here $d_\rho(X_{m_\rho})$ is the probability mass distribution. Considering the polarization of the ρ mesons the general amplitude reads

$$\overline{\left|-i\mathcal{A}_{f_0\to\rho\rho}(m_{f_0},X_{i,m_\rho})\right|}^2 = A_{\rho\rho}^2\left[4-\frac{X_{1,m_\rho}^2+X_{2,m_\rho}^2}{m_\rho^2}+\frac{(m_{f_0}^2-X_{1,m_\rho}^2-X_{2,m_\rho}^2)^2}{4m_\rho^4}\right]\ , \quad \text{(A.49)}$$

where $i = 1, 2$ and $A_{\rho\rho}$ is one of the corresponding constants

$$A_{\sigma_N\rho\rho} = \frac{\phi_N}{2}\left(h_1 + h_2 + h_3\right) \ , \tag{A.50}$$

$$A_{\sigma_S\rho\rho} = \frac{\phi_S}{2} h_1 \ , \tag{A.51}$$

$$A_{G\rho\rho} = \frac{m_1^2}{G_0} \ . \tag{A.52}$$

The physical amplitudes of the scalar-isoscalar fields read

$$\begin{aligned}
&\overline{\left|-i\mathcal{A}_{\sigma'_N\to\rho\rho}(m_{f_0}, X_{i,m_\rho})\right|}^2 \\
&= \left[A_{\sigma_N\rho\rho}b_{11} + A_{\sigma_S\rho\rho}b_{12} + A_{G\rho\rho}b_{13}\right]^2\left[4 - \frac{X_{1,m_\rho}^2 + X_{2,m_\rho}^2}{m_\rho^2} + \frac{(m_{f_0}^2 - X_{1,m_\rho}^2 - X_{2,m_\rho}^2)^2}{4m_\rho^4}\right] \ ,
\end{aligned} \tag{A.53}$$

$$\begin{aligned}
&\overline{\left|-i\mathcal{A}_{\sigma'_S\to\rho\rho}(m_{f_0}, X_{i,m_\rho})\right|}^2 \\
&= \left[A_{\sigma_N\rho\rho}b_{21} + A_{\sigma_S\rho\rho}b_{22} + A_{G\rho\rho}b_{23}\right]^2\left[4 - \frac{X_{1,m_\rho}^2 + X_{2,m_\rho}^2}{m_\rho^2} + \frac{(m_{f_0}^2 - X_{1,m_\rho}^2 - X_{2,m_\rho}^2)^2}{4m_\rho^4}\right] \ ,
\end{aligned} \tag{A.54}$$

$$\begin{aligned}
&\overline{\left|-i\mathcal{A}_{G'\to\rho\rho}(m_{f_0}, X_{i,m_\rho})\right|}^2 \\
&= \left[A_{\sigma_N\rho\rho}b_{31} + A_{\sigma_S\rho\rho}b_{32} + A_{G\rho\rho}b_{33}\right]^2\left[4 - \frac{X_{1,m_\rho}^2 + X_{2,m_\rho}^2}{m_\rho^2} + \frac{(m_{f_0}^2 - X_{1,m_\rho}^2 - X_{2,m_\rho}^2)^2}{4m_\rho^4}\right] \ .
\end{aligned} \tag{A.55}$$

The formula for the decays of the scalar-isoscalar fields into ρ mesons and 4π, respectively, reads

$$\Gamma_{f_0\to\rho\rho}(m_{f_0}, X_{i,m_\rho}) = 6\frac{k_f(m_{f_0}, X_{i,m_\rho})}{8\pi m_{f_0}^2}\overline{\left|-i\mathcal{A}_{f_0\to\rho\rho}(m_{f_0}, X_{i,m_\rho})\right|}^2\theta(m_{f_0} - X_{1,m_\rho} - X_{2,m_\rho}) \ , \tag{A.56}$$

$$\Gamma_{f_0\to\rho\rho\to4\pi} = \int_0^\infty\int_0^\infty \Gamma_{f_0\to\rho\rho}(m_{f_0}, X_{i,m_\rho})d_\rho(X_{1,m_\rho})d_\rho(X_{2,m_\rho})dX_{1,m_\rho}dX_{2,m_\rho} \ . \tag{A.57}$$

Appendix B

Details of the study of the pseudoscalar Glueball

B.1 Explicit form of the pseudoscalar glueball Lagrangian

After performing the field transformations in Eqs. (2.122) and (2.132)-(2.133), the effective Lagrangian (5.1) takes the form:

$$
\begin{aligned}
\mathcal{L}_{\tilde{G}}^{int} = \frac{c_{\tilde{G}\Phi}}{2\sqrt{2}}\tilde{G}(&\sqrt{2}Z_{K^\star}Z_K a_0^0 K_0^{\star 0}\bar{K}^0 + \sqrt{2}Z_K Z_{K^\star} a_0^0 K^0 \bar{K}_0^{\star 0} - 2Z_{K^\star}Z_K a_0^+ K_0^{\star 0} K^- \\
&- 2Z_{K^\star}Z_K a_0^+ K_0^{\star -} K^0 - 2Z_{K^\star}Z_K a_0^- \bar{K}_0^{\star 0} K^+ - \sqrt{2}Z_{K^\star}Z_K a_0^0 K_0^{\star -} K^+ - \sqrt{2}Z_K^2 Z_{\eta_N} K^0 \bar{K}^0 \eta_N \\
&+ \sqrt{2}Z_{K^\star}^2 Z_{\eta_N} K_0^{\star 0}\bar{K}_0^{\star 0}\eta_N - \sqrt{2}Z_K^2 Z_{\eta_N} K^- K^+ \eta_N + Z_{\eta_S} {a_0^0}^2 \eta_S + 2Z_{\eta_S} a_0^- a_0^+ \eta_S \\
&+ Z_{\eta_N}^2 Z_{\eta_S}\eta_N^2\eta_S - \sqrt{2}Z_K^2 Z_\pi K^0\bar{K}^0\pi^0 + \sqrt{2}Z_{K^\star}^2 Z_\pi K_0^{\star 0}\bar{K}_0^{\star 0}\pi^0 + \sqrt{2}Z_K^2 Z_\pi K^- K^+\pi^0 \\
&- Z_{\eta_S}Z_\pi^2\eta_S\,{\pi^0}^2 + 2Z_K^2 Z_\pi \bar{K}^0 K^+\pi^- + 2Z_K^2 Z_\pi K^0 K^-\pi^+ - 2Z_{K^\star}^2 Z_\pi K_0^{\star 0}K_0^{\star -}\pi^+ \\
&- 2Z_{\eta_S}Z_\pi^2\eta_S\pi^-\pi^+ - 2Z_{K^\star}Z_K a_0^- K_0^{\star +}\bar{K}^0 + \sqrt{2}Z_{K^\star}^2 Z_{\eta_N} K_0^{\star +}K_0^{\star -}\eta_N - \sqrt{2}Z_{K^\star}^2 Z_\pi K_0^{\star +}K_0^{\star -}\pi^0 \\
&- 2Z_{K^\star}^2 Z_\pi K_0^{\star +}\bar{K}_0^{\star 0}\pi^- - \sqrt{2}Z_{K^\star}Z_K a_0^0 K_0^{\star +}K^- + \sqrt{2}Z_K Z_{K^\star}K^- K_0^{\star +}\phi_N + \sqrt{2}Z_K Z_{K^\star}K^- K_0^{\star +}\sigma_N \\
&+ \sqrt{2}Z_{K^\star}Z_K K_0^{\star 0}\bar{K}^0\phi_N + \sqrt{2}Z_{K^\star}Z_K K_0^{\star 0}\bar{K}^0\sigma_N + \sqrt{2}Z_K Z_{K^\star}K^0\bar{K}_0^{\star 0}\phi_N + \sqrt{2}Z_K Z_{K^\star}K^0\bar{K}_0^{\star 0}\sigma_N \\
&+ \sqrt{2}Z_{K^\star}Z_K K_0^{\star -}K^+\phi_N + \sqrt{2}Z_{K^\star}Z_K K_0^{\star -}K^+\sigma_N - Z_{\eta_S}\eta_S\phi_N^2 - Z_{\eta_S}\eta_S\sigma_N^2 - 2Z_{\eta_S}\eta_S\phi_N\sigma_N \\
&+ 2Z_\pi a_0^0\pi^0\phi_S + 2Z_\pi a_0^0\pi^0\sigma_S + 2Z_\pi a_0^+\pi^-\phi_S + 2Z_\pi a_0^+\pi^-\sigma_S + 2Z_\pi a_0^-\pi^+\phi_S + 2Z_\pi a_0^-\pi^+\sigma_S \\
&- 2Z_{\eta_N}\eta_N\phi_N\phi_S - 2Z_{\eta_N}\eta_N\phi_N\sigma_S - 2Z_{\eta_N}\eta_N\sigma_N\phi_S - 2Z_{\eta_N}\eta_N\sigma_N\sigma_S) \ . \qquad \text{(B.1)}
\end{aligned}
$$

This expression is used to determine the coupling of the field $\tilde{G}$ to scalar and pseudoscalar mesons.

B.2 Further results for the decays $\tilde{G} \to P f_0$

In order to calculate the decay of the pseudoscalar glueball into an ordinary pseudoscalar meson and an f_0 resonance we consider, as in Refs. [6, 8], other solutions of mixing of the resonances $f_0(1370), f_0(1500)$, and $f_0(1710)$. Two solutions are from Ref. [207] and one solution is from

Ref. [213]. The corresponding mixing matrices read:

$$B_1 = \begin{pmatrix} 0.86 & 0.24 & 0.45 \\ -0.45 & -0.06 & 0.89 \\ -0.24 & 0.97 & -0.06 \end{pmatrix}, \tag{B.2}$$

$$B_2 = \begin{pmatrix} 0.81 & 0.19 & 0.54 \\ -0.49 & 0.72 & 0.49 \\ 0.30 & 0.67 & -0.68 \end{pmatrix}, \tag{B.3}$$

$$B_3 = \begin{pmatrix} 0.78 & 0.51 & -0.36 \\ -0.54 & 0.84 & 0.03 \\ 0.32 & 0.18 & 0.93 \end{pmatrix}. \tag{B.4}$$

In all three solutions $f_0(1370)$ is predominantly described by the bare field σ_N, but the assignments for the other resonances vary. In the first solution of Ref. [207], Eq. (B.2), the resonance $f_0(1500)$ is predominantly gluonic, while in the other two solutions, Eqs. (B.3) and (B.4), the resonance $f_0(1710)$ has the largest gluonic content. The corresponding branching ratios are reported in Table B.1.

Quantity	**Sol. 1 of Ref. [207]**	**Sol. 2 of Ref. [207]**	**Sol. of Ref. [213]**
$\Gamma_{\tilde{G}\to\eta f_0(1370)}/\Gamma^{tot}_{\tilde{G}}$	0.00093 (0.0011)	0.00058 (0.00068)	0.0044 (0.0052)
$\Gamma_{\tilde{G}\to\eta f_0(1500)}/\Gamma^{tot}_{\tilde{G}}$	0.000046 (0.000051)	0.0082 (0.0090)	0.011 (0.012)
$\Gamma_{\tilde{G}\to\eta f_0(1710)}/\Gamma^{tot}_{\tilde{G}}$	0.011 (0.0089)	0.0053 (0.0042)	0.00037 (0.00029)
$\Gamma_{\tilde{G}\to\eta' f_0(1370)}/\Gamma^{tot}_{\tilde{G}}$	0.038 (0.026)	0.033 (0.022)	0.043 (0.029)
$\Gamma_{\tilde{G}\to\eta' f_0(1500)}/\Gamma^{tot}_{\tilde{G}}$	0.0062 (0)	0.00020 (0)	0.00013 (0)
$\Gamma_{\tilde{G}\to\eta' f_0(1710)}/\Gamma^{tot}_{\tilde{G}}$	0 (0)	0 (0)	0 (0)

Table B.1: Branching ratios for the decays of the pseudoscalar glueball $\tilde{G}$ into η and η', respectively and one of the scalar-isoscalar resonances $f_0(1370), f_0(1500)$, and $f_0(1710)$ by using three different mixing scenarios of these scalar-isoscalar states reported in Refs. [207, 213]. The mass of the pseudoscalar glueball is $m_{\tilde{G}} = 2.6$ GeV and $m_{\tilde{G}} = 2.37$ GeV (values in parentheses), respectively.

Deutschsprachige Zusammenfassung

Theoretische Grundlagen

Das Standardmodell der Elementarteilchen Das gegenwärtige physikalische Weltbild beruht auf den vier uns bekannten fundamentalen Kräften bzw. Wechselwirkungen. Drei dieser Wechselwirkungen, die elektromagnetische, die schwache und die starke, bilden das Standardmodell der Elementarteilchen (SM) und werden mit lokalen Quantenfeldtheorien (QFT) beschrieben[1]. Diese Theorien basieren auf einigen wenigen Symmetrien, die sich in der Natur beobachten lassen. Die fundamentalen Symmetrien dieser Wechselwirkungen bzw. des SM, $U(1) \times SU(2) \times SU(3)$, resultieren aus der Forderung nach einer lokalen Eichinvarianz, wodurch die entsprechenden Eichbosonen mit Spin $S = 1$ hervorgehen und diese als Austauschteilchen zwischen den Materieteilchen, die der jeweiligen Wechselwirkung unterliegen, interpretiert werden. Sowohl die zwölf Eichbosonen des SM als auch die Materieteilchen, zu denen die sechs Quarks und sechs Leptonen zählen und auf Grund ihres halbzahligen Spins $S = \frac{1}{2}$ zu den Fermionen gehören, weisen im Rahmen der Genauigkeit heutiger Hochenergie-Experimente keine Substruktur auf und gelten daher als elementar[2]. Die Beschreibung der Natur auf der Basis solcher lokalen QFT hat sich als erfolgreich und vielversprechend herausgestellt. Dies belegen einerseits viele experimentelle Befunde, einige, für diese Arbeit relevante, werden wir noch erwähnen, andererseits ist beispielsweise die Quantenelektrodynamik (QED), die die elektromagnetische Wechselwirkung beschreibt, derzeitig die am genauesten experimentell überprüfte Theorie. Darüberhinaus konnte diese mit der Eichtheorie der schwachen Wechselwirkung zur elektroschwachen Theorie vereinheitlicht werden. Eine weitere Vereinheitlichung, bei der noch die Theorie der starken Wechselwirkung, die Quantenchromodynamik (QCD), einbezogen ist, die Große Vereinheitlichte Theorie (Grand Unified Theory), konnte bis jetzt noch nicht erfolgreich umgesetzt werden, da beispielsweise entsprechende Theorien einen Zerfall des Protons vorhersagen und dies konnte bis jetzt noch nicht experimentell bestätigt werden. Außerdem sind zu weiteren experimentellen Verifikationen solcher Theorien Beschleunigerenergien, die der Planckskala (10^{19} GeV) entsprechen,

[1] Die vierte fundamentale Wechselwirkung ist die Gravitation und wird durch die allgemeine Relativitätstheorie beschrieben. Diese konnte bis jetzt noch nicht einwandfrei in das SM implementiert werden, da konzeptionelle Schwierigkeiten, wie ihre Nicht-Renormierbarkeit und die tensorielle Natur der Gravitonen, vorliegen und noch nicht überbrückt werden konnten.

[2] Man beachte, dass zu jedem Materieteilchen des SM ein entsprechendes Antiteilchen existiert. Ihr Unterschied liegt in den entgegengesetzten additiven Quantenzahlen, während ihre Massen, falls vorhanden, exakt gleich sind.

notwendig, die jedoch (noch) nicht realistisch sind.

Hadronen Die vorliegende Arbeit beschäftigt sich mit der Untersuchung von Hadronen. Dies sind Teilchen, die der starken Wechselwirkung unterliegen und aus Quarks[3] und Gluonen, den Eichbosonen der QCD, zusammengesetzt sind. Eine besondere Eigenschaft der QCD ist, dass sowohl Quarks als auch Gluonen nicht isoliert, sondern in Hadronen eingeschlossen sind. Diese Hadronen haben eine Ausdehnung von Λ_{QCD}^{-1}, wobei $\Lambda_{QCD} \simeq 200$ MeV die typische hadronische Energieskala ist. Diesen experimentell bewiesenen, theoretisch jedoch nicht vollkommen verstandenen Umstand bezeichnet man als Confinement. Hadronen werden bezüglich ihres Spins in Baryonen und Mesonen unterschieden.

Die Baryonen besitzen einen halbzahligen Spin, sind somit Fermionen, und bestehen aus drei Quarks. Die bekanntesten Vertreter dieser Hadronen-Gruppe stellen die Protonen und Neutronen dar, die als Nukleonen zusammengefasst werden und aus den up und down Quarks aufgebaut sind. Eine wichtige Erhaltungsgröße der Baryonen in der QCD ist die Baryonenzahl $B = 1$ bzw. Antibaryonen $B = -1$. Dies impliziert, dass die Quarks $B_q = \frac{1}{3}$ und die Antiquarks entsprechend $B_{\bar{q}} = -\frac{1}{3}$ besitzen.

Die Mesonen, die relevant für diese Arbeit sind, besitzen einen ganzzahligen Spin, wodurch sie den Bosonen angehören und deren allgemeinste Definition durch die Baryonenzahl $B = 0$ gewährleistet ist. Die Konstituenten der gewöhnlichen Mesonen sind Quarks und Antiquarks. Um jedoch die große Breite des bekannten hadronischen Spektrums theoretisch beschreiben zu können, insbesondere im skalaren Bereich $J^{PC} = 0^{++}$, wurden weitere Mesonen postuliert, welche die Bedingung $B = 0$ erfüllen. Dies sind beispielsweise Tetraquarks, die aus einem Diquark und einem Antidiquark ($qq\bar{q}\bar{q}$) bestehen. Darüber hinaus werden Mesonen vorhergesagt, deren Konstituenten nicht Quarks, genauer gesagt Valenzquarks, sind, sondern Gluonen bzw. Valenzgluonen, die sogenannten Gluebälle, die eine zentrale Rolle in dieser Arbeit spielen. Im Folgenden werden wir auf deren Rechtfertigung sowie ihre Eigenschaften und Bedeutung kurz eingehen.

Farbladung und Eigenschaften der Gluonen Hinsichtlich der Tatsache, dass Quarks in drei Farbzuständen, i. d. R. als rot, grün und blau bezeichnet, vorkommen, wurde zu deren Beschreibung die lokale $SU_c(N_c)$-Farbsymmetrie, wobei $N_c = 3$ die Anzahl der Farben ist, gewählt. Die Farbladung wurde zunächst postuliert, um die Wellenfunktion der Delta-Resonanz Δ^{++} bzw. heute bezeichnet als $\Delta(1232)$ zu antisymmetrisieren und dadurch die Gültigkeit des als physikalisch fundamental betrachteten Spin-Statistik-Theorems von Wolfgang Pauli zu erhalten. Die späteren experimentellen Beweise, wie beispielsweise der Zerfall des neutralen Pions in zwei Photonen, $\pi \to \gamma\gamma$, oder das Verhältnis der Wirkungsquerschnitte für hadronische und leptonische Elektron-Positron-Vernichtung, konnten mit theoretischen Berechnungen nur dann übereinstimmten, wenn angenommen wurde, dass drei Farbfreiheitsgrade ($N_c = 3$) existieren. Diese experimentellen Befunde führten schließlich dazu, dass die lokale Farbsymmetrie der QCD als physikalisch fundamental angesehen wurde. Dies begünstigte ihre Weiterentwicklung und nach

[3]Genauer gesagt bestehen sie aus drei Valenz- bzw. Konstituentenquarks, die die Quantenzahlen sowie die Massen der Hadronen bestimmen.

dem theoretischen Beweis der Renormierbarkeit der nicht-abelschen Yang-Mills-Theorien sowie der asymptotischen Freiheit wurde QCD zur wohletablierten Theorie der starken Wechselwirkung. Als Konsequenz der nicht-abelschen Natur der $SU_c(3)$-Farbsymmetrie sind die Gluonen selbst Träger der Farbladung, was eine Selbstkopplung der Gluonen impliziert. Auf Grund dieser Selbstkopplung zusammen mit dem Confinement erwartet man gebundene gluonische Zustände, die Gluebälle, die invariant unter den Transformationen der Farbsymmetrie sind, sowie entsprechend ihrer Konstituenten $B = 0$ aufweisen. Aus experimenteller Sicht konnten Gluonen einerseits direkt bei Elektron-Positron-Vernichtungsprozessen durch Beobachtung von Drei-Jet-Ereignissen nachgewiesen werden. Andererseits konnte durch Analyse von Vier-Jet-Ereignissen die Selbstkopplung der Gluonen experimentell verifiziert werden. Der eindeutige experimentelle Beweis von Gluebällen steht jedoch noch aus und ist mit großen Herausforderungen verbunden. Eine eindeutige Identifikation von Gluebällen würde zum Einen ein weiterer stützender Beweis für die QCD als fundamentale Theorie der Natur sein. Zum Anderen würde man wichtige Erkenntnisse über die Natur des Confinements bzw. den nicht-störungstheoretischen Bereich der QCD gewinnen.

Gluebälle, Motivation und das hadronische Modell

Zugang und Eigenschaften von Gluebällen Aus theoretischer Sicht ist die Existenz von Gluebällen eine eindeutige Vorhersage der QCD. Um deren Eigenschaften zu studieren bzw. zu erhalten müsste man die QCD-Lagrangedichte, insbesondere den Eichsektor der QCD, analytisch in (3+1) Dimensionen lösen. Dies ist aufgrund der Nichtlinearität der Yang-Mills-Gleichungen gegenwärtig leider noch nicht gelungen. Überdies ist die Anwendung von störungstheoretischen Methoden nicht möglich, da im niederenergetischen Bereich der QCD, welcher unter anderem für Gluebälle interessant ist, die von Energie bzw. einer Renormierungsskala abhängige starke Kopplungskonstante groß ist, $g_s \gtrsim 1$. Dennoch gibt es andere vielversprechende Methoden, die einen Zugang zur Untersuchung von Gluebällen bzw. diesen nicht-störungstheoretischen Bereich der QCD liefern. Dies sind einerseits auf der QCD, und insbesondere auf ihren Symmetrieeigenschaften, basierende effektive quantenfeldtheoretische Modelle. Im Rahmen solcher Modelle haben sich auch Betrachtungen der QCD in der N_c^{-1} Entwicklung mit dem Grenzfall $N_c \to \infty$ als sehr nützlich erwiesen. Dadurch können Größenordnungen freier Parameter sowie das Verhalten wichtiger physikalischer Größen, wie z. B. Massen, Amplituden und folglich auch Zerfallsbreiten, abgeschätzt werden. Mit dem sogenannten erweiterten Linearen Sigma Modell (eLSM) werden wir in der vorliegenden Arbeit diese Herangehensweise verfolgen und werden im weiteren Verlauf auf Eigenschaften unseres Modells zu sprechen kommen. Andererseits kann die QCD auf dem Gitter simuliert werden. In diesem Fall bedient man sich direkt den ersten Prinzipien der QCD, indem man die Zwei-Punkt-Korrelations-Funktion heranzieht und aus deren Zerfall die Massen der Gluebälle extrahiert. Mit solchen QCD-Gitterrechnungen konnte ein komplettes Massenspektrum der Gluebälle berechnet werden, bei dem ein skalarer Glueball ($J^{PC} = 0^{++}$) mit einer Masse von etwa $m_G^{lat} \approx 1.7$ GeV den leichtesten Zustand darstellt. Eine wichtige Eigenschaft der Gluebälle ist ihre Flavorblindheit, da die Gluonen mit der gleichen Stärke an alle Quarkflavors koppeln. Außerdem erwartet man eine Mischung zwischen Gluebällen und Quark-Antiquark-Mesonen, sofern ihre Quantenzahlen übereinstimmen. Entsprechend der Stärke der

Mischung kann dies eine große und zusätzliche Herausforderung bei der experimentellen Suche nach Gluebällen sein, da die Unterscheidung zwischen einem Zustand, der überwiegend Glueball, und einem, der überwiegend ein gewöhnliches Meson ist, nicht trivial ist. Um Gluebälle zu untersuchen, eignen sich besonders die sogenannten gluon-reichen Prozesse, da in solchen eine Formierung von Gluebällen sehr wahrscheinlich ist. Eine große Bedeutung haben dabei die radiativen J/ψ Zerfälle $J/\psi \to G \to \gamma Hadronen$, welche z. B. beim *BEijing Spectrometer* (BES) III-Experiment intensiv und mit einem sehr großen Umfang an Daten untersucht wurden. Weitere solche gluon-reichen Prozesse sind die zentralen Kollisionen, bei denen hochenergetische Hadronen gestreut werden, sowie die Proton-Antiproton-Vernichtung. Bei Letzteren können Gluebälle direkt oder zusammen mit anderen Teilchen als Zwischenzustände erzeugt werden, die ihrerseits weiter zerfallen. Ein vielversprechendes, auf $\bar{p}p$ Vernichtung basierendes Experiment, bei dem unter anderem Gluebälle im Massenbereich von $2.1 - 5.5$ GeV erzeugt und studiert werden können, ist das *AntiProton ANnihilations at DArmstadt* ($\bar{\text{P}}$ANDA) Experiment innerhalb der sich im Aufbau befindenden *Facility for Antiproton and Ion Research* (FAIR)-Anlage bei Darmstadt, sowie auch das *GLUonic EXcitations* (GlueX) Experiment am *Jefferson national LABoratory* (JLAB).

Der skalare Glueball Eine der größten Herausforderungen der hadronischen Physik ist das Verständnis des skalaren-isoskalaren Sektors, $I^G(J^{PC}) = 0^+(0^{++})$, unterhalb der Energie von 2 GeV. In diesem Energiebereich werden gegenwärtig fünf f_0-Resonanzen der Particle Data Group (PDG) aufgeführt. Viele Studien deuten daraufhin, dass die beiden Resonanzen $f_0(500)$ und $f_0(980)$, deren Massen unterhalb 1 GeV liegen, keine Quark-Antiquark-Mesonen sind, sondern zu einem Tetraquark-Nonet gehören oder sie sind mesonische Moleküle. Im Energiebereich zwischen 1 und 2 GeV befinden sich die weiteren Resonanzen $f_0(1370)$, $f_0(1500)$ und $f_0(1710)$. Allerdings können höchstens zwei dieser Resonanzen als überwiegende $\bar{q}q$ Zustände interpretiert werden, und zwar eine als ein nicht-seltsames $\sigma_N \cong \left(\bar{u}u + \bar{d}d\right)/\sqrt{2}$ und die andere als ein seltsames $\sigma_S \cong \bar{s}s$ Meson. Folglich stellt sich die Frage, ob sich der skalare Glueball unter diesen drei Resonanzen befindet, welcher wegen seiner Quantenzahlen des Vakuums direkt mit der Spuranomalie des Yang-Mills-Sektors der QCD zusammenhängt. Falls ja, dann ergibt sich eine weitere Frage, nämlich, welche dieser f_0-Resonanzen besitzt den größten gluonischen Anteil.

Der pseudoskalare und vektorielle Glueball Wie schon bereits angedeutet, wird es mit dem $\bar{\text{P}}$ANDA Experiment möglich sein, schwere Zustände zu erzeugen und somit auch mögliche schwere Gluebälle. Man erwartet, dass diese Gluebälle weniger mit gewöhnlichen Quark-Antiquark-Mesonen mischen und daher möglicherweise leichter zu identifizieren sein werden, im Gegensatz zu dem skalaren Glueball, der sich wahrscheinlich unter den f_0-Resonanzen verbirgt. Aus diesem Grund interessieren wir uns in dieser Arbeit einerseits für den pseudoskalaren Glueball ($J^{PC} = 0^{-+}$) mit der Masse von etwa 2.6 GeV, wie Gitterrechnungen der QCD vorhersagen. Andererseits ist es der Vektorglueball ($J^{PC} = 1^{--}$) mit der Masse von etwa 3.8 GeV, die ebenfalls aus den Gitterrechnungen der QCD folgt. Auf Grund der Quantenzahlen ist der Vektorglueball aus mindestens drei Gluonen zusammengesetzt und damit sollte seine Umwandlung in einen Quark-Antiquark-Meson unwahrscheinlich sein. Folglich wird eine kleine Zerfallsbreite dieses Glueballs erwartet.

Das hadronische Modell Um die bereits diskutierten Fragestellungen der hadronischen Physik im mesonischen Sektor zu untersuchen, wird das eLSM herangezogen. Die Freiheitsgrade des eLSM sind auf Grund des Confinements von Beginn an Hadronen, nämlich Quark-Antiquark-Mesonen sowie ein skalarer Glueball, welcher durch die Anregungen des skalaren Dilatons beschrieben wird. Weitere Gluebälle lassen sich leicht in das eLSM einbetten. Die $\bar{q}q$-Felder beinhalten nicht nur skalare ($S, 0^{++}$) und pseudoskalare (P, 0^{-+}) Mesonen, sondern auch Vektor- (V_μ, 1^{--}) und Axial-Vektor (A_μ, 1^{++}) Mesonen. Die letztgenannten Vektorfelder sind von großer Bedeutung, um die Phänomenologie korrekt zu beschreiben, da diese auch den (pseudo)skalaren Sektor beeinflussen. Das effektive feldtheoretische Modell ist im Einklang mit den Eigenschaften der QCD bzw. ihrer Lagrangedichte. Da das eLSM eine auf dem Confinement basierende effektive Feldtheorie ist, wird die Dynamik durch die globale chirale und die Dilatations-Symmetrie bestimmt und weniger durch die lokale $SU_c(3)$-Farbsymmetrie, die folglich trivial erfüllt ist. Die Realisierung des eLSM mit drei Quarkflavors beinhaltet im skalaren-isoskalaren Sektor zwei nackte Quark-Antiquark-Mesonen, nämlich σ_N und σ_S, als auch einen skalaren Glueball G, die allesamt miteinander mischen und die physikalischen Resonanzen $f_0(1370)$, $f_0(1500)$ und $f_0(1710)$ generieren. Da die Felder σ_N, σ_S und G die Quantenzahlen des Vakuums besitzen, treten in unserem Modell drei verschiedene Kondensate in Erscheinung, nämlich das nicht-seltsame und das seltsame Quarkkondensat $\left\langle \bar{u}u + \bar{d}d \right\rangle / \sqrt{2} \neq 0$ und $\langle \bar{s}s \rangle \neq 0$, als auch das Gluonkondensat $\left\langle \frac{\alpha_s}{\pi} G^a_{\mu\nu} G^{\mu\nu}_a \right\rangle \neq 0$. Folglich ist es interessant zu lernen, wie groß die entsprechenden Beiträge zur Erzeugung der Hadronenmassen sind.

Mischung im skalaren-isoskalaren Sektor des eLSM

Das eLSM im Fall von $N_f = 2$ Die Untersuchungen des skalaren Glueballs im eLSM wurden zunächst für den Fall $N_f = 2$ durchgeführt. In dieser Realisierung des eLSM sind Mesonen, die aus den seltsamen Quarks zusammengesetzt sind, nicht enthalten. Ferner ergibt sich im skalaren-isoskalaren Sektor ein Zwei-Körper-Mischungsszenario, in dem das nackte nicht-seltsame Quark-Antiquark-Meson σ_N und der nackte skalare Glueball G mischen und zwei physikalische f_0-Resonanzen erzeugen. Folglich lassen sich verschiedene Zuweisungen der nackten Felder σ_N und G zu den f_0-Resonanzen durchführen und mit Hilfe der χ^2-Methode untersuchen. Dazu wurden physikalische Größen der skalaren-isoskalaren Resonanzen, wie beispielsweise ihre Massen und Zerfallsbreiten, herangezogen. Die Rechnungen wurden durchgeführt im Vakuum, d. h. bei verschwindender Temperatur ($T = 0$) und bei verschwindendem chemischen Potential ($\mu = 0$), und auf Baumdiagrammniveau, d. h. ohne Schleifenkorrekturen. Dabei wurden zwei akzeptable Lösungen gefunden, bei denen jeweils die Resonanz $f_0(1370)$ überwiegend das nicht-seltsame $\bar{q}q$-Meson ist, während der Glueball in einer Lösung überwiegend $f_0(1500)$ und in der anderen überwiegend $f_0(1710)$ ist. Der Grund für das nicht eindeutige Ergebnis liegt darin, dass die Realisierung des eLSM mit $N_f = 2$ unvollständig ist, da das nackte seltsame Feld σ_S vernachlässigt wurde.

Es gibt jedoch eine Reihe von Argumenten, die die Resonanz $f_0(1710)$ als überwiegenden Glueball-Zustand unterstützen. Die wichtige Eigenschaft der Flavorblindheit erfordert für einen reinen

Glueball

$$\frac{\Gamma_{G'\to\pi\pi}}{\Gamma_{G'\to KK}} = \frac{3}{4} \, .$$

Die entsprechenden Verzweigungsverhältnisse für die zwei mutmaßlichen Kandidaten für den skalaren Glueball lauten

$$\frac{\Gamma_{f_0(1500)\to\pi\pi}}{\Gamma_{f_0(1500)\to KK}} = 4.06$$

und

$$\frac{\Gamma_{f_0(1710)\to\pi\pi}}{\Gamma_{f_0(1710)\to KK}} = 0.41 \, .$$

Dies zeigt, dass die Forderung nach der Flavorblindheit eher für die Resonanz $f_0(1710)$ als für die $f_0(1500)$ erfüllt ist. An dieser Stelle wollen wir noch anmerken, dass die Verzweigungsverhältnisse der f_0-Resonanzen $\bar{q}q$-Komponenten enthalten. Außerdem sind die experimentellen Fehler der Zerfallsbreiten von $f_0(1710)$ hinreichend groß, so dass eine Übereinstimmung zwischen den theoretischen und experimentellen Werten möglich ist, während eine entsprechende Übereinstimmung für die Resonanz $f_0(1500)$ nicht vorliegt. Des Weiteren sagen Gitterrechnungen der QCD eine Masse des skalaren Glueballs von $m_G^{lat} \approx 1.7$ GeV voraus, welcher der Masse von $f_0(1710)$ sehr nah ist. Schließlich soll noch auf die Produktionsrate in den radiativen J/ψ Zerfällen hingewiesen werden, die für $f_0(1710)$ höher ist als für $f_0(1500)$.

Diese Argumente sprechen für das Szenario, in dem $G' \equiv f_0(1710)$ ist. Um jedoch ein schlüssiges Ergebnis innerhalb des eLSM zu erzielen, ist eine Studie notwendig, die ein Drei-Körper-Mischungsszenario beinhaltet, in dem die nackten Felder σ_N, σ_S und G involviert sind und die Resonanzen $f_0(1370)$, $f_0(1500)$ und $f_0(1710)$ erzeugen.

Abschließend haben wir auch Szenarien untersucht, in denen die Resonanz $f_0(500)$ überwiegend als das nicht-seltsame $\bar{q}q$-Meson interpretiert wurde. Es stellte sich jedoch heraus, dass diese Szenarien stark nicht-favorisiert sind, da sie die experimentellen Daten nicht beschreiben können z. B. ist die Zerfallsbreite $\Gamma_{\sigma'_N\to\pi\pi} \lesssim 180$ MeV deutlich schmaler als der entsprechende experimentelle Wert $\Gamma^{ex}_{f_0(500)\to\pi\pi} = (400 - 700)$ MeV.

Das eLSM im Fall von $N_f = 3$ Die Realisierung des eLSM mit drei Quarkflavors erfordert die Lösung eines Drei-Körper-Mischungsproblems, um herauszufinden, welche f_0-Resonanz man als den skalaren Glueball interpretieren kann. Im Gegensatz zur Realisierung des eLSM im Fall von zwei Quarkflavors konnten wir in diesem Fall eine eindeutige Lösung finden, die die Phänomenologie in dem skalaren-isoskalaren Sektor sehr gut beschreibt. Wir fanden heraus, dass die Resonanz $f_0(1710)$ überwiegend der skalare Glueball ist, während die Resonanzen $f_0(1370)$ und $f_0(1500)$ überwiegend das nicht-seltsame σ_N und das seltsame σ_S Quark-Antiquark-Meson sind

$$\begin{pmatrix} f_0(1370) \\ f_0(1500) \\ f_0(1710) \end{pmatrix} = \begin{pmatrix} -0.91 & 0.24 & -0.33 \\ 0.30 & 0.94 & -0.17 \\ -0.27 & 0.26 & 0.93 \end{pmatrix} = \begin{pmatrix} \sigma_N \cong \left(\bar{u}u + \bar{d}d\right)/\sqrt{2} \\ \sigma_S \cong \bar{s}s \\ G \cong glueball \end{pmatrix} .$$

Diese Lösung basiert auf der Annahme, dass die Zerfallsbreite des Glueballs schmal ist ($\Gamma_G \lesssim 100$ GeV), was mit den Argumenten des large-N_c Formalismus übereinstimmt. Dies hat eine interessante Konsequenz zur Folge, nämlich einen großen Energieskalenparameter Λ_{dil}, dessen Ursprung

in der Spuranomalie liegt, und das impliziert ein großes Gluonkondensat $\left\langle \frac{\alpha_s}{\pi} G^a_{\mu\nu} G^{\mu\nu}_a \right\rangle$.

An dieser Stelle wollen wir noch einmal hervorheben, dass die Einbindung der (Axial-)Vektor-Freiheitsgrade entscheidend für die erzielten Ergebnisse des eLSM war. Durch ihre Beeinflussung des (pseudo)skalaren Sektors, beispielsweise geht aus unserem Modell hervor, dass der chirale Partner des Pions die Resonanz $f_0(1370)$ ist. Des Weiteren ist es nach unserer Kenntnis das erste Mal, dass eine vollständige Mischung, N_f = 3, über der Energie von 1 GeV von zwei skalaren-isoskalaren Quarkonia und einem skalaren Glueball, der durch das Dilaton-Feld beschrieben wird, in einem chiralen hadronischen Modell mit (axial-)vektor Mesonen, untersucht wurde.

Der pseudoskalare Glueball im Rahmen des eLSM

Ferner wurden in dieser Arbeit die Vakuumeigenschaften des pseudoskalaren Glueballs $\tilde{G}$ untersucht. In diesem Zusammenhang haben wir im Einklang mit dem eLSM eine effektive Lagrangedichte konstruiert, die diesen pseudoskalaren Glueball mit Quark-Antiquark-Mesonen koppelt. Die entsprechende Masse ist $m_{\tilde{G}}$ = 2.6 GeV, die aus den Gitterrechnungen der QCD in der sogenannten quenched-Näherung folgt. Diese Masse liegt im Energiebereich der geplanten Experimente $\bar{\text{P}}$ANDA oder GlueX. Wir präsentieren die entsprechenden Ergebnisse als Verzweigungsverhältnisse, um eine parameterfreie Vorhersage machen zu können, die als eine Richtlinie für die Suche nach Gluebällen dienen kann. Unsere Rechnungen zeigen, dass $\tilde{G} \to KK\pi$ der dominierende Zerfallskanal des pseudoskalaren Glueballs ist ($\sim$ 47%), gefolgt von $\tilde{G} \to \eta\pi\pi$ ($\sim$ 16%) und $\tilde{G} \to \eta'\pi\pi$ ($\sim$ 10%), während der Zerfall $\tilde{G} \to \pi\pi\pi$ verschwindet. Wir wiederholten diese Berechnungen für eine Glueballmasse von 2.37 GeV. Diese entspricht der Masse der pseudoskalaren Resonanz $X(2370)$, welche im BESIII-Experiment beobachtet wurde. Die gleiche Prozedur kann in naher Zukunft auf andere Gluebälle angewendet werden. Einen sehr interessanten Fall bietet der Vektorglueball $\mathcal{O}_\mu$ mit einer Masse von $m_{\mathcal{O}_\mu}$ = 3.8 GeV, welche ebenfalls durch Gitterrechnungen der QCD erhalten wurde, dessen Zerfall in Quark-Antiquark-Mesonen studiert werden kann. In der vorliegenden Arbeit haben wir die entsprechende Lagrangedichte präsentiert und ihre wesentlichen Eigenschaften diskutiert.

Danksagung

An dieser Stelle möchte ich ein paar Worte an die Personen richten, die zur Entstehung meiner Doktorarbeit beigetragen haben.

Ich möchte Prof. Dr. Dirk-Hermann Rischke für die Aufnahme in seiner Arbeitsgruppe, wo ich bereits meine Diplomarbeit geschrieben und meine Arbeit dort im Rahmen der Promotion fortsetzen konnte, ganz herzlich danken. Ich habe seine Unterstützung und die anregenden Diskussionen, die für mich eine Bereicherung waren, während dieser Zeit sehr geschätzt und mich stets sehr gut betreut gefühlt.

Prof. Dr. Francesco Giacosa danke ich ganz herzlich für die seit Beginn meiner Diplomarbeit andauernde, stets sehr gute Betreuung und Unterstützung. Die vielen interessanten und fruchtbaren Gespräche, für die ich sehr dankbar bin, waren für mich eine große Bereicherung. Auch nach Antritt seiner Professur in Polen bestand die Intensität und Qualität der Betreuung und Zusammenarbeit unverändert fort.

Prof. Dr. Igor Mishustin möchte ich danken für die interessanten Anregungen und Diskussionen im Rahmen der PhD Committee-Meetings.

Bei meiner gesamten Arbeitsgruppe möchte ich mich für die vielen interessanten Gespräche, die Unterstützung und die angenehme Arbeitsatmosphäre ganz herzlich bedanken.

Für die Kollaboration im Rahmen verschiedener Projekte bedanke ich mich bei Prof. Dr. Dirk-Hermann Rischke und Prof. Dr. Francesco Giacosa. Dr. Denis Parganlija danke ich für die Zusammenarbeit beim skalaren Glueball sowie für viele interessante und anregende Gespräche. Dr. Walaa Eshraim danke ich für die Zusammenarbeit beim pseudoskalaren Glueball. Antje Peters danke ich für die Rechnungen zu Wechselwirkung des pseudoskalaren Glueballs mit Baryonen und Klaus Neuschwander danke ich für die Rechnungen zu Interferenzeffekten beim Zerfall des pseudoskalaren Glueballs, die sie jeweils im Rahmen ihrer Bachelorarbeit durchgeführt haben und deren Ergebnisse in meine Arbeit eingeflossen sind.

HGS-HIRe und HIC for FAIR möchte ich für die Aufnahme in dem Stipendien-Programm und die Finanzierung meiner Promotion, die die Vereinbarkeit mit Familie fördern, sowie den stets engagierten und hilfsbereiten Mitarbeitern danken. Die Qualifikationen im Rahmen des Pro-

gramms, sowohl fachlich als auch fachübergreifend, waren eine Bereicherung für mich.

Ein ganz großes Dankeschön gilt meiner Familie und Freunden, die mich in der Zeit der Promotion begleitet und unterstützt haben.

Ich weiß es sehr zu schätzen, dass ich in jeder Situation die uneingeschränkte Unterstützung durch meine Eltern, Marta und Ulrich, und Schwiegereltern, Doris und Rüdiger, erfahren habe und dafür möchte ich mich ganz herzlich bedanken.

Darüber hinaus möchte ich Anna, Rafael, Selina, Lionel, Martin, Marie, Victor, Vincent, Charlotte und Clemens danken, von denen mich jeder auf seine Weise unterstützt und ab und an für eine Ablenkung gesorgt hat.

Mein aller größte Dank gebührt meiner einzigartigen Frau Ulrike. Du hast mich während meiner gesamten Promotion grenzenlos unterstützt. Insbesondere in der Zeit der Fertigstellung meiner Arbeit standest Du mir stets kraftvoll zu Seite. Vielen Dank!

Meiner Tochter Sophie danke ich von Herzen, dass sie Teil meines Lebens ist - Du mein kleiner Sonnenschein!

Curriculum Vitae

Pesonal Data

Name	Stanislaus Janowski
Date of birth	04. February 1975, Langendorf (Poland)
Nationality	German
Marital status	married, 1 child

Education

04/2011-11/2015	Ph.D. in Physics (ongoing)
Title	*Phenomenology of glueballs and scalar-isoscalar quarkonia within an effective hadronic model of QCD in vacuum*
Supervisor	Prof. Dr. Francesco Giacosa
Mentor	Prof. Dr. Dirk H. Rischke
10/2003-01/2011	Diploma in Physics (grade: very good with honors)
Title	*Phänomenologie des Dilatons in einem chiralen Modell mit (Axial-) Vektormesonen*
Supervisor	Prof. Dr. Dirk H. Rischke
05/2006	Intermediate Diploma in Physics (grade: very good)
10/2003-09/2015	Study of Physics, Goethe-University, Frankfurt am Main
08/1999-12/2002	Abitur, Hessenkolleg, Frankfurt am Main

Scholarships and Memberships

04/2011-09/2015	Participant of the Helmholtz Graduate School for Hadron and Ion Research - HGS-HIRe for FAIR
01/2012-09/2015	Participant of the Helmholtz Research School for Quark Matter Studies - H-QM
05/2011-04/2015	Scholarships of HIC for FAIR and GSI/GU
since 01/2013	Member of Deutsche Physikalische Gesellschaft e.V. - DPG

Training

04/2013	HGS-HIRe - Softskill Basic Course III *Leadership and Career Development* Abbey of Hoechst, Germany
04/2013	H-QM Lecture Week *Heavy Flavor in Heavy Ion Collisions* San Gimignano, Italy
11/2012	H-QM Lecture Week *Electromagnetic Probes in Heavy Ion Collisions* Ebernburg, Germany
10/2012	HGS-HIRe - Softskill Basic Course II *Leading a Team in a Research Environment* Castle Buchenau, Germany
02/2012	HGS-HIRe Lecture Week *Hot and Dense Matter - Aspects of QCD* Manigod, French Alpes
09/2011	HGS-HIRe - Softskill Basic Course I *Making an Impact as an Effective Researcher* Castle Buchenau, Germany

Teaching Experience

10/2006-09/2009	Teaching assistant
	Theoretical Mechanics I and II Institute for Theoretical Physics Prof. Dr. J. Maruhn
	Theoretical Astrophysics II Institute for Theoretical Physics Prof. Dr. T. Boller
	Experimental Physics: Practical course I *Mechanics, Optics and Thermodynamics* Physical Institute PD. Dr. G. Bruls

Presentations

Talks at international Conferences, Workshops and at Universities

11/2014	*Is f0(1710) a Scalar Glueball?* Instytut Fizyki Uniwersytet Jana Kochanowskiego Kielce, Poland
04/2014	*The Resonances* $f_0(1370), f_0(1500)$ *and* $f_0(1710)$ *in the extended Linear Sigma Model* DPG Spring Meeting Hadronic and Nuclear Physics, Physics Education Frankfurt am Main, Germany
09/2013	*Nature of* $f_0(1370), f_0(1500)$ *and* $f_0(1710)$ *within the extended Linear Sigma Model* 2nd FAIR NExt generation ScientistS - FAIRNESS Berlin, Germany
03/2013	*Phenomenology of the scalar-isoscalar resonances* $f_0(1370)$, $f_0(1500)$ *and* $f_0(1710)$ DPG Spring Meeting Hadronic and Nuclear Physics, Particle Physics Dresden, Germany

02/2013	*Phenomenology of the scalar-isoscalar resonances* $f_0(1370)$ *,* $f_0(1500)$ *and* $f_0(1710)$ 5th International Winter Workshop Excited QCD Sarajevo, Bosnia-Herzegovina
04/2012	*Phenomenology of Dilaton in a Chiral Linear Sigma Model with Vector Mesons* Focus Program at APCPT-WCU From dense matter to compact stars in QCD and in hQCD Pohang, South Korea
05/2012	*Phenomenology of Dilaton in a Chiral Linear Sigma Model with Vector Mesons* 4th International Winter Workshop Excited QCD Peniche, Portugal
03/2011	*The Glueball in a chiral linear sigma model with vector mesons* DPG Spring Meeting Hadronic and Nuclear Physics, Physics Education Münster, Germany

Palaver, Institute for Theoretical Physics, Goethe-University

07/2014	*Scalar-Isoscalar Quarkonia and Glueball within the Extended Linear Sigma Model (eLSM)*
11/2011	*Phenomenology of Dilaton in a two flavored Chiral Linear Sigma Model*
02/2010	*Decays in chiral model with vectors and axial-vectors and dilaton*

Chiral Symmetry Group, Institute for Theoretical Physics, Goethe-University

02/2014	*The scalar glueball and scalar-isoscalar quarkonia*
01/2012	*The pseudoscalar glueball*
10/2011	*Superluminal neutrinos?*
11/2009	*The dilaton in the sigma model: latest results*

05/2009	*The dilaton in the sigma model: first results*
11/2008	*Embedding the dilaton into a generalized sigma model with vector mesons*

HGS-HIRe and H-QM

11/2012	*How to measure dimuons with CMS* H-QM Lecture Week Alte Lokhalle Ebernburg, Germany
10/2012	*Effctive Model of QCD with Glueball* HGS-HIRe Graduate Days Alte Lokhalle Mainz, Germany

Publications

Refereed Journal Articles

12/2014	*Is $f_0(1710)$ a glueball?* S. Janowski, F. Giacosa and D. H. Rischke Phys. Rev. D **90**, no. 11, 114005 (2014) [arXiv:1408.4921[hep-ph]]
03/2013	*Decay of the pseudoscalar glueball into scalar and pseudoscalar mesons* W. I. Eshraim, S. Janowski, F. Giacosa and D. H. Rischke Phys. Rev. D **87**, no. 5, 054036 (2013) [arXiv:1208.6474 [hep-ph]]
09/2011	*Glueball in a chiral linear sigma model with vector mesons* S. Janowski, D. Parganlija, F. Giacosa and D. H. Rischke Phys. Rev. D **84**, 054007 (2011) [arXiv:1103.3238 [hep-ph]]

Conference Proceedings

04/2014 *Resonances $f_0(1370)$, $f_0(1500)$ and $f_0(1710)$within the extended Linear Sigma Model*
S. Janowski and F. Giacosa
J. Phys. Conf. Ser. **503**, 012029 (2014) [arXiv:1312.1605 [hep-ph]]

06/2013 *Quarkonium and glueball admixtures of the scalar-isoscalar resonances$f_0(1370)$, $f_0(1500)$ and $f_0(1710)$*
S. Janowski
Acta Phys. Polon. Supp. **6**, no. 3, 899 (2013) [arXiv:1306.3155 [hep-ph]]

05/2013 *Branching ratios of the pseudoscalar glueball with a mass of 2.6 GeV*
W. I. Eshraim and S. Janowski
PoS ConfinementX , 118 (2012) [arXiv:1301.3345 [hep-ph]]

04/2013 *Phenomenology of the pseudoscalar glueball with a mass of 2.6 GeV*
W. I. Eshraim and S. Janowski
J. Phys. Conf. Ser. **426**, 012018 (2013) [arXiv:1211.7323 [hep-ph]]

12/2012 *Interaction of the pseudoscalar glueball with (pseudo)scalar mesons and nucleons*
W. I. Eshraim, S. Janowski, A. Peters, K. Neuschwander and F. Giacosa
Acta Phys. Polon. Supp. **5**, 1101 (2012) [arXiv:1209.3976 [hep-ph]]

12/2012 *Phenomenology of dilaton in a chiral linear sigma model with vector mesons*
S. Janowski
Acta Phys. Polon. Supp. **5**, 1071 (2012) [arXiv:1208.5397 [hep-ph]]

Manuscript in Preparation

Decay of the vector glueball
S. Janowski, F. Giacosa, *et al.*

Computer Skills

Operative systems	Linux (Ubuntu), Windows
Software	LaTex, Scientic Word, Origin, office applications
Programming	Mathematica, Maple, C++

Languages

German	mother tongue
Polish	mother tongue
English	fluent

Bibliography

[1] S. Janowski, D. Parganlija, F. Giacosa and D. H. Rischke, *Glueball in a chiral linear sigma model with vector mesons*, Phys. Rev. D **84**, 054007 (2011) [arXiv:1103.3238 [hep-ph]].

[2] S. Janowski, *Phenomenology of dilaton in a chiral linear sigma model with vector mesons*, Acta Phys. Polon. Supp. **5**, 1071 (2012) [arXiv:1208.5397 [hep-ph]].

[3] S. Janowski, F. Giacosa and D. H. Rischke, *Is $f_0(1710)$ a glueball?*, Phys. Rev. D **90**, no. 11, 114005 (2014) [arXiv:1408.4921 [hep-ph]].

[4] S. Janowski, *Quarkonium and glueball admixtures of the scalar-isoscalar resonances $f_0(1370)$, $f_0(1500)$ and $f_0(1710)$*, Acta Phys. Polon. Supp. **6**, no. 3, 899 (2013) [arXiv:1306.3155 [hep-ph]].

[5] S. Janowski and F. Giacosa, *Resonances $f_0(1370)$, $f_0(1500)$ and $f_0(1710)$ within the extended Linear Sigma Model*, J. Phys. Conf. Ser. **503**, 012029 (2014) [arXiv:1312.1605 [hep-ph]].

[6] W. I. Eshraim, S. Janowski, F. Giacosa and D. H. Rischke, *Decay of the pseudoscalar glueball into scalar and pseudoscalar mesons*, Phys. Rev. D **87**, no. 5, 054036 (2013) [arXiv:1208.6474 [hep-ph]].

[7] W. I. Eshraim, S. Janowski, A. Peters, K. Neuschwander and F. Giacosa, *Interaction of the pseudoscalar glueball with (pseudo)scalar mesons and nucleons*, Acta Phys. Polon. Supp. **5**, 1101 (2012) [arXiv:1209.3976 [hep-ph]].

[8] W. I. Eshraim and S. Janowski, *Branching ratios of the pseudoscalar glueball with a mass of 2.6 GeV*, PoS ConfinementX , 118 (2012) [arXiv:1301.3345 [hep-ph]].

[9] W. I. Eshraim and S. Janowski, *Phenomenology of the pseudoscalar glueball with a mass of 2.6 GeV*, J. Phys. Conf. Ser. **426**, 012018 (2013) [arXiv:1211.7323 [hep-ph]].

[10] M. E. Peskin, D. V. Schroeder, *An Introduction to Quantum Field Theory*, Addison-Wesley Publishing Company (1995).

[11] K. A. Olive *et al.* [Particle Data Group Collaboration], *Review of Particle Physics*, Chin. Phys. C **38**, 090001 (2014).

[12] L. H. Ryder, *Quantum Field Theory*, Cambridge University Press (1996).

[13] A. Zee, *Quantum Field Theory in a Nutshell*, Princeton University Press (2003).

[14] P. Schmüser, *Feynman-Graphen und Eichtheorien für Experimentalphysiker*, Springer-Verlag (1995).

[15] A. W. Thomas, W. Weise, *The Structure of the Nucleon*, WILEY-VCH (2001).

[16] B. Povh *et al.*, *Teilchen und Kerne - Eine Einführung in die physikalischen Konzepte*, Springer-Verlag (2006).

[17] S. Janowski, *Phänomenologie des Dilatons in einem chiralen Modell mit (Axial-) Vektormesonen,* Diploma Thesis, Faculty of Physics at the J. W. Goethe University in Frankfurt am Main (2010).

[18] F. Giacosa, *Ein effektives chirales Modell der QCD mit Vektormesonen, Dilaton und Tetraquarks: Physik im Vakuum und bei nichtverschwindender Dichte und Temperatur*, Habilitation Thesis, Faculty of Physics at the J. W. Goethe University in Frankfurt am Main (2012).

[19] D. Parganlija, *Quarkonium Phenomenology in Vacuum*, PhD Thesis, Faculty of Physics at the J. W. Goethe University in Frankfurt am Main (2012) arXiv:1208.0204 [hep-ph].

[20] V. Mathieu, N. Kochelev and V. Vento, *The Physics of Glueballs*, Int. J. Mod. Phys. E **18**, 1 (2009) [arXiv:0810.4453 [hep-ph]].

[21] S. Weinberg, *Gravitation and Cosmology: Principles and Applications of the General Theory of Relativity*, John Wiley & Sons, Inc. (1972).

[22] S. Weinberg, *The Making of the standard model*, Eur. Phys. J. C **34**, 5 (2004) [hep-ph/0401010].

[23] W. Greiner, B. Müller, *Quantenmechanik Symmetrien*, Verlag Harri Deutsch (2005).

[24] M. Gell-Mann, *The Eightfold Way: A Theory of strong interaction symmetry*, Synchrotron Laboratory Report CTSL-20, California Institute of Technology (1961).

[25] M. Gell-Mann, *A Schematic Model of Baryons and Mesons*, Phys. Lett. **8**, 214 (1964).

[26] G. Zweig, *An $SU(3)$ model for strong interaction symmetry and its breaking. Version 1*, CERN-TH-401, (1964).

[27] G. Zweig, *An $SU(3)$ model for strong interaction symmetry and its breaking. Version 2*, Developments in the Quark Theory of Hadrons, Volume 1. Edited by D. Lichtenberg and S. Rosen. pp. 22-101, (1964).

[28] H. Fritzsch, M. Gell-Mann and H. Leutwyler, *Advantages of the Color Octet Gluon Picture*, Phys. Lett. B **47**, 365 (1973).

[29] W. Pauli, *The Connection Between Spin and Statistics*, Phys. Rev. **58**, 716 (1940).

[30] R. Aaij *et al.* [LHCb Collaboration], *Observation of $J/\psi p$ resonances consistent with pentaquark states in $\Lambda_b^0 \to J/\psi K^- p$ decays*, arXiv:1507.03414 [hep-ex].

[31] M. Y. Han and Y. Nambu, *Three Triplet Model with Double SU(3) Symmetry*, Phys. Rev. **139**, B1006 (1965).

[32] D. P. Barber, U. Becker, H. Benda, A. Boehm, J. G. Branson, J. Bron, D. Buikman and J. Burger *et al.*, *Discovery of Three Jet Events and a Test of Quantum Chromodynamics at PETRA Energies*, Phys. Rev. Lett. **43**, 830 (1979).

[33] P. Soding, *On the discovery of the gluon*, Eur. Phys. J. H **35**, 3 (2010).

[34] P. Duinker, *Review of e^+e^- physics at PETRA*, Rev. Mod. Phys. **54**, 325 (1982).

[35] B. R. Stella and H. J. Meyer, *Υ(9.46 GeV) and the gluon discovery (a critical recollection of PLUTO results)*, Eur. Phys. J. H **36**, 203 (2011) [arXiv:1008.1869 [hep-ex]].

[36] P. Abreu *et al.* [DELPHI Collaboration], *Experimental study of the triple gluon vertex*, Phys. Lett. B **255**, 466 (1991).

[37] P. Abreu *et al.* [DELPHI Collaboration], *Study of orientation of three jet events in Z^0 hadronic decays using the DELPHI detector* Phys. Lett. B **274**, 498 (1992).

[38] P. M. Zerwas, *QCD: Testing basic properties in jet physics*, DESY-92-139, C91-11-26.

[39] http://www.quantumdiaries.org/author/flip-tanedo/page/5/

[40] G. 't Hooft and M. J. G. Veltman, *Regularization and Renormalization of Gauge Fields*, Nucl. Phys. B **44**, 189 (1972).

[41] D. J. Gross and F. Wilczek, *Ultraviolet Behavior of Nonabelian Gauge Theories*, Phys. Rev. Lett. **30**, 1343 (1973).

[42] H. D. Politzer, *Reliable Perturbative Results for Strong Interactions?*, Phys. Rev. Lett. **30**, 1346 (1973).

[43] M. Gell-Mann and M. Levy, *The axial vector current in beta decay*, Nuovo Cim. **16**, 705 (1960).

[44] Y. Nambu and G. Jona-Lasinio, *Dynamical Model of Elementary Particles Based on an Analogy with Superconductivity. I.*, Phys. Rev. **122**, 345 (1961).

[45] Y. Nambu and G. Jona-Lasinio, *Dynamical Model Of Elementary Particles Based On An Analogy With Superconductivity. II.*, Phys. Rev. **124**, 246 (1961).

[46] P. Ko and S. Rudaz, *Phenomenology of scalar and vector mesons in the linear sigma model*, Phys. Rev. D **50**, 6877 (1994).

[47] J. Schechter, *Introduction to effective Lagrangians for QCD*, eConf C **010815**, 76 (2002) [hep-ph/0112205].

[48] T. Hatsuda and T. Kunihiro, *QCD phenomenology based on a chiral effective Lagrangian*, Phys. Rept. **247**, 221 (1994) [hep-ph/9401310].

[49] http://th.physik.uni-frankfurt.de/ ~giacosa/effectivehadronictheories.html

[50] G. 't Hooft, *A planar diagram theory for strong interactions*, Nucl. Phys. B **72**, 461 (1974).

[51] E. Witten, *Baryons in the* $1/N$ *expansion*, Nucl. Phys. B **160**, 57 (1979).

[52] C. J. Morningstar and M. J. Peardon, *Efficient glueball simulations on anisotropic lattices*, Phys. Rev. D **56**, 4043 (1997) [hep-lat/9704011].

[53] C. J. Morningstar and M. J. Peardon, *Glueball spectrum from an anisotropic lattice study*, Phys. Rev. D **60**, 034509 (1999) [hep-lat/9901004].

[54] C. J. Morningstar and M. J. Peardon, *Simulating the scalar glueball on the lattice*, AIP Conf. Proc. **688**, 220 (2004) [nucl-th/0309068].

[55] Y. Chen, A. Alexandru, S. J. Dong, T. Draper, I. Horvath, F. X. Lee, K. F. Liu and N. Mathur *et al.*, *Glueball spectrum and matrix elements on anisotropic lattices*, Phys. Rev. D **73**, 014516 (2006) [hep-lat/0510074].

[56] M. Loan, X. Q. Luo and Z. H. Luo, *Monte Carlo study of glueball masses in the Hamiltonian limit of* $SU(3)$ *lattice gauge theory*, Int. J. Mod. Phys. A **21**, 2905 (2006) [hep-lat/0503038].

[57] E. B. Gregory, A. C. Irving, C. C. McNeile, S. Miller and Z. Sroczynski, *Scalar glueball and meson spectroscopy in unquenched lattice QCD with improved staggered quarks*, PoS LAT **2005**, 027 (2006) [hep-lat/0510066].

[58] E. B. Gregory, A. C. Irving, B. Lucini, C. C. McNeile, A. Rago, C. Richards and E. Rinaldi, *Towards the glueball spectrum from unquenched lattice QCD*, JHEP **1210**, 170 (2012) [arXiv:1208.1858 [hep-lat]].

[59] W. Ochs, *The Status of Glueballs*, J. Phys. G **40**, 043001 (2013) [arXiv:1301.5183 [hep-ph]].

[60] E. Klempt and A. Zaitsev, *Glueballs, Hybrids, Multiquarks. Experimental facts versus QCD inspired concepts*, Phys. Rept. **454**, 1 (2007) [arXiv:0708.4016 [hep-ph]].

[61] M. Wagner, S. Diehl, T. Kuske and J. Weber, *An introduction to lattice hadron spectroscopy for students without quantum field theoretical background* arXiv:1310.1760 [hep-lat].

[62] K. G. Wilson, *Confinement of Quarks*, Phys. Rev. D **10**, 2445 (1974).

[63] D. H. Rischke, *The Quark gluon plasma in equilibrium*, Prog. Part. Nucl. Phys. **52**, 197 (2004) [nucl-th/0305030].

[64] R. D. Pisarski, *Notes on the deconfining phase transition*, hep-ph/0203271 (2002).

[65] G. 't Hooft, *On the Phase Transition Towards Permanent Quark Confinement*, Nucl. Phys. B **138**, 1 (1978).

[66] A. M. Polyakov, *Thermal Properties of Gauge Fields and Quark Liberation*, Phys. Lett. B **72**, 477 (1978).

[67] O. W. Greenberg, *CPT violation implies violation of Lorentz invariance*, Phys. Rev. Lett. **89**, 231602 (2002) [hep-ph/0201258].

[68] F. Halzen, A. D. Martin, *Quarks and Leptons: An Introductory Course in Modern Particle Physics*, John Wiley & Sons, Inc. (1984).

[69] E. Noether, *Invariante Variationsprobleme*, Nachr. v. d. Ges. d. Wiss. zu Göttingen, 235 (1918).

[70] K. Fujikawa, *Path Integral Measure for Gauge Invariant Fermion Theories*, Phys. Rev. Lett. **42**, 1195 (1979).

[71] P. W. Higgs, *Broken Symmetries and the Masses of Gauge Bosons*, Phys. Rev. Lett. **13**, 508 (1964).

[72] F. Englert and R. Brout, *Broken Symmetry and the Mass of Gauge Vector Mesons*, Phys. Rev. Lett. **13**, 321 (1964).

[73] P. W. Higgs, *Broken symmetries, massless particles and gauge fields*, Phys. Lett. **12**, 132 (1964).

[74] G. Aad *et al.* [ATLAS Collaboration], *Observation of a new particle in the search for the Standard Model Higgs boson with the ATLAS detector at the LHC*, Phys. Lett. B **716**, 1 (2012) [arXiv:1207.7214 [hep-ex]].

[75] S. Chatrchyan *et al.* [CMS Collaboration], Phys. Lett. B **716**, 30 (2012) [arXiv:1207.7235 [hep-ex]].

[76] V. Koch, *Aspects of chiral symmetry*, Int. J. Mod. Phys. E **6**, 203 (1997) [nucl-th/9706075].

[77] J. Bernstein, *Spontaneous symmetry breaking, gauge theories, the higgs mechanism and all that*, Rev. Mod. Phys. **46**, 7 (1974) [Rev. Mod. Phys. **47**, 259 (1975)] [Rev. Mod. Phys. **46**, 855 (1974)].

[78] W. Weise, *The QCD vacuum and its hadronic excitations*, nucl-th/0504087.

[79] J. Goldstone, *Field Theories with Superconductor Solutions*, Nuovo Cim. **19**, 154 (1961).

[80] D. Parganlija, F. Giacosa and D. H. Rischke, *Vacuum properties of mesons in a linear sigma model with vector mesons and global chiral invariance*, Phys. Rev. D **82**, 054024 (2010) [arXiv:1003.4934 [hep-ph]].

[81] D. Parganlija, P. Kovacs, G. Wolf, F. Giacosa and D. H. Rischke, *Meson vacuum phenomenology in a three-flavor linear sigma model with (axial-)vector mesons*, Phys. Rev. D **87**, 014011 (2013) [arXiv:1208.0585 [hep-ph]].

[82] J. T. Lenaghan, D. H. Rischke and J. Schaffner-Bielich, *Chiral symmetry restoration at nonzero temperature in the $SU(3)_r \times SU(3)_l$ linear sigma model*, Phys. Rev. D **62**, 085008 (2000) [nucl-th/0004006].

[83] S. Struber and D. H. Rischke, *Vector and axialvector mesons at nonzero temperature within a gauged linear sigma model*, Phys. Rev. D **77**, 085004 (2008) [arXiv:0708.2389 [hep-th]].

[84] V. M. Braun, G. P. Korchemsky and D. Mueller, *The Uses of conformal symmetry in QCD*, Prog. Part. Nucl. Phys. **51**, 311 (2003) [hep-ph/0306057].

[85] D. J. Gross and J. Wess, *Scale invariance, conformal invariance, and the high-energy behavior of scattering amplitudes*, Phys. Rev. D **2**, 753 (1970).

[86] F. Karbstein, A. Peters and M. Wagner, $\Lambda_{\overline{\rm MS}}^{(n_f=2)}$ *from a momentum space analysis of the quark-antiquark static potential*, JHEP **1409**, 114 (2014) [arXiv:1407.7503 [hep-ph]].

[87] M. A. Shifman, A. I. Vainshtein and V. I. Zakharov, *QCD and Resonance Physics. Sum Rules*, Nucl. Phys. B **147**, 385 (1979).

[88] L. J. Reinders, H. R. Rubinstein and S. Yazaki, *QCD Sum Rules for Heavy Quark Systems*, Nucl. Phys. B **186**, 109 (1981).

[89] J. Marrow, J. Parker and G. Shaw, *QCD Sum Rules: Charmonium*, Z. Phys. C **37**, 103 (1987).

[90] B. V. Geshkenbein, *On the Value of Gluonic Condensate in Quantum Chromodynamics*, Sov. J. Nucl. Phys. **51**, 719 (1990) [Yad. Fiz. **51**, 1121 (1990)].

[91] D. J. Broadhurst, P. A. Baikov, V. A. Ilyin, J. Fleischer, O. V. Tarasov and V. A. Smirnov, *Two loop gluon condensate contributions to heavy quark current correlators: Exact results and approximations*, Phys. Lett. B **329**, 103 (1994) [hep-ph/9403274].

[92] F. J. Yndurain, *Gluon condensate from superconvergent QCD sum rule*, Phys. Rept. **320**, 287 (1999) [hep-ph/9903457].

[93] B. L. Ioffe and K. N. Zyablyuk, *Gluon condensate in charmonium sum rules with three loop corrections*, Eur. Phys. J. C **27**, 229 (2003) [hep-ph/0207183].

[94] K. N. Zyablyuk, *Gluon condensate and c quark mass in pseudoscalar sum rules at three loop order*, JHEP **0301**, 081 (2003) [hep-ph/0210103].

[95] A. Samsonov, *Gluon condensate in charmonium sum rules for the axial-vector current*, hep-ph/0407199.

[96] J. Kripfganz, *Gluon Condensate From $SU(2)$ Lattice Gauge Theory*, Phys. Lett. B **101**, 169 (1981).

[97] A. Di Giacomo and G. C. Rossi, *Extracting $\left\langle (\alpha/\pi) \sum_{a,\mu\nu} G^a_{\mu\nu} G^a_{\mu\nu} \right\rangle$ from gauge theories on a lattice*, Phys. Lett. B **100**, 481 (1981).

[98] A. Di Giacomo and G. Paffuti, *Precise determination of* $\left\langle (\alpha/\pi) \sum_{a,\mu\nu} G^a_{\mu\nu} G^a_{\mu\nu} \right\rangle$ *from lattice gauge theories*, Phys. Lett. B **108**, 327 (1982).

[99] E. M. Ilgenfritz and M. Müller-Preussker, $SU(3)$ *Gluon Condensate From Lattice MC Data*, Phys. Lett. B **119**, 395 (1982).

[100] S. s. Xue, *Gluon Condensate Matter From Analytic Data in* $SU(2)$ *Lattice Theory*, Phys. Lett. B **191**, 147 (1987).

[101] M. Campostrini, A. Di Giacomo and Y. Gunduc, *Gluon Condensation in* $SU(3)$ *Lattice Gauge Theory*, Phys. Lett. B **225**, 393 (1989).

[102] A. Di Giacomo, H. Panagopoulos and E. Vicari, *The Topological Susceptibility and Lattice Universality*, Nucl. Phys. B **338**, 294 (1990).

[103] X. D. Ji, *Gluon condensate from lattice QCD*, hep-ph/9506413.

[104] G. Boyd and D. E. Miller, *The Temperature dependence of the* $SU(N_c)$ *gluon condensate from lattice gauge theory*, hep-ph/9608482.

[105] A. Di Giacomo, H. G. Dosch, V. I. Shevchenko and Y. A. Simonov, *Field correlators in QCD: Theory and applications*, Phys. Rept. **372**, 319 (2002) [hep-ph/0007223].

[106] S. Strauss, C. S. Fischer and C. Kellermann, *Analytic structure of the Landau gauge gluon propagator*, Phys. Rev. Lett. **109**, 252001 (2012) [arXiv:1208.6239 [hep-ph]].

[107] D. Binosi, D. Ibanez and J. Papavassiliou, *The all-order equation of the effective gluon mass*, Phys. Rev. D **86**, 085033 (2012) [arXiv:1208.1451 [hep-ph]].

[108] A. C. Aguilar and A. A. Natale, *A Dynamical gluon mass solution in a coupled system of the Schwinger-Dyson equations*, JHEP **0408**, 057 (2004) [hep-ph/0408254].

[109] K. Johnson, The M.I.T. Bag Model, Acta Phys. Polon. B **6**, 865 (1975).

[110] R. L. Jaffe and K. Johnson, *Unconventional States of Confined Quarks and Gluons*, Phys. Lett. B **60**, 201 (1976).

[111] R. Konoplich and M. Shchepkin, *Glueballs' Masses in the Bag Model*, Nuovo Cim. A **67**, 211 (1982).

[112] M. Jezabek and J. Szwed, *Glueballs In The Bag Models*, Acta Phys. Polon. B **14**, 599 (1983).

[113] R. L. Jaffe, K. Johnson and Z. Ryzak, *Qualitative Features of the Glueball Spectrum*, Annals Phys. **168**, 344 (1986).

[114] M. Strohmeier-Presicek, T. Gutsche, R. Vinh Mau and A. Faessler, *Glueball quarkonia content and decay of scalar-isoscalar mesons*, Phys. Rev. D **60**, 054010 (1999) [hep-ph/9904461].

[115] F. E. Close, *Gluonic Hadrons*, Rept. Prog. Phys. **51**, 833 (1988).

[116] S. Godfrey and J. Napolitano, *Light meson spectroscopy*, Rev. Mod. Phys. **71**, 1411 (1999) [hep-ph/9811410].

[117] C. Amsler and N. A. Tornqvist, *Mesons beyond the naive quark model*, Phys. Rept. **389**, 61 (2004).

[118] V. Crede and C. A. Meyer, *The Experimental Status of Glueballs*, Prog. Part. Nucl. Phys. **63**, 74 (2009) [arXiv:0812.0600 [hep-ex]].

[119] S. Okubo, *φ-meson and unitary symmetry model*, Phys. Lett. **5** (1963) 165.

[120] J. Iizuka, K. Okada and O. Shito, *Systematics and phenomenology of boson mass levels. 3*, Prog. Theor. Phys. **35**, 1061 (1966).

[121] J. Iizuka, *Systematics and phenomenology of meson family*, Prog. Theor. Phys. Suppl. **37**, 21 (1966).

[122] S. Okubo, *Consequences of Quark Line (Okubo-Zweig-Iizuka) Rule*, Phys. Rev. D **16**, 2336 (1977).

[123] D. M. Asner, T. Barnes, J. M. Bian, I. I. Bigi, N. Brambilla, I. R. Boyko, V. Bytev and K. T. Chao *et al.* [BESIII Collaboration], *Physics at BES-III*, Int. J. Mod. Phys. A **24**, S1 (2009) [arXiv:0809.1869 [hep-ex]].

[124] M. F. M. Lutz *et al.* [$\bar{\text{P}}$ANDA Collaboration], *Physics Performance Report for $\bar{P}ANDA$: Strong Interaction Studies with Antiprotons*, arXiv:0903.3905 [hep-ex].

[125] J. G. Messchendorp [$\bar{\text{P}}$ANDA Collaboration], *Hadron Physics with Anti-Protons: The $\bar{P}ANDA$ Experiment at FAIR*, eConf C **070910**, 123 (2007) [arXiv:0711.1598 [nucl-ex]].

[126] D. Bettoni, *The $\bar{P}ANDA$ experiment at FAIR*, eConf C **070805**, 39 (2007) [arXiv:0710.5664 [hep-ex]].

[127] F. Giacosa, *Non-conventional mesons at $\bar{P}ANDA$*, J. Phys. Conf. Ser. **599**, no. 1, 012004 (2015) [arXiv:1502.02682 [hep-ph]].

[128] J. R. Ellis and J. Lanik, *Is Scalar Gluonium Observable?*, Phys. Lett. B **150**, 289 (1985).

[129] P. Minkowski and W. Ochs, *B decays into light scalar particles and glueball*, Eur. Phys. J. C **39**, 71 (2005) [hep-ph/0404194].

[130] P. Minkowski and W. Ochs, *The Glueball among the light scalar mesons*, Nucl. Phys. Proc. Suppl. **121**, 123 (2003) [hep-ph/0209225].

[131] P. Minkowski and W. Ochs, *Identification of the glueballs and the scalar meson nonet of lowest mass*, Eur. Phys. J. C **9**, 283 (1999) [hep-ph/9811518].

[132] G. Mennessier, S. Narison and W. Ochs, *Glueball nature of the $\sigma/f_0(600)$ from $\pi\pi$ and $\gamma\gamma$ scatterings*, Phys. Lett. B **665**, 205 (2008) [arXiv:0804.4452 [hep-ph]].

[133] R. L. Jaffe, *Multi-Quark Hadrons. 1. The Phenomenology of (2 Quark 2 anti-Quark) Mesons*, Phys. Rev. D **15**, 267 (1977).

[134] R. L. Jaffe, *Multi-Quark Hadrons. 2. Methods*, Phys. Rev. D **15**, 281 (1977).

[135] L. Maiani, F. Piccinini, A. D. Polosa and V. Riquer, *A New look at scalar mesons*, Phys. Rev. Lett. **93**, 212002 (2004) [hep-ph/0407017].

[136] F. Giacosa, *Strong and electromagnetic decays of the light scalar mesons interpreted as tetraquark states*, Phys. Rev. D **74**, 014028 (2006) [hep-ph/0605191].

[137] F. Giacosa and G. Pagliara, *Decay of light scalar mesons into vector-photon and into pseudoscalar mesons*, Nucl. Phys. A **833**, 138 (2010) [arXiv:0905.3706 [hep-ph]].

[138] F. Giacosa, *Mixing of scalar tetraquark and quarkonia states in a chiral approach*, Phys. Rev. D **75**, 054007 (2007) [hep-ph/0611388].

[139] E. van Beveren, T. A. Rijken, K. Metzger, C. Dullemond, G. Rupp and J. E. Ribeiro, *A Low Lying Scalar Meson Nonet in a Unitarized Meson Mode*, Z. Phys. C **30**, 615 (1986) [arXiv:0710.4067 [hep-ph]].

[140] N. A. Tornqvist, *Understanding the scalar meson q anti-q nonet*, Z. Phys. C **68**, 647 (1995) [hep-ph/9504372].

[141] M. Boglione and M. R. Pennington, *Dynamical generation of scalar mesons*, Phys. Rev. D **65**, 114010 (2002) [hep-ph/0203149].

[142] E. van Beveren, D. V. Bugg, F. Kleefeld and G. Rupp, *The Nature of σ, κ, $a_0(980)$ and $f_0(980)$*, Phys. Lett. B **641**, 265 (2006) [hep-ph/0606022].

[143] J. R. Pelaez, *On the Nature of Light Scalar Mesons from their Large-N_c Behavior*, Phys. Rev. Lett. **92**, 102001 (2004) [hep-ph/0309292].

[144] J. A. Oller and E. Oset, *Chiral symmetry amplitudes in the S wave isoscalar and isovector channels and the σ, $f_0(980)$, $a_0(980)$ scalar mesons*, Nucl. Phys. A **620**, 438 (1997) [Erratum-ibid. A **652**, 407 (1999)] [hep-ph/9702314].

[145] A. H. Fariborz, R. Jora and J. Schechter, *Toy model for two chiral nonets*, Phys. Rev. D **72**, 034001 (2005) [hep-ph/0506170].

[146] A. H. Fariborz, *Isosinglet scalar mesons below 2-GeV and the scalar glueball mass*, Int. J. Mod. Phys. A **19**, 2095 (2004) [hep-ph/0302133].

[147] M. Napsuciale and S. Rodriguez, *A Chiral model for $\bar{q}q$ and $\bar{q}\bar{q}qq$ mesons*, Phys. Rev. D **70**, 094043 (2004) [hep-ph/0407037].

[148] S. Gallas, F. Giacosa and D. H. Rischke, *Vacuum phenomenology of the chiral partner of the nucleon in a linear sigma model with vector mesons*, Phys. Rev. D **82**, 014004 (2010) [arXiv:0907.5084 [hep-ph]].

[149] F. Giacosa, T. Gutsche, V. E. Lyubovitskij and A. Faessler, *Decays of tensor mesons and the tensor glueball in an effective field approach*, Phys. Rev. D **72**, 114021 (2005) hep-ph/0511171].

[150] L. Burakovsky and J. T. Goldman, *Towards resolution of the enigmas of P wave meson spectroscopy*, Phys. Rev. D **57**, 2879 (1998) [hep-ph/9703271].

[151] A. Masoni, C. Cicalo and G. L. Usai, *The case of the pseudoscalar glueball*, J. Phys. G **32**, R293 (2006).

[152] T. Gutsche, V. E. Lyubovitskij and M. C. Tichy, $\eta(1405)$ *in a chiral approach based on mixing of the pseudoscalar glueball with the first radial excitations of eta and eta-prime*, Phys. Rev. D **80**, 014014 (2009) [arXiv:0904.3414 [hep-ph]].

[153] H. Y. Cheng, H. n. Li and K. F. Liu, *Pseudoscalar glueball mass from η-η'-G mixing*, Phys. Rev. D **79**, 014024 (2009) [arXiv:0811.2577 [hep-ph]].

[154] V. Mathieu and V. Vento, *Pseudoscalar glueball and η-η' mixing*, Phys. Rev. D **81**, 034004 (2010) [arXiv:0910.0212 [hep-ph]].

[155] C. Di Donato, G. Ricciardi and I. Bigi, *η-η' Mixing - From electromagnetic transitions to weak decays of charm and beauty hadrons*, Phys. Rev. D **85**, 013016 (2012) [arXiv:1105.3557 [hep-ph]].

[156] B. A. Li, *Chiral field theory of 0^{-+} glueball*, Phys. Rev. D **81**, 114002 (2010) [arXiv:0912.2323 [hep-ph]].

[157] F. Ambrosino, A. Antonelli, M. Antonelli, F. Archilli, P. Beltrame, G. Bencivenni, S. Bertolucci and C. Bini *et al.* [KLOE Collaboration], *A Global fit to determine the pseudoscalar mixing angle and the gluonium content of the eta-prime meson*, JHEP **0907**, 105 (2009) [arXiv:0906.3819 [hep-ph]].

[158] R. Escribano and J. Nadal, *On the gluon content of the η and η' mesons* JHEP **0705**, 006 (2007) [hep-ph/0703187].

[159] R. Escribano, *$J/\psi \to VP$ decays and the quark and gluon content of the η and η'*, Eur. Phys. J. C **65**, 467 (2010) [arXiv:0807.4201 [hep-ph]].

[160] D. Robson, *Identification of a Vector Glueball?*, Phys. Lett. B **66**, 267 (1977).

[161] G. W. S. Hou, *(Vector) glueballs and charmonium decay revisited*, In *Minneapolis 1996, Particles and fields, vol. 1* 399-401 [hep-ph/9609363].

[162] J. Z. Bai *et al.* [BES Collaboration], *Search for a vector glueball by a scan of the J/ψ resonance*, Phys. Rev. D **54**, 1221 (1996) [Phys. Rev. D **57**, 3187 (1998)].

[163] M. Suzuki, *Elusive vector glueball*, Phys. Rev. D **65**, 097507 (2002) [hep-ph/0203012].

[164] W. S. Hou, *Glueballs: Charmonium decay and $\bar{p}p$ annihilation*, Phys. Rev. D **55**, 6952 (1997) [hep-ph/9610411].

[165] G. W. S. Hou, *The Case for a vector glueball*, hep-ph/9707526 (1997).

[166] S. Janowski and F. Giacosa *et al.*, in preparation.

[167] M. E. B. Franklin *et al.*, *Measurement of* $\psi(3097)$ *and* $\psi'(3686)$ *Decays Into Selected Hadronic Modes* Phys. Rev. Lett. **51**, 963 (1983).

[168] S. J. Brodsky, G. P. Lepage and S. F. Tuan, *Exclusive Charmonium Decays: The* $J/\psi(\psi')$ $\to \rho\pi$, $K^*\bar{K}$ *Puzzle*, Phys. Rev. Lett. **59**, 621 (1987).

[169] D. S. Carman, *GlueX: The Search for gluonic excitations at Jefferson Laboratory*, AIP Conf. Proc. **814**, 173 (2006) [hep-ex/0511030].

[170] F. Giacosa and G. Pagliara, *On the spectral functions of scalar mesons*, Phys. Rev. C **76**, 065204 (2007) [arXiv:0707.3594 [hep-ph]].

[171] D. J. Griffiths, *Introduction to Elementary Particles*, by John Wiley & Sons, Inc. (1987).

[172] http://th.physik.uni-frankfurt.de/˜ giacosa/decays.html.

[173] S. Weinberg, *Tetraquark Mesons in Large N Quantum Chromodynamics*, Phys. Rev. Lett. **110**, 261601 (2013) [arXiv:1303.0342 [hep-ph]].

[174] C. Rosenzweig, A. Salomone and J. Schechter, *A Pseudoscalar Glueball, the Axial Anomaly and the Mixing Problem for Pseudoscalar Mesons*, Phys. Rev. D **24**, 2545 (1981).

[175] A. Salomone, J. Schechter and T. Tudron, *Properties of Scalar Gluonium*, Phys. Rev. D **23**, 1143 (1981).

[176] C. Rosenzweig, A. Salomone and J. Schechter, *How Does A Pseudoscalar Glueball Come Unglued?*, Nucl. Phys. B **206**, 12 (1982) [Erratum-ibid. B **207**, 546 (1982)].

[177] H. Gomm and J. Schechter, *Goldstone Bosons and Scalar Gluonium*, Phys. Lett. B **158**, 449 (1985).

[178] R. Gomm, P. Jain, R. Johnson and J. Schechter, *Scale Anomaly and the Scalars*, Phys. Rev. D **33**, 801 (1986).

[179] A. A. Migdal and M. A. Shifman, *Dilaton Effective Lagrangian in Gluodynamics*, Phys. Lett. B **114**, 445 (1982).

[180] V. A. Novikov, M. A. Shifman, A. I. Vainshtein and V. I. Zakharov, *Are All Hadrons Alike?*,Nucl. Phys. B **191**, 301 (1981).

[181] D. Parganlija, F. Giacosa and D. H. Rischke, *How Universal is the Coupling in the Sigma Model?*, AIP Conf. Proc. **1030**, 160 (2008) [arXiv:0804.3949 [hep-ph]].

[182] S. Vandoren and P. van Nieuwenhuizen, *Lectures on instantons*, arXiv:0802.1862 [hep-th].

[183] G. 't Hooft, *How Instantons Solve the* $U(1)$ *Problem*, Phys. Rept. **142**, 357 (1986).

[184] E. Witten, *Current Algebra Theorems for the $U(1)$ Goldstone Boson*, Nucl. Phys. B **156**, 269 (1979).

[185] G. Veneziano, *$U(1)$ Without Instantons*, Nucl. Phys. B **159**, 213 (1979).

[186] D. Parganlija, P. Kovacs, G. Wolf, F. Giacosa and D. H. Rischke, *Eta, Eta' and eLSM*, PoS ConfinementX , 117 (2012) [arXiv:1301.3478 [hep-ph]].

[187] C. Rosenzweig, J. Schechter and C. G. Trahern, *Is the effective Lagrangian for quantum chromodynamics a σ model?*, Phys. Rev. D **21**, 3388 (1980).

[188] K. Kawarabayashi and N. Ohta, *The problem of η in the Large N limit: Effective Lagrangian approach*, Nucl. Phys. B **175**, 477 (1980).

[189] L. S. Geng and E. Oset, *Vector meson-vector meson interaction in a hidden gauge unitary approach*, Phys. Rev. D **79**, 074009 (2009) [arXiv:0812.1199 [hep-ph]].

[190] L. S. Geng, F. K. Guo, C. Hanhart, R. Molina, E. Oset and B. S. Zou, *Study of the $f_2(1270)$, $f_2'(1525)$, $f_0(1370)$ and $f_0(1710)$ in the J/ψ radiative decays*, Eur. Phys. J. A **44**, 305 (2010) [arXiv:0910.5192 [hep-ph]].

[191] A. Martinez Torres, K. P. Khemchandani, F. S. Navarra, M. Nielsen and E. Oset, *The Role of $f_0(1710)$ in the $\phi\omega$ Threshold Peak of $J/\psi \to \gamma\phi\omega$*, Phys. Lett. B **719**, 388 (2013) [arXiv:1210.6392 [hep-ph]].

[192] F. Divotgey, L. Olbrich and F. Giacosa, *Phenomenology of axial-vector and pseudovector mesons: decays and mixing in the kaonic sector*, Eur. Phys. J. A **49**, 135 (2013) [arXiv:1306.1193 [hep-ph]].

[193] S. Gasiorowicz and D. A. Geffen, *Effective Lagrangians and field algebras with chiral symmetry*, Rev. Mod. Phys. **41**, 531 (1969).

[194] K. Nakamura *et al.* [Particle Data Group Collaboration], *Review of particle physics*, J. Phys. G **37**, 075021 (2010).

[195] J. Beringer *et al.* [Particle Data Group Collaboration], *Review of particle physics*, Phys. Rev. D **86**, 010001 (2012).

[196] I. Caprini, G. Colangelo and H. Leutwyler, *Mass and width of the lowest resonance in QCD*, Phys. Rev. Lett. **96**, 132001 (2006) [hep-ph/0512364].

[197] F. J. Yndurain, R. Garcia-Martin and J. R. Pelaez, *Experimental status of the $\pi\pi$ isoscalar S wave at low energy: $f_0(600)$ pole and scattering length* Phys. Rev. D **76**, 074034 (2007) [hep-ph/0701025].

[198] R. Kaminski, R. Garcia-Martin, P. Grynkiewicz and J. R. Pelaez, *Sigma pole position and errors of a once and twice subtracted dispersive analysis of pi-pi scattering data*, Nucl. Phys. Proc. Suppl. **186**, 318 (2009) [arXiv:0811.4510 [hep-ph]].

[199] R. Garcia-Martin, R. Kaminski, J. R. Pelaez and J. Ruiz de Elvira, *Precise determination of the $f_0(600)$ and $f_0(980)$ pole parameters from a dispersive data analysis*, Phys. Rev. Lett. **107**, 072001 (2011) [arXiv:1107.1635 [hep-ph]].

[200] F. Giacosa, *Two-photon decay of light scalars: A Comparison of tetraquark and quarkonium assignments*, in XII International Conference on Hadron Spectroscopy, Frascati, Italy, 2007 (Istituto Nazionale di Fisica Nucleare, Frascati, Italy, 2007), arXiv:0712.0186 [hep-ph].

[201] D. Parganlija, F. Giacosa and D. H. Rischke, *Decay widths of resonances and pion scattering lengths in a globally invariant linear sigma model with vector mesons*, PoS CONFINEMENT **8**, 070 (2008) [arXiv:0812.2183 [hep-ph]].

[202] M. Urban, M. Buballa and J. Wambach, *Vector and axial vector correlators in a chirally symmetric model*, Nucl. Phys. A **697**, 338 (2002) [hep-ph/0102260].

[203] C. Amsler and F. E. Close, *Is $f_0(1500)$ a scalar glueball?*, Phys. Rev. D **53**, 295 (1996) [hep-ph/9507326].

[204] F. E. Close and A. Kirk, *Scalar glueball-$q\bar{q}$ mixing above 1 GeV and implications for lattice QCD*, Eur. Phys. J. C **21**, 531 (2001) [hep-ph/0103173].

[205] F. Giacosa, T. Gutsche and A. Faessler, *Covariant constituent quark-gluon model for the glueball-quarkonia content of scalar-isoscalar mesons*, Phys. Rev. C **71**, 025202 (2005) [hep-ph/0408085].

[206] T. Teshima, I. Kitamura and N. Morisita, *Effects to scalar meson decays of strong mixing between low and high mass scalar mesons*, J. Phys. G **30**, 663 (2004) [hep-ph/0305296].

[207] F. Giacosa, T. Gutsche, V. E. Lyubovitskij and A. Faessler, *Scalar nonet quarkonia and the scalar glueball: Mixing and decays in an effective chiral approach*, Phys. Rev. D **72**, 094006 (2005) [hep-ph/0509247].

[208] F. Giacosa, T. Gutsche, V. E. Lyubovitskij and A. Faessler, *Scalar meson and glueball decays within a effective chiral approach*, Phys. Lett. B **622**, 277 (2005) [hep-ph/0504033].

[209] A. H. Fariborz, *Mass Uncertainties of $f_0(600)$ and $f_0(1370)$ and their Effects on Determination of the Quark and Glueball Admixtures of the I=0 Scalar Mesons* Phys. Rev. D **74**, 054030 (2006) [hep-ph/0607105].

[210] D. V. Bugg, *A Study in Depth of $f_0(1370)$*, Eur. Phys. J. C **52**, 55 (2007) [arXiv:0706.1341 [hep-ex]].

[211] G. E. Brown and M. Rho, *Scaling effective Lagrangians in a dense medium*, Phys. Rev. Lett. **66**, 2720 (1991).

[212] D. Parganlija, F. Giacosa and D. H. Rischke, *Influence of Vector Mesons on the $f_0(600)$ Decay Width in a Linear Sigma Model with Global Chiral Invariance*, arXiv:0911.3996 [nucl-th].

[213] H. Y. Cheng, C. K. Chua and K. F. Liu, *Scalar glueball, scalar quarkonia, and their mixing*, Phys. Rev. D **74**, 094005 (2006) [hep-ph/0607206].

[214] W. J. Lee and D. Weingarten, *Scalar quarkonium masses and mixing with the lightest scalar glueball*, Phys. Rev. D **61**, 014015 (2000) [hep-lat/9910008].

[215] L. C. Gui, Y. Chen, G. Li, C. Liu, Y. B. Liu, J. P. Ma, Y. B. Yang and J. B. Zhang, *Scalar glueball in radiative J/ψ decay on lattice*, Phys. Rev. Lett. **110**, 021601 (2013) [arXiv:1206.0125 [hep-lat]].

[216] H. Y. Cheng, C. K. Chua and K. F. Liu, *Revisiting Scalar Glueballs*, arXiv:1503.06827 [hep-ph].

[217] V. Vento, *Glueball-Meson Mixing*, arXiv:1505.05355 [hep-ph].

[218] M. Albaladejo and J. A. Oller, *Identification of a Scalar Glueball*, Phys. Rev. Lett. **101**, 252002 (2008) [arXiv:0801.4929 [hep-ph]].

[219] M. Ablikim *et al.*, *Partial wave analyses of $J/\psi \to \gamma\pi^+\pi^-$ and $\gamma\pi^0\pi^0$*, Phys. Lett. B **642**, 441 (2006) [hep-ex/0603048].

[220] S. Dobbs, A. Tomaradze, T. Xiao and K. K. Seth, *Comprehensive Study of the Radiative Decays of J/ψ and $\psi(2S)$ to Pseudoscalar Meson Pairs, and Search for Glueballs*, Phys. Rev. D **91**, no. 5, 052006 (2015) [arXiv:1502.01686 [hep-ex]].

[221] F. Brünner, D. Parganlija and A. Rebhan, *Glueball Decay Rates in the Witten-Sakai-Sugimoto Model*, Phys. Rev. D **91**, no. 10, 106002 (2015) [arXiv:1501.07906 [hep-ph]].

[222] J. M. Frère and J. Heeck, *Scalar glueball: seeking help from $\eta\eta'$ decays*, arXiv:1506.04766 [hep-ph].

[223] K. Neuschwander, *Three-body decays in effective hadronic models,* Bachelor Thesis, Faculty of Physics at the J. W. Goethe University in Frankfurt am Main (2012).

[224] A. Peters, *Baryonic decays in the eLSM,* Bachelor Thesis, Faculty of Physics at the J. W. Goethe University in Frankfurt am Main (2012).

[225] M. Ablikim *et al.* [BES Collaboration], *Observation of a Resonance $X(1835)$ in $J/\psi \to \gamma\pi^+\pi^-\eta'$*, Phys. Rev. Lett. **95**, 262001 (2005) [hep-ex/0508025].

[226] N. Kochelev and D. P. Min, *$X(1835)$ as thelowest mass pseudoscalar glueball and proton spin problem*, Phys. Lett. B **633**, 283 (2006) [hep-ph/0508288].

[227] M. Ablikim *et al.* [BESIII Collaboration], *Confirmation of the $X(1835)$ and Observation of the Resonances $X(2120)$ and $X(2370)$ in $J/\psi \to \gamma\pi^+\pi^-\eta'$*, Phys. Rev. Lett. **106**, 072002 (2011) [arXiv:1012.3510 [hep-ex]].

[228] D. V. Bugg, *An Alternative interpretation of Belle data on $\gamma\gamma \to \eta'\pi^+\pi^-$*, Phys. Rev. D **86**, 114006 (2012) [arXiv:1209.3480 [hep-ex]].

[229] P. Chatzis, A. Faessler, T. Gutsche and V. E. Lyubovitskij, *Hadronic and radiative three-body decays of J/ψ involving the scalars $f_0(1370)$, $f_0(1500)$ and $f_0(1710)$*, Phys. Rev. D **84**, 034027 (2011) [arXiv:1105.1676 [hep-ph]].

[230] C. E. Detar and T. Kunihiro, *Linear σ Model With Parity Doubling*, Phys. Rev. D **39**, 2805 (1989).

[231] A. Heinz, S. Struber, F. Giacosa and D. H. Rischke, *Role of the tetraquark in the chiral phase transition*, Phys. Rev. D **79**, 037502 (2009) [arXiv:0805.1134 [hep-ph]].

[232] S. Gallas, F. Giacosa and G. Pagliara, *Nuclear matter within a dilatation-invariant parity doublet model: the role of the tetraquark at nonzero density*, Nucl. Phys. A **872**, 13 (2011) [arXiv:1105.5003 [hep-ph]].

[233] A. Heinz, F. Giacosa and D. H. Rischke, *Chiral density wave in nuclear matter*, Nucl. Phys. A **933**, 34 (2015) [arXiv:1312.3244 [nucl-th]].